DX

184648

STUDIES ON CONDUCTING POLYMERS: THE SYNTHESES AND ANODIC ELECTROPOLYMERISATION OF NOVEL β-FUNCTIONALISED THIOPHENES

DAVID O. B. A. ADEBIMPE

A thesis submitted in partial fulfilment of
the requirements of the University of North London
for the degree of *Doctor of Philosophy (Ph.D.)*

THIS RESAEARCH PROGRAMME WAS CARRIED OUT IN COLLABORATION WITH COOKSON GROUP PLC., AND THE UNIT FOR SPECIALITY ELECTRONIC POLYMERS, UNIVERSITY COLLEGE, UNIVERSITY OF LONDON

JUNE 1994

ACKNOWLEDGEMENT

I would like to express my profound gratitude to my mentor and director of studies Dr. Michael K. Shepherd, and supervisors Drs. Poopathy Kathirgamanathan, Dominic Spillane and Prof. Harry R. Hudson for their invaluable guidance and assistance. I would also like to heartily acknowledge Dr. John Coyle and the Cookson Group plc. for allowing the use of facilities at the Central Research Centre at Kidlington; Prof. Dr. Gerhart Koßmehl (Freie Universität Berlin) for useful discussions; Prof. John C. Charalambous for being a continuous source of assistance and encouragement, and Prof. Mary McPartlin for granting the use of her publishing facilities.

Mark Rümmeli deserves thanks for being a true (and timely) friend, and gratitude is also due to my sister Scooby-doo and of course, to "MJP" for their love, support, sustenance, comfort and lots of patience.

This thesis is dedicated to my much-cherished father, Engr. Adésòkàn Bódúnrìn Adébimpé, a bastion of inspiration who holds loyalty above all other, except honour.

A man would do nothing,
if he waited until he could do it so well
that no one would find fault
with what he has done.

CARDINAL NEWMAN (1801 - 90)

DAVID O.B.A ADEBIMPE

**STUDIES ON CONDUCTING POLYMERS:
THE SYNTHESES AND ANODIC ELECTROPOLYMERISATION OF NOVEL β-FUNCTIONALISED THIOPHENES.**

ABSTRACT

Following a brief review on conducting polymers, eight β-functionalised thiophene derivatives *viz*; *trans*-1,2-bis(3´-thienyl)ethene, [1]; *trans*-1-(1´-pyrenyl)-2-(3˝-thienyl)ethene, [2]; *trans*-1-(p-N,N-dimethylaminophenyl)-2-(3´-thienyl)ethene, [3]; *trans*-1-(ferrocenyl)-2-(3´-thienyl)ethene, [4]; (*E,E*)-3,4-*bis*-(2´-ethenylferrocenyl)thiophene, [5]; 1-(ferrocenyl)-3-(3´-thienyl)prop-2-en-1-one, [6]; (*E,E*)-1,5-*bis*(3´-thienyl)penta-1,4-dien-3-one, [7]; *all-trans* 1,9-*bis*(3´-thienyl)nona-1,3,6,8-tetraen-5-one, [8]; and 3-(trimethylsilyl)thiophene, [9] were synthesised as precursors for anodic electropolymerisation though an anticipated 2,5´-coupling of their respective thiophene moieties. The spectroscopic properties of these novel compounds, including their electrochemical behaviour, are presented.

The oxidation of the ferrocene-containing compounds, [4] to [6], resulted in the formation of quasi-reversible metal-centred cations. The heterogenous oxidation of compound [5] resulted in the formation of a mixed-valent Fe(II)/Fe(III) ion which underwent dispropotionation to yield a stable dication. Compounds [7] and [8] also resisted oxidative polymerisation due to the overwhelming electron withdrawing effect of the carbonyl function, resulting in proton abstraction from the electron-rich carbonyl oxygen followed by dimerisation.

However oxidised polymers were generated from compounds [1], [2] and [9]. Typical PF_6-doped polymeric materials obtained from compounds [1] and [2] exhibited conductivities of 3.5×10^{-2} S cm^{-1} and 5.60×10^{-3} S cm^{-1} respectively, whilst the ClO_4-doped polymer of [2] exhibited a conductivity of 4.20×10^{-3} S cm^{-1}. The flexible and compressible PF_6-doped polymer derived from the electropolymerisation of [9] displayed disparate conductivities of 15 and 100 S cm^{-1} for the solvent and electrode sides of the polymer respectively. It was also noted that the oxidation process had resulted in desilylation of the monomeric species and thus, in the formation of a polymer predominantly composed of 2,5 and 2,4-thienylene.

As a result of Scanning Electron Microscopy (SEM), Electron Probe Microanalysis (EPMA), Thermogravimetric Analysis (TGA), Fourier-Transform Infra-Red spectroscopy and Solid-State ^{13}C-Nuclear Magnetic Resonance studies, some of the physicochemical properties of these polymeric materials are described.

TABLE OF CONTENTS

LIST OF FIGURES

LIST OF TABLES

CHAPTER 1

INTRODUCTION

1.1 GENERAL INTRODUCTION

Polymers (e.g., polyethylene, polyvinylchloride (PVC), and polymethylacrylate), well known for their intrinsic inability to conduct electricity, are widely employed as insulators. This inability arises from a lack of charge carriers and a path for their conduction. Hence, electrically conducting polymers are traditionally achieved via the fabrication of filled-polymer composites,[1,2] obtained by milling or compounding the polymer of interest with flakes of an organic or inorganic conductive filler such as nickel, metallised glass spheres and fibres, indium tin oxide, copper, aluminium, brass, stainless steel, and graphite powder,[3] to form composites such as those shown below (figure 1.1).

Rubber + Graphite Powder = Conductive Rubber.

Polyethylene Powder + Nickel Powder = Conductive Polyethylene.

Polyester film + Aluminium Powder = Metallised Polyester film.

Figure 1.1
Some examples of filled polymer composites.[4]

Another method by which conducting polymer composites are prepared is by complexation of inert and insulating polymers with charge-transfer compounds. This is realised by the co-crystallisation of the polymer of interest with a pre-determined amount of a charge-transfer compound such as tetrathiafulvalene (TTF) or 7,7,8,8,-tetracyanoquinodimethane (TCNQ), along with a prudent manipulation of such factors as purity, additive solvent and polymer interactions, temperature, and the rate of solvent evaporation. In these two distinct techniques the polymer itself remains non-conducting, and conduction is made possible by the presence of the dispersed filler embedded within its matrix. In addition to this, the maximum conductivity achievable in a polymer composite is dependent solely on the conductivity of the dispersed filler, and the amount used (i.e its loading level). Although fillers generally give high conductivity values at low loading levels, applications of filled polymer composites are mainly geared towards

charge dissipation (antistatics) and electromagnetic interference (EMI) shielding applications.[5]

Although the first report on a polymer capable of "intrinsically" conducting electricity was made by Naarmann *et al.*,[6] three factors have contributed to the significant development in the search for "intrinsically" conducting polymers (ICP's). The first was the discovery of metallic[7] and later, superconductivity,[8] in single crystals of poly(sulphur nitride) $[(SN)_n]$. Then in 1977, Heeger and McDiarmid[9] discovered that polyacetylene $[(CH)_n]$, synthesised by the Shirakawa method[10] (and which untill then attracted little attention), entailing the passage of pure, dry acetylene gas over titanium tetrabutoxide-triethyl aluminium (Ziegler-Natta catalyst) in toluene at -78°C, underwent a 12-fold increase in conductivity upon oxidative doping. Two years later, Diaz and colleagues adopted the use of anodic oxidation methods in the generation of conducting polymers from targeted aromatic compounds, with a revised and improved anodic oxidation technique that led to the electrosynthesis of p-doped polypyrrole.[11] Although most of todays well known ICP's were first chemically synthesised as insulating powders or films which are later doped,[12] they are now preferably obtained through anodic oxidation techniques. This is because of the following factors:

1. chemical coupling methods usually lead to the production of polymers with structural defects and/or impurities.[13]

2. Anodic oxidation concludes in electropolymerisation accompanied by *in situ* doping. This results in the "one-pot" synthesis of a doped, free-standing polymer.

3. The polymer formed can be reversibly cycled between its oxidised (doped and conducting) and reduced (undoped & insulating) states respectively.

4. The process allows for the incorporation of a diverse range of chemical species as dopants.

5. The rate of polymer growth is controllable by a manipulation of either the applied oxidation potential or deposition charge. In order to optimise the quality and the physicochemical properties of a conducting polymer, the rate at which polymerisation proceeds is apparently important.[14]

6. With the use of anodic oxidation as a polymerisation technique, it is possible to undertake a systematic study of the polymerisation and doping processes through in-situ electrochemical analytical techniques. Cyclic voltammetry, one of the simplest and most popular of such techniques, was used during the course of this research, and is briefly discussed in Chapter 4.

Since Diaz's electrosynthesis of p-doped polypyrrole, an array of benzenoid, non-benzenoid and heterocyclic compounds such as benzene,[15] phenol,[16] N,N-dimethylaniline,[17] carbazole,[18] azulene,[19] pyrene,[20] furan and indole,[21] have been subjected to anodic oxidation methods to yield highly conductive polymeric films which display a wealth of electro-optic,[22] electronic junction, electrochemical and redox properties which are arousing the curiosities of industrial and academic scientists worldwide. Several articles have now been devoted to the key aspects involved in the electrochemical synthesis of conducting polymers. These include reviews involving their general electrochemistry,[23] environmental stability,[24] and optical properties.[25]

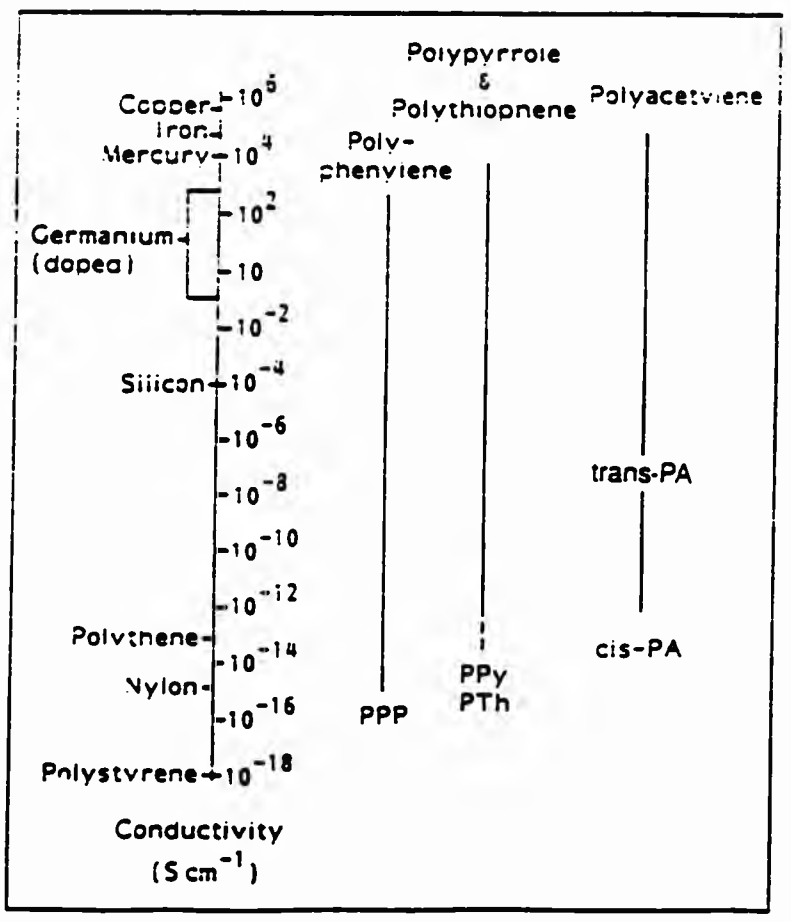

Figure 1.2
A comparison of conductivity ranges for several polymers with some conventional materials.[26]

1.2 THE THEORY OF CONDUCTION IN ICP's[27]

Electricity is defined as the flow of electrons. Unlike electrical conduction in metals, which results from the movement of electrons across atoms that are in a lattice devoid of an energy barrier or band gap,[28] the band gap between the valence and conduction bands in polymeric compounds is very large (figure 1.3).

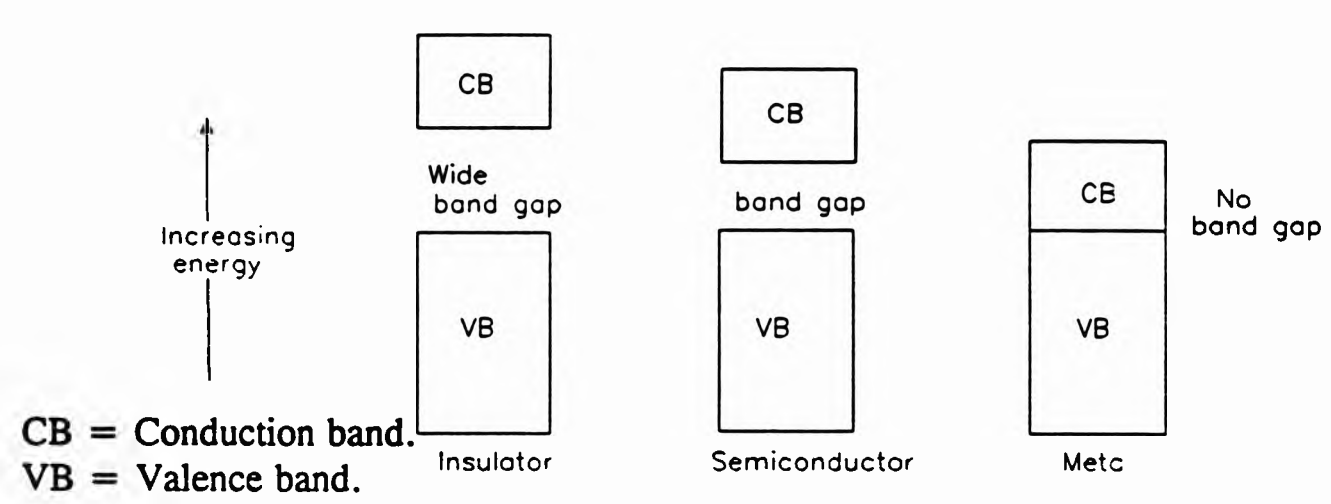

Figure 1.3
The electronic structure of conventional materials.

In conducting polymers charge transport or conduction is achieved by doping. The two different types of charge carriers generated by the doping process, derived from basic solid-state theory,[29] are called polarons and bipolarons respectively. The energy levels associated with these carriers represent destabilising bonding orbitals with an energy higher than that of the valence band,[30] and so, leads to the introduction of intermediate energy levels into the band-gap region. The carriers then jump from chain to chain through a smaller potential energy barrier, and they also move along polymer chains by the rearrangement of single and double bonds along a conjugated π-system that extends over several repeating monomeric units. This leads to the "intrinsic conductivity" of the material.

1.2.1 Low-level doping

The low-level doping of a conjugated polymer through any of the known liquid, vapour phase or anodic oxidation techniques results in the removal of an electron from its' top valence band and the formation of a polaron, which is a radical cation with a spin of ½. The presence of the polaron leads to two new states in the otherwise large band gap, symmetrically placed about the mid-gap energy (figure 1.4b). The partial delocalisation induced by the polaron is accompanied by a geometric distortion of the conjugated polymer in the vicinity of the charge, whereby the single bonds between the monomeric units (the α-α linkages) shorten and assume a double-bond character. The quinoidal portion between the positive charge and the free electron in figure 1.5 represents the polaron. It has been forecasted from quantum mechanical calculations that polypyrrole must contain a minimum of four monomers in order to achieve the polaron state.

1.2.2 Increased doping

An increase in doping results in the removal of a second electron from the first polaron level (i.e the unpaired electron is removed), and the formation of a bipolaron. In chemical terms the bipolaron is a dicationic spinless state of a system, after oxidation from the neutral state. The two positive charges of a bipolaron are not independent, instead they act as a pair. Its mode of formation is in preference to an alternative route involving the removal of the second electron from another portion of the polymer chain, leading to the formation of a second independent polaron. The preferential formation of a bipolaron instead of two polarons is a consequence of the greater thermodynamic stability of the bipolaron model[31,32] and its requirement of a lower ionisation potential.

At very high doping levels (25 - 30 mol %) the energies of the multitude of bipolaron states elicited may combine to form "bipolaron bands" within the gap.[33] A hypothetical 100 mol % doping level is postulated to result in the merging of the lower and upper bipolaron bands with the valence and conduction bands respectively (figure 1.4d), leading to a decrease in the band gap value to as low as 0.14 eV in polythiophene,[34] and the instigation of quasi-metallic behaviour.

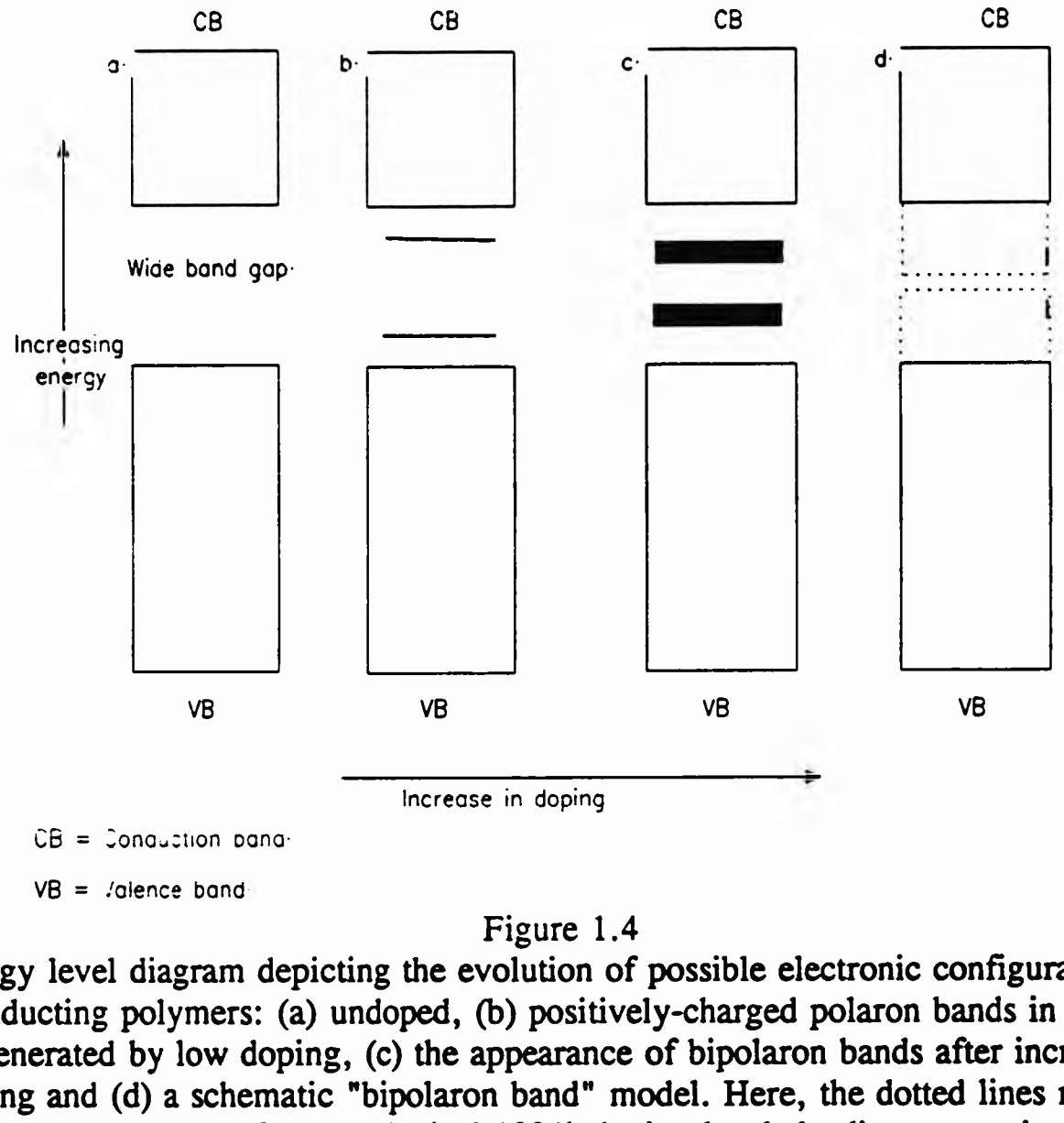

Figure 1.4
Energy level diagram depicting the evolution of possible electronic configurations for conducting polymers: (a) undoped, (b) positively-charged polaron bands in the gap generated by low doping, (c) the appearance of bipolaron bands after increased doping and (d) a schematic "bipolaron band" model. Here, the dotted lines represent the low band gap of a hypothetical 100% doping level, leading to quasi-metallic behaviour.

The conduction model proposed above is applicable to all polymers exhibiting non-degenerate ground states. The unique ground state degeneracy of *trans*-polyacetylene (due to the equivalence of its two possible resonance forms) presents it with a charge-carrier system different from all other conducting polymers. Here, the bipolaron dissociates into two independent charged carriers; known as charged solitons (cations).[35] Various models based on soliton excitation[36,37] have been used to explain the charge-transport phenomena in such polymers.

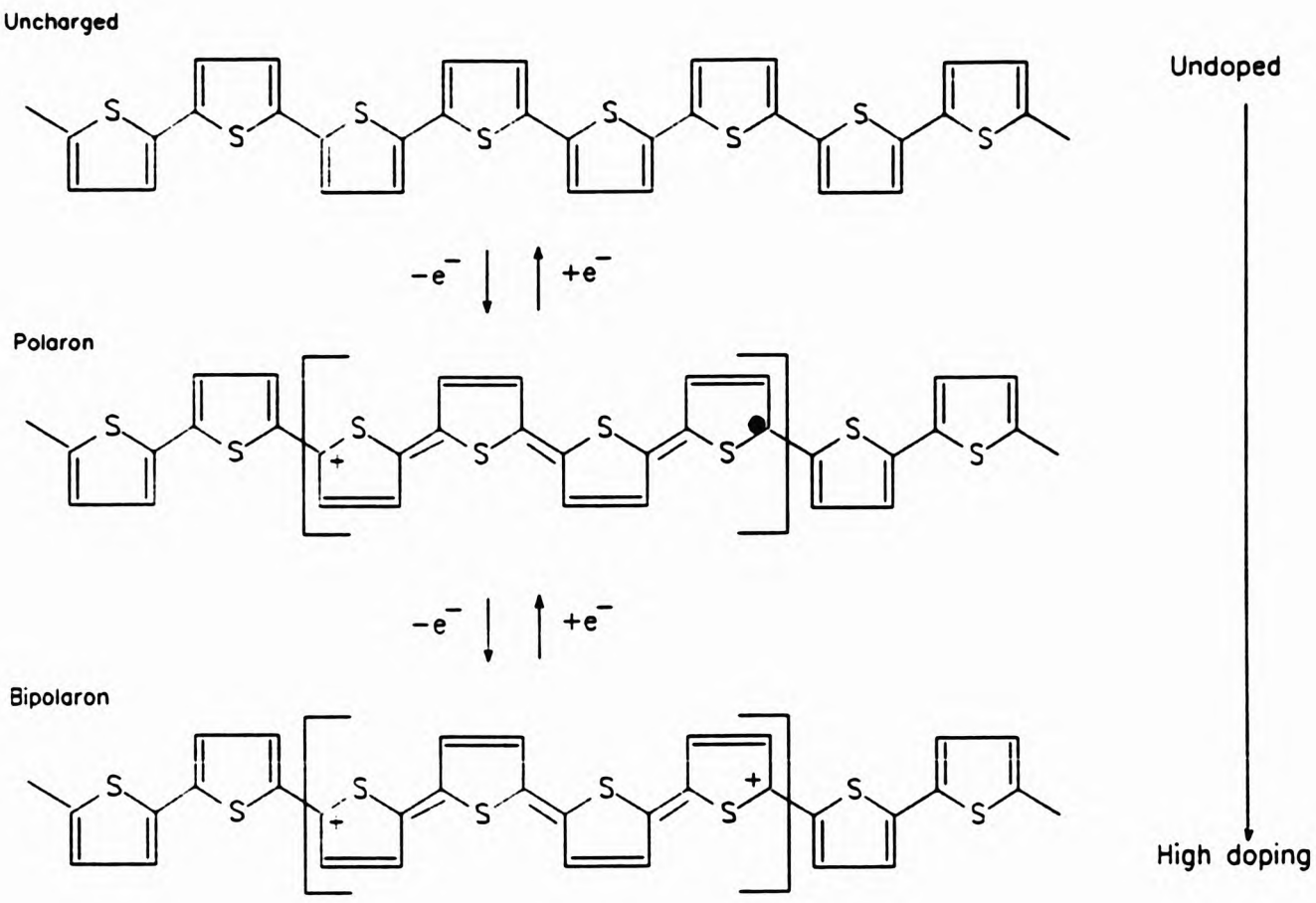

Figure 1.5
A proposed mechanism for the formation of polaron and bipolaron along a polythiophene chain.

1.3 THE TECHNOLOGICAL APPLICATIONS OF INHERENTLY CONDUCTING POLYMERS

The market potential of the physicochemical and electronic properties of conducting polymers; part of a larger class of materials called "synthetic metals"* has resulted in collaborations between research teams from the traditionally independent subject areas of chemistry, physics, electronic device engineering and materials science. Unlike conventional electrical and semi-conductors, the quasi one-dimensional structure of these polymers allows for a 10 - 10,000 fold anisotropic current flow favouring the parallel direction over the perpendicular. The electrochemical syntheses of composites from materials like PVC and polypyrrole have produced films of polymer composites which retain both the mechanical superiority of the host polymer and the high electrical conductivity of the oxidised polymer.[38] On-going research has also resulted in the production of conducting polymers that exhibit specific dc conductivities analogous to that of copper,[39] whilst theoretical predictions indicate optimal conductivity values ranging from two orders of magnitude higher[40] to superconductivity.[41] Practical applications currently undergoing development involve technologies as diverse as power cable shielding,[42] gas[43] and electrochemical[44] sensing, the fabrication of artificial nerves and masking of metal-implant surfaces against blood clotting and rejection,[45] the introduction of biocidal properties in protective surface coatings,[46] the protection of photoelectrode and semiconductor surfaces against photocorrosion,[47] electrochromic displays,[48] electrical energy storage in rechargeable batteries,[49] p-n junction diodes,[50] high-density information storage,[51] a variety of biological applications,[52] and the conversion of solar energy into electricity.[53]

---

*Other materials that fall under this category are charge-transfer complexes and metalo-organic assemblies.

1.4 CONDUCTING POLYTHIOPHENE AND ITS DERIVATIVES

1.4.1 Historical Background and General Properties

Although polymeric materials have been obtained from thiophene derivatives for over forty years,[54] electrochemically-generated and conducting polythiophene was first obtained in 1981 as a result of the anodic electropolymerisation of bithiophene.[55] Over the past few years, thiophene,[21] and a large number of substituted polythiophenes have been synthesised by the electropolymerisation of the appropriate derivatised monomeric unit.

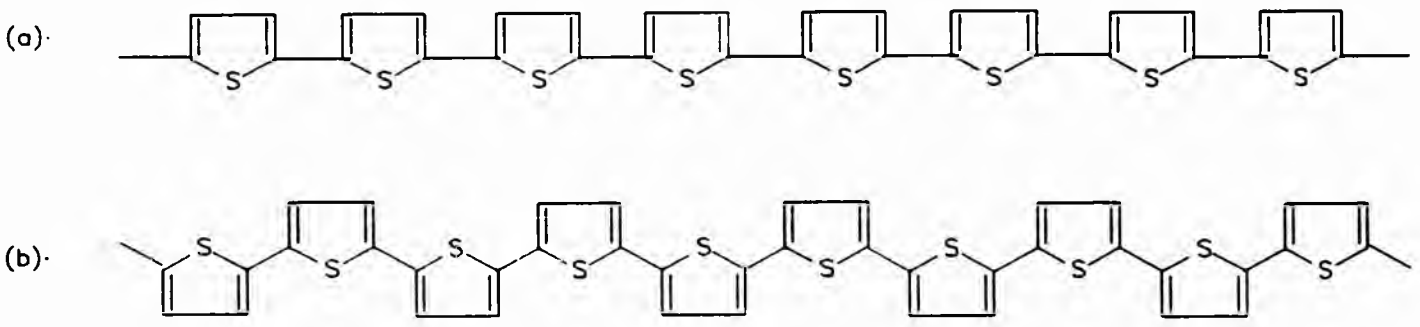

Figure 1.6
The S-*cis* (a) and S-*trans* (b) polythiophene models that can be derived from an ideal ordering of the monomer units. It is assumed that the S-*cis* structure, leading to a helical arrangement,[56] best represents polythiophene.

Derivatisation is normally carried out by substitution of one or both of the β-hydrogens of the thiophene ring with electron donating groups. The oxidation potentials of several substituted thiophenes are presented in figure 1.7. Groups exerting either an inductive or mesomeric effect have been targeted with the aim of producing monomers with low oxidation potentials and stable radical cations. This is postulated to facilitate a swift formation of polymer and may impart improved mechanical properties (for example: adhesion & flexibility), higher environmental stability and increased conductivities. Polymers have been generated from 3,4-disubstituted thiophenes,[56] thiophene dimers,[57,58] trimers,[59] tetramers,[55b] and fused thiophene rings systems.[60,61] Composite polymers have also been generated from the anodic oxidation of mixtures of pyrrole/bithiophene[62] and pyrrole/terthiophene.[63] A variety of 3-alkylsubstituted thiophenes[64] are now known to form stable polymers which are soluble in various organic and inorganic solvents (including water),[65] whilst still maintaining their electrical properties; thus paving way for the development of solution-proccessible conducting polymers and expanding the scope of device applicability. In terms of

stability, comparative studies with polypyrrole have demonstrated the superior chemical and electrochemical stability of both doped and undoped polythiophene-derivatised polymers,[66] which also manifest a reversible doping level higher than those obtained for polypyrrole, polyacetylene or polyparaphenylene.[67]

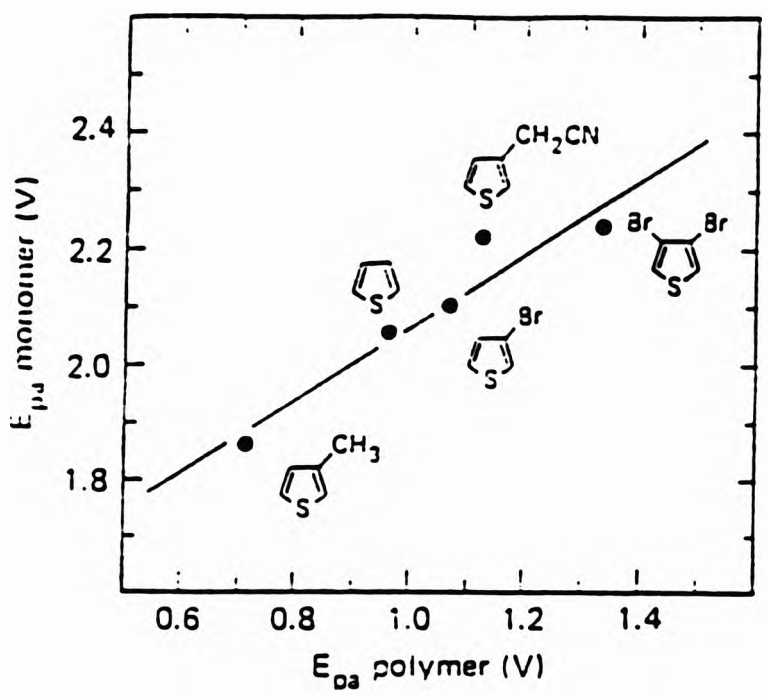

Figure 1.7
Peak oxidation potential of thiophene monomers versus their respective polymers in 0.10 mol dm^{-3} $(CH_3CH_2)_4NBF_4$ / CH_3CN (vs. SCE).[68]

1.4.2 The Electropolymerisation of Thiophene and its derivatives

The mechanism of anodic electropolymerisation of thiophene and its derivatives, which is analogous to that proposed for pyrrole and other heterocycles, proceeds with an electrochemical stoichiometry of 2.07 faraday/mol (i.e. two electrons per molecule) for the film-forming process.[69]

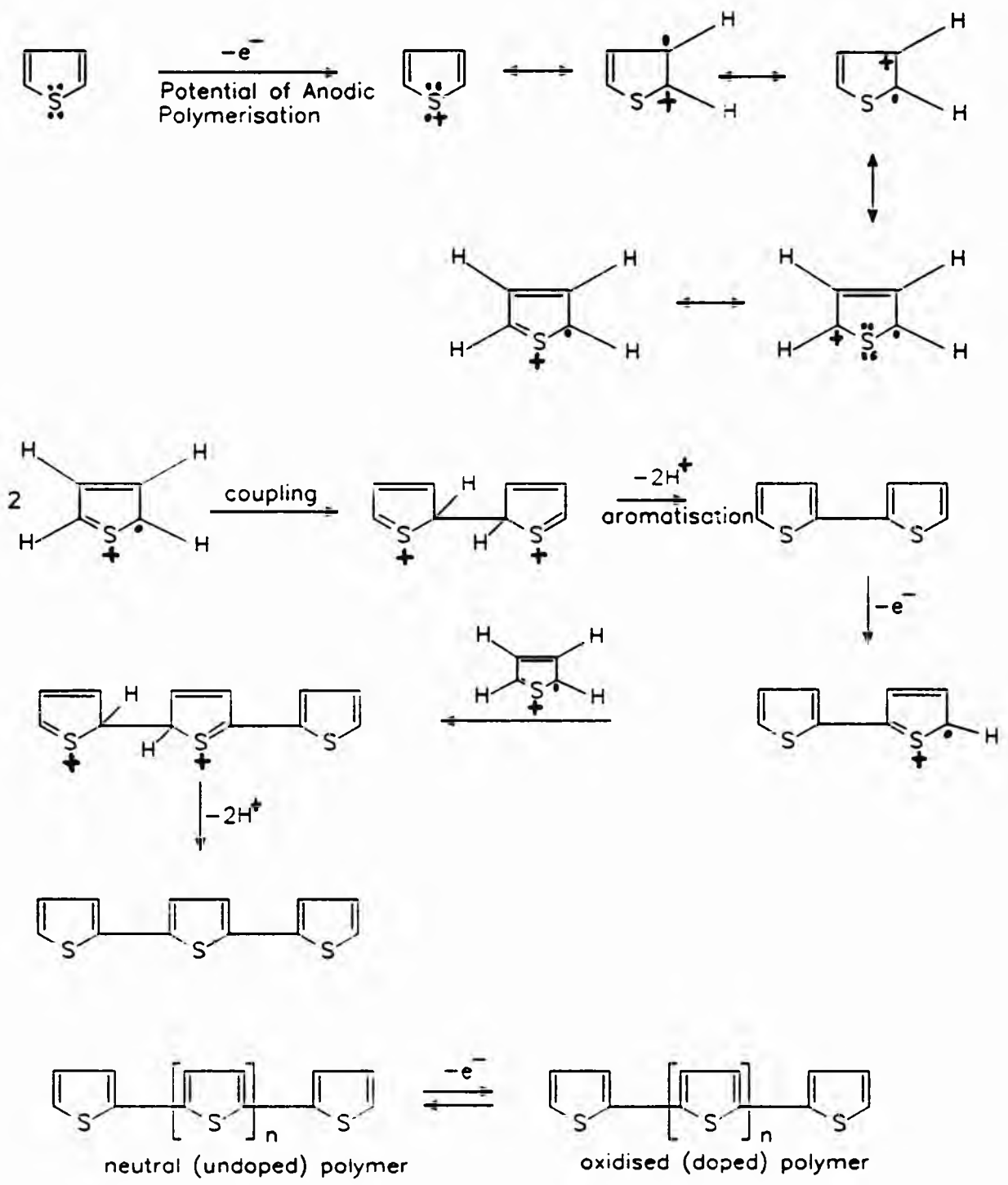

Figure 1.8
Proposed scheme for the electropolymerisation of thiophene.

As depicted in figure 1.8, the first step of this process involves the electrochemical (E) oxidation of monomers (and the oligomers already formed) to their respective radical cations via heterogenous charge transfer. The radical cations generated then undergo

chemical coupling (C) with a monomeric cation, to form a neutral dimer through a process of aromatisation, involving the loss of two protons from a doubly-charged dihydrodimer intermediate.[70] A cascade of successive electrochemical (E) and chemical (C) reactions in an $E(CE)_n$ process culminates in the precipitation of an insoluble polymer upon the electrode surface. The relative stability of the radical cation formed is the essential parameter determining the propensity of a given monomer to polymerise.[68, 71]

Since the electron transfer reaction(s) leading to the generation of the radical cation species is much faster than the diffusion of the monomer from the bulk solution, a very high concentration of radical cations is guaranteed at the electrode surface. Although α-α couplings are favoured theoretically due to a 95 : 5 relative reactivity of the α and β positions of the thiophene moiety[71,72,73] a significant amount of undesirable α-β linkages occur, leading to amorphous polymers that are branched or crosslinked. These undesirable couplings break the conjugation of the polymer and adversely affect conductivity.

The standard oxidation potential of the engendered polymer is lower than that of its corresponding monomer, therefore anodic oxidation always leads to the production of a polymer in its oxidised (p-doped) form. Also, the electropolymerisation of a derivatised thiophene occurs at a lower potential on a polymer-modified electrode than on a bare electrode.[74] The physicochemical properties and conductivities of the engendered polymers are always affected by experimental parameters. These include the types of dopant, solvent,[75] electrolyte, and electrode material used,[76] the oxygen and water content, current density, temperature, and steric constraints imposed by the bulk of the β-thienyl substituent.

1.5 AIM OF THE RESEARCH

This thesis treats the synthesis and characterisation of some novel, β-functionalised thiophene monomers and their respective p-doped, semi-conducting 2,5-thiophenediyl polymers.

PART I

MONOMER SYNTHESES
&
CHARACTERISATION

The work presented in Chapters 2 and 3 was accomplished at the Chemistry department of the University of North London, London.

CHAPTER 2

MONOMER SYNTHESES

2.1 MONOMER DESIGN

The monomers synthesised as precursors for oxidative electropolymerisation were designed to encompass the following material requirements:

- The supression of undesirable α-β linkages in the polymerisation process.
- Stability of the monomer and the polymer.
- A significant delocalisation of π-electrons along the envisaged polymer chain.
- The incorporation of moieties which harness chemical phenomena that could complement the intrinsic electronic and electrochemical properties of the charged conjugated backbone e.g redox centres (ferrocene), fluorescence (pyrene), reactivity (trimethylsilane).

In response to these requirements, the following monomers [1 - 9] were prepared:

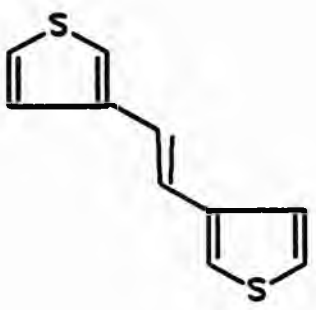

[1]

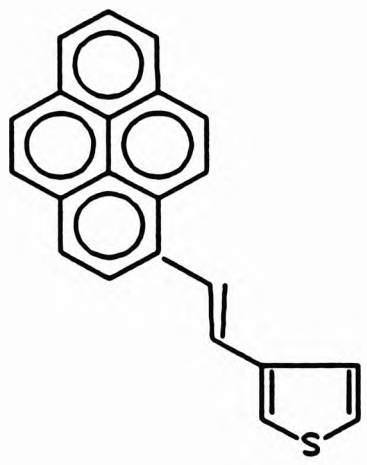

[2]

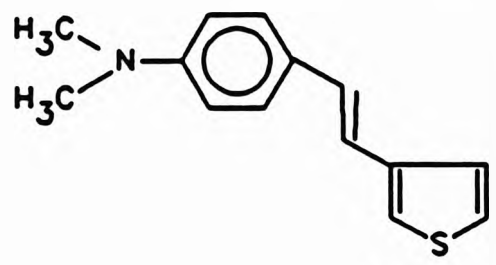

[3]

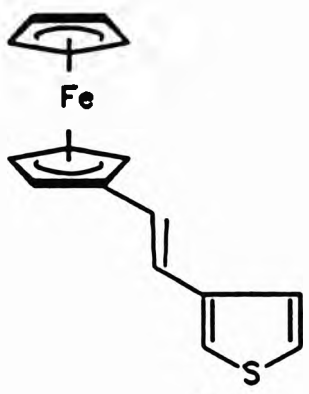

[4]

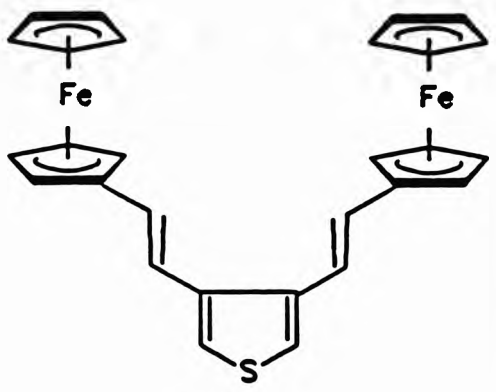

[5]

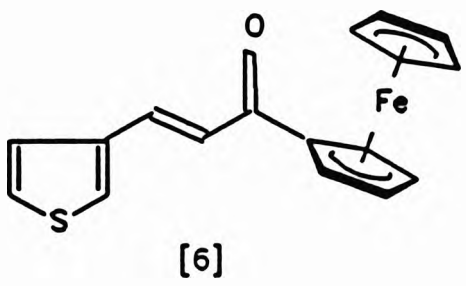

[6]

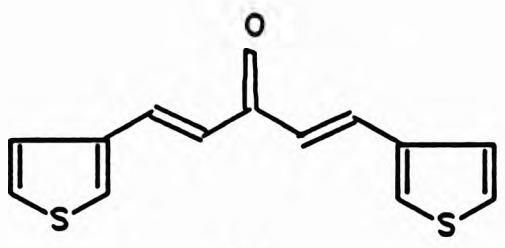

[7]

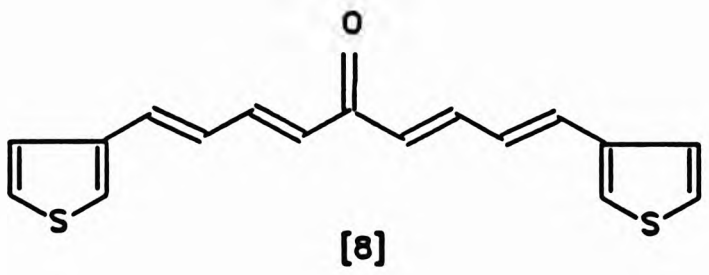

[8]

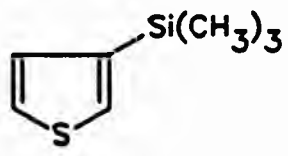

[9]

Figure 2.1
Structures of the synthesised monomers designated for anodic electropolymerisation

2.2 MONOMER SYNTHESES

The initial anticipation that success in the aims of this project would culminate in the large-scale preparation of the monomer(s) concerned prompted a search for synthetic routes that accorded an ease of procedure, cost effectiveness, and optimal yields. The following four synthetic routes satisfied necessary requirements, including the propensity for large-scale reactions.

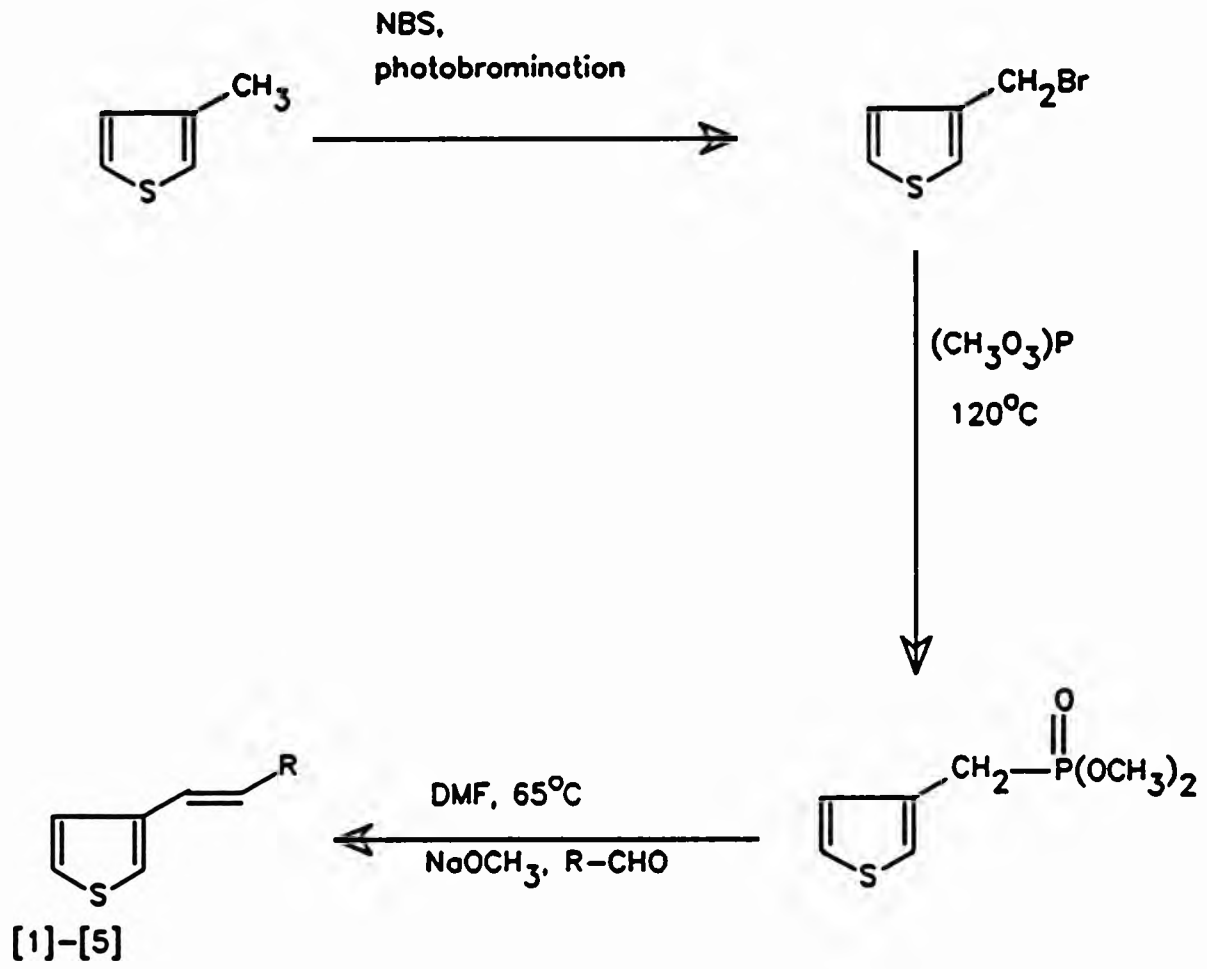

Figure 2.2
Schematic diagram reflecting the synthetic route leading to the generation of the type-1 monomers....

the type-2 monomer;

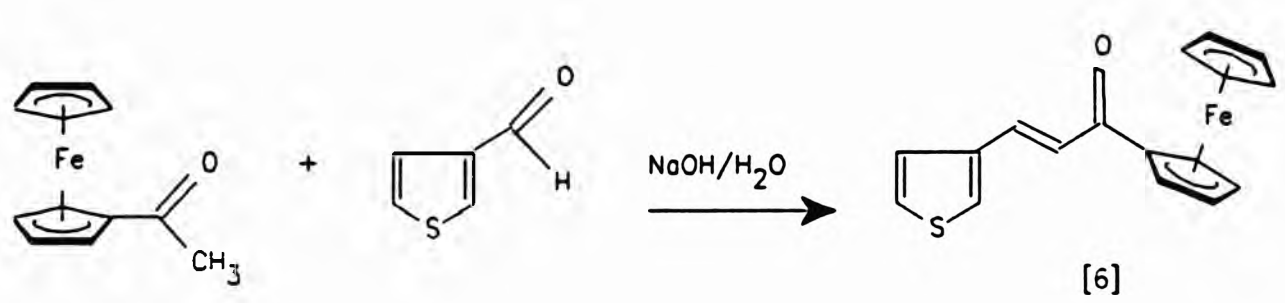

the type-3-monomers;

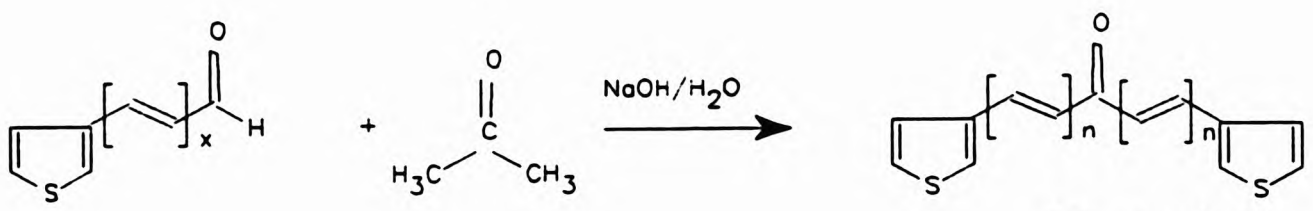

[7] n=1 (x=0)
[8] n=2 (x=1)

and lastly, the type-4 monomer:

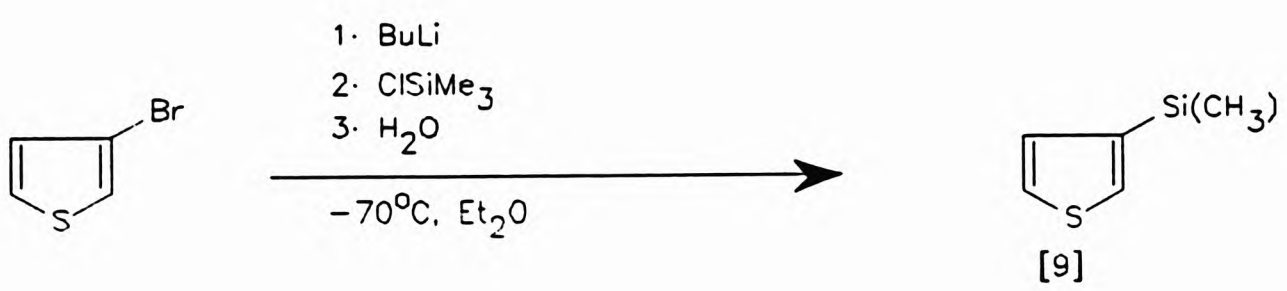

[9]

2.3 DISCUSSION OF MONOMER SYNTHESES

2.3.1 The formation of dimethyl 3-thenyl phosphonate

[10]

The preparation of the phosphonate [10] was achieved by the utilisation of a reaction developed by Arbuzov,[77] but pioneered by Michaelis and Kaehoe.[78] The use of the Michaelis-Arbuzov reaction in the synthesis of a wide array of phosphonates has been reviewed.[79] In this case, it involves the treatment of a tervalent phosphorus alkyl ester with 3-(bromomethyl)thiophene (prepared by the free radical bromination of 3-methylthiophene with N-bromosuccinimide in carbon tetrachloride). This results in the formation of an alkoxyphosphonium salt [11] which, between 110-120°C, undergoes rapid dealkylation with the formation of a highly stable P=O bond via nucleophillic attack of the halide ion, on the saturated α-carbon.

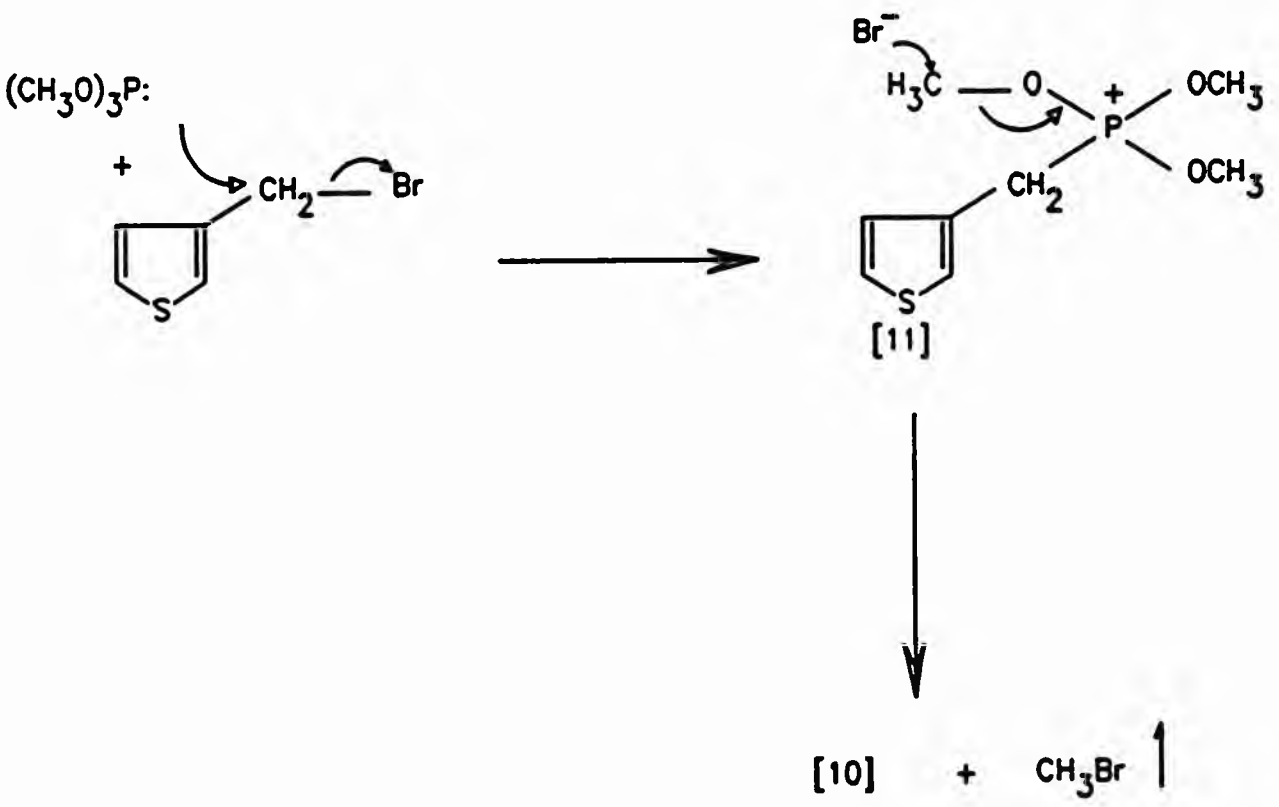

Bromomethane, the by-product formed during the course of the reaction, is readily removed due to its low boiling point. This helps to minimise its competition with the thenylhalide, for the phosphite.

2.3.2 The Horner-Wandsworth-Emmons(HWE) Reaction

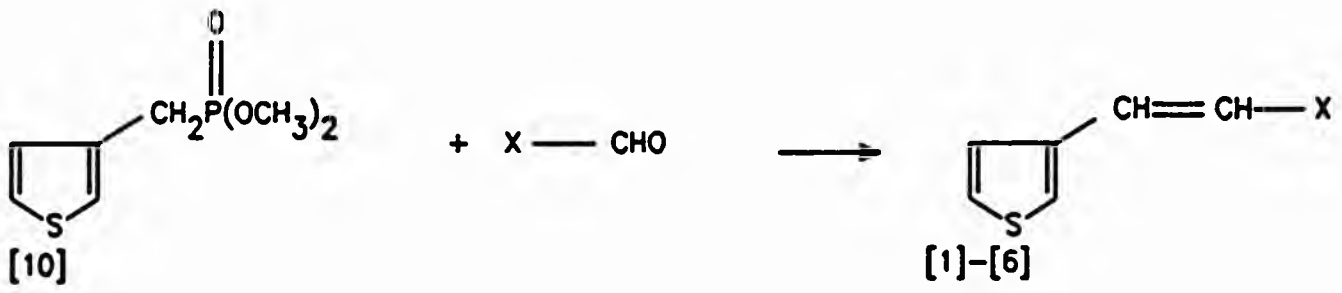

[10] [1]–[6]

Although Horner's group was the first to condense funtionalised phosphonates with aldehydes and ketones to form alkenes,[80] Wadsworth and Emmons showed its versatility.[81] The reaction is restricted to phosphonates bearing α-substituents with a capacity to stabilise a carbanion (e.g. CN, OR, aryl, vinyl). In comparison with their Wittig analogues,[82*] the enhanced reactivity of these phosphonate anions, coupled with the ease of preparation of a wide array of derivatised phosphonates by means of the Arbuzov reaction, the *E*-selectivity of the oxyanion intermediate, and the ease of removal of the phosphate anion formed as a by-product (due to its solubility in water), made it the synthetic proceedure of choice. Several key reviews have documented the scope of use of the Wittig[83] and HWE[84] reactions.

The mechanism for the formation of the ethene linkage is analogous to that of the Wittig reaction involving triarylphosphoranes with aldehydes and ketones.[81,85] Deprotonation of [10] with sodium methoxide leads to the generation of a carbanion [12] that owes its stabilisation to resonance with the conjugated thienyl moiety. The reaction of numerous phosphonate reagents with sodium ethoxide and substituted benzaldehydes has been shown to be first order in aldehyde, ethoxide and phosphonate; with the rate limiting step being the initial condensation of phosphonate with aldehyde.[86] The carbanion formed [12] reversibly condenses with the carbonyl-carbon of the respective aldehydes to form the oxyanion intermediate [13]; which irreversibly decomposes by a process involving oxygen transfer to the phosphorous atom by means of a transient 4-centred oxaphosphetane intermediate [14], to yield the ethenyl functionalised thiophenes [1-5], plus a water-soluble phosphate anion [15].

At room temperature, the syntheses of the thiophenes [1-4] was non-stereospecific and

---

*Attempts to synthesise [1-4] via the Wittig reaction led to a near-equal mixture of geometric isomers in relatively low yields (<30% gross) which were inversely proportional to the bulk of the β-substituent. The *cis*-isomer of [1] underwent transformation to its *trans*- form upon prolonged exposure to sunlight.

led to low yields of a mixture of geometric isomers; comparable to those obtained using the classical Wittig reaction. This reflects a sluggish formation of an equilibrium mixture of the diastereoisomers [13a] & [13b]. However, stirring the reactants at elevated temperatures lead to stereoconvergence and the exclusive formation of trans-products [1-5] in high yield. Presumably, the *threo*-[13a] initially formed is either interconverted at elevated temperatures to the thermodynamically favoured *erythro*-[13b] through a direct cis ⇔ trans isomerisation, or via dissociation to starting material in a retro-HWE reaction reminiscent of that exhibited by *erytho*-β-hydroxyphosphonium salts,[87] and some other betaine intermediates.[88] An excellent summary on the effects of the relative rates of formation, dissociation, and decomposition of oxyanion intermediates on the ratios of stereoisomers formed in the closely-related Wiitg reaction is furnished by House.[89]

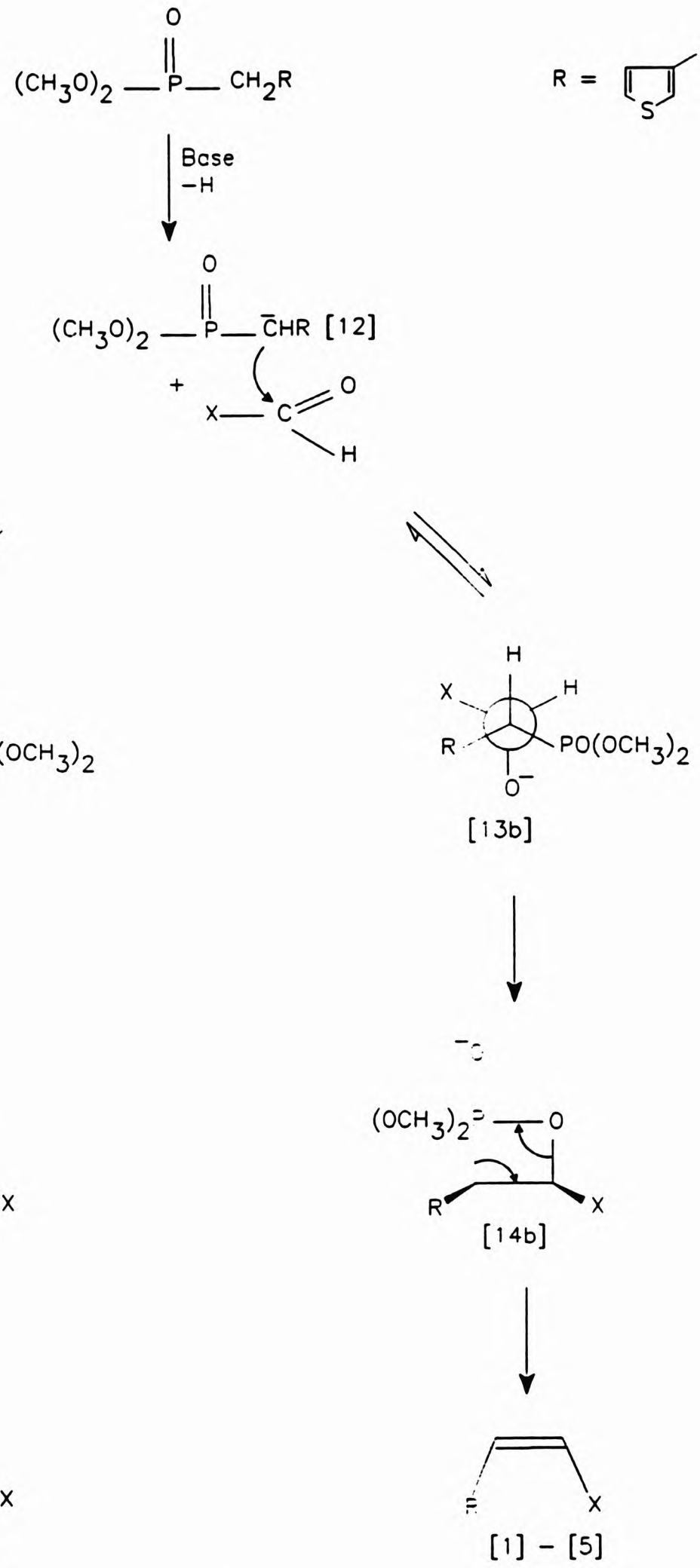
(CH3O)2 — P — CH2R
R =
S
Base
−H
(CH3O)2 — P — ĊHR [12]
+
X — C = O
H
[13a]
[13b]
PO(OCH3)2
[14a]
[14b]
[1] – [5]
[1] – [5]
+
(CH3O)2P = O
O
[15]

2.3.3 The Claisen-Schmidt Reaction

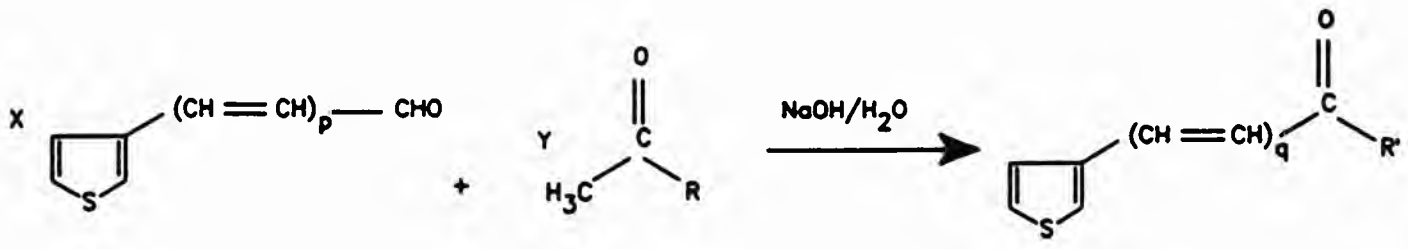

Compound	X	p	Y	R	q	R^1
[6]	1	0	1	Fc	1	Fc
[7]	2	0	1	CH_3	1	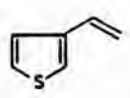
[8]	2	1	1	CH_3	2	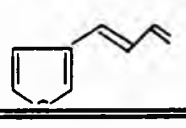 *

Fc = Ferrocene.

1-Ferrocenyl-3-(3'-thienyl)-prop-2-ene-1-one[6], 1,5-bis(3-thienyl)-penta-1,4-dien-3-one [7], and 1,9-bis(3-thienyl)nona-1,3,6,8-tetraen-5-one [8] were prepared with the aid of the Claisen-Schmidt reaction. This is essentially a base-catalysed, crossed-aldol condensation reaction leading to the formation of an α,β-unsaturated ketone whose carbonyl function is *trans* to the larger substituent on the β-carbon atom.[90,91] The first step in the mechanism of this reaction involves the abstraction of a proton from the α-carbon of the slowly-added methyl ketone, by the hydroxide ion. The carbanion formed [16] attacks the carbonyl carbon of the aromatic aldehyde in a rate limiting nucleophilic addition reaction to generate the anion [17]. Orientation of the spontaneous elimination of water from the β-hydroxyketone [18] is driven by the stability of a *trans* configuration about the ethylenic linkage.

---

*_trans_-3-(3-thienyl)acrolein was prepared by a crossed-aldol condensation reaction involving 3-thiophene carboxaldehyde and acetaldehyde. Further details are in the experimental section (chapter 8).

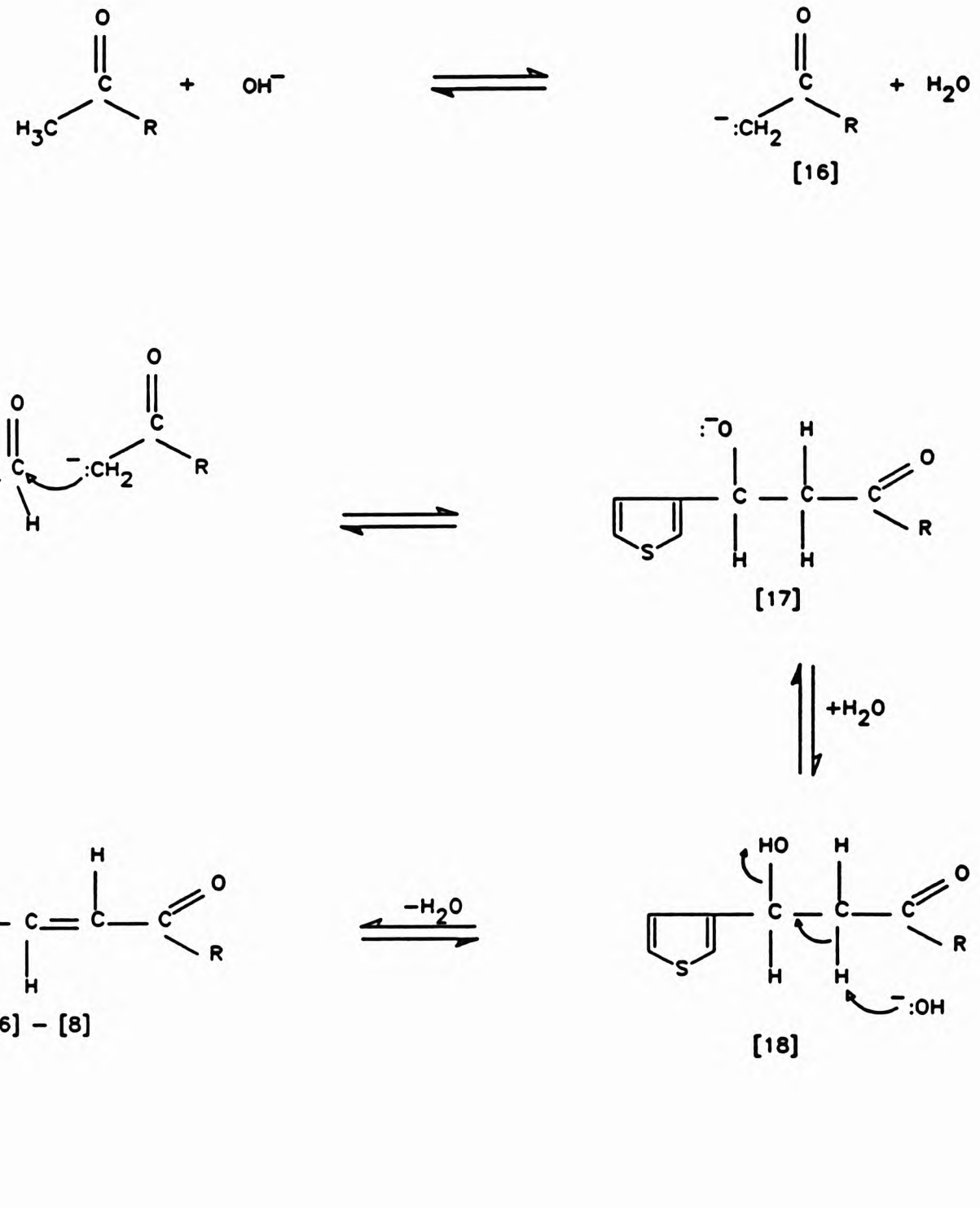
O
C
H3C
R
+
OH⁻
O
C
⁻:CH2
R
+ H2O
[16]
O
O
C
⁻:CH2
R
H
S
:⁻O
H
O
C
C
C
R
H
H
S
[17]
+H2O
H
O
C
C
C
R
H
S
[6] - [8]
-H2O
HO
H
O
C
C
C
R
H
H
S
⁻:OH
[18]

2.3.4 The Syntheses of 3-(trimethylsilyl)thiophene

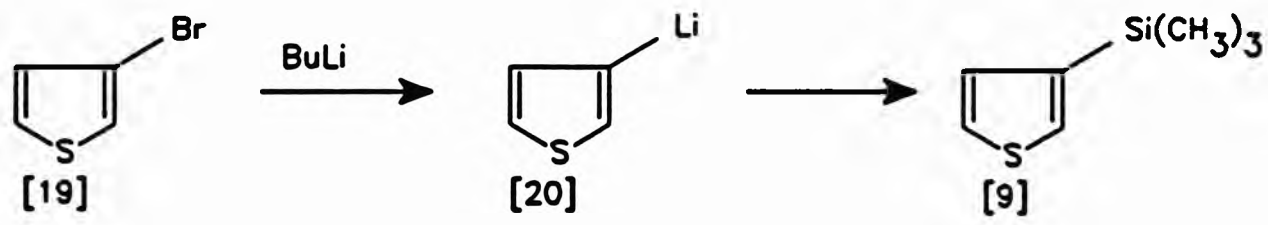

3-(Trimethylsilyl)thiophene [9] was prepared via the use of 3-thienyllithium [20]; generated by the halogen-metal exchange of 3-bromothiophene [19] as described by Gronowitz.[92] The selectivity of lithium for the 3-position is due to the higher relative acidity of the Br atom in comparison to the α-hydrogens normally involved in the metalation of thiophene. The polarity of the metal-carbon bond formed in [20] imparts a high electron density on carbon. This accounts for its strong nucleophilic character and the ease of silylation upon addition of a molar equivalent of etheral trimethylsilyl chloride.

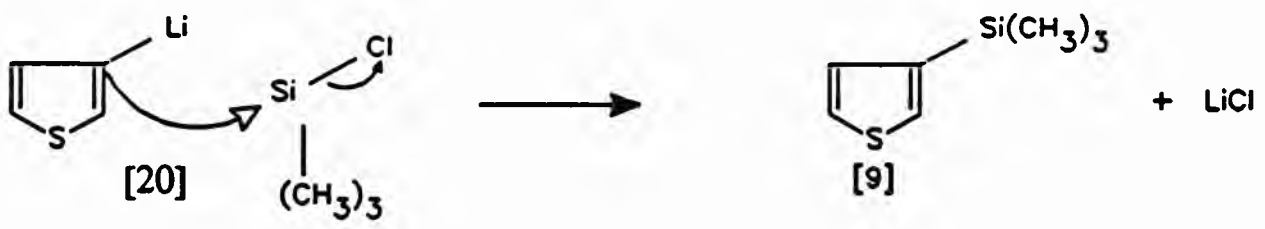

CHAPTER 3

SPECTROSCOPIC STUDIES

3.1 INFRA-RED TRANSMISSION SPECTROSCOPY[93,94]

The earliest IR study of thiophene was conducted by Coblentz.[95] Since then, several reports regarding the IR study of thiophene, including its mono- and disubstituted derivatives, have been published.[96] Amongst these reports was the definitive characterisation of thiophene and all its deuterated derivatives (except 2,4 dideuteriothiophene)[97] which culminated in the development of a complete set of harmonic symmetry force constants for thiophene and later, tetradeuteriothiophene.[98] The results discussed below are based on the homologous assignments of 3-substituted thiophenes,[99] benzeneoid systems,[100] ferrocene,[101] and deuterated thiophenes.

3.1.1 Results and discussion

[I]. <u>The 3000 cm^{-1} region</u>

The C-H str. mode of the parent thiophene molecule absorbs between 3000 & 3100 cm^{-1} and at slightly shorter wavelengths than benzeniod systems. In comparing the spectra of *trans*-1-(ferrocenyl)-2-(3´-thienyl)ethene [4] (figure 3.1.4) and 1-(ferroceny)l-3-(3´-thienyl)-prop-2-en-1-one [6] (figure 3.1.6) within this region, it is apparent that the intensity of this mode is dependent on the pendant substituent, as the introduction of an electron withdrawing moiety led to a diminished absorption. The C-H str. vibration of the methyl group of [3] could be observed as multiple bands between 2900 - 2800 cm^{-1} (figure 3.1.3).

[II] <u>The 1600 cm^{-1} region</u>

The series of weak bands displayed by [1] between 1875 and 1576 cm^{-1} are as a result of overtones and combination bands of the out-of-plane(o.o.p) C-H def. vibrations (figure 3.1.1). With the conjugation of the ring with the electron-accepting C=O function, all absorptions corresponding to the ring C=C skeletal fundamentals are intensified. Thus, the α,β-unsaturated ketone [6] exhibited enhanced absorptions at 1452 and 1377 cm^{-1} respectively (figure 3.1.6), in comparison with its *trans*-disubstituted ethylene analogue [4] (figure 3.1.4).

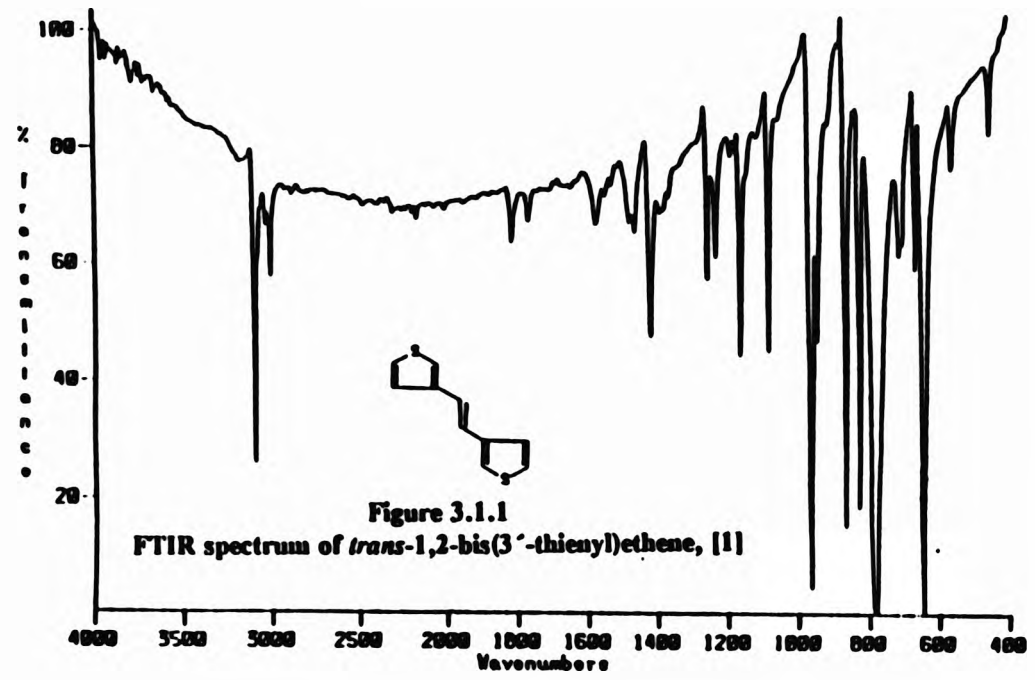

Figure 3.1.1
FTIR spectrum of *trans*-1,2-bis(3´-thienyl)ethene, [1]

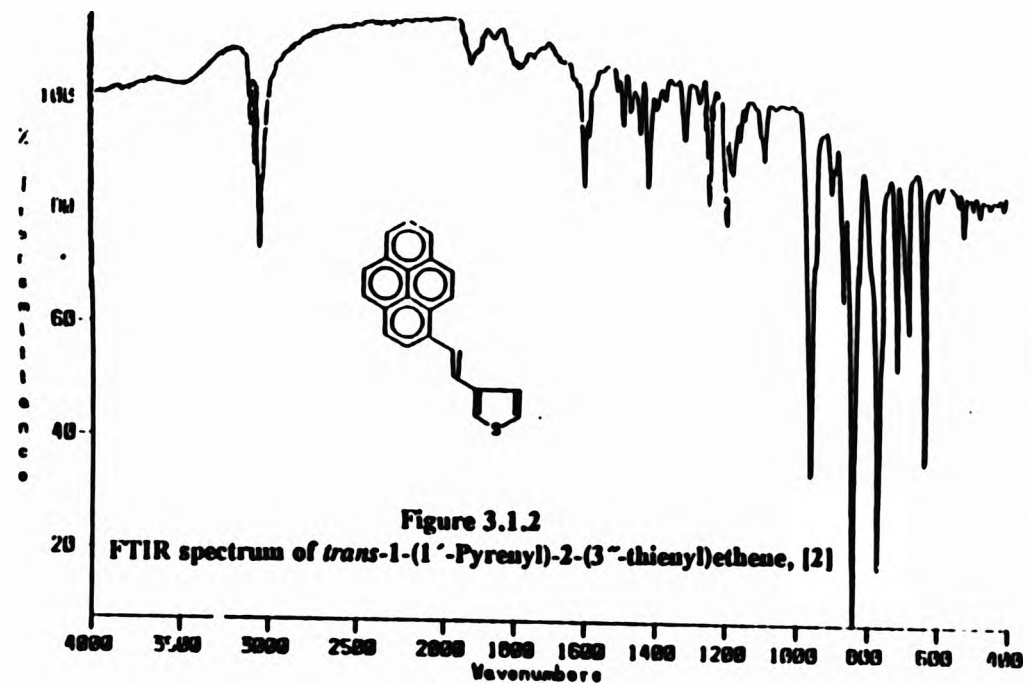

Figure 3.1.2
FTIR spectrum of *trans*-1-(1´-Pyrenyl)-2-(3´´-thienyl)ethene, [2]

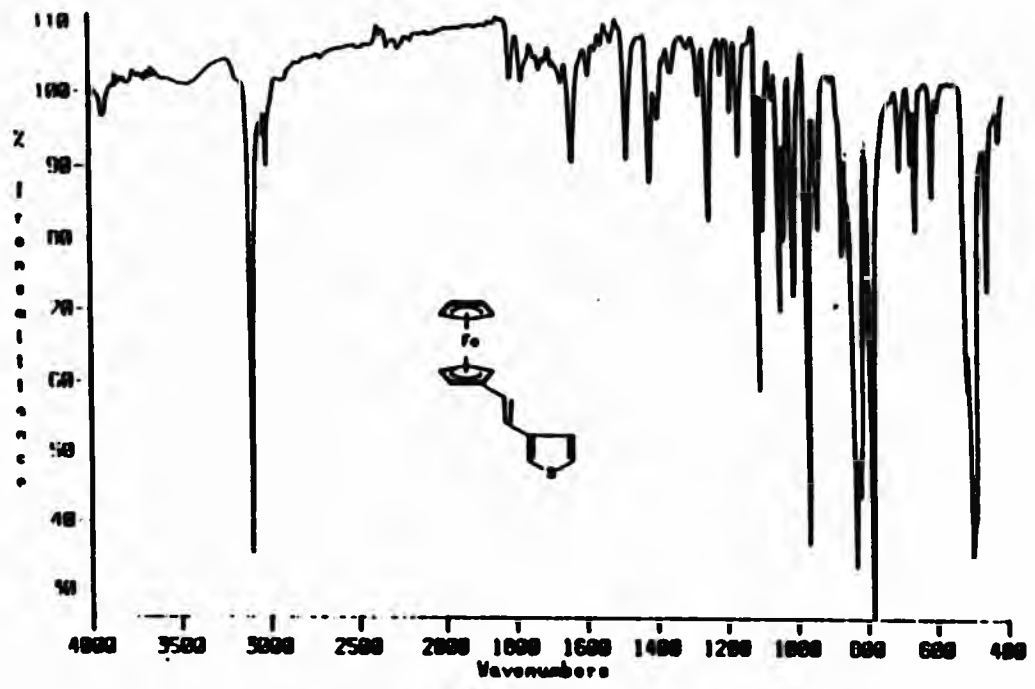

Figure 3.1.4
FTIR spectrum of *trans*-1-(Ferrocenyl)-2-(3´-thienyl)ethene, [4]

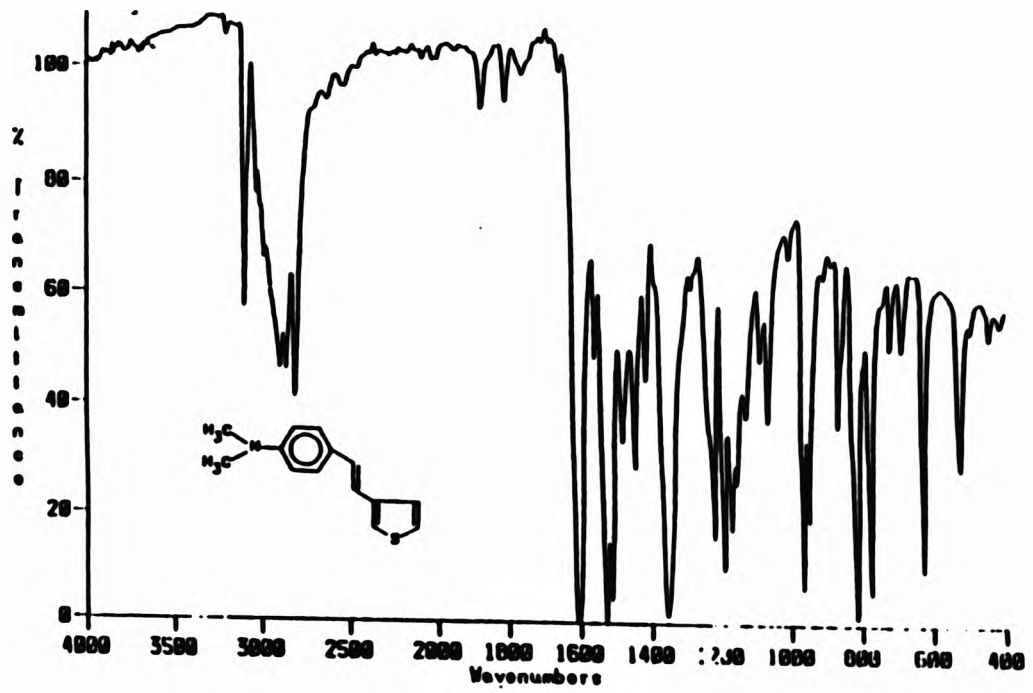

Figure 3.1.3
FTIR spectrum of *trans*-1-(p-N,N-Dimethylaminophenyl)-2-(3´-thienyl)ethene, [3]

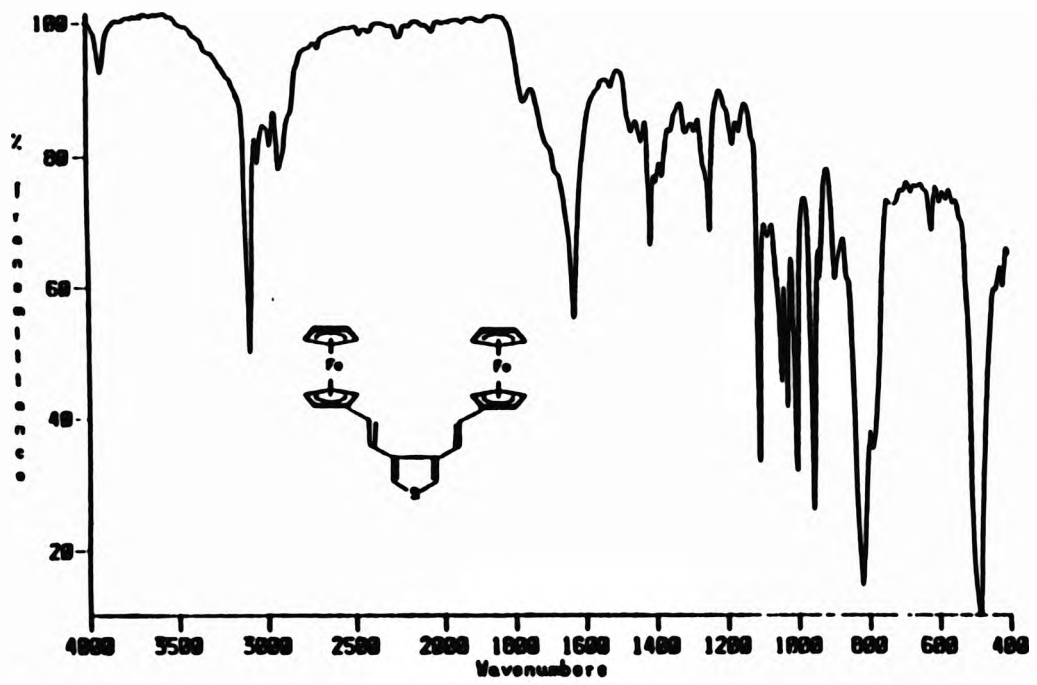

Figure 3.1.5

FTIR spectrum of (*E,E*)-3,4 *Bis*-(2´-ethenylferrocenyl)thiophene, [5]

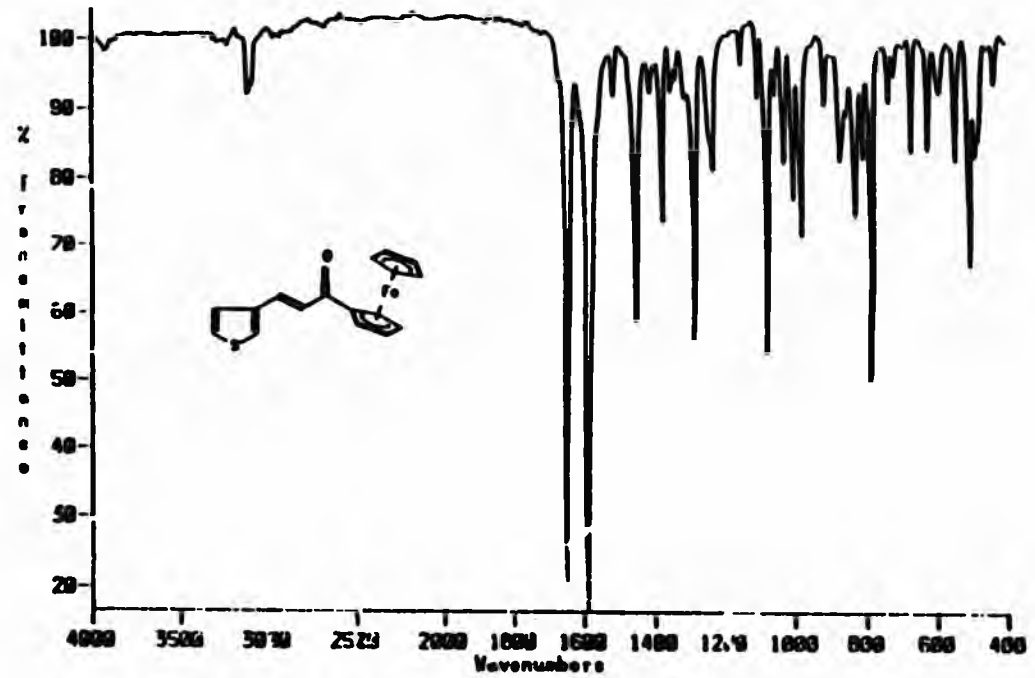

Figure 3.1.6

FTIR spectrum of 1-(Ferrocenyl)-3-(3´-thienyl)prop-2-en-1-one, [6]

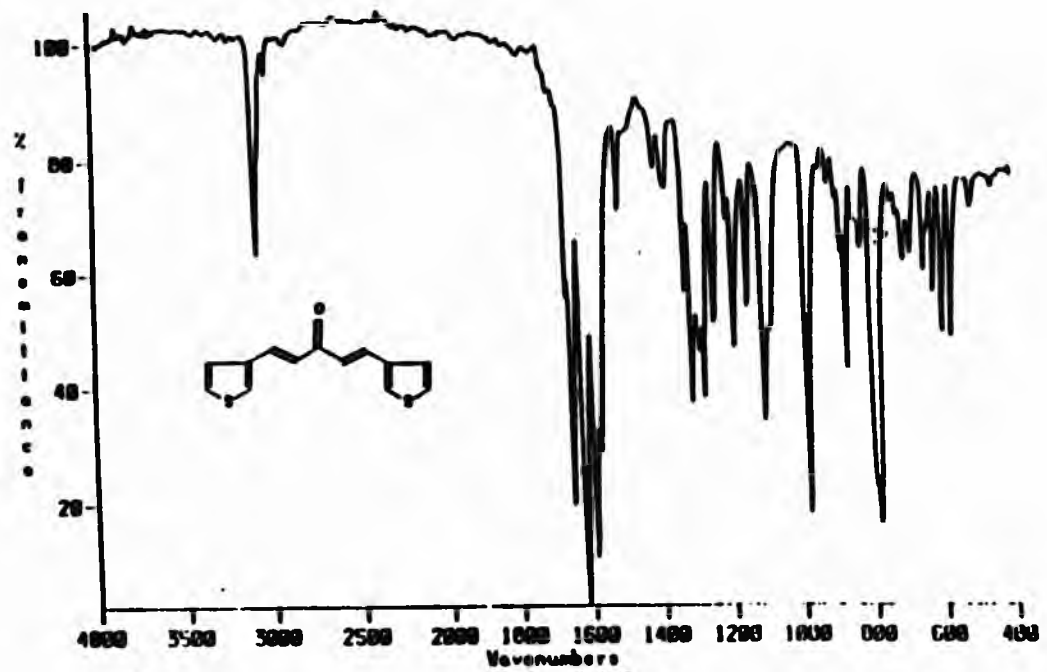

Figure 3.1.7

FTIR spectrum of (*E,E*)-1,5-*Bis*(3´-thienyl)penta-1,4-dien-3-one, [7]

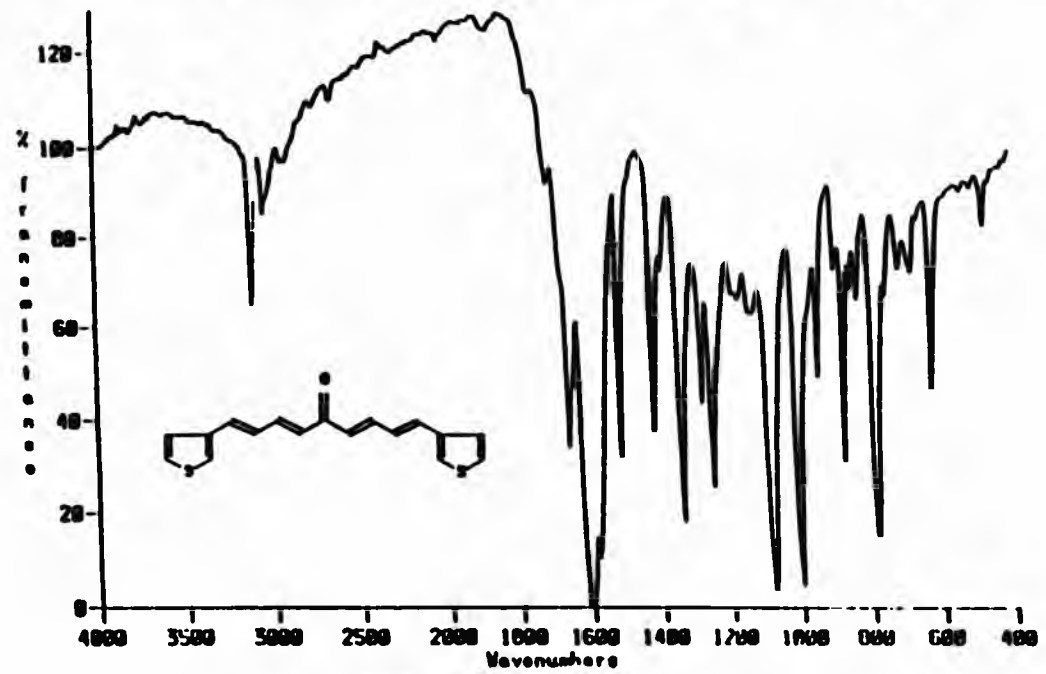

Figure 3.1.8

FTIR spectrum of 1,9-*Bis*(3´-thienyl)nona-1,3,6,8-tetraen-5-one, [8]

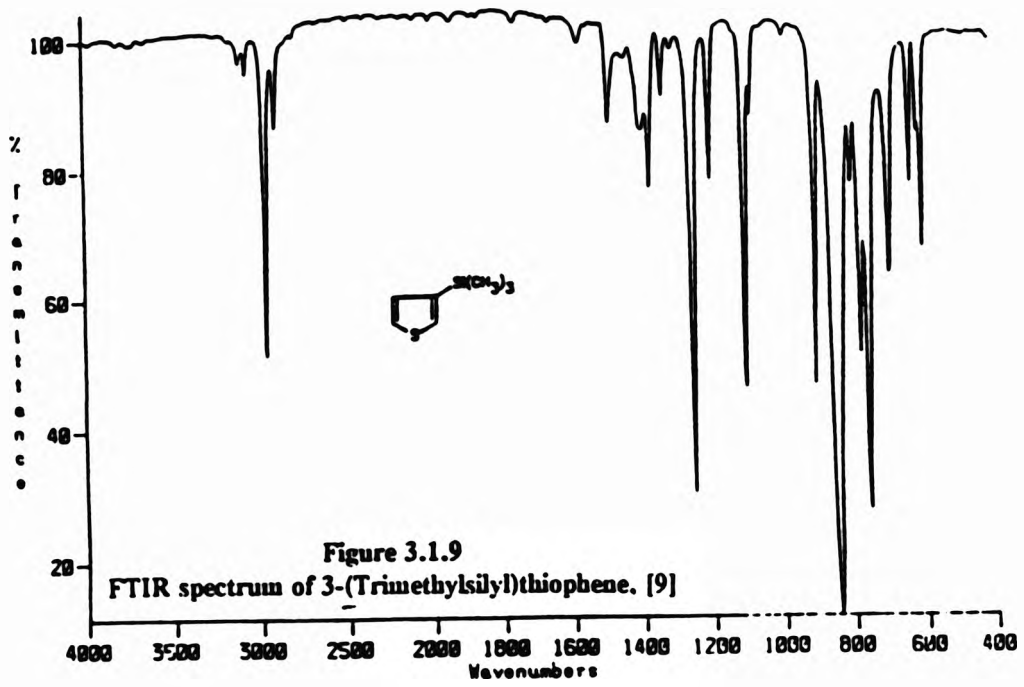

Figure 3.1.9
FTIR spectrum of 3-(Trimethylsilyl)thiophene. [9]

[III] The C=O moiety

The dramatic shift of the ν(C=O) fundamental to longer wavelengths demonstrates the effective conjugation of this functional group with the ring. This is also indicative of the single-bond character of the C=O bond and (as observed in the NMR spectra of [7] & [8]) of the rings' electron releasing ability.

It has been suggested that a "push-pull" effect of the type depicted below (see box) is responsible for the observation of a more intense absorption for the ν(C=C) mode in relation to that of a ν(C=O) mode.[102] This is in addition to the observation that the intensity of the ν(C=O) mode decreased with an increase in the number of conjugated ethylenic linkages. Also, the multiplicity of bands found within the 1600 cm^{-1} region in the spectra of [7] (figure 3.1.7) & [8] (figure 3.1.8) implicates both the C=C and C=O groups as manifesting multiple absorptions. Multiple absorptions accorded to the carbonyl group could be due to the operation of Fermi resonance; which has been implicated in the multiple bands observed in substituted thiophene carboxaldehydes,[103,104] alkyl thiophene carboxylates,[105] and some chalcone analogues of thiophene.[106]

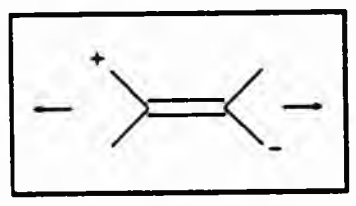

[IV] In-plane vibrations

All the compounds studied displayed a series of bands between 1277 and 1061 cm^{-1} assigned to in-plane C-H deformation and "ring breathing" modes. There was also an overall similarity in the positions of bands that are accorded to those compounds which have parallel functionalities. The ethylenic β(C-H) mode was observed between 1415 $\pm$ 6 cm^{-1} in applicable compounds, while the monosubstituted ferrocenyl pendants of [4] - [6] displayed three intense characteristic bands at 1043, 1028, and 1000 cm^{-1}; attributed to the β(C-H) mode of the cyclopentadieneyl moiety.

[V] Out-of-plane (o.o.p.) vibrations

Absorptions accorded to the monosubstituted thienyl parent ring could be interpreted in terms of a C_s symmetry; whereby all its vibrational modes are IR and Raman active, and the IR spectra gives rise to strong o.o.p. absorptions.[107] Disubstituted thiophenes however exhibit a C_{2v} symmetry; whence all the o.o.p. C-H def. fundamentals of the A_2-symmetry type are forbidden in the IR. This accounts for the reduced number of absorption bands attributable to the ν(C-H) mode of the thiopene moiety of [5] (figure 3.1.5), and has been of particular help in the characterisation of the o.o.p. absorbances displayed by the other monomers.

The increase in the number of out-of-plane C-H deformation vibrations in polycyclic benzenoid, benzenoid, and heteroaromatic compounds is proportional to the number of adjacent hydrogens present,[100a,108] thus [2] and [4] exhibit more absorptions relating to this vibrational mode than the rest of the monomers. The Si-CH_3 rocking mode appears in the same range as one of the rocking modes of the parent thiophene moiety (835 cm^{-1}), and their absorptions overlap to form one sharp and very strong band (figure 3.1.9). Also, compound [3] depicts a strong and broad absorption band at 813 cm^{-1} characteristic of a 1,4-disubstituted benzene ring, while the monosubstituted cyclopentadienyl moieties exhibit their characteristic absorpton for this vibrational mode at 816 cm^{-1}.

A strong band exhibited by all monomers at 776 $\pm$ 10 cm^{-1} is indicative of β-substitution of the thiophene ring,[109] while the absorption at 964 cm^{-1} confirms the *trans*- stereochemistry of the ethylenic linkage.

[VI] The presence of a C-X mode?

A distinctive and intense low-frequency vibration whose position and intensity varied with a change of substituent, was observed in all compounds except in those that contain a ketone group. This vibration is speculatively assigned to a substituent-sensitive ring stretch (C-X) mode. A comparison of the FTIR spectra of [4] and its disubstituted counterpart [5] reveals a difference in the band pattern of this mode, seen between 400 and 500 cm^{-1}. The frequency-shift and enhanced absorbance of this vibration in [5] leads to the assumption that it is sensitive to both substituent orientation and molecular weight respectively. The absence of this band in compounds [6] - [8], which harness carbonyl functionalities, also suggests its dependency on the effective electron density, as it is probable that the absorbance in these compounds have been moved to longer wavelengths ($< 400\ cm^{-1}$) due to the deshielding of the thiophene ring by the carbonyl oxygen.

3.2 ELECTRON-IMPACT MASS SPECTROSCOPY

The major fragments formed in the electron-impact (EI) mass-spectrometry of thoiphene at 70eV are $C_2H_2S^+$ [*m/z* 58]; $C_3H_3^+$ [*m/z* 39]; CHS^+ [*m/z* 45]; CH_3S^+ [*m/z* 69]; and $C_4H_3S^+$ [*m/z* 83].[110] The relative abundances of these ions in compounds [1] - [8] are summarised overleaf in Table 3.2.1.

Compound	Mol. wt.	Molecular ions expressed as percentages of the base peak										
		$[M^+ + 1]$	$[M^+ + 2]$	$[M^+]$	$[M^+ - 1]$	$[M^+ - 2]$	$[M^+ - CHS]$	*m/z* 97	*m/z* 65	*m/z* 58	*m/z* 45	*m/z* 39
[1]	192	40	11	61	100	26	64	3	3	8	34	15
[2]	310	-	0.40	100	34	22	0.70	-	-	0.20	4	0.90
[3]	229	17	3	100	50	-	21	0.20	5	0.30	7	5
[4]	294	-	-	100	5	19	-	0.30	0.70	0.10	9	7
[5]	504	-	-	100	-	7	-	3	2	0.30	7	11
[6]	322	-	-	100	-	9	-	0.40	8	0.60	7	10
[7]	246	11	5.30	51	13	2	39	40	55	8	39	45
[8]	298	-	-	38	-	-	1	62	43	16	100	72
[10]	206	2	1	22	0.70	-	0.10	100	0.80	1.30	23	5

Table 3. 2.1
The relatve intensities of some of the principal ions in the electron-impact mass spectra of the synthesised compounds [1] - [8].

3.2.1 Results and Discussion

[I] General Observations

The parent molecular ion was of at least 50% intensity for all compounds except for [7]. It also constituted the base peak in compounds [2] - [6]. The base peak of the intermediate phosphonate [10] is attributed to β-sidechain cleavage followed by ring enlargement of the thenyl cation to form the thiopyrilium ion [21]. This mode of cleavage is typical of α- and β-alkylthiophenes and constitutes their base peak in most cases.[111]

Although no trans(3-thienyl)ethylene residue appears to have been examined by electron impact mass-spectrometry, its conjugation with an aromatic substituent (as in compounds [1] - [6]) resulted in the loss of two protons from the molecular ion in a fashion analogous to that of stilbene and its 4,4´-disubstitued derivatives.[112] Compounds [1] - [6] exhibited both $[M^+ - 1]$ and $[M^+ - 2]$ peaks, from both a stepwise loss of 2(H) and a molecular loss of H_2 (as evidenced by the presence of metastable ions for this process in [2], [4], and [6]), and which leads to the formation of an aromatised rearrangement entity in a manner akin to that proposed for compound [1] in figure 3.2.1.

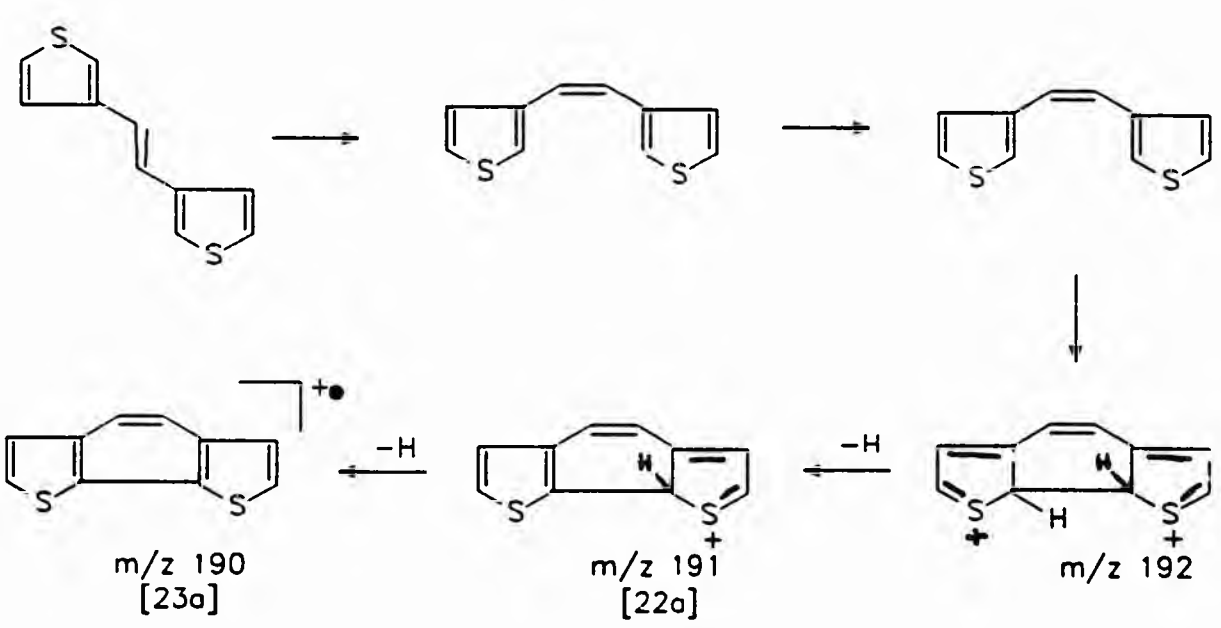

Figure 3.2.1
The proposed fragmentation route leading to the generation of the $[M^+ - 2]$ radical cation.

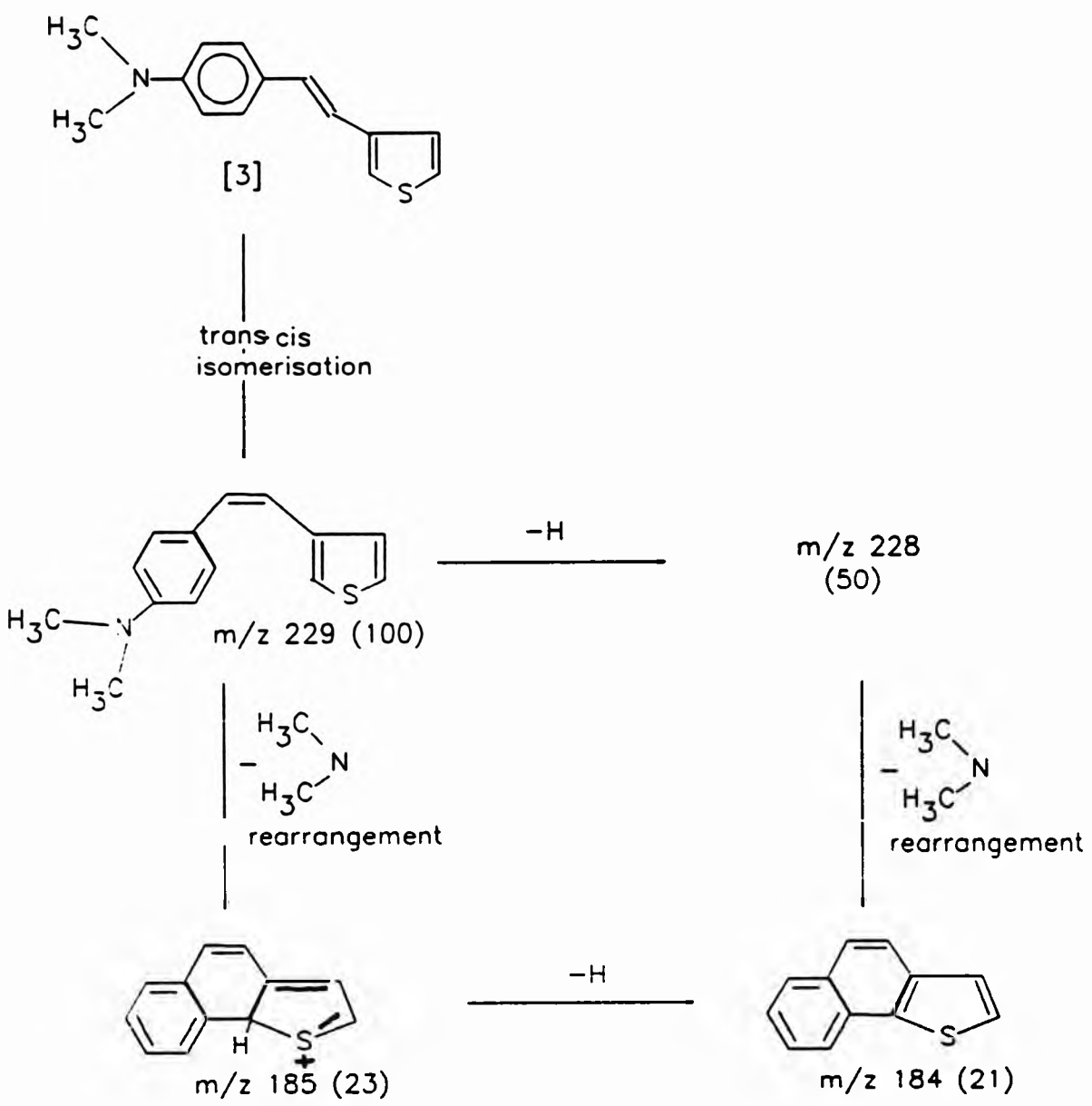

Figure 3.2.2
Schematic diagram illustrating the proposed fragmentation route leading to the formation of the cyclised radical cation (*m/z* 184). The relative intensities of the daughter ions are in brackets ().

It is plausible to infer that the *trans* → *cis* isomerisation that occurs prior to the formation of this aromatised entity [23a] is preceded by the randomisation of all carbon and hydrogen atoms. This is because randomisation, leading to complex skeletal rearrangements, frequently occurs during the electron-impact ionisation of heterocyclic compounds,[113] the pyrolysis of some substituted stilbenes and thiophenes,[114] or their irradiation with UV light.[112,115] In view of this, the intensity of an [M^+ - 2] process could reflect the ease with which the synthesised compounds undergo structural reorganisation in order to attain the geometry required to achieve a *cis* → *trans* isomerisation upon randomisation, and this is a view substantiated by the lack of this process in [8] which does not have the ability to attain the geometry that favours this phenomenon.

Compound [3], which does not have the $[M^+ - 2]$ peak, is proposed to undergo *trans* → *cis* isomerisation and subsequent molecular contraction not by the loss of two protons, but by the competitive expulsion of an α-proton (from the 2-position of the thiophene ring) and the dimethylamino group from the aniline moiety (figure 3.2.2). The preferential cleavage of the C-N bond to the loss of a proton from the benzene ring is due to the lower ionisation energy of the former.

[II] Specific Observations

[A] *trans*-1,2-Bis(3´-thienyl)ethene, [1]

The overall mass-spectrum of compound [1] bears a similarity to the fragementation patterns of the bithienyls and of 2,2´dithienylethylene,[116] the striking and most important difference being that while the latter compound shows its parent ion as its base peak, compound [1] depicts the $[M^+ - 1]$ fragment (*m/z* 191) as its most abundant ion (table 3.2.1). This discrepancy in base peaks cannot be divorced from the configurational propensity of compound [1] to undergo an $[M^+ - 2]$ process leading to the formation of [23a] (due to the availability of the labile α-protons of the 2-position of the respective thiophene units), and via an $[M^+ - 1]$ isomer [22a].

In addition to this, there were losses of S, CHS^+ (*m/z* 45), CS^+, H_2S^+, CH_3S^+, SH^+, $C_2H_2^+$, and $C_3H_3^+$ from both of the thiophene rings. These explusions are indicative of complex rearrangements. Studies of deuterium labelled thiophenes have revealed that carbon scrambling is the predominating randomisation process during losses of CHS^+ and $C_3H_3^+$, whilst hydrogen scrambling is the most important randomisation process in the loss of $C_2H_2^+$.[117] Two intense daughter ions formed from such losses are ascribed the structures of benzo[b]thiophene [25] and benzocyclobutadiene [26] radical cations respectively, as their further fragmentation is analogous to those of these compounds.[118]

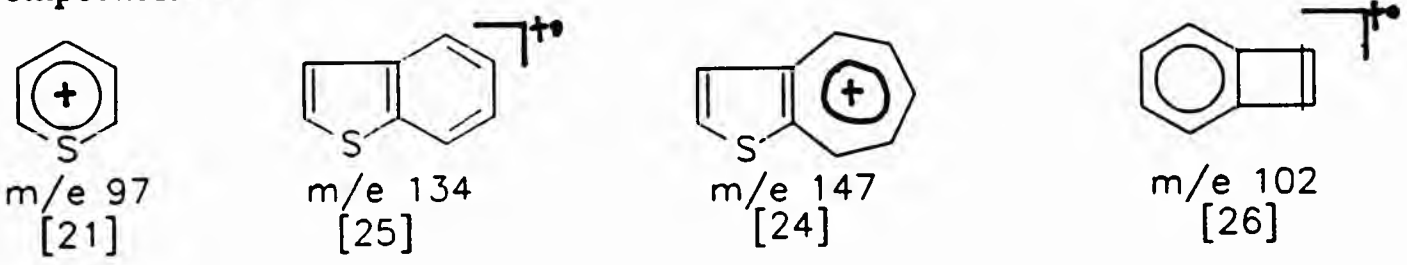

The generation of daughter ion *m/z* 147 in 64% intensity represents one out of four competing $[M^+ - CHS]$ processes (figure 3.2.3). This ion is proposed to have the same structure as [24]; the $[M^+ - 1]$ ion in 5- and 7-methylbenzo[b]thiophenes.[118a]

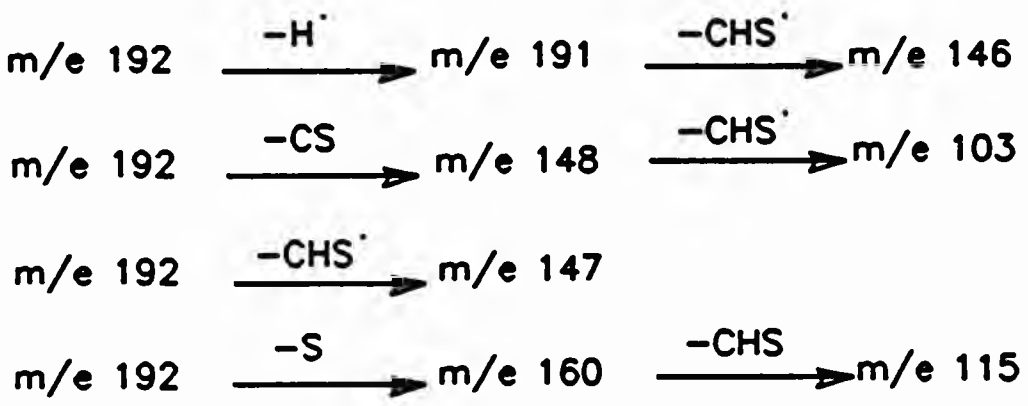

Figure 3.2.3
Competing [M^+ - CHS] processes attributed to the electron-impact ionisation of compound [1].

[B] *trans*-1-(1´-Pyrenyl)-2-(3˝-thienyl)ethene, [2]

The fragmentation of [2] was characterised by an intense parent ion which also constituted the base peak. Apart from this, only two other processes led to the formation of daughter ions of any appreciable intensity. The first of these processes resulted in molecular contraction through *trans* → *cis* isomerisation followed by a stepwise or molecular loss of hydrogen, while the second process led to the formation of a polynuclear ion [27], via the loss of atomic sulphur from the product of the first process, [23b] (figure 3.2.4). It is suggested that molecular contraction results in the formation of a cation [23b] which, through conjugation, acquires the property of high stability normally attributed to the pyrene radical cation. This stability is such that it leads to the suppression of the normal fragmentation modes expected of the thiophene moiety, and results in the expulsion of sulphur as the only other major process.

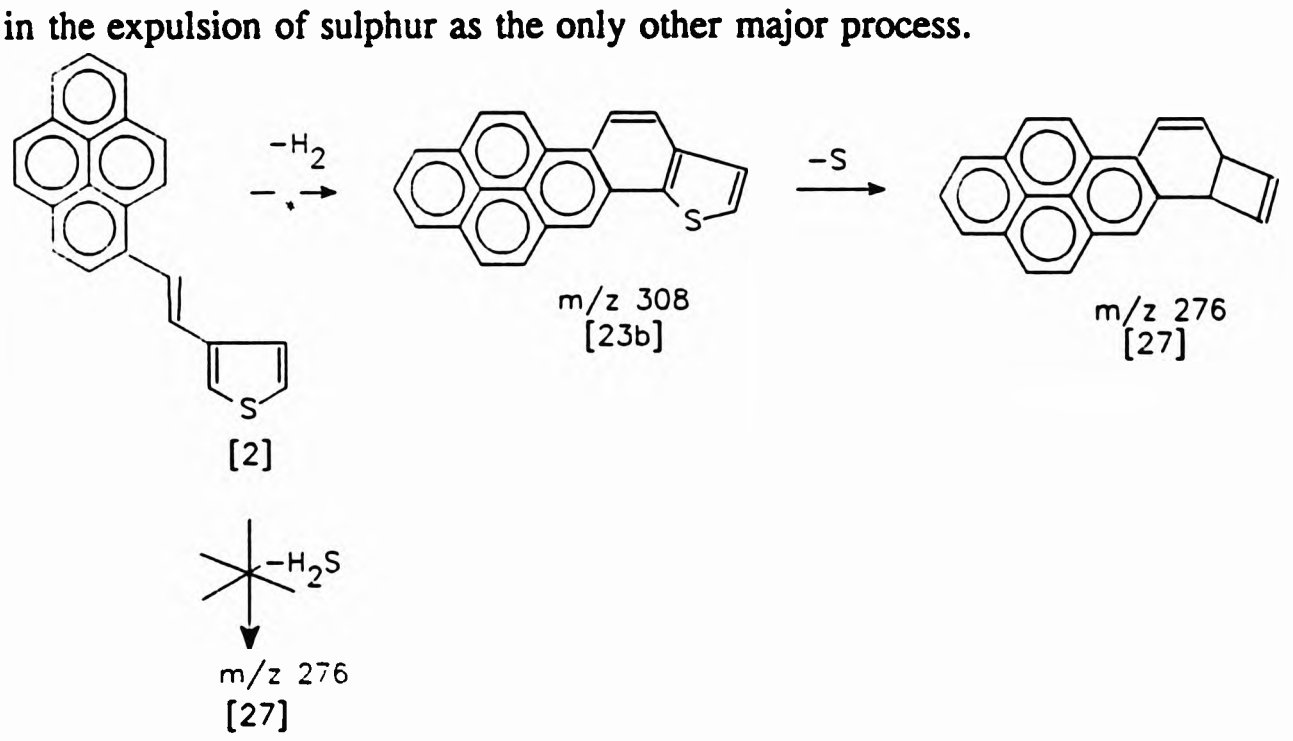

Figure 3.2.4
The major fragmentation processes observed in the EI ionisation of [2].

[C]. The ferrocenyl monomers [4] - [6]

The parent molecular ions constituted the base peaks for the ferrocenyl compounds [4], [5] and [6]. This signifies a relative stability of the molecular radical cations generated from these compounds. In addition to an $[M^+ - 2]$ process to form radical cations like [23d], and which provides evidence of an interaction between the thiophene unit and the ferrocene groups (since it is a process that decrees a delocalisation of electrons beween the two moieties), the fragmentation of the generated molecular radical cations were dominated by cleavages of the charge-localised ferrocene moiety. Daughter ions ascribed to this fragmentations are presented in table 3.2.2 overleaf.

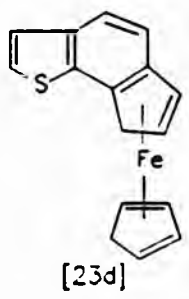

[23d]

[D] 1,5-bis(3´-thienyl)-penta-1,4-dien-3-one [7] &
1,9-bis(3´-thienyl)nona-1,3,6,8-tetraen-5-one [8]

The electron-impact ionisation of [7] and [8] was accompanied by a fragementation pattern comparable to that of thiophene. Ionisation thus yielded similar fragments (table 3.2.1), and resulted in base peaks of CHS^+ [*m/z* 45], and S^+ [*m/z* 32] for [7] and [8] respectively. There were also losses of CO^+, $C_2H_2^+$, and a variety of cleavages about the ethylenic linkages, to yield daughter ions whose structures were dependent on whether cleavage was effected with or without rearrangement.

Cyclic products were also generated by simple cleavages, followed by single or double hydrogen transfer. Unlike in the ionisation of 1-(ferrocenyl)-3-(3´-thienyl)prop-2-ene-1-one [6], the formation of the cyclopentadienyl cation (*m/z* 65) and the thiopyrilium ion [21] from β-carbon cleavage of the ethylenic linkage accompanied by hydrogen transfer and ring formation, featured with high relative intensities (table 3.2.1).

Compound	Molecular ions expressed as percentages of the base peak.						
	$[C_5H_5FeC_5H_5]^+$ *m/z* 186	$[C_5H_5FeC_5H_4]^+$ *m/z* 185	$[C_9H_7Fe]^+$ *m/z* 171	$[C_5H_5FeC_3H_3]^+$ *m/z* 160	$[C_5H_5 - C_5H_5]^+$ *m/z* 130	$[C_5H_5 - C_5H_4]^+$ *m/z* 129	$[C_5H_4 = C_5H_4]^+$ *m/z* 128
[4]	3	2	19	-	0.20	5	5
[5]	12	4	7	-	-	1	2
[6]	5	5	7	1	1	10	6

Compound	Molecular ions expressed as percentages of the base peak.					
	$[C_4H_3S - Fe]^+$ *m/z* 139	$[C_5H_5Fe]^+$ *m/z* 121	$[C_3H_3 Fe]^+$ *m/z* 95	$[C_2H Fe]^+$ *m/z* 81	$[C_5H_5]^+$ *m/z* 65	Fe^+ *m/z* 56
[4]	11	18	3	3	0.70	30
[5]	6	38	6	6	2	36
[6]	12	31	4	6	8	32

Table 3.2.2
The relative intensities of some of the principal ions in the electron-impact mass spectra of the ferrocenyl compounds [4], [5], and [6].

3.3 NUCLEAR MAGNETIC RESONANCE[119,120]

Table 3.3.1 overleaf lists the ^{1}H-chemical shifts and coupling constants of [1] - [10] in $CDCl_3$, using TMS as an internal standard.

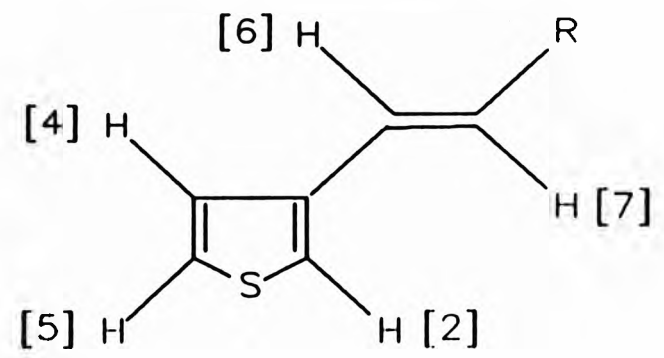

Figure 3.3.1
Numbering system used for the protons of the trans(3-thienyl)ethene residue.

Compound	Chemical Shifts (ppm)					Coupling Constants (Hz)			
	δ_2	δ_4	δ_5	δ_6	δ_7	$J_{2,4}$	$J_{2,5}$	$J_{4,5}$	$J_{6,7}$
[1]	7.30 (d)	7.21 (d)	7.30 (d)	6.96 (s)	6.96 (s)	*	*	*	*
[2]	7.39 (m)	7.39 (m)	7.51 (m)	7.27 (d)	8.04 (d)	1.40	2.80	4.70	17.10
[3]	7.14 (q)	7.31 (dd)	7.27 (dd)	6.95 (d)	6.87 (d)	1.36	2.89	5.10	16.30
[4]	7.28 (d)	7.13 (t)	7.28 (d)	6.71 (d)	6.71 (d)	*	*	*	*
[5]	7.25 (d)	-	7.25 (d)	6.69 (d)	6.77 (d)	-	-	-	16.01
[6]	7.60(q)	7.43(dd)	7.39(dq)	6.95(d)	7.79(d)	1.32	2.70	5.40	15.53
[7]	7.57(t)	7.38(m)	7.35(m)	6.77(d)	7.71(d)	1.31	2.80	4.91	15.81
[8]	7.32(m)	7.32(m)	7.32(m)	6.52(d)	7.67(m)	*	*	*	15.42
[9]	7.40(q)	7.20(dd)	7.33(q)	-	-	1.26	2.60	4.81	-
[10]	7.15(m)	7.04(dt)	7.27(qd)	-	-	1.32	2.99	4.98	-

* = exact values not determined

Table 3.3.1
Chemical shifts and Coupling Constants for the Compounds [1] - [10].

3.3.1 Results and Discussion

[I] Chemical Shifts

The chemical shifts of the designated protons are expected to be directly related to their respective electron densities. The marked electron-withdrawing capacity of the carbonyl function is established by a comparison of the differences in the 2-*H* chemical shift between the thienylethylenes [1] & [4] and their respective ketones [7] & [6] (Table 3.3.2).

Compound	$\Delta\delta_2$	$\Delta\delta_4$	$\Delta\delta_5$
[6]	-0.26	-0.31	-0.05
[7]	-0.23	-0.26	-0.01
[2]	-0.17	-0.27	-0.05
[9]	-0.06	-0.04	+0.01
Thiophene	0.00	0.00	0.00
[8]	+0.02*	*	*
[1]	+0.04	-0.09	+0.04
[4]	+0.06	-0.01	+0.06
[5]	+0.09	-	+0.09
[3]	+0.20	-0.19	+0.07
[10]	+0.30	-0.03	+0.07

Table 3.3.2
Chemical shifts (ppm), of the engineered monomers, arranged in an increasing order relative to the shift of the 2-*H* of thiophene.

The introduction of a carbonyl group, as in the progression from [1]→[7] and [4]→[6], decreases the electron density about 2-*H*, and results in a downfield shift of this proton by 0.27 ppm and 0.32 ppm respectively. This effect however, is dependent on the number of adjoining bonds, and is alleviated by the insertion of an additional ethylenic link, as evident in *all-trans*-1,9-bis(3´-thienyl)nona-1,3,6,8-tetraen-5-one [8], which has a 2-*H* chemical shift comparable to that of *trans*-1,2-bis(3´-thienyl)ethene [1] (figure 3.3.2).

---

* exact chemical shifts were undeterminable.

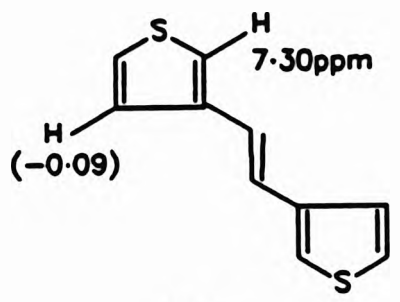

[1]

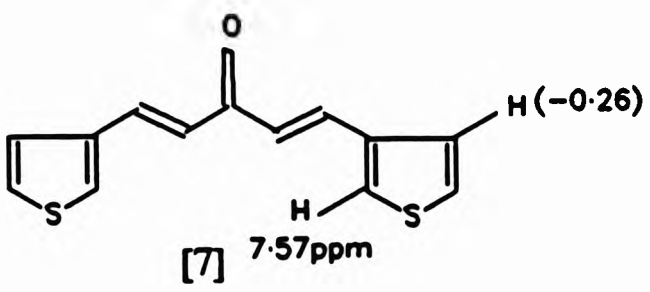

[7]

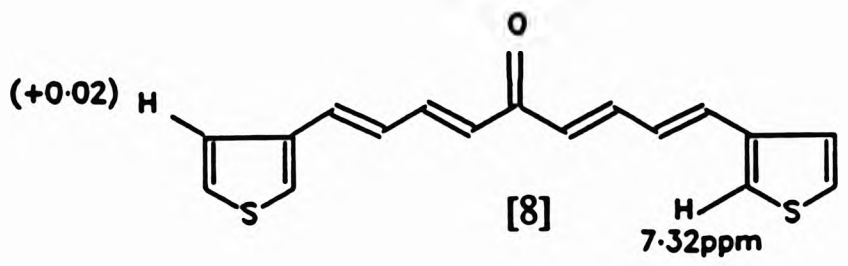

[8]

Figure 3.3.2
Effects of the carbonyl group and the number of adjoining ethylenic linkages, on chemical shifts of the 2-*H* and 4-*H* positions of compounds [1], [7] and [8]. The 4-*H* shift is relative to thiophene.

[II] Coupling Constants

The spin-spin coupling constants of the thiophene-ring protons fall within their average attributed coupling ranges.[121] The average coupling constant of 16.03 Hz for the ethylenic protons ($^3J_{6,7}$) is consistent with a trans configuration about the double bonds.[122]

The coupling constants of the the protons in compounds [1] and [4] were not quoted because their spectra seemed deceptively simple. It is suspected to be overlaid and of second order. However, long range coupling was evident between the ring and methyl protons of [10]. This is typical of thiophene thiols and acetylenes,[123] thiophene carboxaldehydes,[124] and methylthiophenes.[125]

CHAPTER 4

ELECTROCHEMICAL STUDIES

The work presented in this chapter was undertaken at the Central Research Centre of Cookson Group PLC., Kidlington, Oxfordshire.

4.1 INTRODUCTION

The candidature of any compound for electrochemical polymerisation is strictly dependent on its interaction with the fundamental laws of electricity as proposed by Faraday.[126] As a pre-requisite to oxidative polymerisation by constant potential electrolysis, it is imperative that potentials suitable for the optimised oxidation of the synthesised compounds are established and structure-reactivity relationships, including any pattern of chemical transforamations, determined. This section therefore describes the use of cyclic (stationary-electrode) voltammetry as an analytical tool in the study of the electroactivity of the compounds [1] - [9], within specified potential limits.

4.2 THE CV EXPERIMENT[127]

Cyclic voltammetry (CV) is an electrochemical technique used for the direct measurement of the formal potential of an electrode process, provided that the oxidised and/or reduced forms of the compound(s) being investigated are stable during the time required to obtain the voltammogram.[128]

Starting from an initial potential value, a linear potential sweep (or scan) of a known velocity (in volts per second) is applied to the working electrode (WE), to a final potential limit. Upon reaching this limit, the sweep is reversed to its initial potential value, or any other value of interest. The most pertinent data features of a cyclic voltammogram are the anodic and/or cathodic peak potentials ($E_{p(a)}$ and $E_{p(c)}$ respectively), the anodic and cathodic peak current density measured from the residual current axis I_r to the peak wave ($I_{p(a)}$ and $I_{p(c)}$ respectively), and the half-wave potential, $E_{1/2}$. Some of these features are represented in figure 4.1.

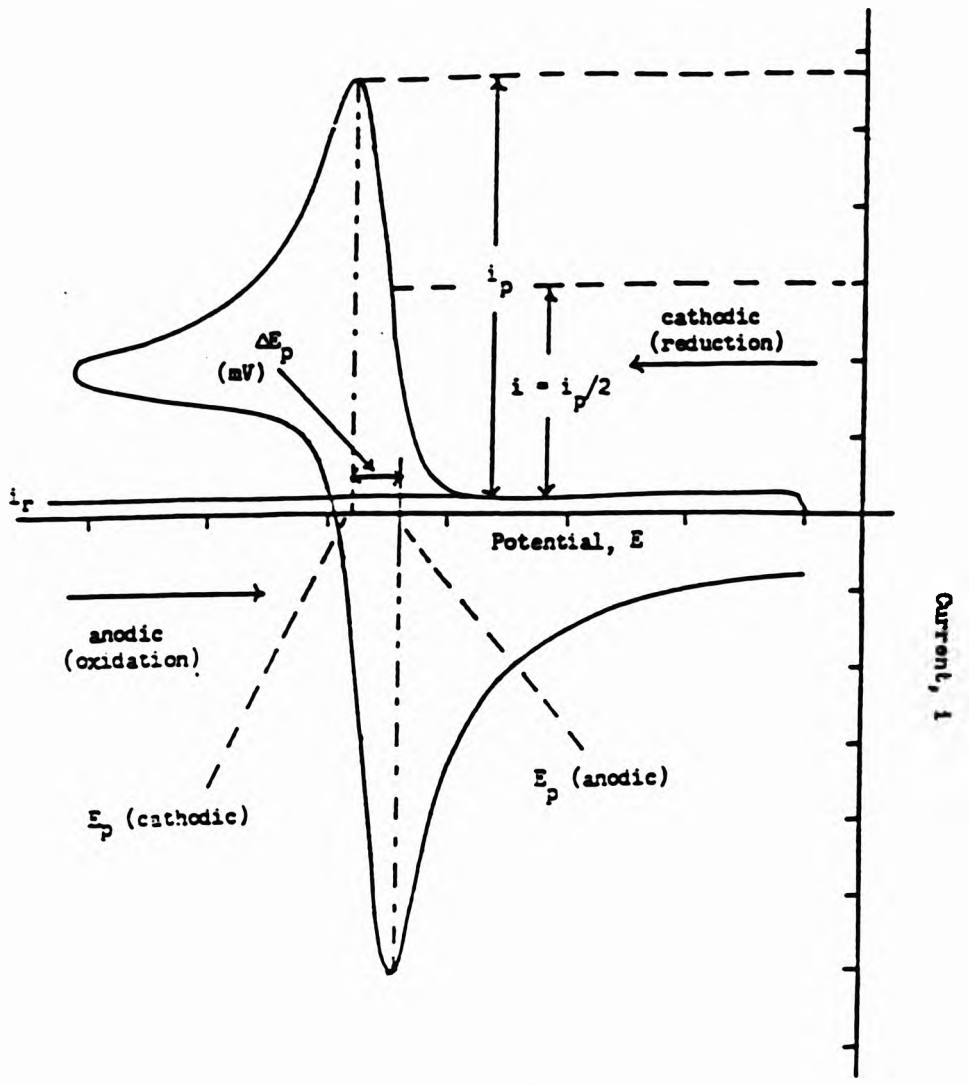

Figure 4.1
A typical Cyclic Voltammogram showing some of the pertinent data features.[129]

A generalised 3-electrode setup used in the CV studies is illustrated below (figure 4.2) It is important to place the non-polarised reference electrode (RE) as physically close to the working electrode as possible (without shielding it) in order to minimise an uncompensated drop in internal resistance (IR). An auxiliary electrode (AE) was also used in order to counteract any drop in potential that might be incurred due to the inherently-high internal resistances of the low-conducting aprotic solvents used.

The potentiometric circuitry adjusts the current passing through the working and auxiliary electrodes so that the potential between the working and reference electrodes is uniform with the applied cell voltage. No universal reference electrode is available for use in electrochemical studies, and in the course of this research, the saturated calomel electrode (SCE)[130] was employed; with all measurements completed within 5 minutes in order to prevent drifting of its intrinsic liquid junction potential. A signal generator usually provides the fast responses needed at high sweep rates.

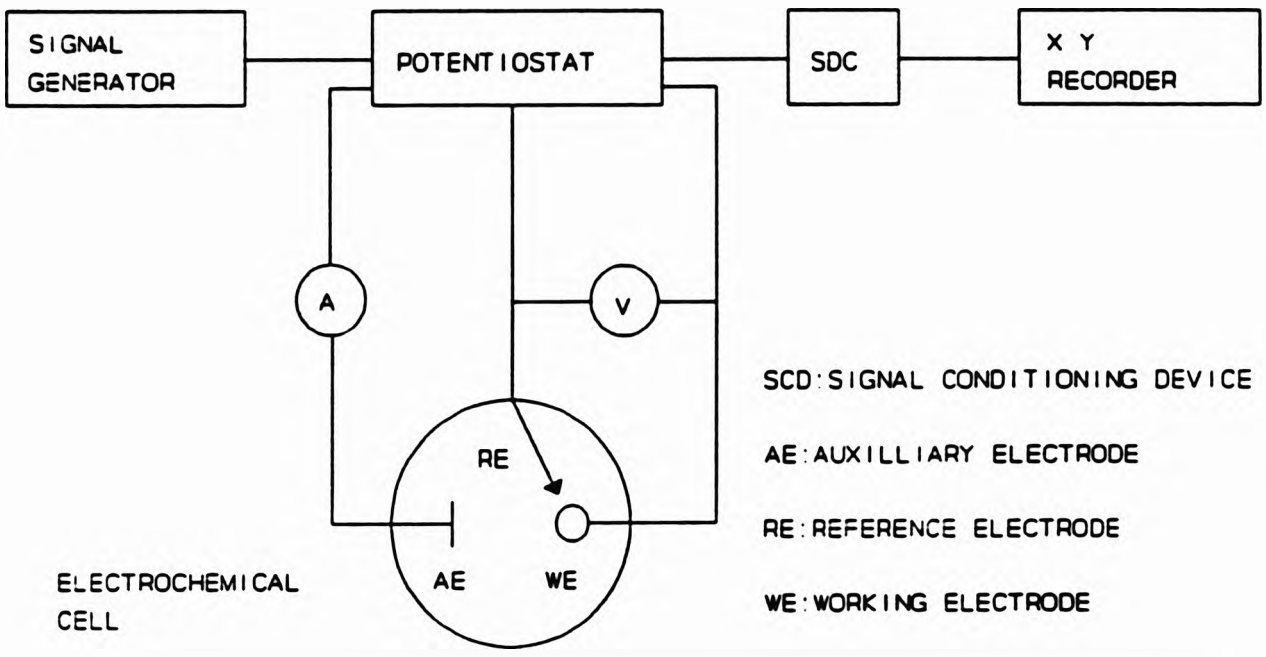

Figure 4.2
Experimental setup for CV.

Although platinum is conventionally used as the working electrode in oxidative processes, other materials can be employed. Materials used as anodes have included graphite, stainless steel, gold, Indium tin (IV) oxide, and oxides of silver, manganese and iron. The choice and limitations of electrode materials have been discussed,[131] while Mann has reviewed the suitability of a variety of reference electrodes in a range of solvents.[132]

4.3 THEORETICAL CONSIDERATIONS

A characteristic cyclic voltammogram is actually a current-voltage curve. The measurable current in a CV profile at, or within a range of potentials, is a product of the faradaic current density of the working electrode (resulting from heterogeneous charge transfer between electrode and the electroactive solution species), plus some current contributions from a "charging current", which flows to charge up the capaticance which is ever-present at electrode/electrolyte interfaces. This capacitance current normally increases with an increase in scan rate. The faradic current density is solely determined by two interlinked processes; heterogenous charge transfer and diffusional mass transport. These two variables, discussed in detail below, help to provide a direct insight into the kinetic, mechanistic and thermodynamic aspects of an electrochemical reaction.

4.3.1 Heterogenous Charge Transfer

This is the rate at which electrons transfer from the electrode to the solution species and vice-versa. The current density associated with heterogenous charge transfer at an electrode interface and leading, for example, to the oxidative process, A - e^- $\overset{E}{\rightleftharpoons}$ B, is dependent on the applied electrode potential, the surface concentrations of the redox partners involved and the heterogeneous standard rate constant. This is expressed by the Butler-Volmer equation,[133]

$$J_A(0,t) = \frac{i}{nFA} = C_A(0,t)\ K^o \exp\left[-\alpha \frac{nF}{RT}(E-E^o)\right]$$
$$-C_B(0,t)\ K^o \exp\left[(1-\alpha) \frac{nF}{RT}(E-E^o)\right] \ldots\ldots\ldots(i)$$

where:

J	=	Flux at the Electrode Interface.
K^o	=	Heterogenous Standard Rate Constant.[134]
α	=	Electron Transfer Coefficient.
E^o	=	Standard Redox Potential.
A	=	Electrode Area.
C	=	Potential Dependent Surface Concentration.
F	=	Faraday Constant.

E^o, the thermodynamic standard redox potential, is related to the anodic and cathodic peak potentials E_p, by the expression;

$$E_{1/2} = (E_{p(a)} + E_{p(c)}) / 2 \quad ; \quad E_{1/2} = E^o + (RT / nF) \ln (D_R / D_o)^{1/2} \ldots\ldots\ldots(ii)$$

where D_R and D_o are the diffusion coefficients of the reduced and the oxidised forms of the electroactive species respectively, n is the number of electrons in the half reaction, and because D_R is approximately equal to D_o in a reversible charge transfer process, $E_{1/2}$ largely corresponds to E^o.

During oxidation, there is a depletion in the concentration of the electroactive species $C_A(0,t)$ at the electrode, to zero with time, and a concomitant increase in that of its oxidised primary intermediate, $C_B(0,t)$. The concentration of the intermediate(s) formed at the electrode is dependent on the initial concentration of the electroactive species, and the time taken by the oxidation process. The ensuing difference in concentrations between the electrode and the rest of the solution results in a well-defined concentration gradient, along which the second current determinant; mass transport, occurs.

4.3.2 Mass Transport

Mass transport describes the process by which materials get to the electrode. Theoretical ramifications of mass transport (flux) to the electrode are mathematically expressed in the Nernst-Plank equation:

$$J(x,t) = -D\frac{\delta C(x,t)}{\delta x} - \frac{zF}{RT}DC(x,t)\frac{\delta \Phi(x,t)}{\delta x} + C(x,t)\,v_x(x,t) \ldots (iii)$$

where:

J	=	Flux
D	=	Diffusion Coefficient (addresses diffusional mass transport).
C	=	Concentration
Φ	=	Electrostatic Potential (addresses migrational mass transport).
v_x	=	Hydrodynamic Velocity (addresses convectional mass transport).

Of the three modes of mass transport, viz: convection (the movement of solution species within a stirred solution and as a result of gross physical displacement), diffusion (the movement of solution species under a gradient of chemical potential), and migration (the movement of a charged solution species in the electric field gradient between electrodes), the mass transport of a solution species in linear sweep and cyclic voltammetry should be governed solely by diffusion. In order to achieve this, the effect of convectional transport is circumvented by the maintenance of a quiescent electrolytic solution and the application of a sweep rate of at least 10 mV s^{-1}., whilst migrational transport of the charged electroactive species and its products is suppressed by swamping the solution with a large excess (normally tenfold) of an electrochemically inert supporting electrolyte, which then serves as the major charge carrier. Tetrabutylammonium hexafluorophosphate was the supporting electrolyte (and the ionic dopant) used in the CV studies reported herein. With the elimination of migrational and convectional mass transport, the time-dependent rate of diffusion at the electrode surface becomes proportional to the charge flux. This relationship could be expressed as:

$$J_A(0,t) = -D_A\frac{\delta C_A}{\delta x} = D_B\frac{\delta C_B}{\delta x} \qquad \ldots\ldots\ldots (iv)$$

4.4 TYPES OF VOLTAMMETRIC WAVES AND THE CLASSIFICATION OF ELECTRODE REACTIONS

Three different kinds of waveforms can be obtained in cyclic voltammetry. These are reversible, irreversible, and quasi-reversible waves. The actual type of waveform obtained within a potential range depends on the heterogenous standard rate constant, K^o (and thus the kinetics of electron transfer), and on the conditions of mass transport. It also depends on whether any associated chemical reactions occur prior to electron transfer, after electron transfer, are interposed between electron transfer steps, or do not occur atall.

Nicholson and Shain[134,135] have published diagnostic criteria with which one could unravel and classify the seemingly complex electrode processes that constitute a CV. This was achieved by the study of a series of electrode reactions and an investigtation of the magnitudes by which a number of qualitatively-determined voltammetric parameters deviate from classical norms, and as functions of potential scan rates. Using their adopted notation, the eight electrode processes presented were;

Type I: Reversible charge transfer.

Type II: Irreversible charge transfer.

Type III: Chemical reaction preceding a reversible charge transfer.

Type IV: Chemical reaction preceding an irreversible charge transfer

Type V: Reversible charge transfer followed by a reversible chemical reaction.

Type VI: Reversible charge transfer followed by an irreversible chemical reaction.

Type VII: Catalytic reaction with reversible charge transfer, and

Type VIII: Catalytic reaction with irreversible charge transfer.

These processes could be easily diagnosed from the graphs presented in figures 4.3a and 4.3b.

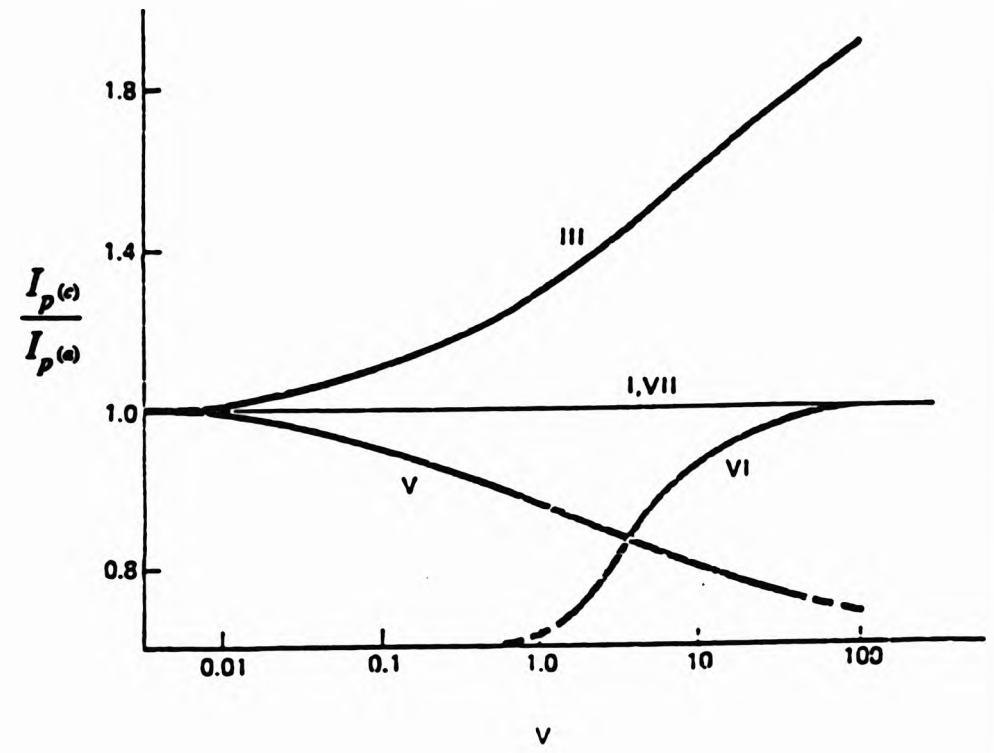

Figure 4. 3a
The Nicholson and Shain plots of the ratio of cathodic to anodic peak current for the various electrode processes, as a function of scan rate.[136]

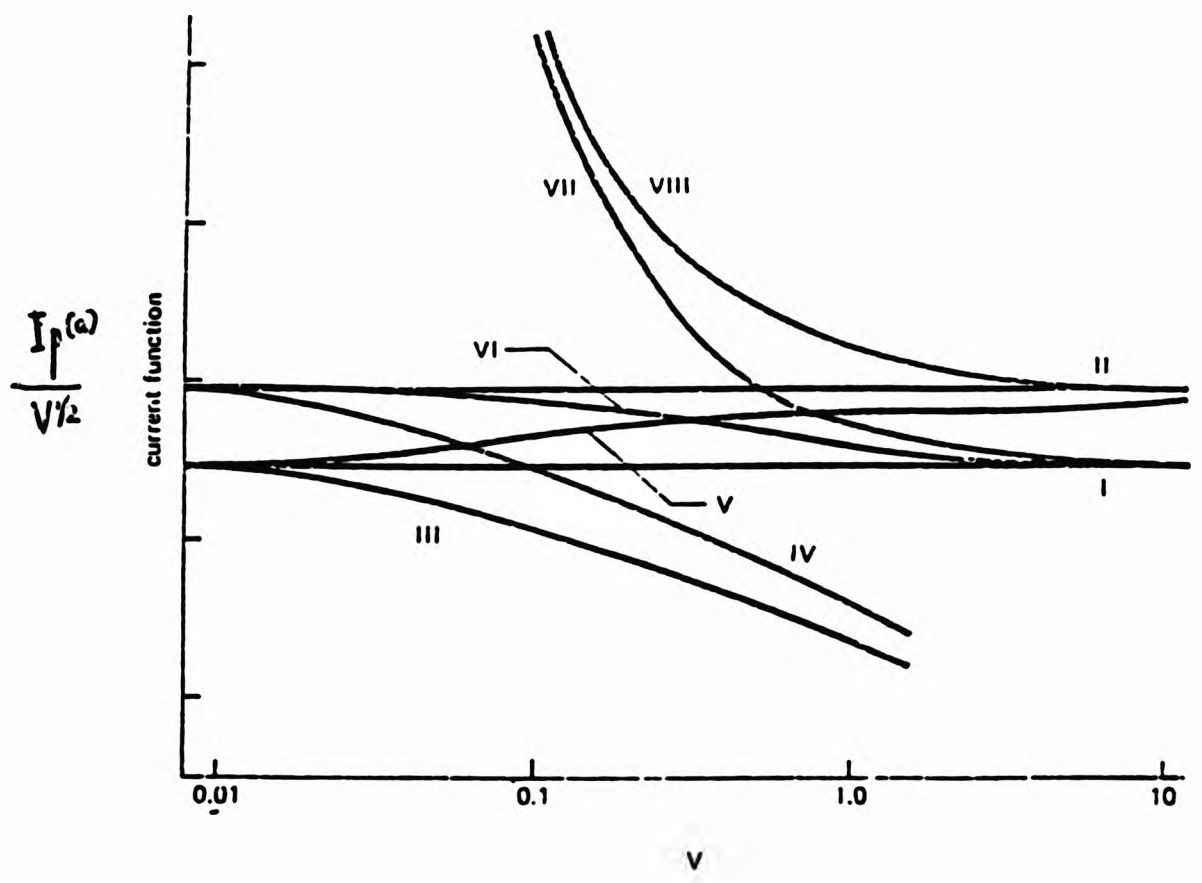

Figure 4.3b
The Nicholson and Shain plots of the anodic current function for the various electrode processes, as a function of scan rate.[136]

4.4.1 The Reversible Charge Transfer, ($K^\circ > 10^{-1}$ cm/s)

$$A \pm ne^- \rightleftharpoons B$$

When the rate of heterogenous charge transfer is by far higher than the rate of mass transport, charge transfer is said to be reversible. Transient charge transfer at the electrode interface results in thermodynamic equilibrium at the phase boundary; even in the presence of a substantial net current and a rapidly-changing potential. The Butler-Volmer equation [Eq. (i)] is reduced to the Nernst equation [Eq. (iii)], as the concentrations of reactants and products (and thus, the current profile) are no longer influenced by the effects of transient heterogenous charge transfer, but by the slower rate of diffusional mass transport (mass-transport control).

CV manifestations of electrochemical reversibility at 25°C are:

1. $I_{p(a)} \div I_{p(c)} = 1$
2. I_p is proportional to $V^{1/2}$
3. E_p is independent of sweep rate, V.
4. $\Delta E_p = E_{p(a)} - E_{p(c)} = 59/n$ mV; where n = no of electrons involved in the redox process.
5. $E_{1/2}$ approximates E°.

4.4.2 The Irreversible Charge Transfer, ($K^\circ < 10^{-5}$ cm/s)

$$A \pm ne^- \rightarrow B$$

The main feature of irreversible charge transfer is that only one of the anodic or cathodic reactions has a measurable rate. This is due to the extremely slow forward or reverse rate of heterogenous charge transfer. As a result, thermodynamic equilibrum is not maintained at the phase boundry and current is therefore pricipally determined by the kinetics of the slow rate of this heterogeneous charge transfer (charge-transfer controlled). Accordingly, the Nernst equation is rendered invalid, and potential values extrapolated from these kinetically-controlled (irreversible) profiles cannot be directly compared with those profiles obtained from the thermodynamically-controlled (reversible) charge-transfer processes.

CV manifestations for total irreversibility are (at 25°C):

1. No reverse peak.
2. $I_{p(a)}$ ($I_{p(c)}$) is proportional to $V^{1/2}$
3. $E_{p(a)}$ ($E_{p(c)}$) shifts 30/n mV for each tenfold increase in sweep rate (V).

4. $E_p - (E_p \div 2) = 48/n$ mV

5. $E_{1/2}$ no longer corresponds to E° because the former is now determined by charge transter kinetics instead of thermodynamics.

An irreversible oxidation peak suggests either the occurence of a slow electron transfer process, or that the generated ionic species is unstable, very reactive, and has undergone a fast follow-up chemical reaction.

4.4.3 The Quasi-Reversible Charge Transfer, ($10^{-1} > K^\circ > 10^{-5}$ cm/s)

The properties of a compound do not pre-determine which waveform occur. It is the time scale of the CV experiment that determines whether the observed electrode process would be charge-transfer or mass-transport controlled. A sufficient decrease in the sweep rates could result in the conversion of a waveform from reversible to irreversible behaviour, *via* a region of quasi-reversibility. Here, processes involving charge-transfer are insufficient in maintaining thermodynamic equilibrium at the electrode surfaces, and the faradaic current is therefore determined by both charge transfer and mass transport. Quasi-reversible charge transfer also fulfils the following CV criteria.

1. $E_{p(c)}$ shifts negatively with increasing V
2. ΔEp is greater than 57/n mV and increases with increasing V
3. $I_{p(a)} \div I_{p(c)} = 1$
4. I_p increases with $V^{1/2}$ but is not proportional to it.

4.5 EXPERIMENTAL RESULTS AND DISCUSSION

The cyclic voltammetric behaviour of the novel thiophene monomers [1] to [9], was studied at room temperature (15°C) in a two-compartment electrochemical cell, and under the experimental conditions stipulated overleaf in table 4.1. The electrolytic solution was initially purged with and continuously maintained under an atmosphere of nitrogen during the course of the studies. A platinum wire served as the auxiliary electrode while either fluorine-doped tin (IV) oxide or a glass-backed 2cm x 2cm platinum flag served as the working electrode. Prior to the experiments, the platinum working electrode was subjected to surface modification by anodisation. This resulted in the growth of a thin oxide veneer on the electrode surface.

	Prefix of compound involved.	Solvent used.	Working Electrode used	Anion used	Concentration ($x\ 10^{-3}\ dm^{-3}$)		Scan Limits (V vs SCE)		Film formation?	Film Colour	
					monomer	anion	anodic	cathodic		anodic scan	cathodic scan
condition 1a	[1]	CH_3CN	Pt	PF_6^-	10	100	1.75	- 0.50	yes	blue-black	gold
condition 1b		CH_3CN	SnO_2	PF_6^-	10	100	1.80	- 0.50	yes	blue-black	
condition 1c		ΦNO_2	Pt	PF_6^-	10	100	2.25	- 0.75	yes	blue-black	
condition 2a	[2]	CH_3CN	Pt	PF_6^-	2	10	2.00	- 0.50	yes	army-green	brick-red
condition 2b		ΦNO_2	SnO_2	PF_6^-	10	100	1.70	- 0.70	yes	blue-black	
condition 3a	[3]	CH_3CN	Pt	PF_6^-	1	10	2.00	-0.50	yes	blue-black	film dissloved
condition 3b		CH_3CN	SnO_2	PF_6^-	1	10	2.80	-0.20	no	-	-
condition 3c		CH_2Cl_2	SnO_2	PF_6^-	10	10	1.70	- 0.75	yes	deep-green	film dissolved
condition 4a	[4]	ΦNO_2	Pt	PF_6^-	10	100	2.25	- 0.75	no	-	-
condition 4b		CH_3CN	Pt	PF_6^-	10	100	2.20	- 0.50		-	-
condition 5	[5]	CH_3CN	Pt	PF_6^-	1	10	2.25	- 0.75	no	-	-
condition 6	[6]	CH_3CN	Pt	PF_6^-	2	200	2.25	- 0.75	no	-	-
condition 7	[7]	CH_3CN	Pt	PF_6^-	10	100			no	-	-
condition 8	[8]	CH_3CN	Pt	PF_6^-	2	20	2.25	- 0.75	no	-	-
condition 9a	[9]	ΦNO_2	Pt	PF_6^-	20	200	2.25	- 0.75	yes	metallic blue-green	deep orange
condition 9b		CH_3CN	Pt	PF_6^-	20	200	1.90	- 0.75	no	-	-

ΦNO_2 = nitrobenzene

Table 4.1

A summary of the Cyclic voltammetric behaviour of the synthesised compounds [1] - [9] at room temperature (15°C).

4.5.1 The CV behaviour of *trans*-1,2-Bis(3´-thienyl)ethene, [1]

The Voltammetric behaviour of [1] in degassed acetonitrile, using both platinum and tin (IV) oxide electrodes (conditions 1 a and b) is depicted in figure 4.4. The use of both platinum (figure 4.4a) and tin-(IV)-oxide (figure 4.4b) working electrodes led to proflies containing broad featureless anodic ramps with the absence of any cathodic profile upon scan reversal. Since $\Delta E_{p(a)}$ for the decade sweep (10 mV - 100 mV) in both profiles was greater than 30 mV, it could be proposed that the initial electron transfer in each case is succeeded by irreversible chemical coupling.

Repetitive cycling in degassed nitrobenzene with a platinum electrode (condition 1c) also resulted in an irreversible monomeric oxidation wave at +1.84 V vs. SCE and the appearance of an oxidised blue-black polymer on the electrode. The oxidation wave of this engendered polymer was located at +1.16 V vs. SCE. There was a cathodic response at +0.68 V vs. SCE as the oxidised polymer underwent reduction (figure 4.4c). The low but steady increase in current densities of the polymeric redox waves however indicated quite a slow buildup of this polymer on the electrode surface. The polymer obtained exhibited electrochromic behaviour, the colour changing from blue to gold in the oxidised and reduced states respectively.

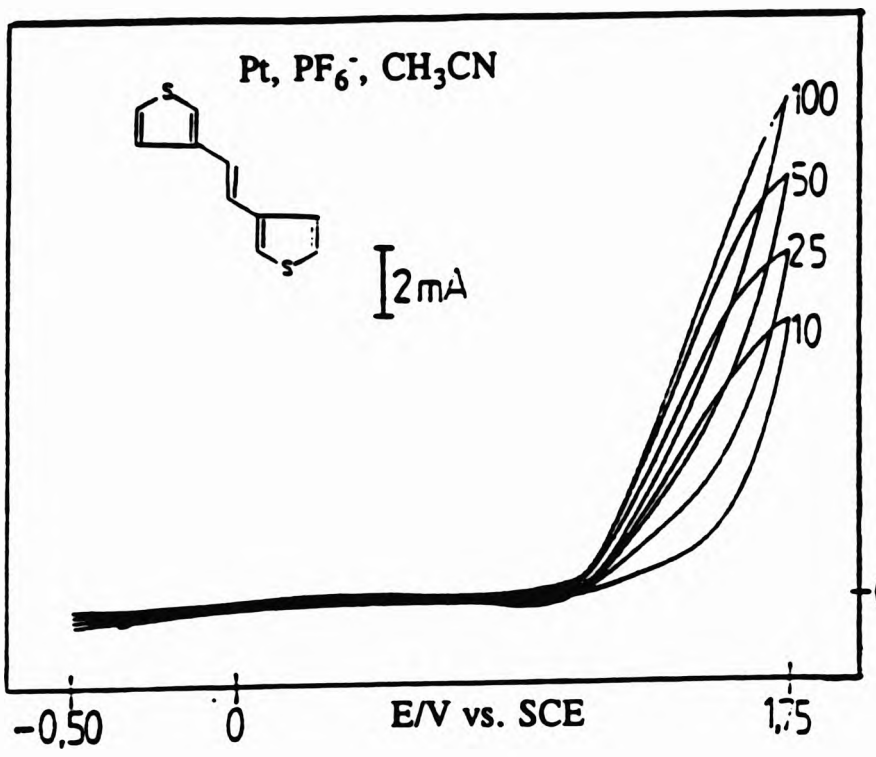

Figure 4.4a
Single-trace CV profile of [1] using condition 1a at different scan speeds (10, 25, 50, and 100 mV sec^{-1}).

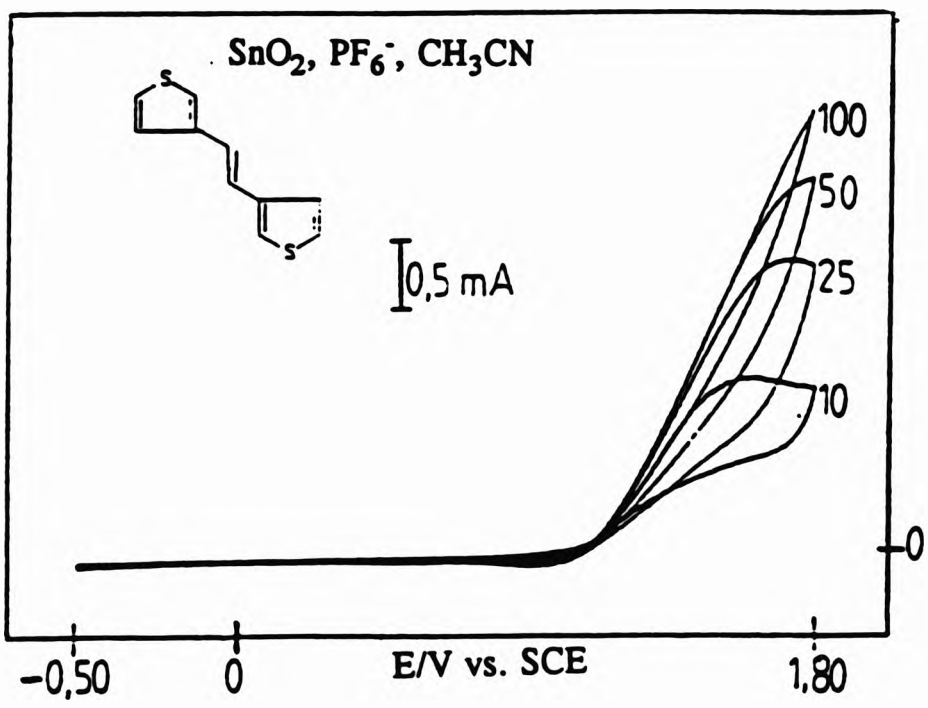

Figure 4.4b
Single-trace CV profile of [1] using condition 1b at different scan speeds (10, 25, 50, and 100 mV sec^{-1}).

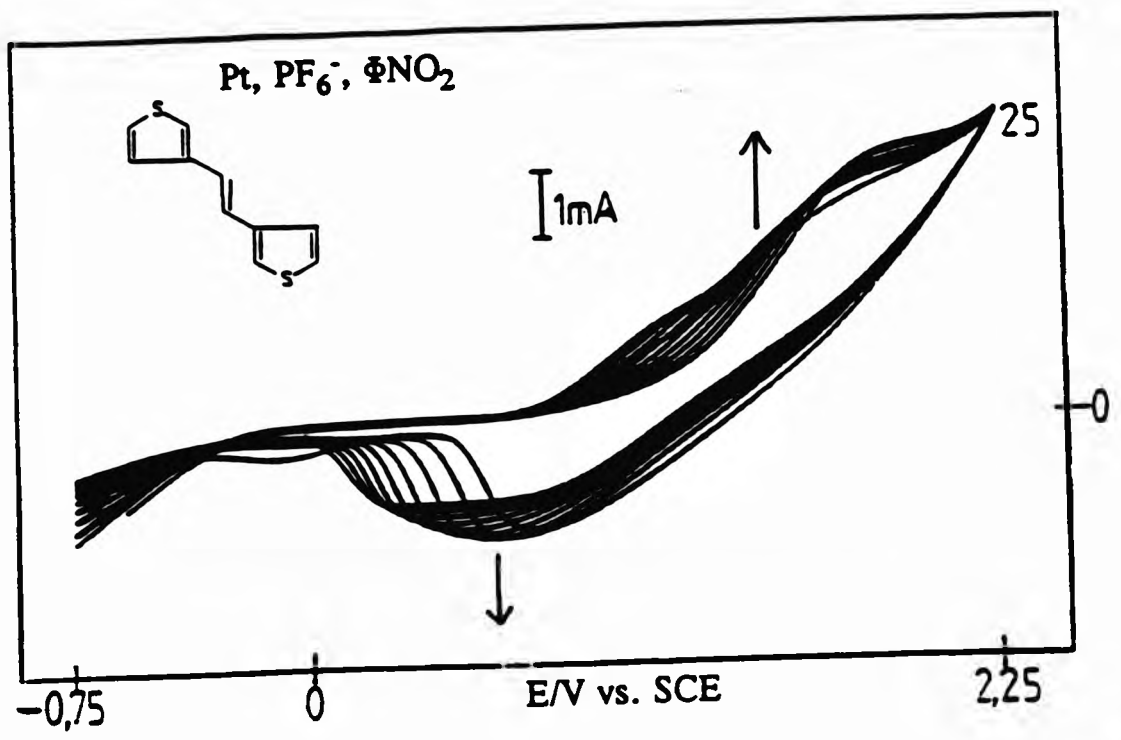

Figure 4.4c
Repetitive-cycling CV profile of [1] using condition 1c at 25 mV sec^{-1}.

4.5.2 The CV behaviour of *trans*-1-(1´-Pyrenyl)-2-(3˝-thienyl)ethene, [2]

The results of the steady state CV of [2] using degassed acetonitrile in conjunction with a platinum working-electrode (condition 2a) and degassed nitrobenzene with a tin (IV) oxide working-electrode (condition 2b) are presented in figures 4.5a & 4.5b respectively. In both cases, the I-E wave representing the oxidation of the thiophene ring was ill-defined and occurred as a shoulder on a much larger anodic ramp. These electron transfer processes were irreversible and consequently led to chemical coupling and the formation of polymer films on the electrode surface. The electrochromicity of these films was such that they were blue-black upon oxidation (doping) and brick-red on reduction (dedoping). The low increase in the anodic current response of the waveform during successive cycling indicates a slow polymer buildup, whilst the low cathodic current response is indicative of a low mobility of cations.

A blue-violet fluorescence of the solution was also noticed during the course of both experiments. This was not investigated any further as equipment for in-situ fluorescence studies was not available.

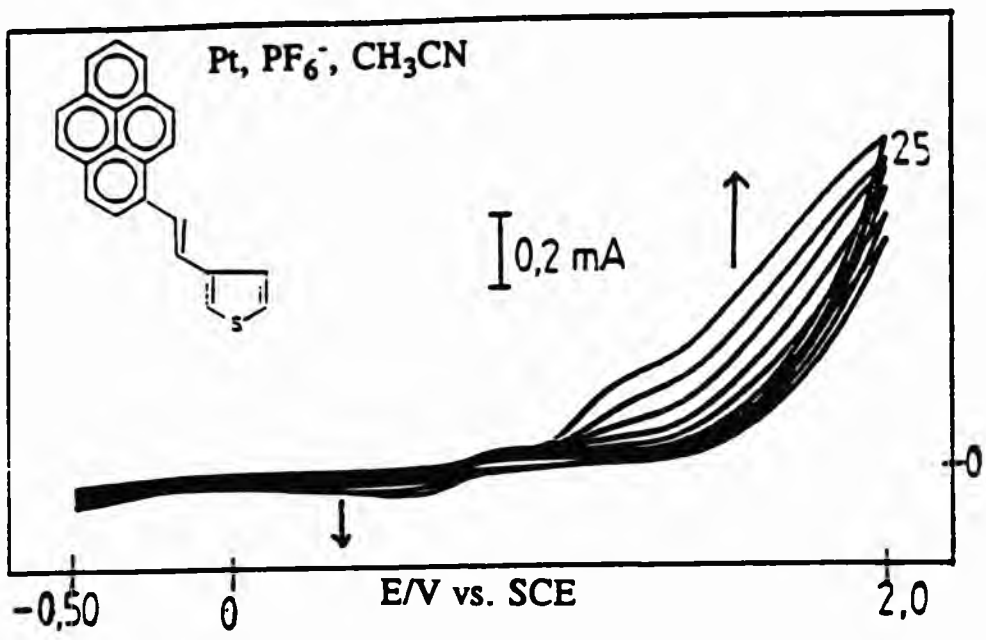

Figure 4.5a
Repetitive-cycling CV profile of [2] at 25 mV sec^{-1}, using condition 2a

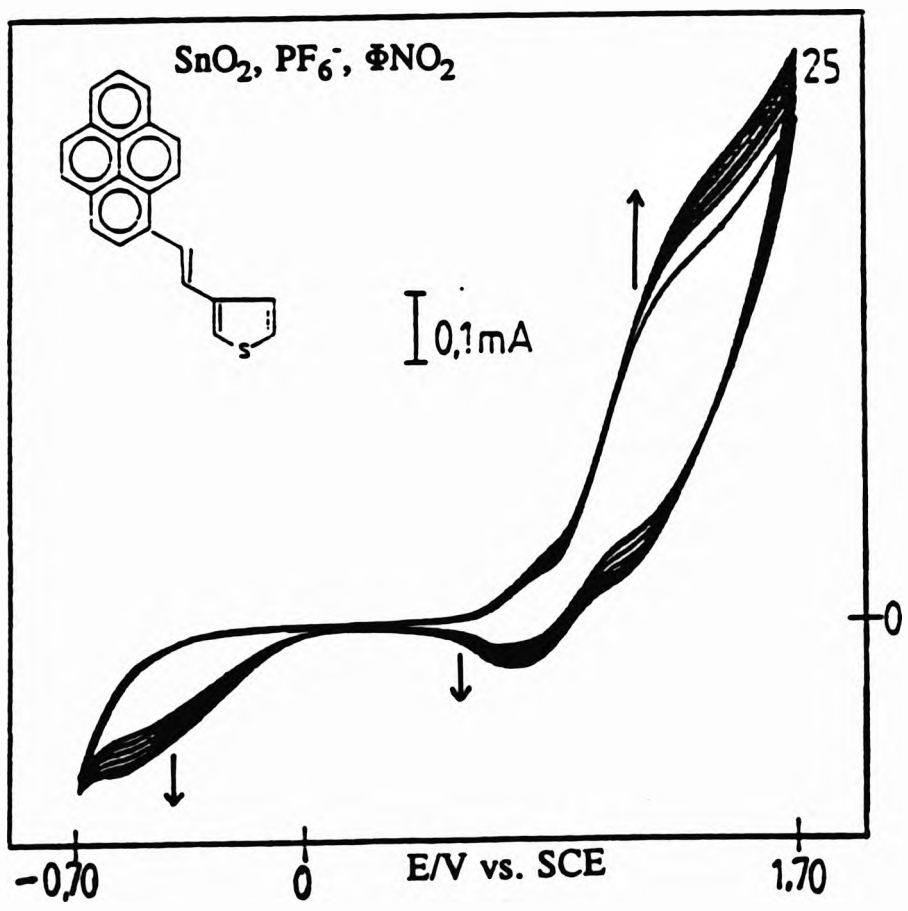

Figure 4.5b
Repetitive-cycling CV profile of [2] at 25 mV sec^{-1}, using condition 2b

4.5.3 The CV behaviour of 1-(p-N,N-Dimethylaminophenyl)-2(3˜-thienyl)ethene, [3]

The electrochemical activity of [3] was dependent on the solvent employed and the type of working electrode used. CV profiles in degassed acetonitrile with a platinum working electrode (condition 3a) depicted a quasi-reversible oxidation peak at +0.68 V vs. SCE attributed to the dimethyl-amino moiety, and an ill-defined oxidation peak at +1.68 V vs. SCE due to oxidation of the thiophene group (figure 4.6a, 25 mV s^{-1}). This latter process resulted in chemical coupling and the formation of a blue-black polymer on the electrode surface that dissolved back into the solution upon sweep-reversal (reduction). A change of the working electrode to tin (IV) oxide whilst maintaining analogous conditions (condition 3b) resulted in a voltammogram which was characterised by an waveform at +1.58 V vs. SCE (figure 4.6b, 25 mV s^{-1}), and which kinetic data revealed to be due to a reversible charge transfer followed by an irreversible chemical reaction. As a result of this, a cathodic peak just starts to appear as the sweep rate is increased to 100 mV s^{-1} (figure 4.6b, 100 mV s^{-1}). Although no polymerisation was observed in this instance, a change in solvent to dichloromethane (condition 3c) yielded a brittle deep-green polymer. The multi-scan CV profile obtained in dichloromethane showed irreversible oxidation peaks (eg., +1.6 V vs. SCE at a scan speed of 25 mV s^{-1}), with no reduction peak on reversal (figure 4.6c).

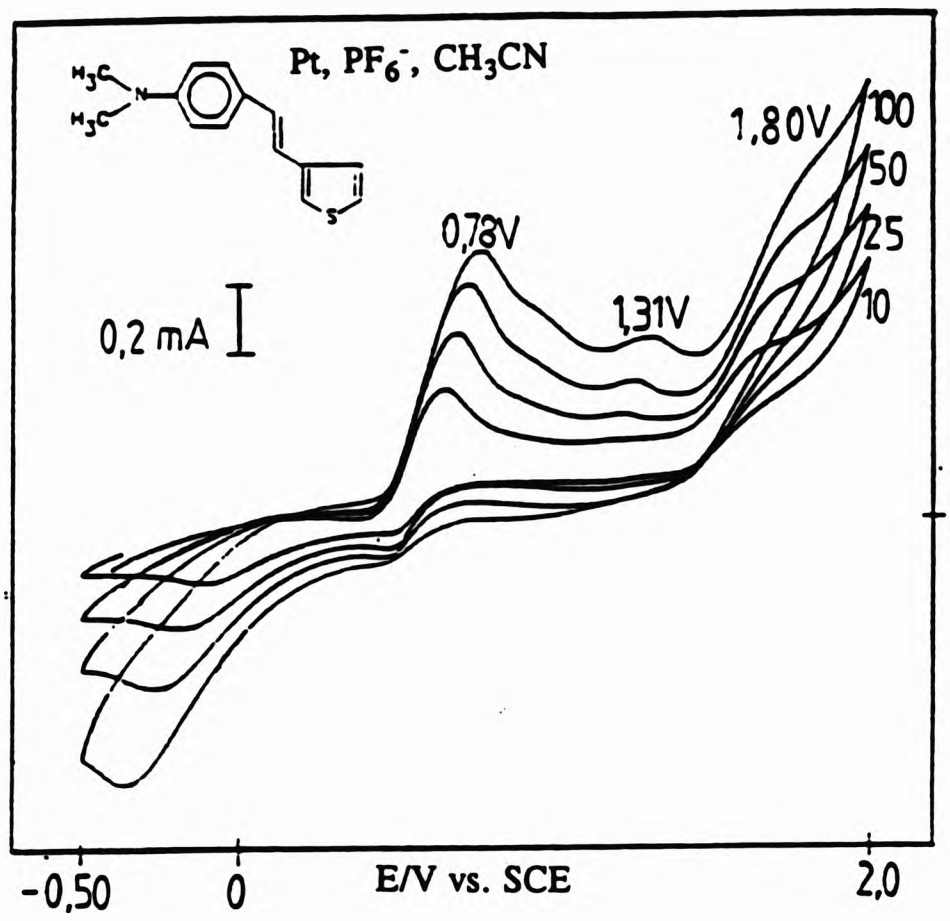

Figure 4.6a
Single-trace CV profile of [3] using condition 3a at different scan speeds (10, 25, 50, and 100 mV sec^{-1}).

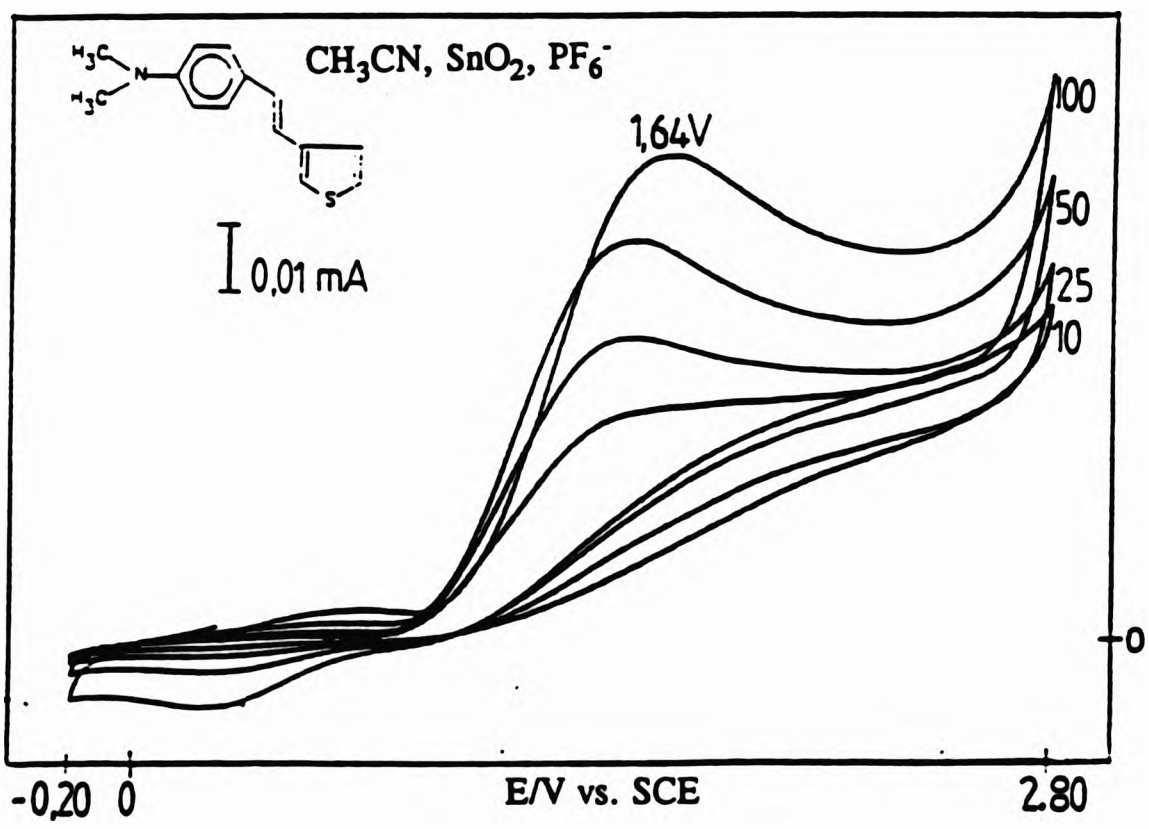

Figure 4.6b
Single-trace CV profile of [2] using condition 3b at different scan speeds (10, 25, 50, and 100 mV sec^{-1}).

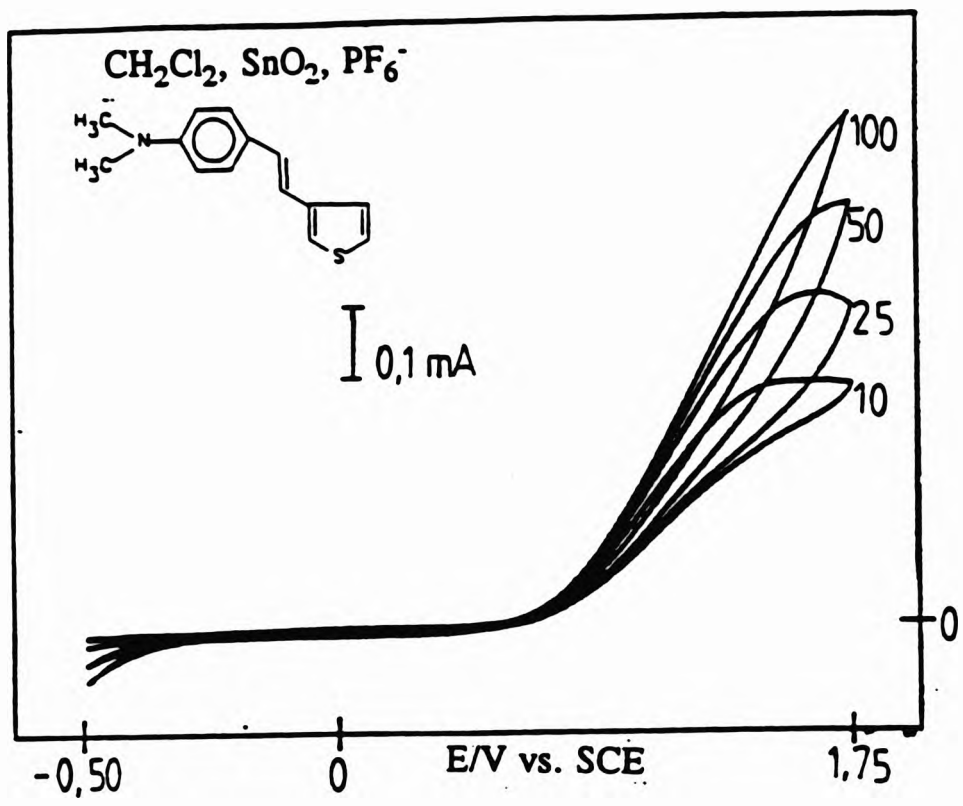

Figure 4.6c

Single-trace CV profile of [2] using condition 3c at different scan speeds (10, 25, 50, and 100 mV sec^{-1}).

4.5.4 The CV behaviour of *trans*-1-(Ferrocenyl)-2-(3´-thienyl)ethene, [4]

The discovery of Wilkinson and Page[137] that ferrocene could be reversibly oxidized to a stable Fe(III) ion initiated extensive investigations into the redox properties of ferrocene. These studies have been summarised in a series of reviews.[138]

The 25 mV s^{-1} repetitive-cycling CV profile of [4] in nitrobenzene, using a platinum electrode (condition 4a), exhibited two clear-cut oxidation processes (figure 4.7a): a quasi-reversible oxidation centred at +0.66 V vs. SCE representing the ferrocene/ ferrocenium redox wave, and an irreversible waveform at +1.68 V vs. SCE, which is due to the oxidation of the thiophene ring. There was no visible formation of polymer on the electrode surface, but irregularities in the portion of the waveform representing the thiophene oxidation and the general increase in both anodic peak potentials upon eight successive cycles suggests that a sluggish and irreversible oxidation leading to some degree of chemical coupling had occured. Futher studies on the electrochemical properties of this compound are in progress.

V (mV/s^{-1})	$E_{p(a)}$ (volts)	$E_{p(c)}$ (volts)	$E_{1/2}$ (volts)	ΔE_p (volts)
50	0.60	0.24	0.42	0.36
100	0.94	-0.12	0.41	1.06
300	1.08	-0.22	0.43	1.30
600	1.22	-0.40	0.41	1.62

Table 4.2
Voltammogrammic data for the Fc / Fc^+ wave of [4] (vs. SCE) whilst employing condition 4a.

The CV profile in acetonitrile using a platinum electrode (condition 4b) was dissimilar to that obtained with the use of nitrobenzene as solvent. Over a series of scan rates, whilst oxidation resulted in a series of distorted peaks, scan reversal (reduction) led to symmetrical waveforms whose traces clearly crossed those of the forward scan at about +1.5 V vs. SCE when the slow scan speeds of 10 and 25 mV sec^{-1} were employed (figure 4.7b). These CV profiles, plus the thin and patchy rust coloured film observed on the working electrode upon termination of the experimental proceedure, suggest the occurence of weak product adsorption due to the oxidation of the iron portion of the

ferrocene moiety of [4], its demetalation, and the weak adsorption of oxidised iron on the working electrode.

V (mV/s^{-1})	$E_{p(a)}$ (volts)	$E_{p(c)}$ (volts)	$E_{½}$ (volts)	ΔE_p (volts)	$\frac{I_p{}^{(c)}}{I_p{}^{(a)}}$	$\frac{I_p{}^{(a)}}{V^{½}}$
10	0.60	0.26	0.43	0.34	0.31	1.10
25	0.64	0.20	0.42	0.44	0.55	0.80
50	0.67	0.17	0.42	0.50	0.81	0.59
100	0.70	0.11	0.41	0.59	0.87	0.55

Table 4.3
Voltammogrammic data for the Fc / Fc^+ wave of [4] (vs. SCE) whilst employing condition 4b.

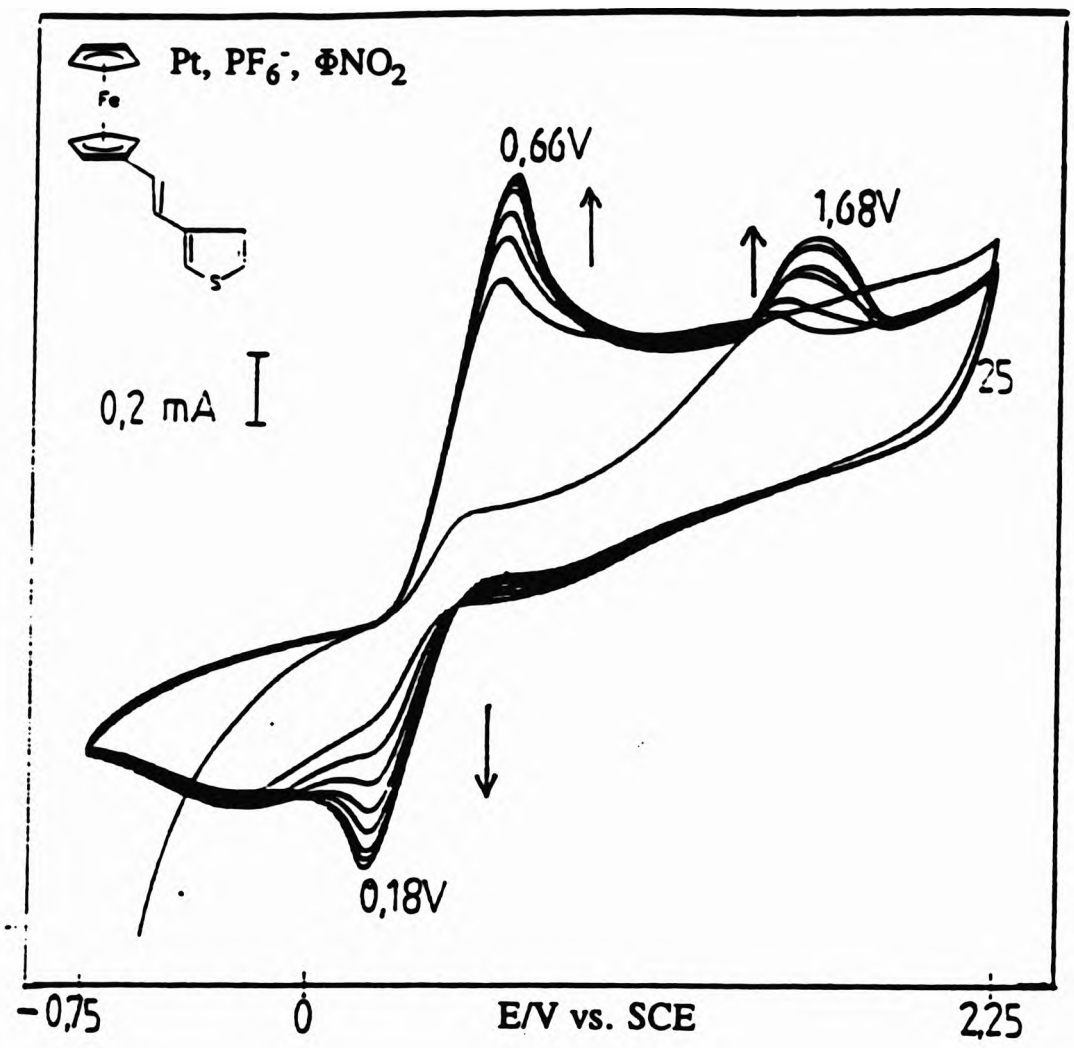

Figure 4.7a
Repetitive-cycling CV profile of [4] at 25 mV sec^{-1}, using condition 4a.

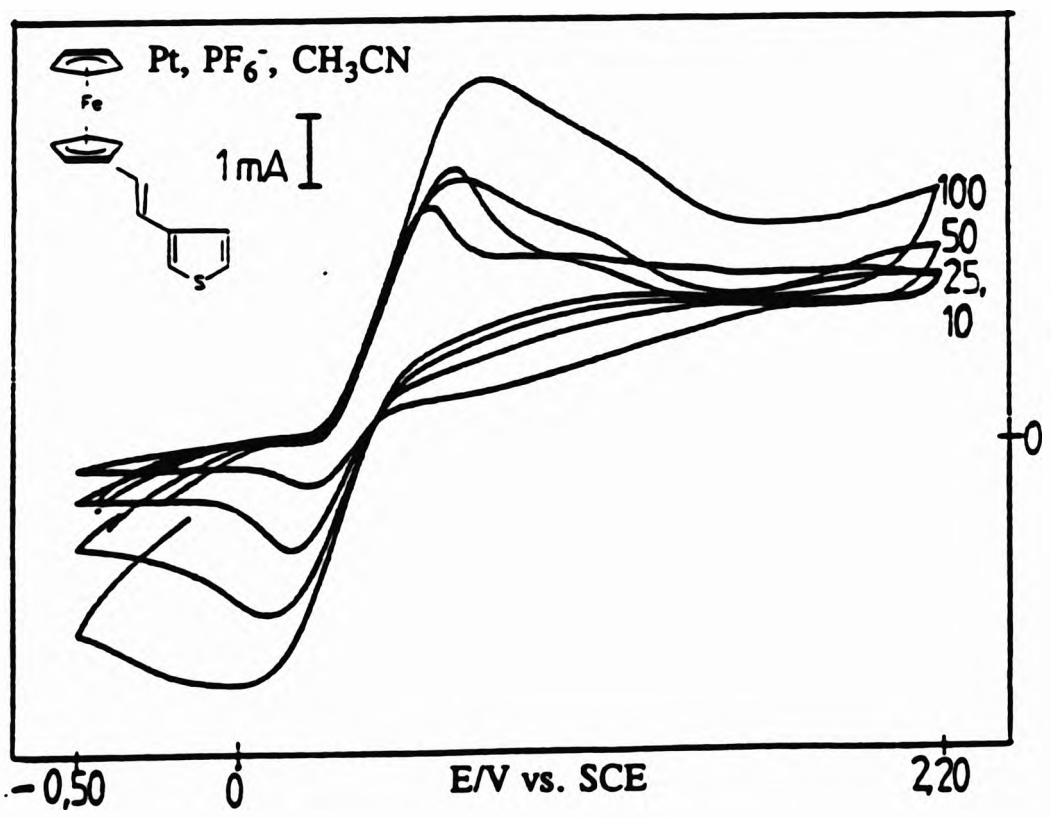

Figure 4.7b
Single-trace CV profile of [4] using condition 4b at different scan speeds (10, 25, 50, and 100 mV/0 sec^{-1}).

4.5.5 The CV behaviour of 3,4-bis(2´-ethenylferrocenyl)thiophene, [5]

Figures 4.8a - 4.8c depicts the CV profiles of [5] in acetonitrile using platinum as a working electrode (condition 5). At sweep rates below 250 mV s^{-1} (figure 4.8a) the waveforms reveal a quasi-reversible electron transfer process with a half-wave potential analogous to that of [4] (+0.45 V vs. SCE). When the scan rate was however increased to, and over 250 mV s^{-1}, a quasi-reversible charge transfer process with a new half-wave potential of +0.24 V vs. SCE resulted (figures 4.8b and 4.8c). It is therefore assumed that, in contrast to a "pure $2e^-$" transfer process, leading to the oxidation of the two structurally identical ferrocene units in one elementary step, the compound [5] undergoes two successive $1e^-$ charge transfer processes. The first quasi-reversible oxidation process at +0.24 V leads to the formation of a stable mixed-valent Fe(II)/Fe(III) monocation [29], which then undergoes a disproportionation reaction to generate the dication in a manner depicted below:

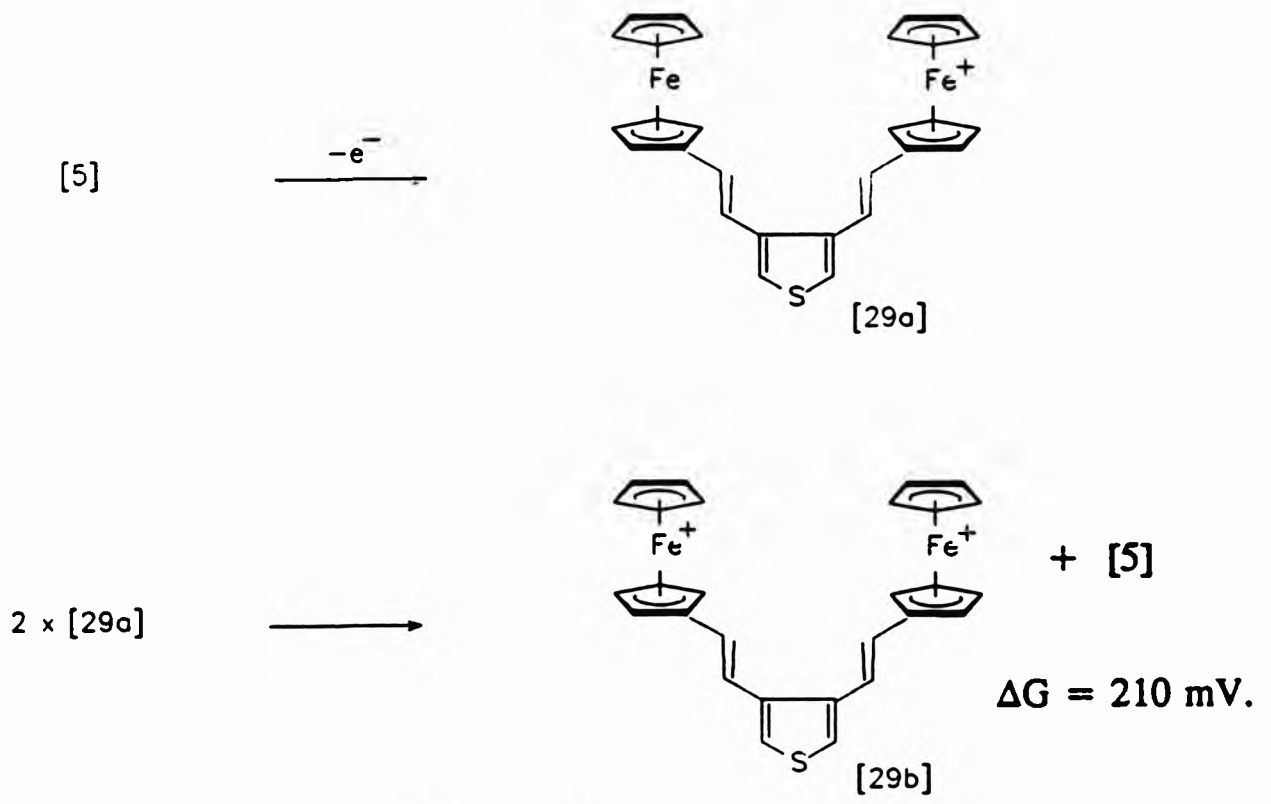

Figure 4.8
A schematic diagram of the two-step oxidation process attibuted to 3,4-bis(2´-ethenylferrocenyl)thiophene, [5].

Normally, when two ferrocenyl groups are separated by a saturated linkage, both iron sites oxidise independently at the same potential because the ferrocenyl groups react weakly, if at all. The +210 mV difference in the half-wave potentials of the two iron sites in [5] however indicate that there is a direct metal-metal interaction, and the presence of the bridging thiophene unit does not prevent the delocalisation of the valence electrons between these two ferrocene groups.

V (mV/s)	$E_{p(a)}$ (volts)	$E_{p(c)}$ (volts)	$E_{½}$ (volts)	ΔE_p	$\frac{I_p{}^{(c)}}{I_p{}^{(a)}}$	$\frac{I_p{}^{(a)}}{V^{½}}$
10	0.63	0.23	0.43	0.40	1	0.19
25	0.72	0.18	0.45	0.54	1	0.18
50	0.79	0.10	0.45	0.69	1	0.16
100	0.86	0.00	0.43	0.86	1	0.14
250	0.80	-0.36	0.22	1.16	1	0.051
500	0.92	-0.44	0.24	1.36	1	0.041

Table 4.4
Voltammogrammic data for the Fc / Fc^+ wave of [5] (vs. SCE) whilst employing condition 5.

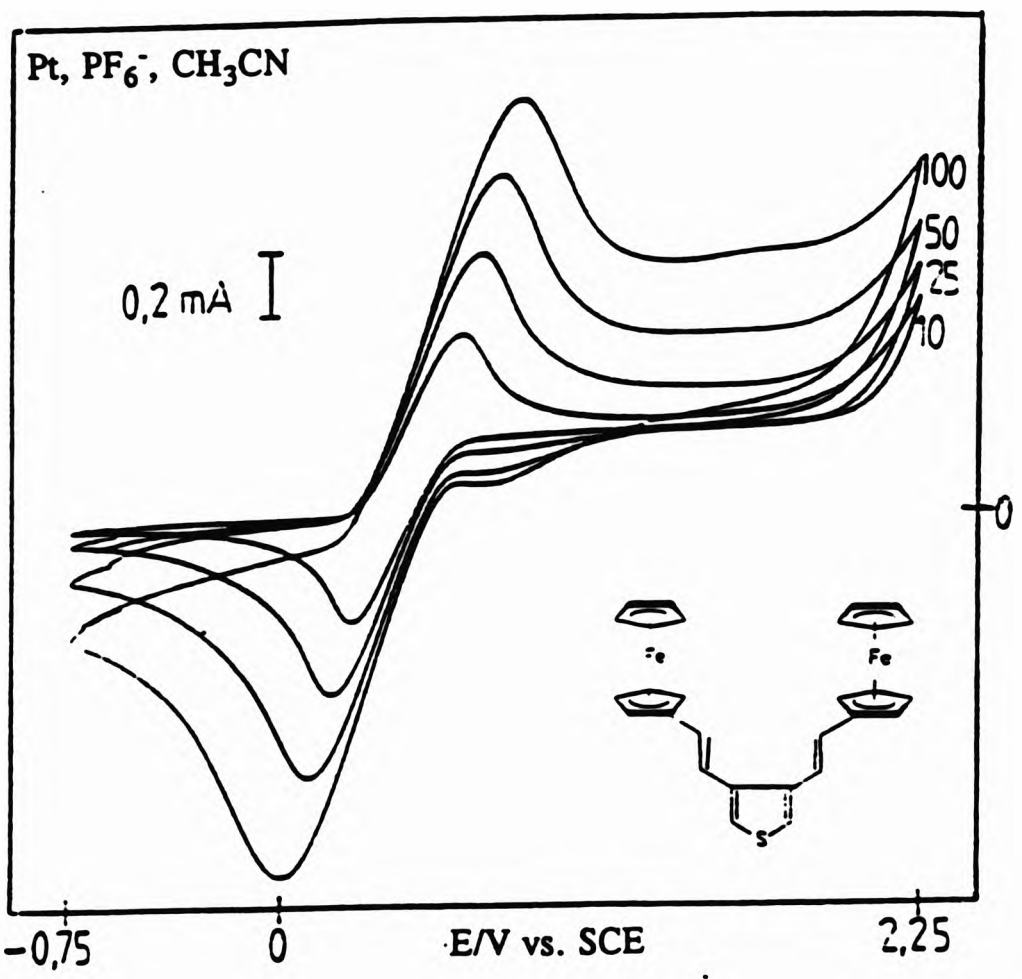

Figure 4.8a
Single-trace CV profile of [5] using condition 5 at different scan speeds (10, 25, 50, and 100 mV sec^{-1}).

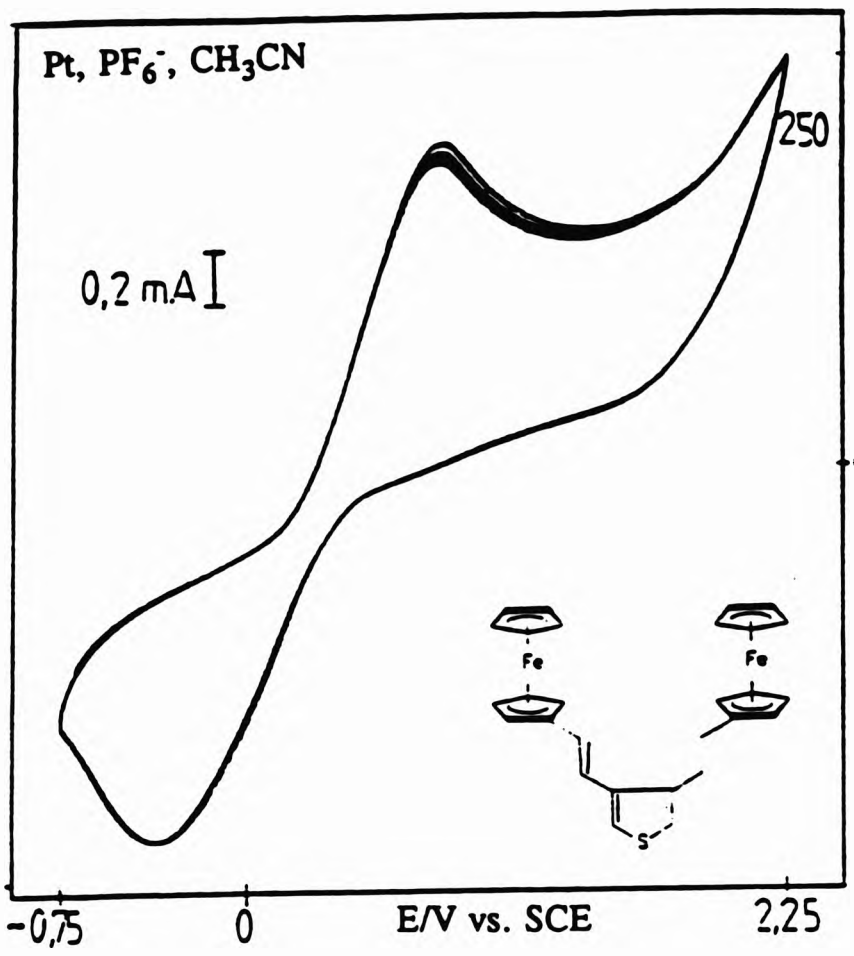

Figure 4.8b
Repetitive-cycling CV profile of [5] at 250 mV sec^{-1}, using condition 5.

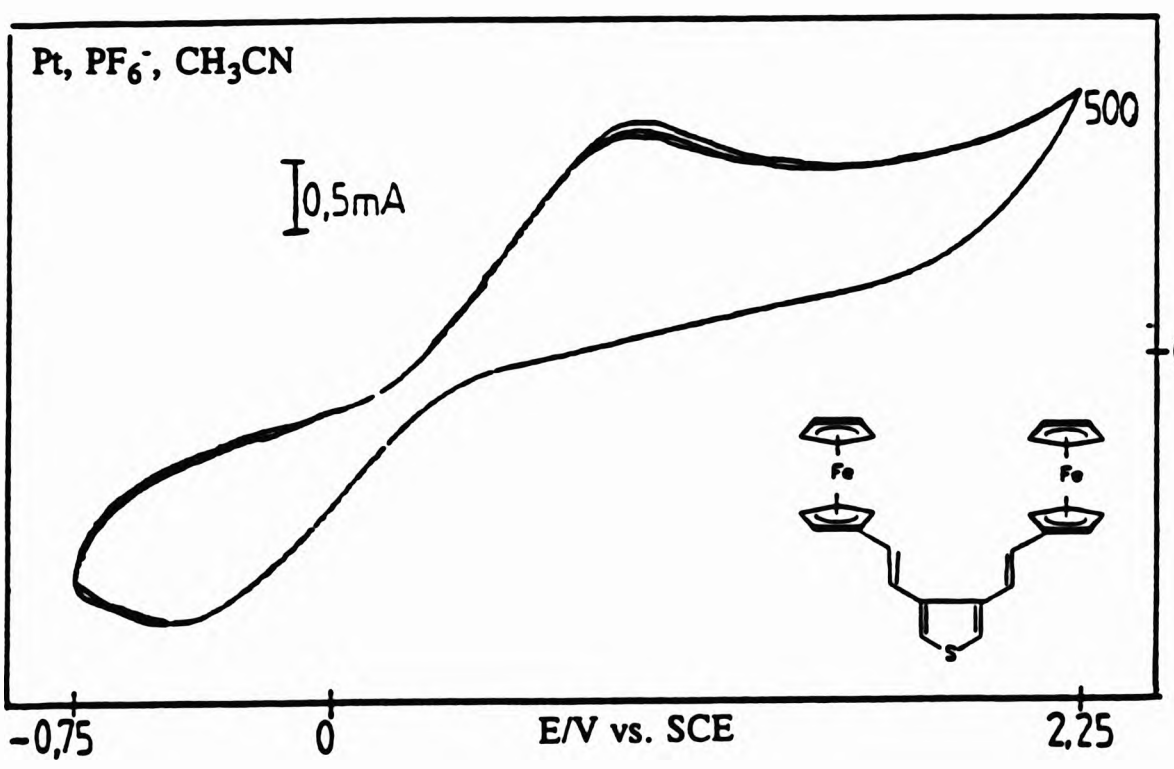

Figure 4.8c
Repetitive-cycling CV profile of [5] at 500 mV sec^{-1}, using condition 5.

Although the disproportionation constant for Scheme 4.1, K = [5][29b]/[29a]^2, can normally be determined from the difference between the standard redox potentials using the equation $-RT \ln K = nF(\Delta E^{\circ})$, there is a difficulty in the accurate determination of the individual standard potentials of this two-step redox process. This is because, due to the quasi-reversibility of the waveform obtained*, the rate of electron transfer is such that mass-transport is incapable of maintaining Nernstian equilibrum at the electrode surface, thus the observed $E_{1/2}$ does not accurately correspond to E°; and the large $\Delta E_{1/2}$ observed (+210 mV) does not indicate a large ΔE°. Moreover, scanning to high potentials at room temperature and on the very slow sweep rates used, leads a formally measurable half-wave potential which is actually (of a value equal to) the mean value of the two individual half-wave potentials. Although this leads to a difficulty in the establishment of the precise E° for either of the two individual oxidative processes illustrated, the observation of a single redox profile in the voltammograms obtained (figure 4.8a) implicates the occurrence of a multielectron transfer process where the difference between the two standard redox potentials is actually not greater than 150 mV.[139]

Generally, the redox values obtained for [5] compare well to that of 1,1´-terferrocene.[140] Stable mixed valence species have also been obtained during the oxidation of biferrocene,[141] acetyldiferrocenes,[142] and [1,1´] ferrocenophanes.[143,144]

*This quasi-reversibility, stemming from large peak separations (ΔEp), could be due to the high solution resistances especially encountered in non-aqueous solvents.

4.5.6 The CV behaviour of 1-(ferrocenyl)-3-(3´-thienyl)-prop-2-ene-1-one, [6]

V (mV/s^{-1})	$E_{p(a)}$ (volts)	$E_{p(c)}$ (volts)	E^{o} (volts)	ΔE_p	$\frac{I_p{}^{(c)}}{I_p{}^{(a)}}$	$\frac{I_p{}^{(a)}}{V^{1/2}}$
10	0.69	0.48	0.58	0.21	0.40	0.080
25	0.71	0.41	0.56	0.30	0.47	0.064
50	0.73	0.34	0.54	0.39	0.57	0.055
100	0.75	0.29	0.52	0.46	0.68	0.044

Table 4.5
Voltammogrammic data for the Fc / Fc^{+} wave of [6] (vs. SCE) whilst employing condition 6.

The CV waveforms of 1-ferroceneyl-3-(3'-thienyl)-prop-2-ene-1-one [6], employing condition 6 (degassed acetonitrile, platinum working electrode), are illustrated in figures 4.9. The quasi-reversible oxidation peak attributed to the formation of the ferricenium cation was, in contrast to the redox profile of [4], shifted to more anodic values. This is possibly as a result of the electron-withdrawing capacity of the carbonyl function which makes the oxidation of the ferrocenyl-iron more difficult. Scan reversal at +2.25 V revealed an attenuation of the cathodic peak; indicating a degree of kinetic sluggishness for the reduction of the cation, and suggesting the existence of an interaction between the carbonyl moiety and the Fe(III) cation generated (figure 4.9a). Continuous cycling at 25 mV s^{-1} did not give rise to any polymer growth, but to a consistent decrease in both the anodic and cathodic peak-current densities due to electrode passivation (Figure 4.9b), whilst a deepening of the red colour of the initial electrolytic solution was observed.

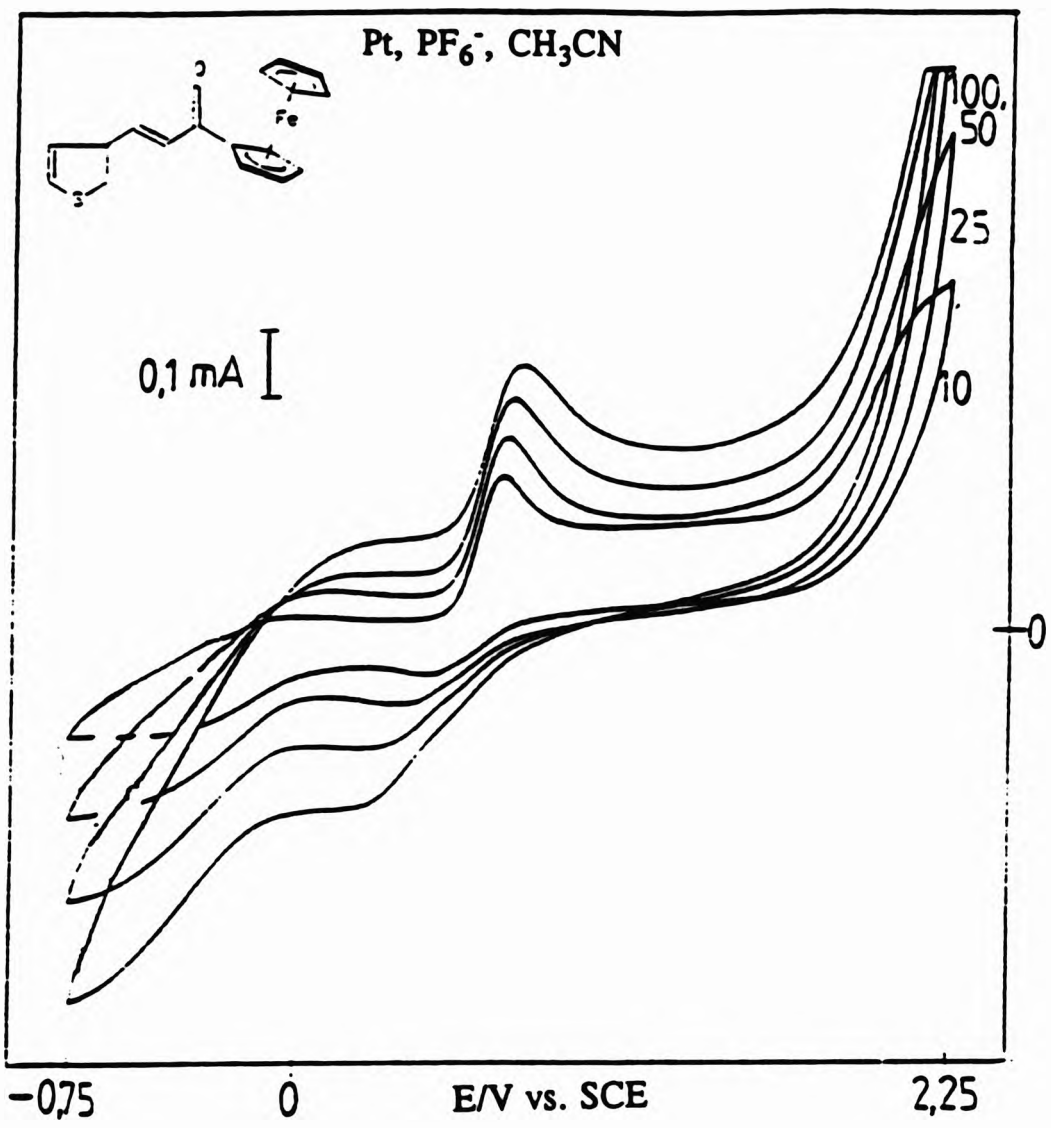

Figure 4.9a
Single-trace CV profile of [6] using condition 6 at different scan speeds (10, 25, 50, and 100 mV sec^{-1}).

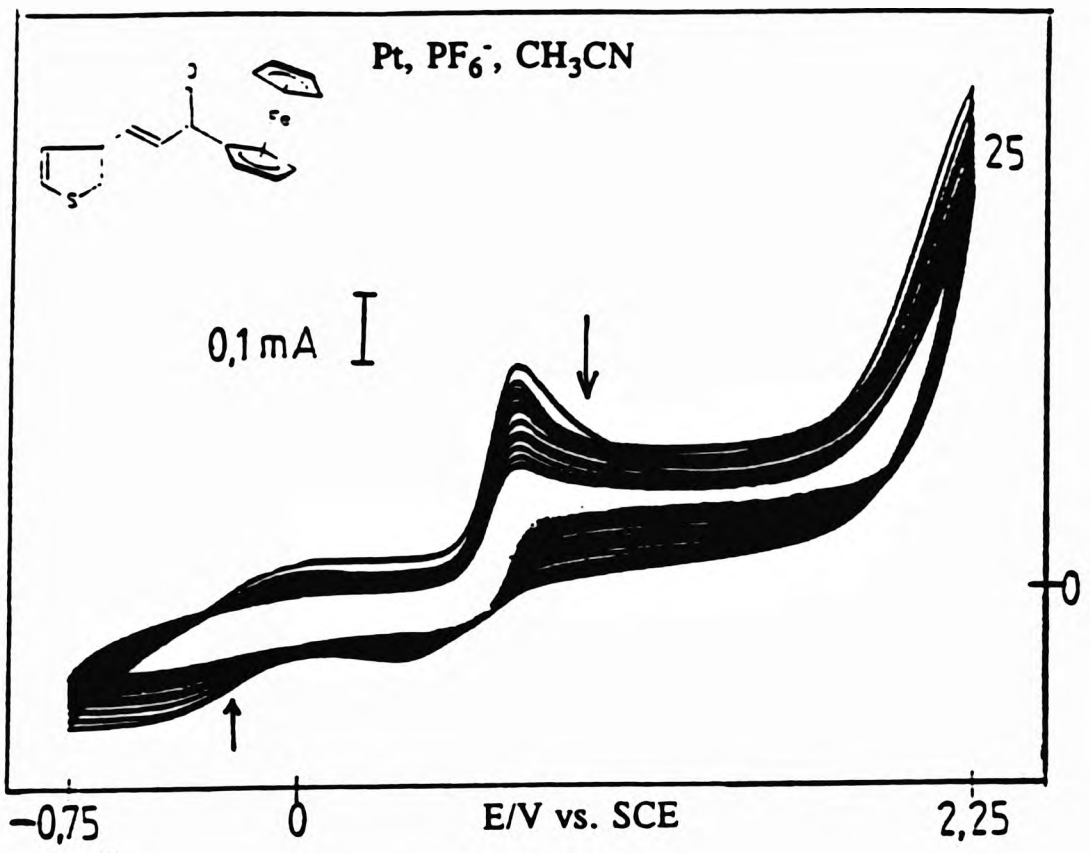

Figure 4.9b
Repetitive-cycling CV profile of [6] at 25 mV sec^{-1}, using condition 6

4.5.7 The CV behaviour of 1,5-bis(3´-thienyl)-penta-1,4-dien-3-one [7] & 1,9-bis(3´-thienyl)nona-1,3,6,8-tetraen-5-one [8]

The CV waveforms of [7] and [8] in degassed acetonitrile using a platinum electrode (figures 4.10 and 4.11 respectively) are characterised by two ill-defined oxidation peaks. It is assumed that the first of these peaks involves the oxidation of the carbonyl function, and the second peak (just before the anodic ramp) is due to an irreversible oxidation of the thiophene moiety. The greater electron withdrawing effect of the carbonyl group of [7], as evidenced in section 3.3.1.[A], is accompanied by a shift of the ionisation potential of its thiophene function to higher values, in comparison to that of [8]. Due to electron withdrawal from the thiophene ring by the carbonyl group, there is a difficulty in effecting the ionisation of the thiophene moiety, and thus a concomitant inability in effecting polymerisation.

The repetitive cycling of these two compounds using analogous conditions resulted in a relative constancy of the anodic peak-current for the first oxidation wave. The peak-current density of the second anodic wave, attributed to the thiophene function, however gradually diminished in intensity (figures 4.10b and 4.11b). The production of a thin gold film on the electrode surface suggests the formation of a passivating layer on the electrode from electrochemical processes attributed to the ketonic moiety.

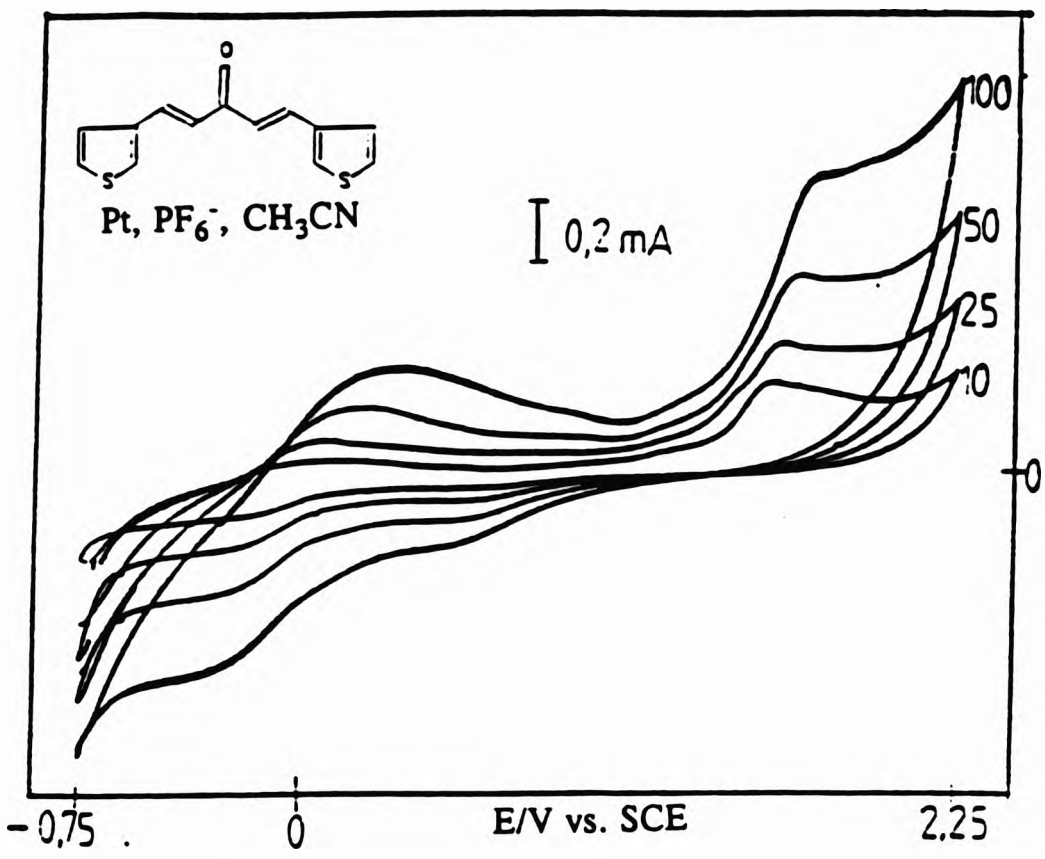

Figure 4.10a
Single-trace CV profile of [7] using condition 7 at different scan speeds (10, 25, 50, and 100 mV sec^{-1}).

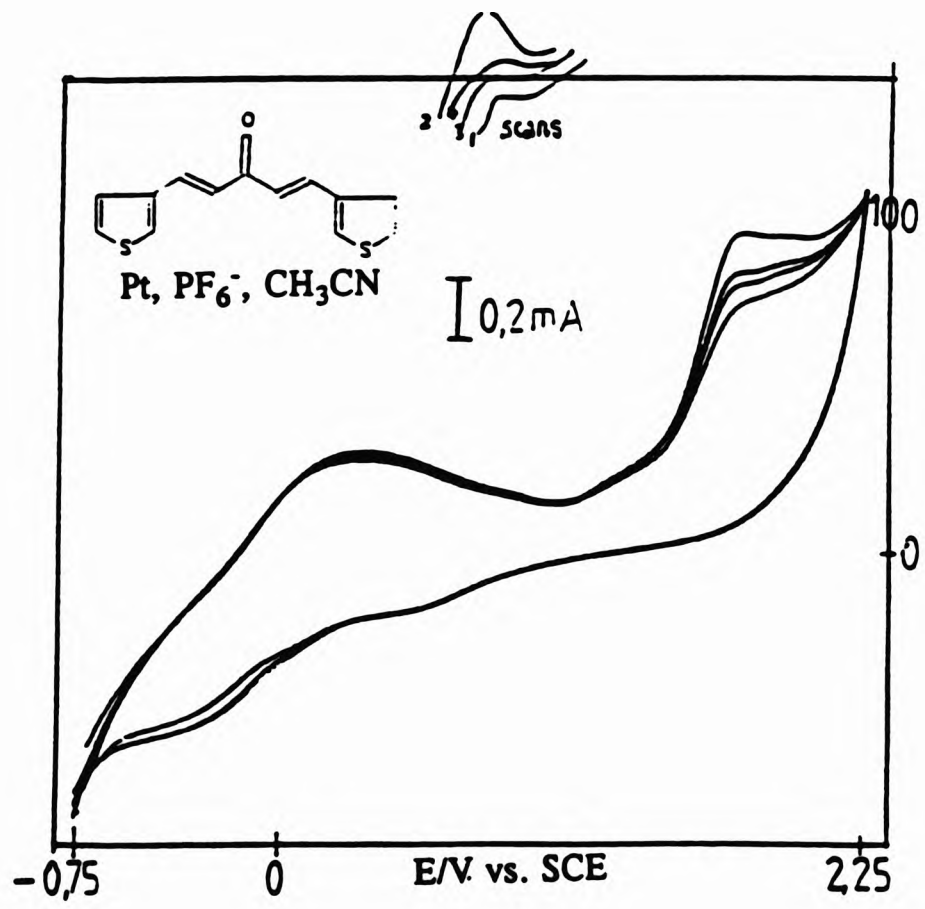

Figure 4.10b
Repetitive-cycling CV profile of [7] at 100 mV sec^{-1}, using condition 7.

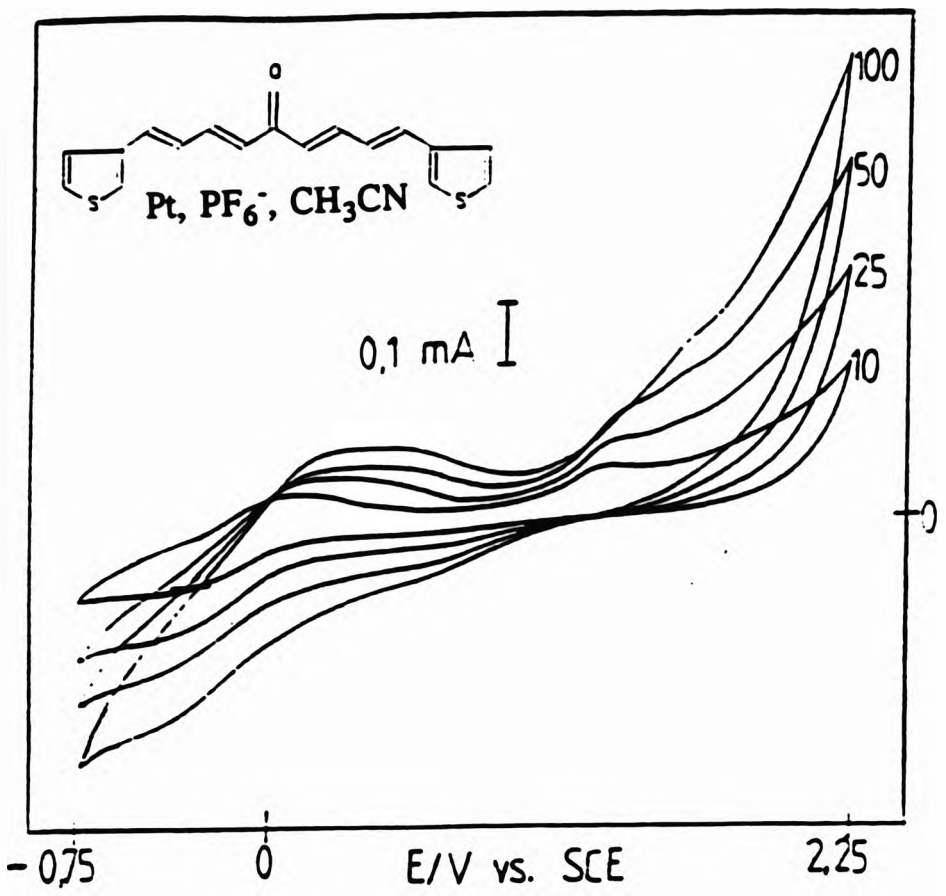

Figure 4.11a
Single-trace CV profile of [8] using condition 8 at different scan speeds (10, 25, 50, and 100 mV sec^{-1}).

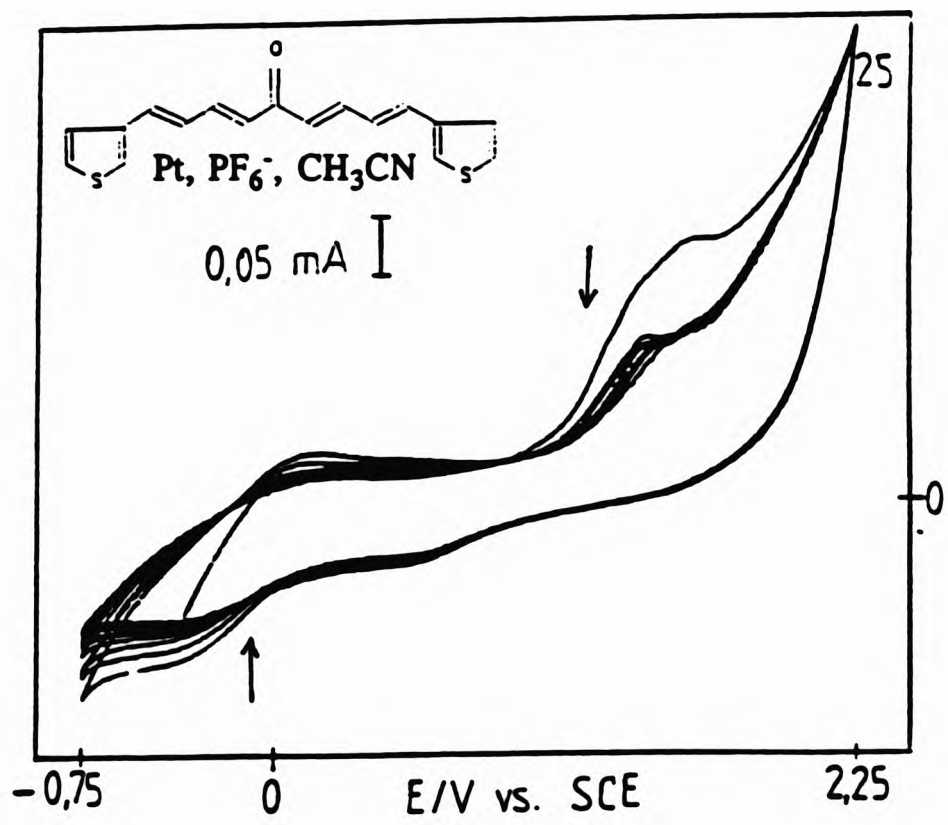

Figure 4.11b
Repetitive-cycling CV profile of [8] at 25 mV sec^{-1}, using condition 8.

4.5.8 The CV behaviour of 3-(Trimethylsilyl)thiophene, [9]

Figure 4.12a depicts the steady state cyclic voltammogram of 3-(trimethylsilyl)thiophene [9], in nitrobenzene using a platinum working electrode, and a scan speed of 25 mV s^{-1} (condition 9a). On the anodic sweep, there is an adsorption prewave at about +0.8 V vs. SCE, followed by the main polymer oxidation peak at +1.11 V vs. SCE. Scan reversal revealed a desorption prewave at about +1.0 V vs. SCE which is followed by a main cathodic peak at +0.84 V vs. SCE. A decrease in the time scale of the cycling process to 600 and 900 mV s^{-1} resulted in the observation of nucleation loops at +2.0 V and +2.19 V, oxidation waves at +1.42 V & +1.67 V, and of reduction waves at +0.60 V and +0.22 V respectively (figures 4.12b and 4.12c).

During these studies, facile polymerisation of [9] on the working electrode was observed. The cathodic profile, corresponding to the dedoping of the adsorbed species could, in principle, be used to quantify the amount of polymer deposited on the electrode. The regular increase of the anodic peak-current of the waveform during successive cycling also indicated a continuous growth of this polymer on the electrode surface,[145] and the broadness of the anodic half-peak width reflects the polymerisation of oligomers with wide range of conjugated chain-lengths, some of which should be due to parasitic 2,4 (and possibly 2,3) coupling caused by a progressive equivalence in the reactivity of the α- and β-positions of the thiophene unit.[71, 73]

The adhered film exhibited a high degree of electrochromicity upon switching; from blue-green (between +0.8 and +1.8 V vs. SCE) on oxidation, to deep orange (from -0.75 to +0.3 V vs. SCE) on reduction. An observed +0.23 V shift of the anodic peak potential upon six consecutive cycles (figure 4.12a) could be attributed to IR drop across the film, resulting from the growth of a polymer whose conductivity is significantly lower than that of the platinum electrode used.

The change of solvent to acetonitrile (condition 9b) also highlighted the solvent dependency of the electroactivity of this monomer (within the potential limits scanned). Unlike the glossy, flexible, blue-green films yielded with the use of nitrobenzene as solvent, cyclic voltammetry in degassed acetonitrile yielded a stream of soluble blue-black material that diffused away from the anode into solution. Scan reversal did not elicit a colour change as there was no polymer on the electrode surface. The CV profile (figure 4.12d) showed a nucleation loop at +0.8 V, a cathodic peak at -0.3 V, but no anodic peak for the polymer was observed. This leads to the proposition that in contrast to the oxidation process in nitrobenzene, chain propagation in acetonitrile is terminated

at an early stage because the newly formed oligomeric cations react more readily with the electrolyte and/or the solvent, rather than participate in reaction(s) that relate to the polymerisation process. This abrupt termination of polymer-chain propagation leads to the diffusion of coloured, soluble and oxidised short-chained oligomers from the electrode, into the electrolytic solution.

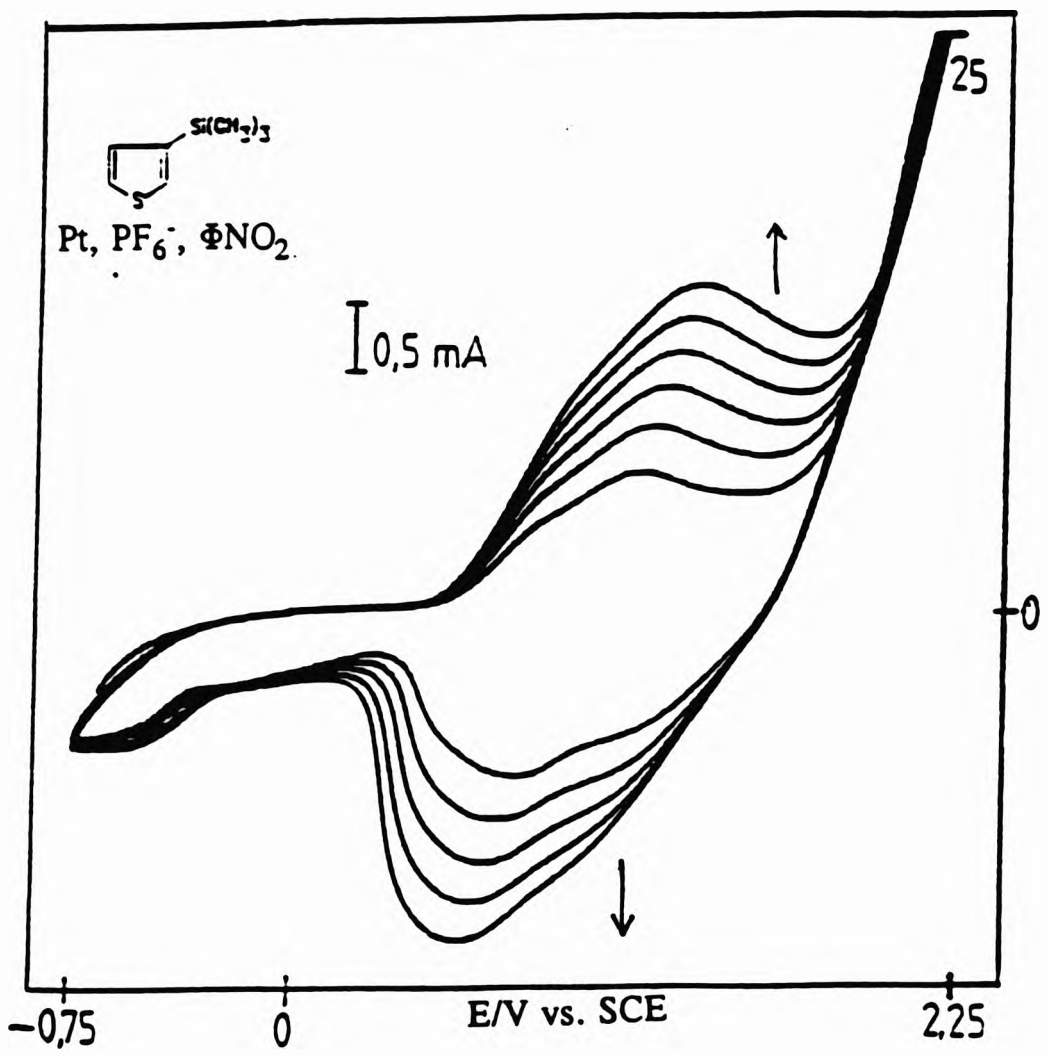

Figure 4.12a
Repetitive-cycling CV profile of [9] at 25 mV sec^{-1}, using condition 9a.

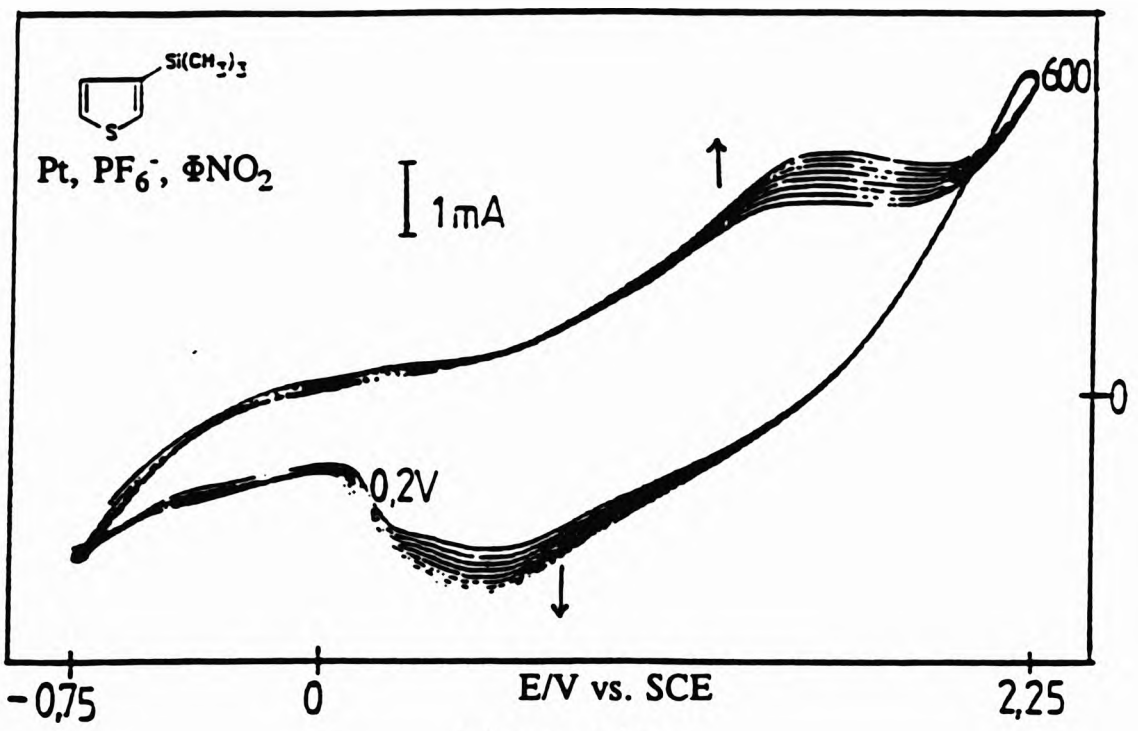

Figure 4.12b
Repetitive-cycling CV profile of [9] at 600 mV sec^{-1}, using condition 9a.

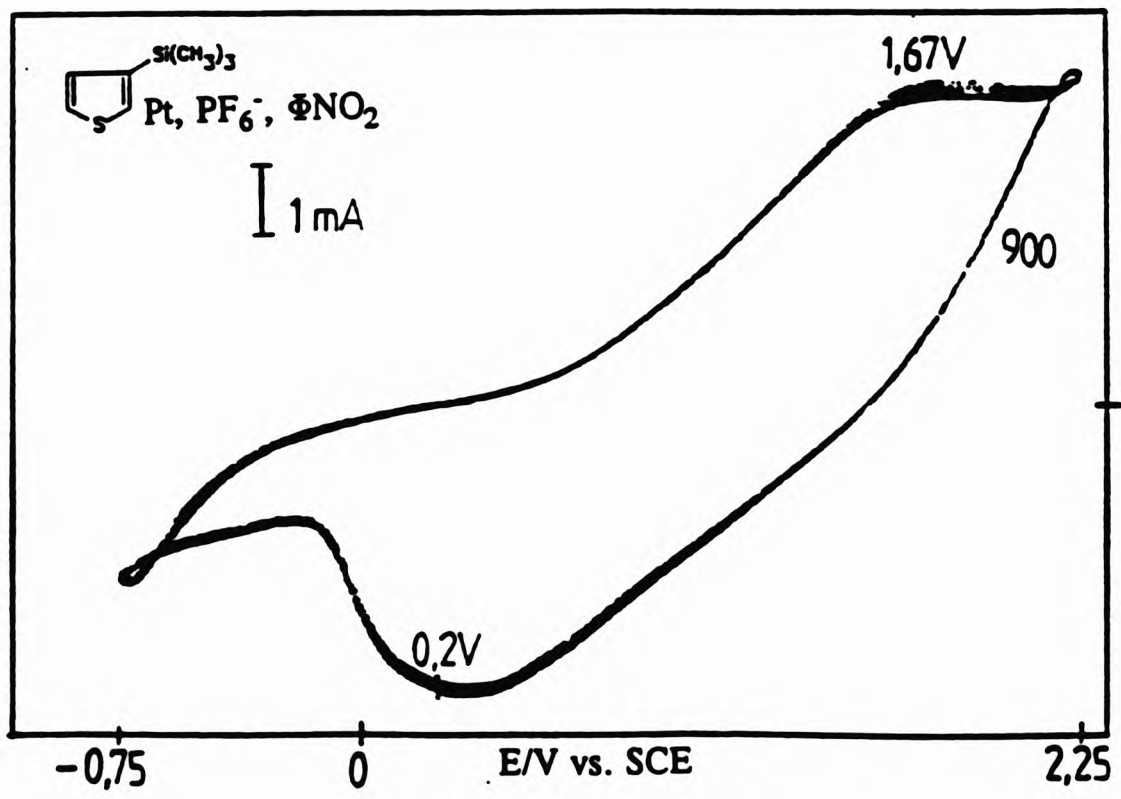

Figure 4.12c
Repetitive-cycling CV profile of [9] at 900 mV sec^{-1}, using condition 9a.

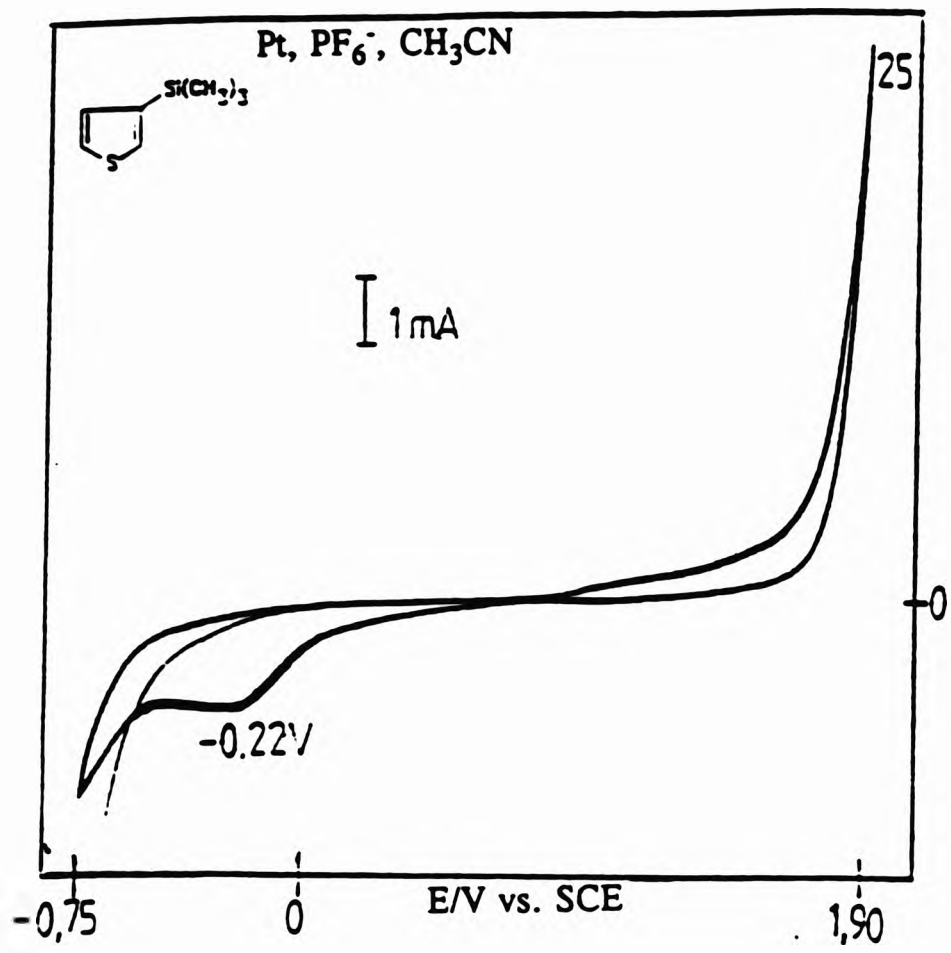

Figure 4.12d
Repetitive-cycling CV profile of [9] at 25 mV sec^{-1}, using condition 9b.

PART II

POLYMER SYNTHESES
&
CHARACTERISATION

The work reported in this section, encompassing chapters 5 and 6, was undertaken at the Unit for Speciality Electronic Polymers, University College, University of London.

CHAPTER 5

ELECTROCHEMICAL POLYMERISATION

5.1 INTRODUCTION

Although all the compounds examined by CV exhibited interesting current-voltage behaviour which deserve a more detailed electrochemical characterisation than was possible in this study, further research was focused on those monomers that exhibited electrochemical behaviour which was consistent with the original objective of the study *i.e,* those that oxidatively polymerised. To this end, anodic polymerisation by preparative constant potential electrolysis at suitable potentials (as extrapolated from respective CV profiles) was carried out on *trans*-1,2-bis(3´-thienyl)ethene [1], *trans*-1-(1´-pyrenyl)-2-(3´-thienyl)ethene [2], and 3-(trimethylsilyl)thiophene [9], using electrolytic solvents that were chosen on the basis of the following criteria:

- dielectric constant,
- anodic voltage limits,
- the mutual solubility of both monomer and supporting electrolytes,
- viscosity.

The features desirable in solvents used for organic electrochemistry have been discussed elsewhere.[146,147] Although polymerisation was attempted in a range of electrolytic solutions in order to acertain the best electrolytic conditions for polymerisation, the preferred supporting-electrolyte at the time these experiments were conducted was tetrabutylammonium-hexafluorophosphate, $(CH_3)_4NPF_6$. This is due to the slightly greater resistance of the PF_6 anion toward anodic oxidation than either its tetrafluoroborate or perchlorate analogues.[148] The PF_6 anion has also been reported to have produced some of the most highly conductive 3-substituted polythiophene films.[149] The choice of the other electrolytes used was based upon their general availability, and all the electrolytes used were of electrochemical grade.

5.2 CONSTANT POTENTIAL ELECTROLYSIS

The constant potential electrochemical polymerisation of monomers [1], [2], and [9] was carried out in a two-compartment electrochemical cell at room temperature (15°C) and under a blanket of nitrogen. In all cases a saturated calomel electrode (SCE) served as the reference electrode while a platinum wire and glass-backed platinum flag (2 cm x 2 cm) served as auxiliary and working electrodes respectively.[150] Polymerisation conditions are detailed in tables 5.1 - 5.3.

Prior to initiation of polymerisation, the platinum working electrode was subjected to surface modification by anodisation. A thin oxide layer was grown on the electrode by subjecting it to 30-second current pulses of 0.5 mA whilst being immersed in an 0.5 mol dm^{-3} solution of sulphuric acid. This was repeated until oxygen evolution occurred at the electrode.

5.2.1 The attempted syntheses of p-doped poly(2,5-thiophenediyl)-3-(trimethylsilyl)thiophene (Poly[9]), by the electropolymerisation of 3-(trimethylsilyl)thiophene [9]

Table 5.1 contains the conditions used in the constant potential electrolysis of [9].

The use of an solution containing lithium perchlorate in degassed acetonitrile (condition 5.1) resulted in neither film formation on the electrode nor the formation and subsequent diffusion of oligomers into the electrolytic solution. Further electropolymerisation attempts in an electrolytic solution of tetrabutylammonium bromide in degassed nitrobenzene (condition 5.4) led to the generation of a deep red solution. This is probably due to the formation of free bromine at the anode, which in turn, might result in the bromination of the thiophene moiety. α-bromination of the thiophene ring would support reports on the electrochemical oxidation of some substituted thiophenes using ammonium bromide as the supporting electrolyte, in which the electrochemical oxidation of 2,5-dimethylthiophene resulted in the exclusive formation of 3-bromo-2,5-dimethyl thiophene,[151] while the oxidation of 2- and 3-methylthiophene yielded 5-bromo-2-methyl thiophene (from 2-methyl thiophene) and a mixture of 2-bromo-3-methyl- and 2,5-dibromo-3-methylthiophene (from the 3-methylthiophene) respectively.[152] However, it is more likely that in this instance, the generation of free bromine would result in the formation of 3-(bromo)thiophene through a displacement of the trimethylsilyl moiety, and as quantitatively obtained when [9] is treated with N-

Bromosuccimide in DMF.[153]

In concordance with CV results, the propagation of the polymer chain was solvent dependent. Whilst constant potential electrolysis in an electrolytic solution containing the PF_6 anion in degassed acetonitrile (condition 5.5) resulted in the formation of oxidised and soluble blue-black, low molecular weight oligomers at such a rate that it completely coloured the electrolytic solution within sixty minutes at the applied potential (+2.0 V vs. SCE), no polymer formation on the electrode surface was observed. A change of solvent to nitrobenzene (condition 5.6) however resulted in the rapid formation of a free-standing, highly flexible and glossy blue-black polymer film that easily peeled off the electrode surface. The film thus formed [30] was rinsed in acetone and briefly dried in a stream of air at room temperature. It was insoluble in common solvents, including propylene carbonate, tetrahydrofuran, dichloromethane, nitrobenzene, toluene, dimethylformamide, butanone, propan-2-ol, and acetone. The polymer film was observed to undergo gradual degradation with time, due to the decomposition of the dopant. This was indicated by the appearance of white deposits on the interior of the vial inside which it was stored, after a three-week period.

	Concentration of monomer (x 10^{-3} mol dm^{-3})	Supporting Electrolyte	Concentration of Supporting electrolyte (x 10^{-3} mol dm^{-3})	Solvent used	Volume of Solvent (cm^3)	Applied Potential (V vs.SCE) (Time in hrs)	Remarks
Condition 5.1	20	$LiClO_4$	200	CH_3CN	50	2 - 2.80 V in 0.2 V intervals. (3 hrs. at each step).	No deposit.
Condition 5.2	40	$^-SO_3CF_3$	20	ΦNO_2	25	2.70 (up to 24).	10% of the electrode was covered with a blue-black film.
Condition 5.3	40	$^-SO_3CF_3$	20	ΦNO_2	25	3.03 (up to 18).	40% of the electrode was covered with a brown film that dissolved in acetone, leaving a black residue.
Condition 5.4	40	$(CH_3)_4NBr_2$	203	ΦNO_2	50	2.80 (8)	No deposit. Solution turned red.
Condition 5.5	20	$(CH_3)_4NPF_6$	200	CH_3CN	50	2.00 (4)	No deposit. There was a blue-black "wisp" from the electrode that dissolved into the solution, turning it completely blue-black within a period of 2 hrs.
Condition 5.6	20	$(CH_3)_4NPF_6$	200	ΦNO_2	50	1.90 (2)	There was the rapid formation of a blue-black film with a metallic lustre. The film was very flexible and easily peeled off the electrode [30].

Table 5.1
Potentiostatic conditions used for the oxidative electropolymerisation of 3-(trimethylsilyl)thiophene at room temperature (15°C).
Φ = phenyl group; PC = Propylene Carbonate; DMF = Dimethylformamide.

5.2.2 The attempted syntheses of p-doped poly-(2´,5´-thiophenediyl)-1-(1˜-pyrenyl)2-(3´-thienyl)ethene (Poly[2]), by the electropolymerisation of *trans*-1-(1´-pyrenyl)-2-(3˜-thienyl)ethene, [2]

The conditions used in the electrolysis of [2] are summarised in table 5.2. The presence of the p-toluenesulphonate anion (PTS^-) suppressed effective polymerisation, even in nitrobenzene and at high electrolyte concentrations, possibly as a consequence of steric constraints imposed by the bulkiness of this anion. This result is consistent with findings obtained from the attempted electropolymerisation of thiophene using similar conditions.[154] The influence of the monomer:electrolyte ratio on the propensity of [2] to undergo electropolymerisation was also apparent, and solvent dependent. An increase in the ratio of monomer ([2]) to electrolyte ($(CH_3)_3NPF_6$) in degassed nitrobenzene from 1:1 to 1:10, as seen in the progresson from condition 5.15 to condition 5.16, was accompanied by facile polymerisation on the electrode surface. Only slight oligomer formation was observed when a 3:1 ratio of the same monomer and electrolyte in propylene carbonate was used (condition 5.7), and electrolysis in a 1:1 ratio resulted in the formation of a thin golden-yellow passivating film on the electrode surface (condition 5.8). A comparison of the analogous results obtained from the use of conditions 5.8 and 5.14 also establishes a concentration dependency of the polymerisation process.

The flexibility and yield of the blue-black film obtained on the electrode surface during the electrolysis of [2] in a medium of degassed acetonitrile and PF_6 anions (condition 5.17), were enhanced by the substitution of degassed nitrobenzene as solvent (condition 5.16). With the use of this latter solvent, polymerisation was also effected at a lower oxidation potential.

Generally, the yield of material obtained from the oxidation of [2] increased in the order acetonitrile (from condition 5.17) < dichloromethane (from condition 5.12) = nitrobenzene (from condition 5.16). The flexibility of these films also increased in the order acetonitrile << dichloromethane < nitrobenzene.

All conditions that led to film formation on the surface of the working electrode (conditions 5.12, 5.16 - 5.18) concomitantly resulted in the streaming of blue-black material (from the electrode) into the solution, and to a low yield of electrode-localised polymeric material. This would suggest the exclusion of most of the intermediate products that have been generated from the oxidation of this compound, from effective coupling and polymer-chain propagation. The profusion of coloured material from the anode also indicates a degree of solubility of the short-chained oligomeric material(s)

formed, in the solvent used.[155]

The materials [32] and [33], realised from the use of degassed acetonitrile containing PF_6 and ClO_4 anions respectively (conditions 5.17 and 5.18) did not undergo any noticeable decomposition upon prolonged storage. Neither did [31], obtained from a solution containing dichloromethane and the ClO_4 anion (condition 5.12). Gradual degradation of the dopant was however evident in [32], obtained from a solution of nitrobenzene and PF_6 anions (condition 5.16), after about four weeks. It is suspected that, in agreement with earlier reports on oxidised poly(3-methyl)thiophene films,[156] the ClO_4 anion is retained more strongly than PF_6^-.

All the polymeric materials produced were insoluble in all solvents in which attempts were made to dissolve them. These included propylene carbonate, tetrahydrofuran, dichloromethane, nitrobenzene, toluene, dimethylformamide, butanone, and propan-2-ol, and acetone.

	Concentration of Monomer. ($\times 10^{-3}$ mol dm^{-3})	Supporting Electrolyte	Concentration of Supporting Electrolyte ($\times 10^{-3}$ mol dm^{-3})	Solvent used	Volume of Solvent (cm^3)	Applied Potential (V vs. SCE). (Time in hours)	Remarks
Condition 5.7	2	$(CH_3)_4NPF_6$	0.67	PC	50	1.65 (5)	Slight blue-black wisp at anode. No deposit.
Condition 5.8	2	$(CH_3)_4NPF_6$	2.0	PC	50	1.65 (2)	Thin golden-yellow film. Possibly a passivating layer.
Condition 5.9	2	$(CH_3)_4NPF_6$	100	PC	50	1.65 (5)	
Condition 5.10	4	$\Phi CH_3SO_3^-$	1.33	PC	30	1.65 (5)	No deposit.
Condition 5.11	4	$\Phi CH_3SO_3^-$	100	PC	30	1.70 (15)	
Condition 5.12	10	$(CH_3)_4NClO_4$	100	CH_2Cl_2	50	1.70 (3)	Glossy blue-black film [31] that easily peeled off the electrode. Colour of solution turned blue-black.
Condition 5.13	2	$(CH_3)_4NPF_6$	0.67	ΦNO_2	50	1.65 (3)	Blue-black wisp from the electrode that dissolved into the solution .
Condition 5.14	2	$(CH_3)_4NPF_6$	2.0	ΦNO_2	50	1.65 (3)	- as above - Slight golden-yellow deposit on anode.
Condition 5.15	10	$(CH_3)_4NPF_6$	10	ΦNO_2	50	1.56 (3.5)	Half of the electrode was covered with a blue-black film. The film slid back into solution upon removal of electrode from solution.
Condition 5.16	10	$(CH_3)_4NPF_6$	100	ΦNO_2	50	1.55 (1)	Electrode was completely covered with a blue-black film [32] that easily peeled off .
Condition 5.17	10	$(CH_3)_4NPF_6$	100	CH_3CN	50	1.65 (3)	A Blue-black film covered the whole electrode. The film was very brittle and adhered firmly to the electrode and its yield was lower than that of [32].
Condition 5.18	10	$LiClO_4$	100	ΦCN	50	1.60 (4)	25% of the electrode was covered with a thin patchy blue-black film [33]. The formation of similar film achieved at 1.4 V.
Condition 5.19	4	$\Phi CH_3SO_3^-$	1.33	ΦNO_2	30	1.70 (4)	No deposit. Colour of solution at cathode turned deep-red.
Condition 5.20	4	$\Phi CH_3SO_3^-$	100	ΦNO_2	30	1.70 (4)	- as above -
Condition 5.21	20	$LiClO_4$	100	CH_3CN/ DMF (5:1)	50	1.70 (4)	No deposit. Electrolytic solution turned deep-yellow

Table 5.2

Potentiostatic conditions used for the oxidative electropolymerisation of *trans*-1-(1-pyrenyl)-2-(3-thienyl)ethene at room temperature (15°C). Φ = phenyl group; PC = Propylene Carbonate; DMF = Dimethylformamide.

5.2.3 The attempted syntheses of p-doped poly(2´,5´-thiophenediyl)-1,2-bis(3´-thienyl)ethene (Poly[1]), by the electropolymerisation of *trans*-1,2-bis(3´-thienyl)ethene, [1]

Table 5.3 (conditions 5.22 - 5.36) summarises the conditions imposed for the constant potential electrolysis of compound [1]. The influence of the type of anion used, on the outcome of the oxidation process, is quite evident. Oxidations involving the use of the bulky p-toluenesulphonate anion in either degassed acetonitrile or dimethylformamide (DMF) led to no obvious polymer or oligomer formation. The colour change observed during the unsuccessful polymerisation attempts in DMF (conditions 5.24 - 5.27) could be indicative of the oxidation of the solvent at the potentials employed.

Solvent effects are displayed in the results obtained in conditions 5.28 - 5.35. The constant potential electrolysis of [1] in a solution of $(CH_3)_3PF_6$ in degassed acetonitrile (condition 5.29) yielded a very brittle dark-blue film [35] that turned brown in colour after being rinsed in acetone and air-dried. The use of nitrobenzene as solvent under analogous conditions (condition 5.35) resulted in the production of a glossy blue-black film [36] which, unlike the film produced in acetonitrile, showed an increased flexibility and it also retained its physical appearance after rinsing and drying. Conditions 5.32 - 5.35 show that the effective generation of this material (and the degree of anion incorporation) is dependent on the applied potential.

The free-standing material [36] was the most flexible of all the films generated from electrosynthetic conditions that led to the formation of films on the electrode surface (conditions 5.28 - 5.31, 5.33 - 5.36). It was insoluble in propylene carbonate, tetrahydrofuran, dichloromethane, nitrobenzene, toluene, dimethylformamide, butanone, propan-2-ol and acetone, showed signs of degradation due to decomposition of dopant after one month's storage in an air-tight vial.

	Concentration of Monomer ($\times 10^{-3}$ mol dm^{-3})	Supporting Electrolyte	Concentration of Supporting Electrolyte ($\times 10^{-3}$ mol dm^{-3})	Solvent used	Volume of Solvent (cm^3)	Applied Potential (V vs. SCE). (Time in hours)	Remarks
Condition 5.22	20	$\Phi CH_2SO_3^-$	20	CH_3CN	50	1.60 (12)	No deposit.
Condition 5.23	20	$\Phi CH_2SO_3^-$	6.70	CH_3CN	50	1.60 (12)	
Condition 5.24	20	$\Phi CH_2SO_3^-$	6.70	DMF	50	1.50 (2)	No deposition on the electrode. The solution in the anodic compartment turned magenta whilst that of the cathodic compartment turned to the colour of "weak-tea".
Condition 5.25	20	$\Phi CH_2SO_3^-$	6.70	DMF	30	1.70 (2)	
Condition 5.26	20	$\Phi CH_2SO_3^-$	6.70	DMF	30	2.00 (4)	
Condition 5.27	20	$\Phi CH_2SO_3^-$	20	DMF	50	2.00 (2)	
Condition 5.28	20	$(CH_3)_4NPF_6$	6.70	CH_3CN	50	1.60 (4)	There was the formation of a brittle, translucent greenish-yellow film [34].
Condition 5.29	20	$(CH_3)_4NPF_6$	20	CH_3CN	50	1.60 (4)	A Blue-black film [35] covered the whole electrode. The film was very brittle and adhered firmly to the electrode.
Condition 5.30	20	$(CH_3)_4NPF_6$	6.70	PC	50	1.60 (6)	An army-green polymer covered approx. half of the anode. The polymer wispily dissolved back into the electrolytic medium.
Condition 5.31	20	$(CH_3)_4NPF_6$	6.70	PC	50	1.60 (6)	
Condition 5.32	20	$(CH_3)_4NPF_6$	200	ΦNO_2	50	1.10 (6)	No deposit.
Condition 5.33	20	$(CH_3)_4NPF_6$	200	ΦNO_2	50	1.20 (6)	
Condition 5.34	20	$(CH_3)_4NPF_6$	200	ΦNO_2	30	1.30 (6)	Blue-green polymer deposited on the electrode.
Condition 5.35	20	$(CH_3)_4NPF_6$	200	ΦNO_2	30	1.60 (6)	There was the formation of a blue-black film [36] which was less brittle than [35], and easily peeled off the electrode.
Condition 5.36	20	$(CH_3)_4NClO_4$	200	CH_3CN	50	1.60 (6)	Formation of a blue-black polymer [37] that adhered so firmly to the electrode that it had to be scraped off. The polymer yield was also quite low, although it completely covered the electrode.

Table 5.3

Potentiostatic conditions used for the oxidative electropolymerisation of *trans*-1,2-di(3-thienyl)ethene at room temperature (15°C).
Φ = phenyl group; PC = Propylene Carbonate; DMF = Dimethylformamide.

5.3 ELEMENTAL ANALYSIS

5.3.1 Material obtained from the electropolymerisation of *trans*-1,2-bis(3´-thienyl)ethene [1]

The percentage composition of the elements present in the film [36], engendered from the electropolymerisation of [1] in nitrobenzene (condition 5.35), was found to be; C: 54.81; H: 2.88; and P: 1.35%. The empirical formular deduced; $C_{10.5}H_{6.5}P_{0.1}$ approximates the stiochiometry of a polymer-anion ensemble which is made up of one dopant ion every ten/eleven monomer units. The slightly higher level of hydrogen in the synthesised material, in comparison to what was anticipated, could be due to an incomplete coupling of all the available α-positions. Since there are two thiophene moities per monomeric unit, there are four of such positions.

5.3.2 Material obtained from the electropolymerisation of *trans*-1-(1´-pyrenyl)2-(3˝-thienyl)ethene [2]

The percentage composition of the elements present in the material [32], obtained from the electropolymerisation of [2] (condition 5.16) was; C: 73.80; H: 3.22; S: 8.12; and P: 0.69%. This stoichiometry equates that of a PF_6-doped 2´,5´-thiophenediyl-1-(1˝-pyrenyl)2-(3´-thienyl)ethene polymer with the empirical formulae $C_{22}H_{11.4}S_{0.91}P_{0.08}$ and thus, with an average doping level of one dopant ion per eleven monomeric units. The slightly low level of hydrogen in the synthesised material might indicate slight coupling of the pyrene moiety.

5.3.3 Material obtained from the electropolymerisation of 3-(trimethylsilyl)thiophene [9]

The percentage composition of elements found in the flexible blue-black film [30], produced from the electropolymerisation of [9] (condition 5.6) was C: 48.75; H: 2.12; S: 24.68 and P: 1.67%. This gives an empirical formulae of $C_{4.06}H_{2.10}S_{0.77}P_{0.054}$ and a polymer stiochiometry of one dopant ion every fourteen coupled monomeric units. Assuming an intact assimilation of compound [9] during the polymerisation process, the elemental composition which should most-closely approximate that of the synthesised material should be that of a polymer that consists of a hydrogen content of about 6%. The calculated elemental composition of a polymer containing fourteen coupled 2,5-

thiophenediyl units of compound [9] and one dopant ion, $C_{98}H_{142}S_{14}Si_{14}^{+}$ PF_6^{-} is C: 51.02; H: 6.20; S: 19.45; Si: 17.04; and P: 1.34%. However, the distinctively low hydrogen level and the high sulphur level in the composition of the material [30] suggested it to be made up of an oligomeric chain that lacks the intact incorporation of the trimethylsilyl moiety, and approximations with thiophene oligomers were sought. The precentage composition of hydrogen in the polymeric material [30] was found to be more closely related to that calculated for a 2,5-thienylene polymer. Calculated for the tetra-decamer, $C_{56}H_{30}S_{14}^{+}$ PF_6^{-}, C: 51.87; H: 2.33; S: 34.62; and P: 2.39%. Calculated for a hypothetical polymer containing an intact assimilation of one monomer (*ie*; a monomer containing the trimethylsilyl moiety) per fourteen coupled monomeric units, $C_{59}H_{38}S_{14}Si^{+}$ PF_6^{-}; C: 51.77; H: 2.80; S: 32.79; Si: 2.05; and P; 2.26. It is noted that the amount of hydrogen in this hypothetical polymer is still greater than that found in the material.

5.4 CONDUCTIVITY MEASUREMENTS

Conductivity measurements, using a linear (four-point) probe electrode arrangement, were carried out only on free-standing films that had been intactly peeled off the working electrode. The current source employed was a Scycopel potentiostat converted into a galvanostat, and the current was measured with a Keithley 160 digital multimeter. Voltage was monitored by a Keithley 195A digital multimeter.
Although partially doped, all the materials measured proved to be semi-conducting.

5.4.1 Polymer(s) obtained from the electropolymerisation of *trans*-1,2-bis(3´-thienyl)ethene [1]

The glossy, blue-back, PF_6-doped film [36], exhibited a conductivity value of 3.5×10^{-2} S cm^{-1}.

5.4.2 Polymer(s) obtained from the electropolymerisation of *trans*-1-(1´-pyrenyl)-2-(3˜-thienyl)ethene [2]

The conductivity of the poly[2]$^{+}ClO_4^{-}$ material [31], derived from condition 5.12 was 4.20×10^{-3} S cm^{-1}, whilst that of poly[2]$^{+}PF_6^{-}$ material [32] (from condition 5.16), was 5.60×10^{-3} S cm^{-1}.

5.4.3 Polymer(s) obtained from the electropolymerisation of 3-(trimethylsilyl)thiophene [9]

The two sides of the film [30], derived from the implementation of condition 5.6 exhibited significant differences in conductivity. The surface that adhered to the electrode (the inner polymer surface) had a volume conductivity of 15 S cm^{-1}, whilst the surface exposed to the electrolytic solution (the outer polymer surface) had a volume conductivity of 100 S cm^{-1}.

CHAPTER 6

POLYMER CHARACTERISATION

6.1 THE ANALYSIS OF SURFACE MORPHOLOGY BY SCANNING ELECTRON MICROSCOPY*

6.1.1 Polymers derived from *trans*-1,2-bis(3´-thienyl)ethene [1]

Scanning electron micrographs of the PF_6-doped polymer [34] (condition 5.28) revealed it to possess a granular morphology (figure 6.1a), although this microstructure could have resulted from a previously-smooth, but very brittle, polymer which had undergone cracking upon contraction due to solvent evaporation. Energy dispersive electron probe X-ray microanalysis (EPMA) disclose the polymer to have a homogeneous distribution of sulphur (figure 6.1b) and of dopant ions (figure 6.1c).

On the other hand, the perchlorate-doped analogue [37] produced from condition 5.36 had a smooth but undulating microstructure with no sign of primary-particle incorporation (figure 6.2a). The observed undulation of the polymer surface could be the result of material contraction upon solvent evaporation. This ClO_4-doped polymer also displayed a greater degree of doping (figure 6.2c) than the PF_6-doped [34].

*Details of the methodology are contained in the experimental section (chapter 8).

Legends for the subsequent micrographs are as follows:

Figure 6.1a (*micrograph 300009*): SEM micrograph of the Poly[1]$^{+}PF_6^{-}$ material [34], synthesised by the use of condition 5.28. The granular morphology might represent the cracking of a brittle film formed by the contraction caused by solvent evaporation.

Figure 6.1b (*micrograph 300011*): EPMA micrographs showing a dotmapping of S-characteristic X-ray images of the same area of [34] represented in Figure 6.1a.

Figure 6.1c (*micrograph 300012*): EPMA micrographs showing a dotmapping of P-characteristic X-ray images of the same area of [34] represented in Figure 6.1a.


300009 20KV X3.90K 7.7um

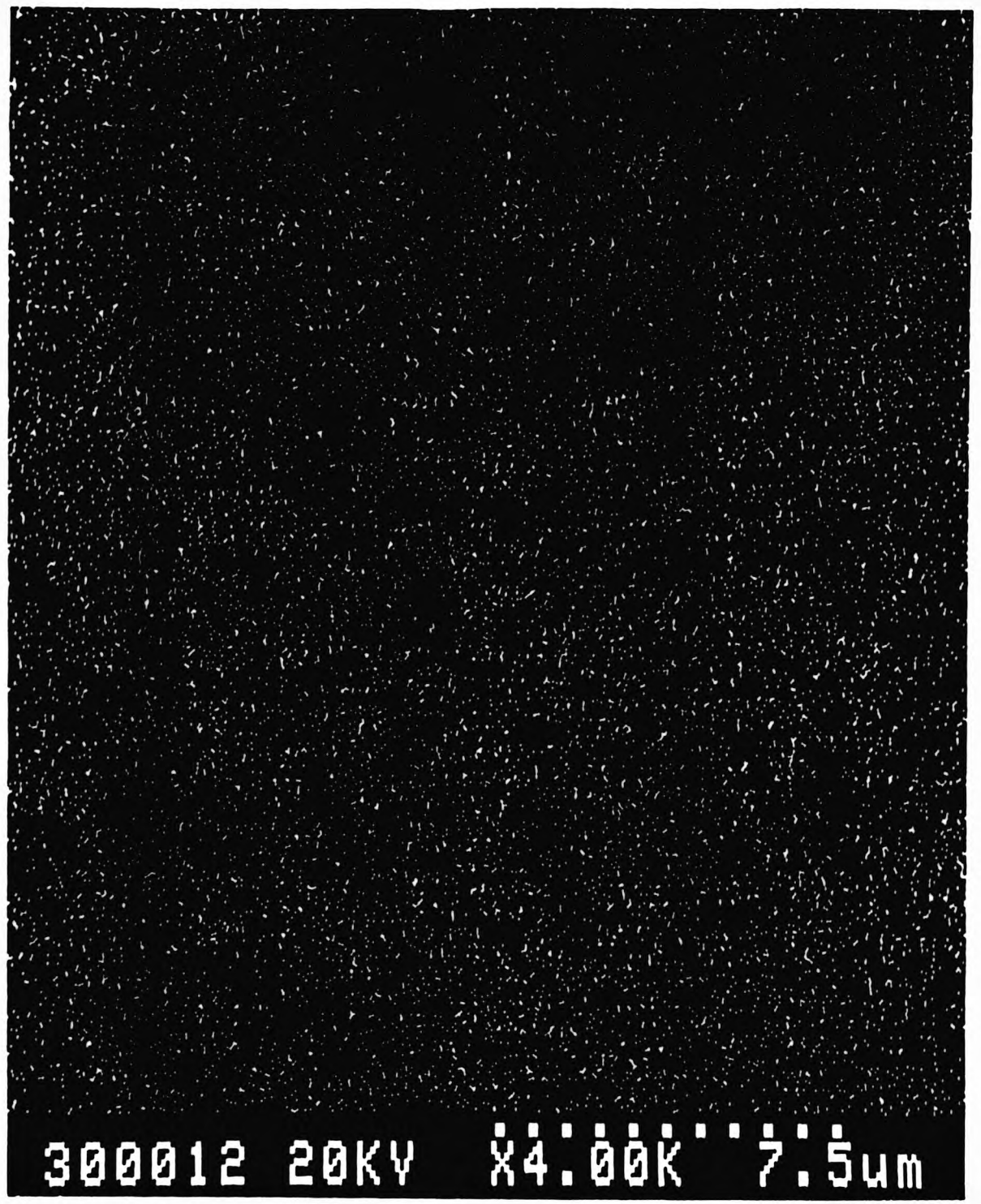
300012 20KV X4.00K 7.5um

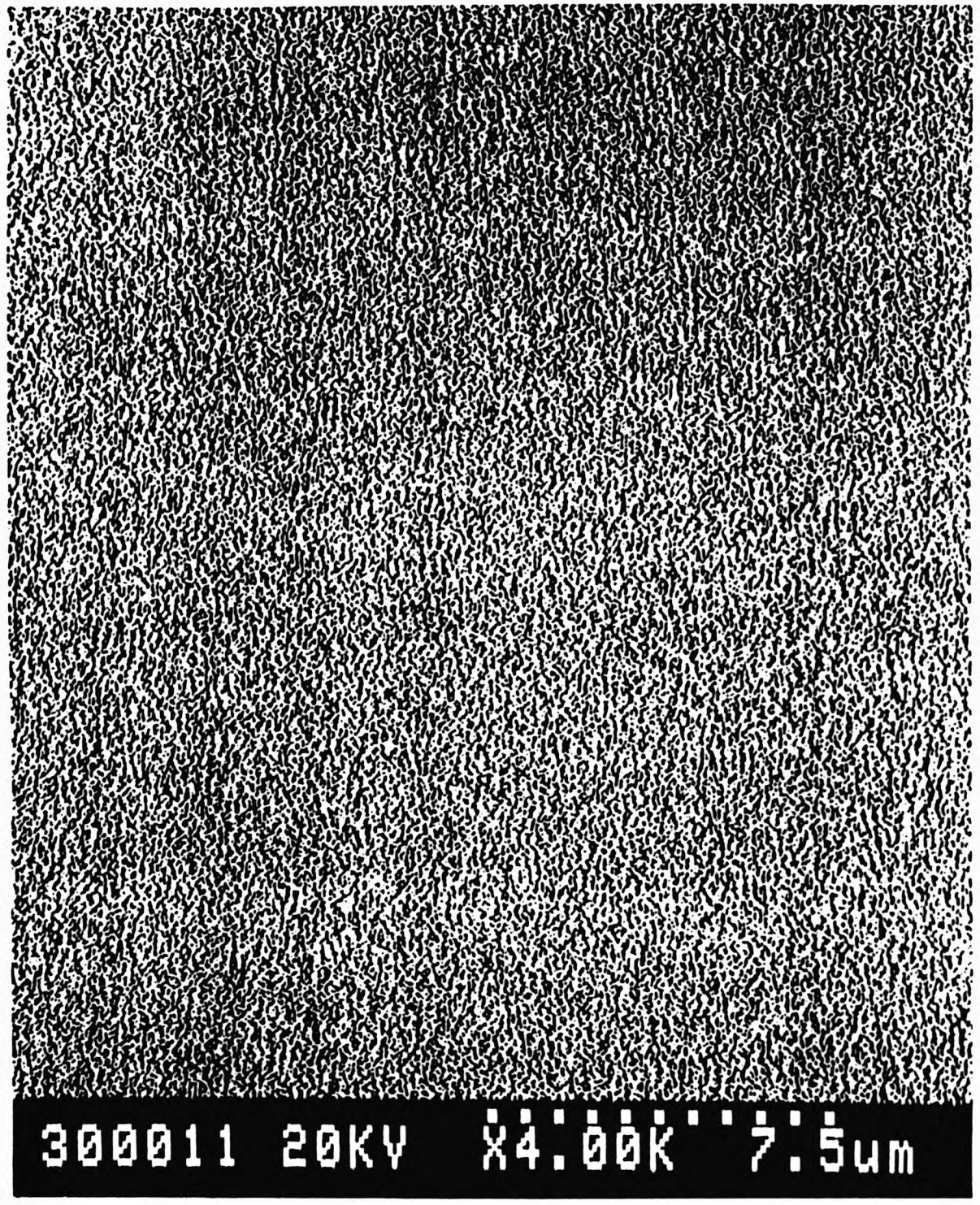
300011 20KV X4.00K 7.5um

Legends for the subsequent micrographs are as follows:

Figure 6.2a (*micrograph 300005*): SEM micrograph of the Poly[1]$^{+}ClO_4^{-}$ material [37], synthesised by the use of condition 5.36. The undulation of the smooth polymer surface might have resulted from the contraction of the film upon solvent evaporation.

Figure 6.2b (*micrograph 300006*): EPMA micrographs showing a dotmapping of S-characteristic X-ray images of the same area of [37] represented in Figure 6.2a.

Figure 6.2c (*micrograph 300007*): EPMA micrographs showing a dotmapping of Cl-characteristic X-ray images of the same area of [37] represented in Figure 6.2a.


300005 20KV X3.50K 8.6um

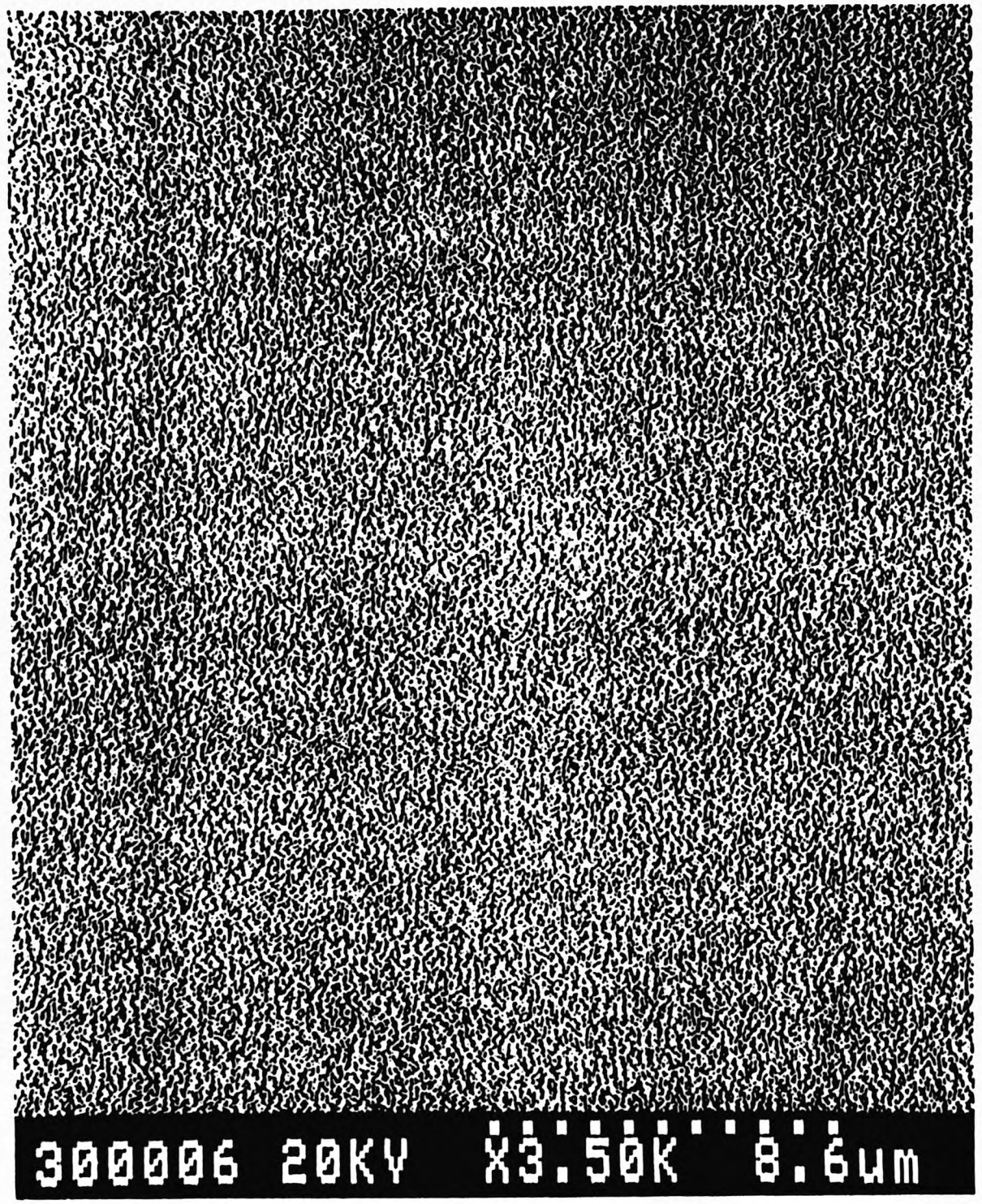
300006 20KV X3.50K 8.6um

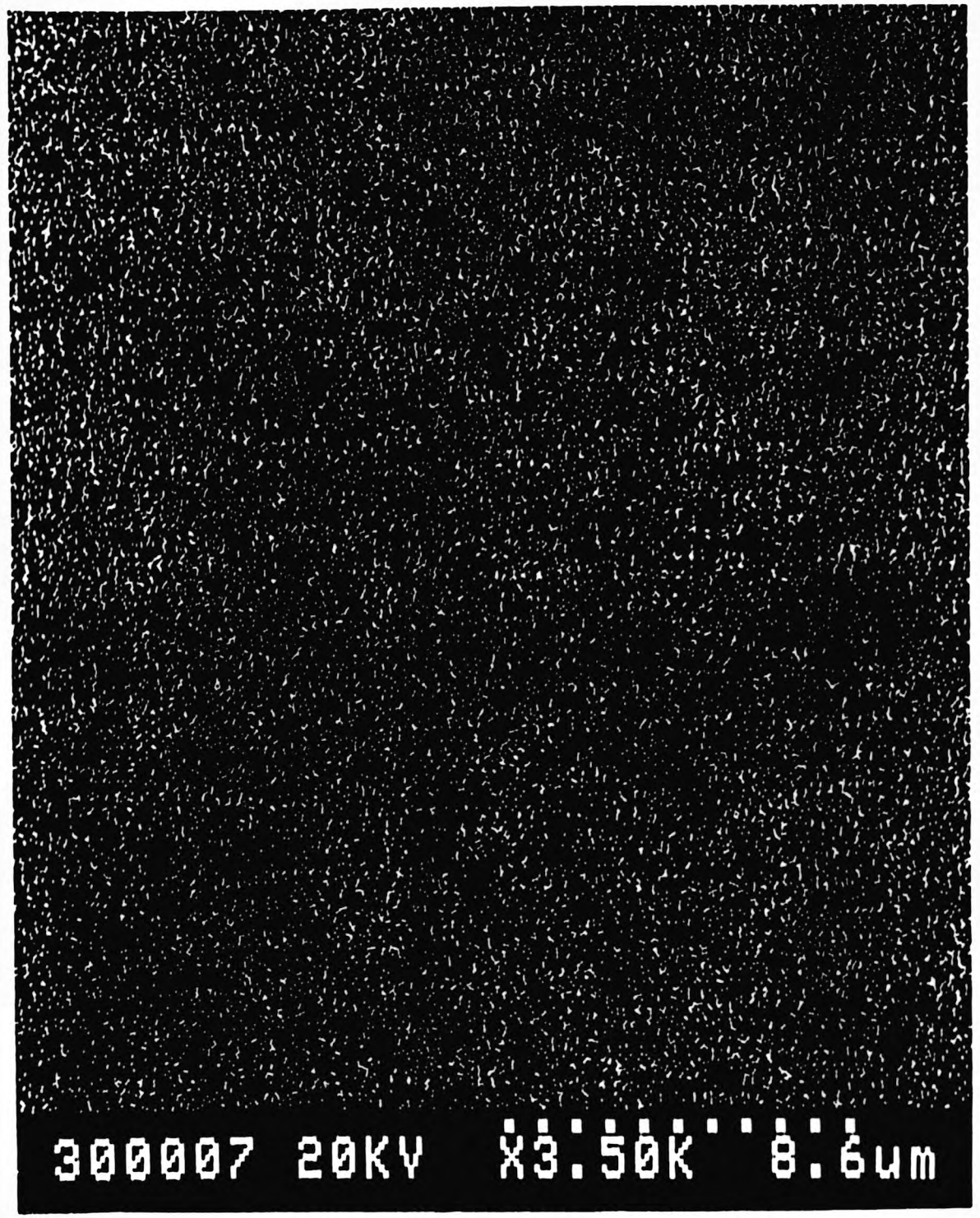
300007 20KV X3.50K 8.6um

6.1.2 Polymers derived from *trans*-1-(1´-pyrenyl)-2-(3˜-thienyl)ethene [2]

Figures 6.3 and 6.4 illustrate the influence of the incorporated dopant ion on the polymer morphology. Although the oxidative polymeriation of pyrene leads to amorphous materials with non-specific surface features,[157] micrographs of the Poly[2]$^{+}PF_6^{-}$ polymer, [32], generated from condition 5.16, revealed its surface to consist of an array of packed cauliflower structures made up of hemispheres averaging 4.5 μm in diameter (figures 6.3a & 6.3b). The dot-mapped X-ray images characteristic of sulphur (figure 6.3c) and phosphorous (figure 6.3d) indicates the uniform distribution of these elements within the polymer matrix although their ratio signifies a very low doping level. The latter could be due to substantial dopant degradation during storage, the leaching of surface dopants as a result of the intensity of the electron beam, or alternatively, most of the the dopant anions could be buried beneath the surface of the material sample, and dot-mapping only reveals the surface localised elements.

The Poly[2]$^{+}ClO_4^{-}$ material [33], engendered from condition 5.18, also had a packed cauliflower microstructure, but with hemispheres averaging 8.2 μm in diameter (figures 6.4a and 6.4b). This latter material [33] thus exhibited an 82% increase in the diameter of its surface features (hemispheres) in contrast to the PF_6^{-} doped counterpart [32]. In analogy with the perchlorate-doped polymer [37], this film was also more densely-packed (figure 6.4c), and there was a marked increase in the degree of anion incorporation (figure 6.4d) in comparison with [32].

Legends for the subsequent micrographs are as follows:

Figure 6.3a,b (*micrographs 000000 & 000001*): Scanning Electron Micrographs of the Poly[2]$^{+}PF_6^{-}$ material [32], synthesised by the use of condition 5.16.

Figure 6.3c (*micrograph 000002*): EPMA micrographs showing a dotmapping of S-characteristic X-ray images of the same area of [32] represented in Figure 6.3b.

Figure 6.3d (*micrograph 000003*): EPMA micrographs showing a dotmapping of P-characteristic X-ray images of the same area of [32] represented in Figure 6.3b.

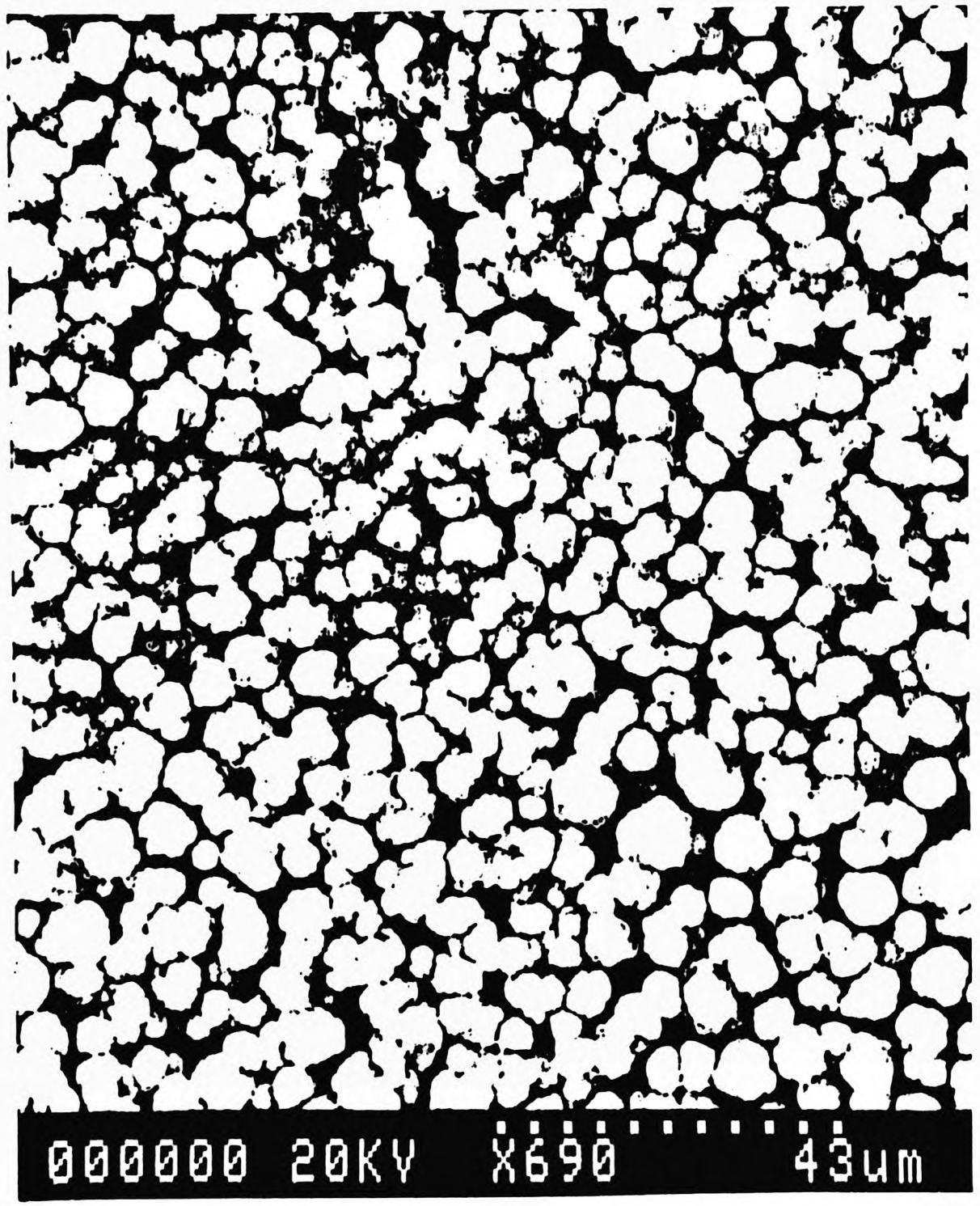
000000 20KV X690 43um


000001 20KV X3.50K 8.6um

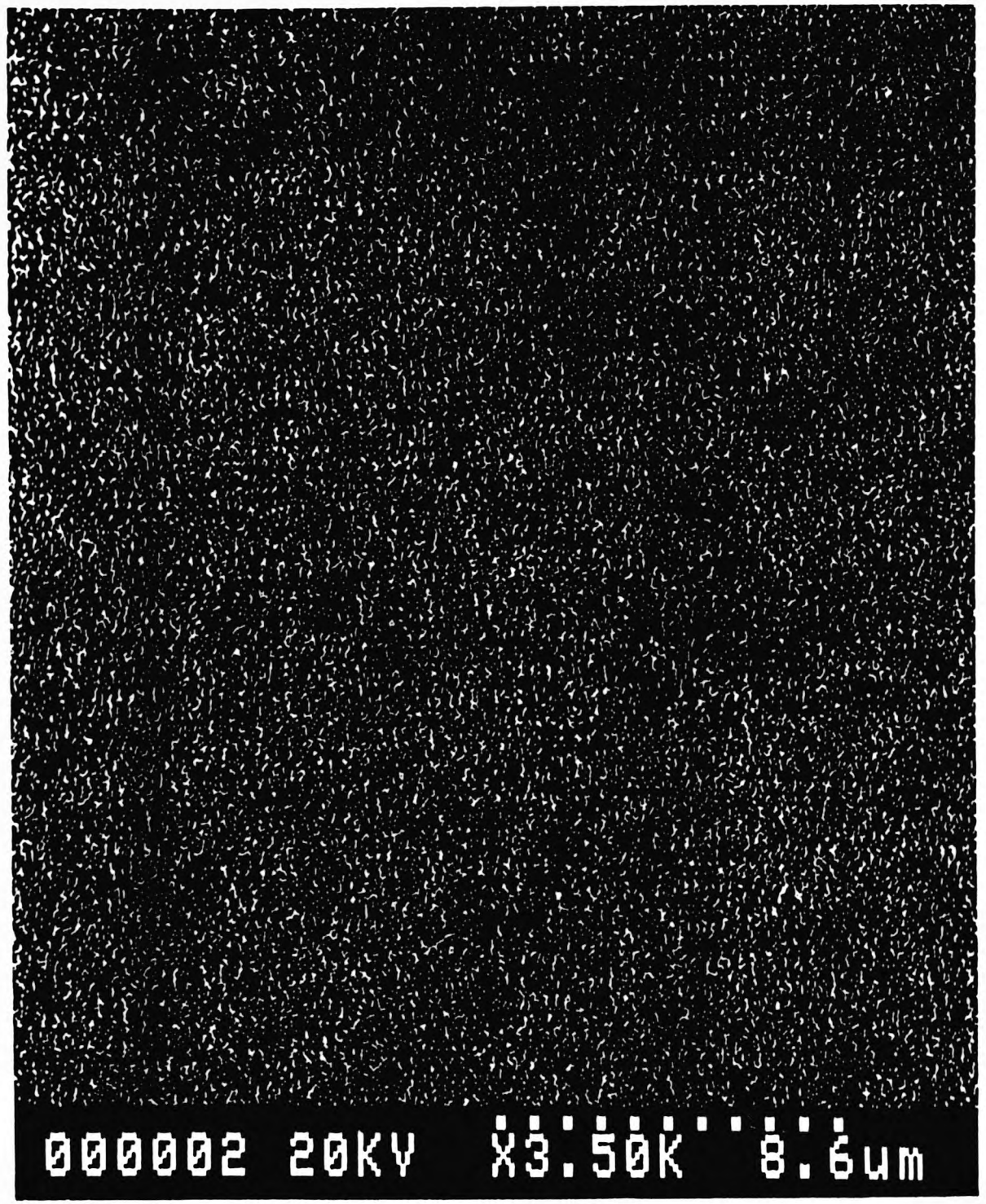
000002 20KV X3.50K 8.6um

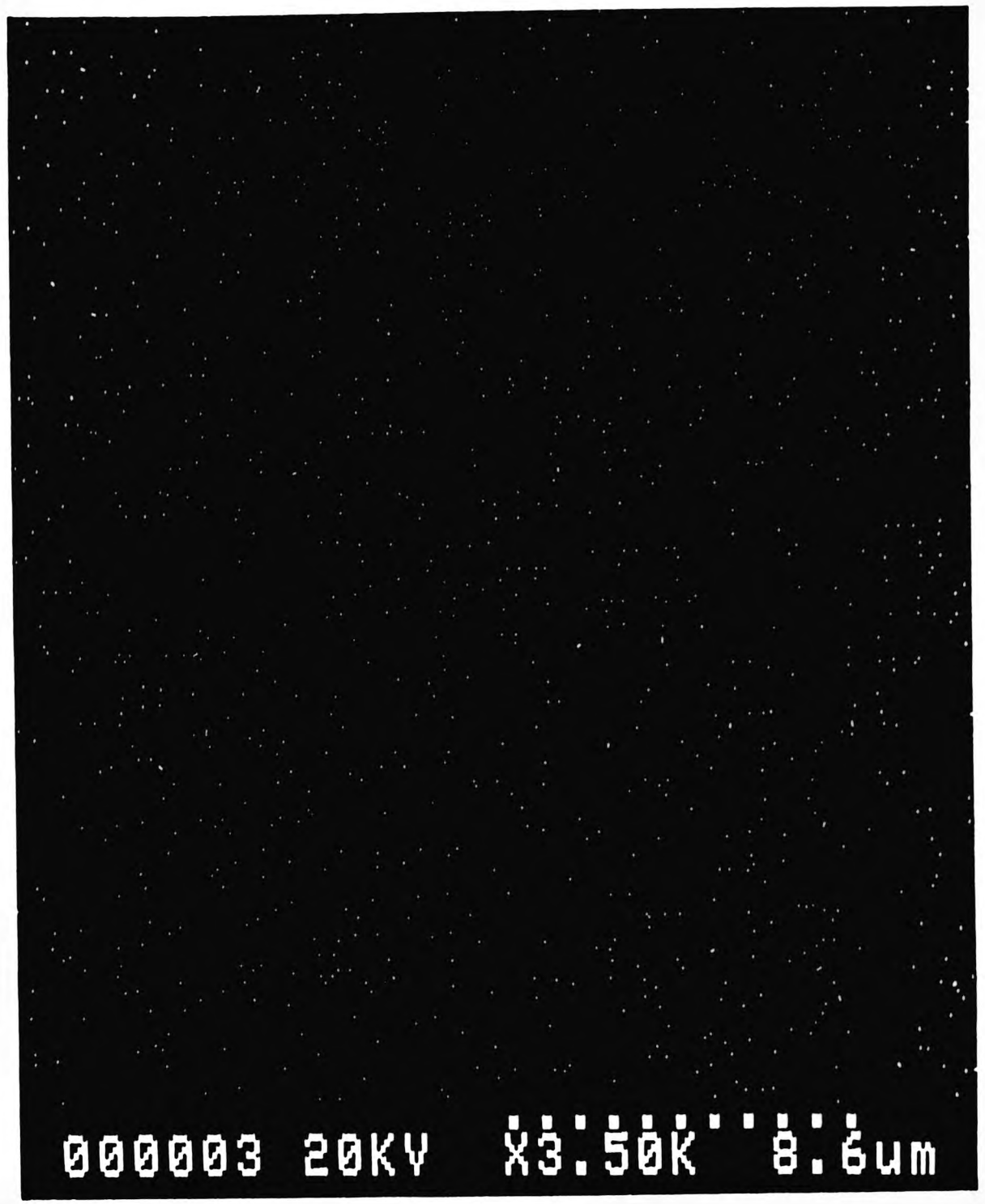
000003 20KV X3.50K 8.6um

Legends for the subsequent micrographs are as follows:

Figures 6.4a,b (*micrographs 300001 & 000005*): Scanning Electron micrographs of the Poly[2]$^{+}ClO_4^{-}$ material [33], synthesised by the use of condition 5.18.

Figure 6.4c (*micrograph 000006*): EPMA micrograph showing a dotmapping of S-characteristic X-ray images of the same area of [33] represented in Figure 6.4b.

Figure 6.4d (*micrograph 000007*): EPMA micrograph showing a dotmapping of Cl-characteristic X-ray images of the same area of [33] represented in Figure 6.4b.

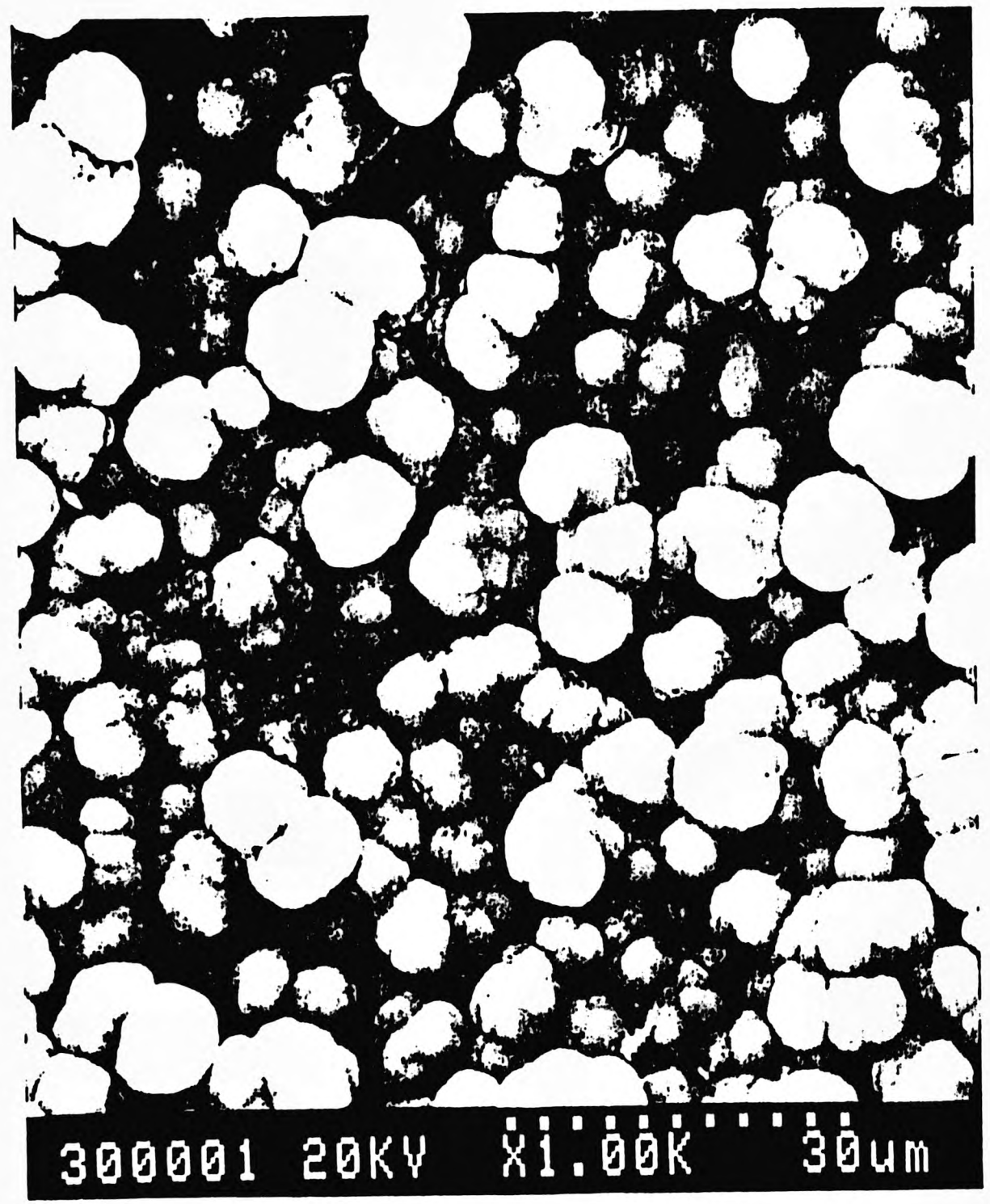
300001 20KV X1.00K 30um

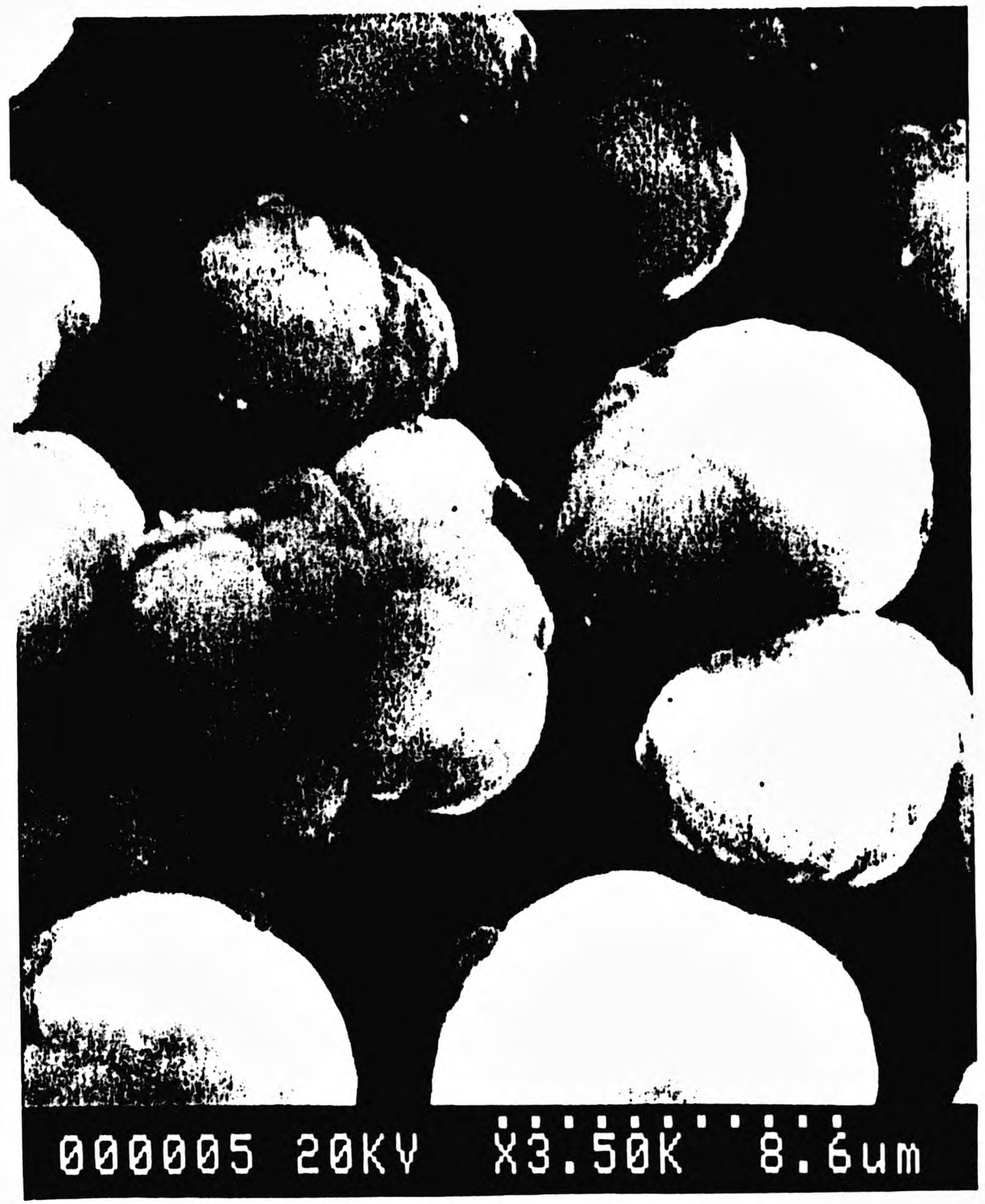
000005 20KV X3.50K 8.6um

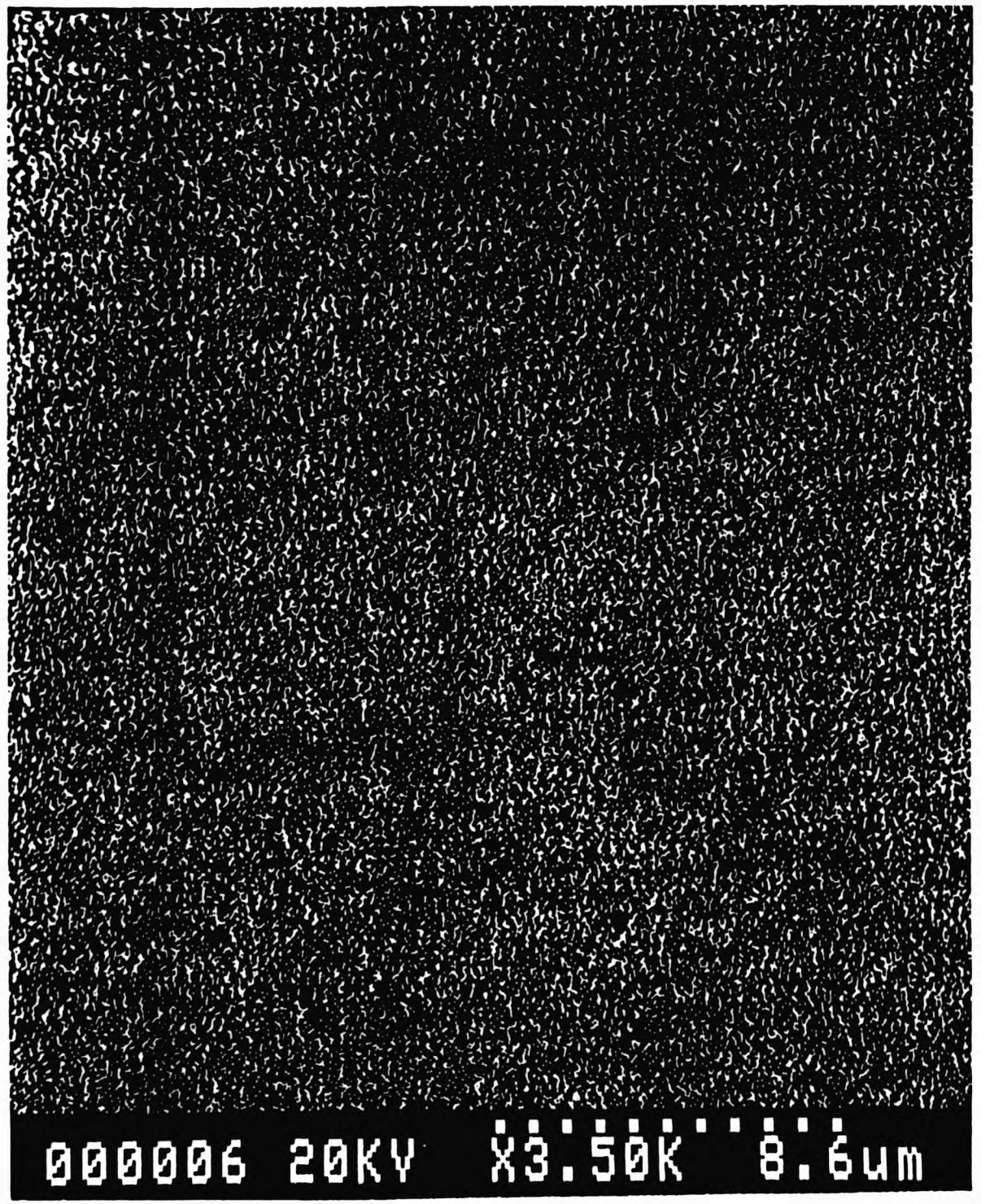
000006 20KV X3.50K 8.6um

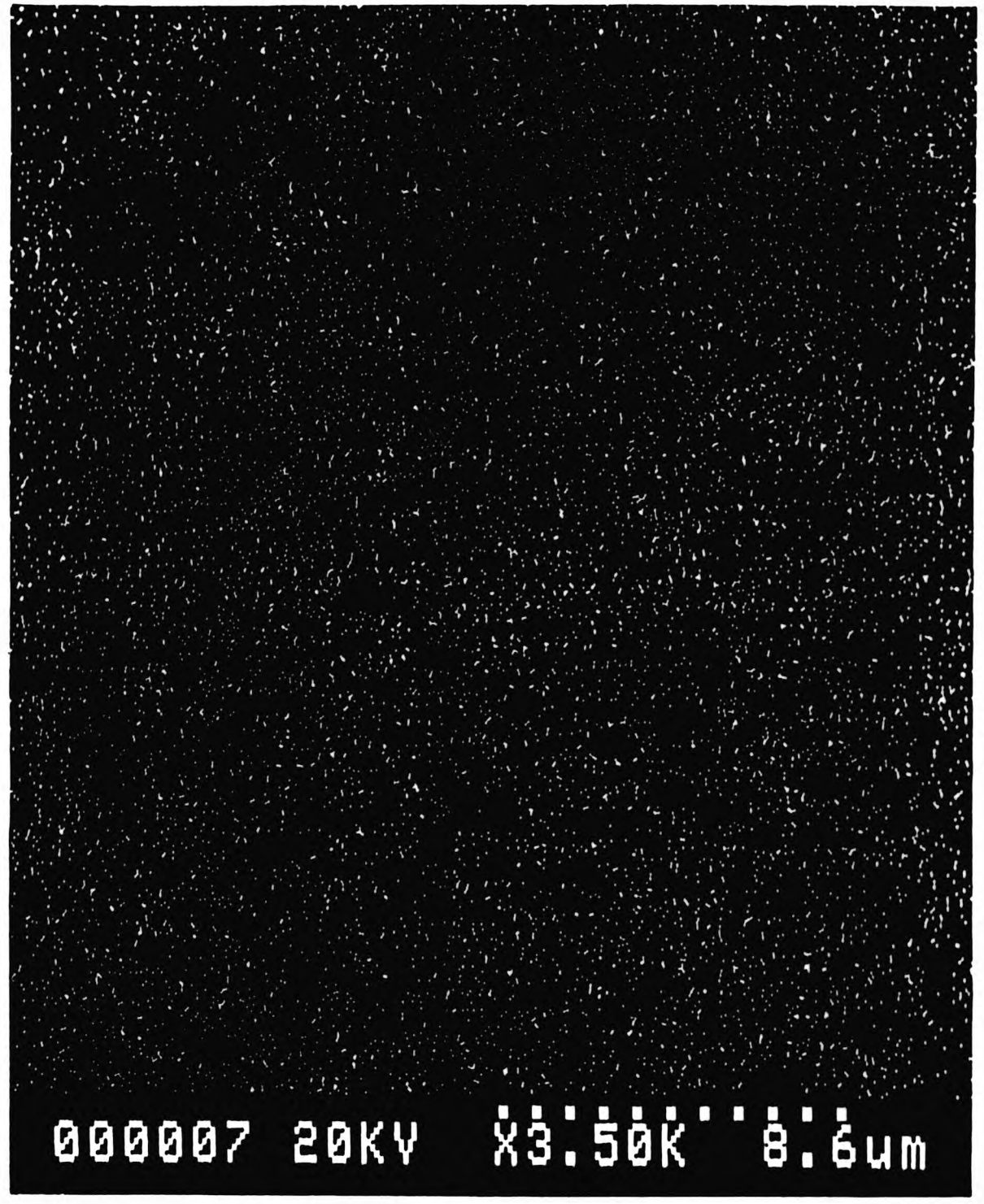
000007 20KV X3.50K 8.6um

6.1.3 Polymers derived from 3-(trimethylsilyl)thiophene [9]

The EPMA micrograph of the flexible and free-standing film [30] obtained under condition 5.6 reveal two areas of significance. First, the distribution of phosphorous was such that it was more concentrated some areas in relation to others (figure 6.6d). These regions of high phosphorus (and thus the dopant) concentration also coincided with areas where low thiophene distributions are located, as was evidenced by the shadowy regions of the dot-mapped, sulphur-characteristic X-ray images (figure 6.6c). It is suspected that these regions are areas of interfibril contact. The high dopant content, corresponding to a high level of charge-carriers in these regions, leads to improved interfibril contacts which correspondingly results in enhanced interfibril charge-hopping and improved electrical conductivity. This observation reinforces earlier suggestions that intermolecular interactions, rather than molecular structure, are responsible for high electrical conductivity.[158] The concept of intra and interchain charge-carrier hopping is illustrated below (figure 6.5).

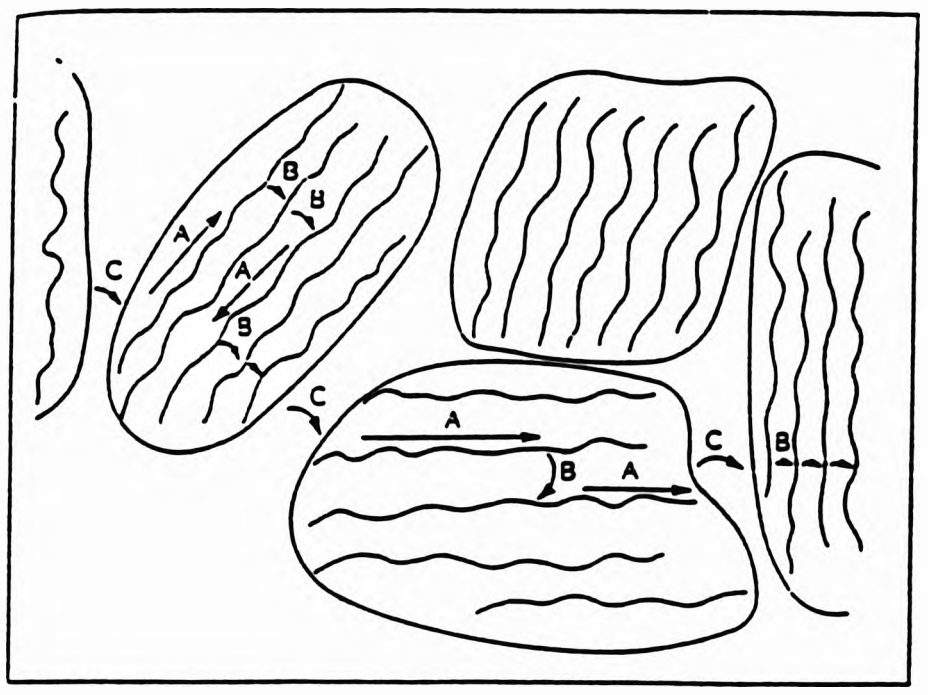

Figure 6.5
A schematic illustration of the conductivity network of a conducting polymer with arrows indicating the possible path of a charge carrier migrating through the polymeric material through (A) intrachain transport; (B) interchain transport; (C) interfibril transport.[26]

Legends for the subsequent micrographs are as follows:

Figure 6.6a (*micrograph 000005*): SEM of the electrode-side of the PF_6-doped polymer derived from the electropolymerisation of compound [9] using condition 5.6. The film is tightly-coiled, showing its flexibility. Also note the microcrystallites on the underside of the film. These make up the dominant structures in the solvent side of the polymer.

Figure 6.6b (*micrograph 000004*): SEM of the solvent-side of the PF_6-doped polymer showing the geometric microcrystallites.

Figures 6.6c,d & e: EPMA micrographs showing a dotmapping of (c) S-characteristic (*micrograph 300016*) (d) P-characteristic (*micrograph 300015*) and (e) Si-characteristic (*micrograph 300014*) X-ray images of the PF_6-doped polymer derived from the electropolymerisation of compound [9] (electrode side). Circumstances analogous to condition 5.6 were employed, the only difference being that a deposition time of 1 hour was used in this instance.


000005 20KV
38um

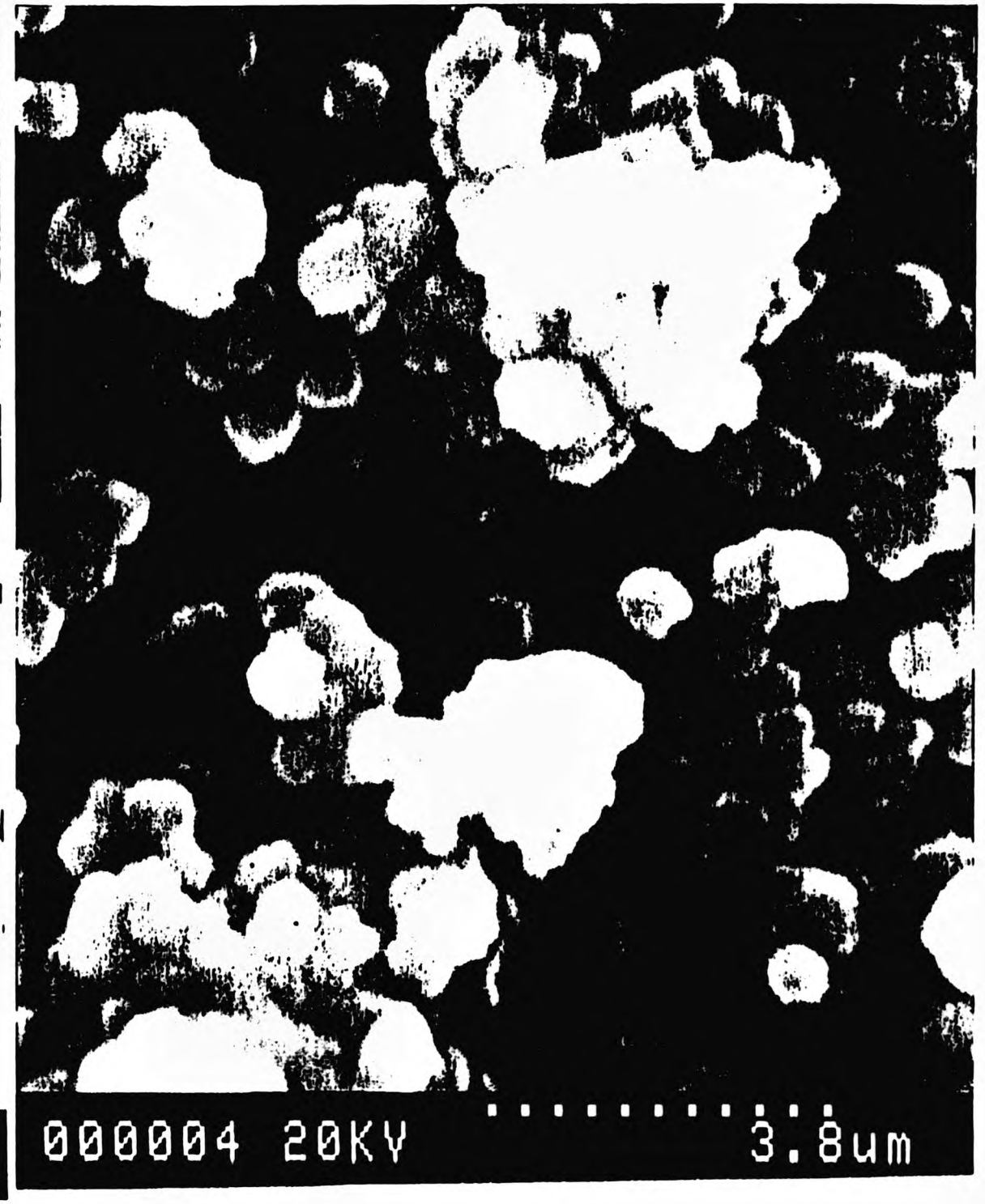
000004 20KV
3.8um

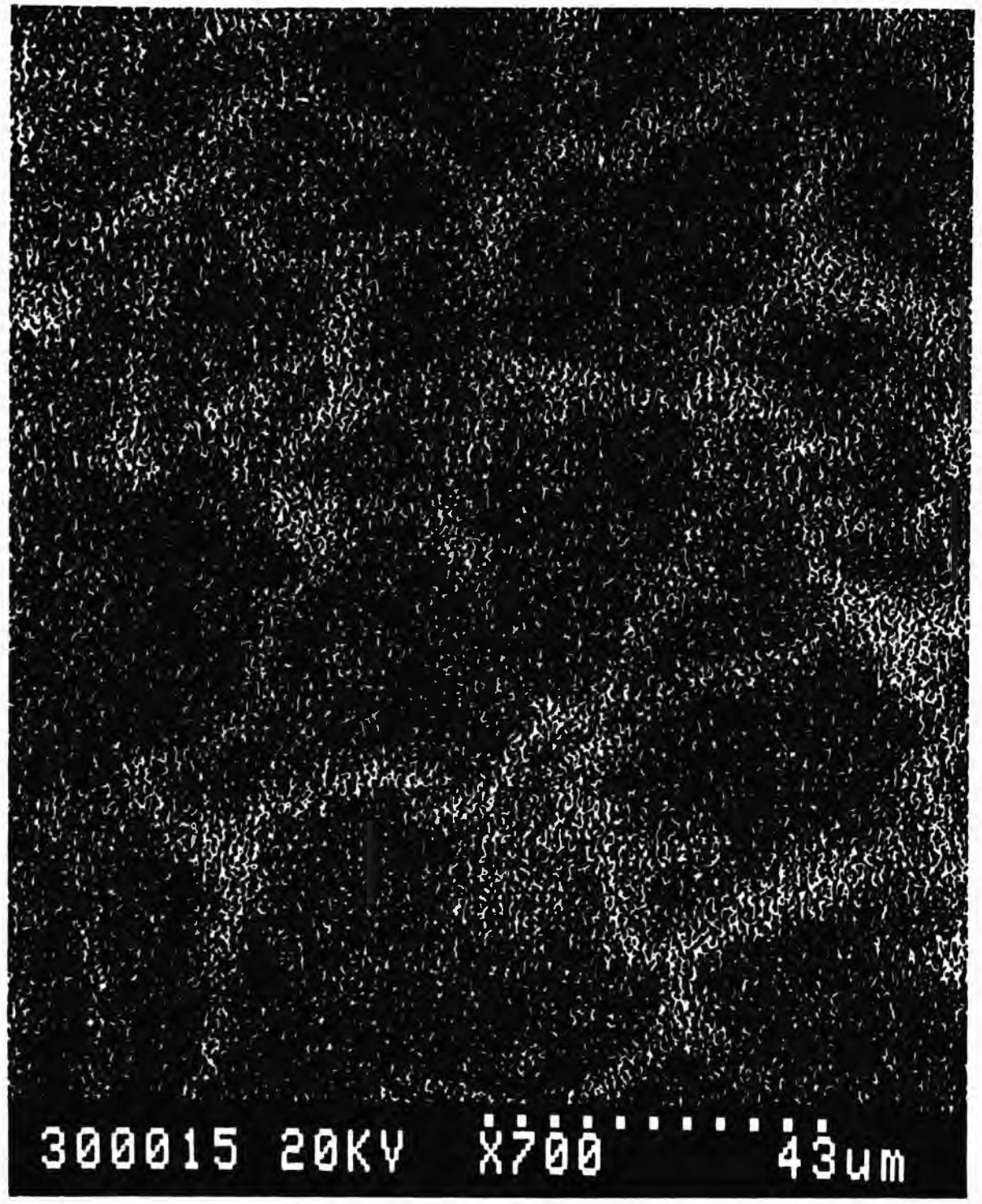
300015 20KV X700 43um

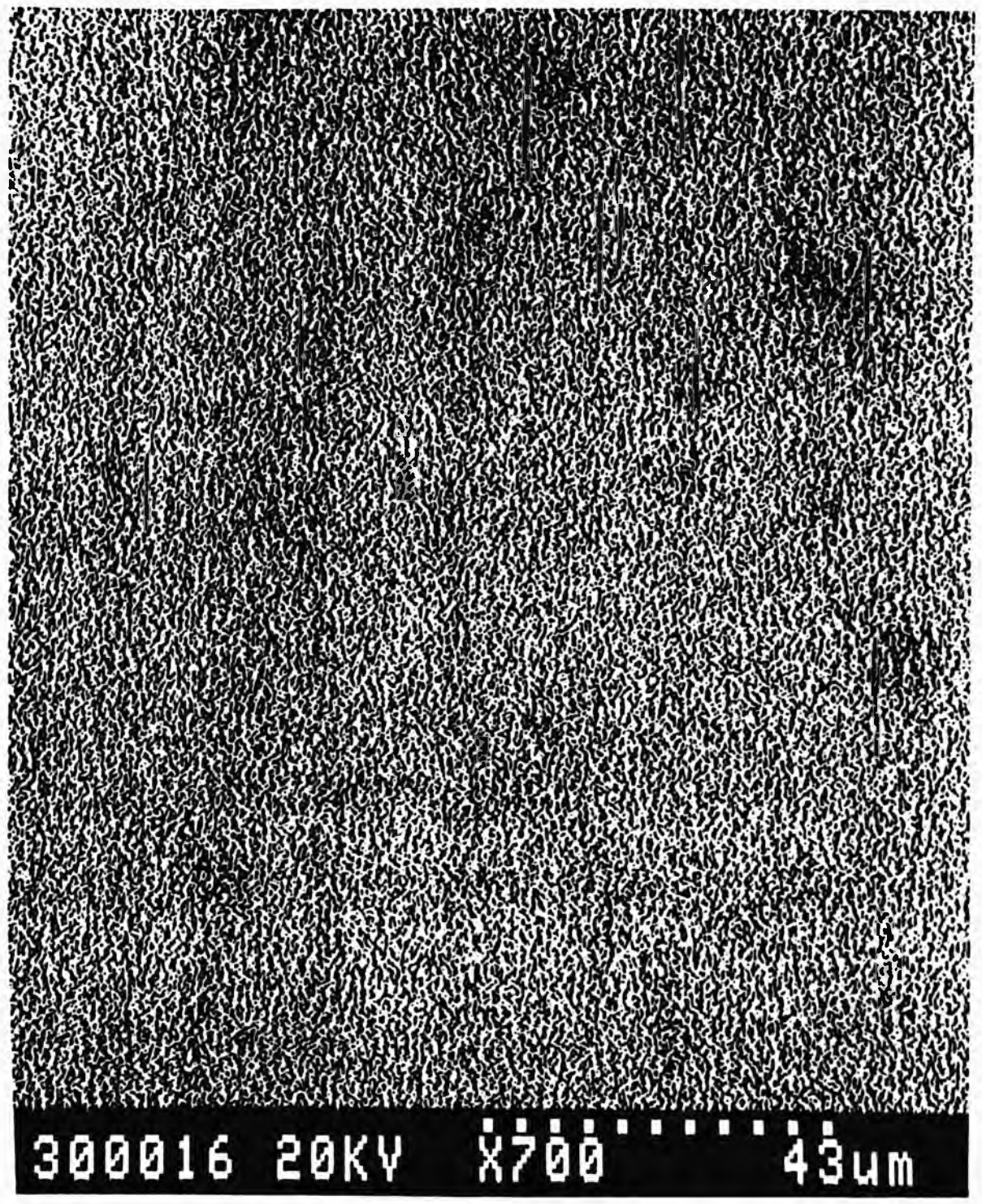
300016 20KV X700 43um

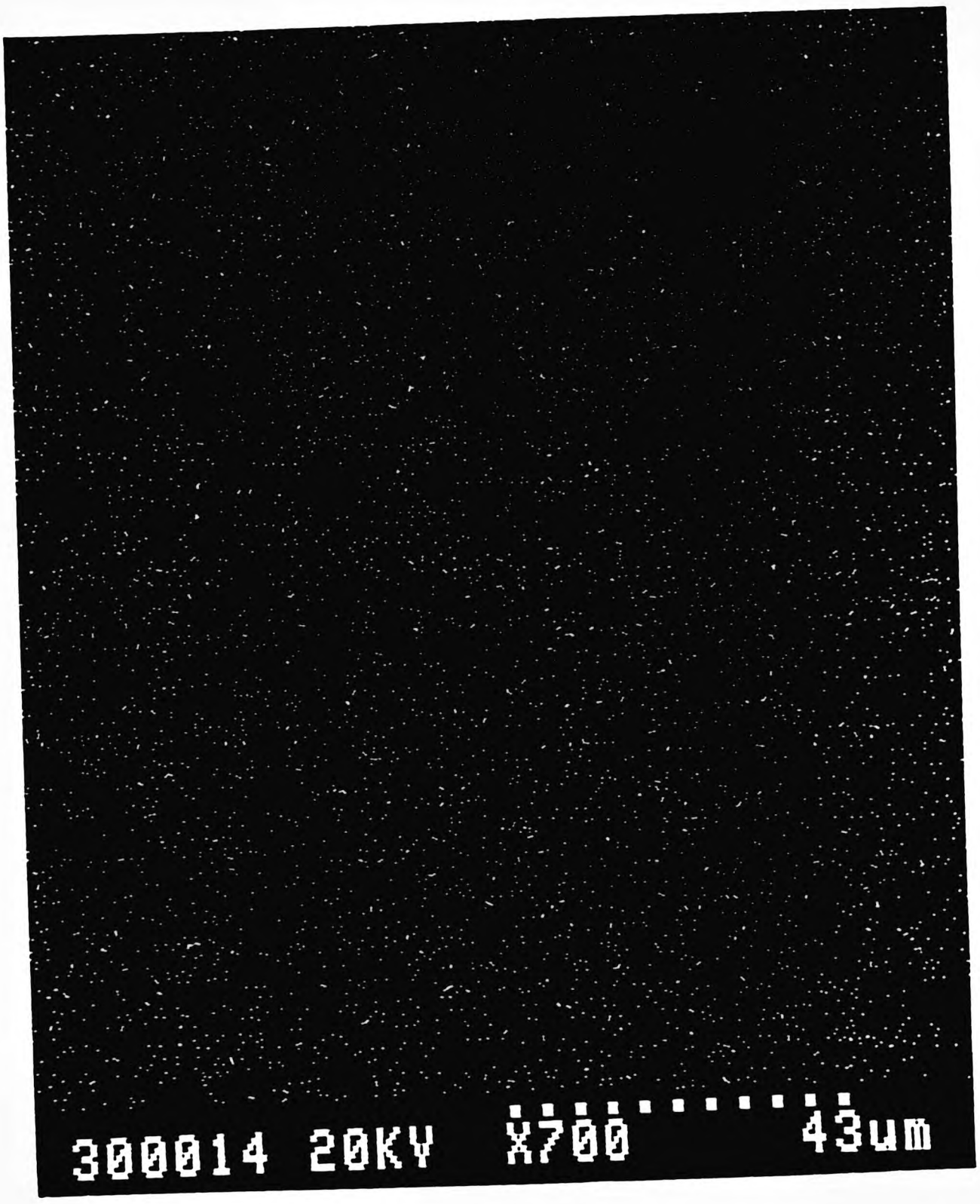
300014 20KV X700 43um

Additionally, the very low level of dot-mapped, silicon-characteristic X-ray images obtained from EPMA studies of the polymer provides evidence that a near-complete desilylation of the monomeric species had occured during the electropolymerisation process (figure 6.6e). The anticipated ratio of dot-mapped S:Si under conditions that provide a polymer in which there is an essential assimilation of the intact monomeric entity, is 1:1 (unity).

From the micrographs produced, the two sides of the film exhibits distinct morphological variations. Whilst the polymer surface adhering to the electrode (the inner polymer surface) was made up of an array of interconnected fibrils (figure 6.6a), the polymer surface exposed to the electrolytic solution (the outer polymer surface) consisted of a collection of nanometer-sized geometric microcrystallites (figure 6.6b). This change in polymer morphology from the fibrillar to the crystalline nature resulted in a 6-fold increase in conductivity (see section 5.4.3).

6.2 FOURIER-TRANSFORM INFRA-RED TRANSMISSION SPECTROSCOPY*

The IR spectra of the oxidised polymers are presented in figures 6.7 - 6.9. The broadening of absorption bands in all the spectra, is an indication of amorphous disorder inherent in these polymers.

6.2.1 The Polymer Structrure

The oxidised polymers of compounds [1] & [2] exhibited strong bands at 844 $\pm$1 cm^{-1} (figures 6.7 and 6.8) which are frequencies assosiated with the δ(C-H) o.o.p. mode of 2,3,5-substituted thiophenes.[149b] This indicates that these polymers are essentially derived from the respective intact units of [1] and [2] which are linked through 2,5-thiophenediyl bonds.

However, this absorption band (corresponding to the band at 839 cm^{-1}), was of diminished intensity in the spectrum of the polymer [30], derived from the oxidation of 3-(trimethylsilyl)thiophene (figure 6.9). This abated absorbance, in conjunction with an absence of the strong absorbances attributable to the methyl ν(C-H) fundamental of the trimethylsilyl group (this absorbance occurs at 2956 cm^{-1} in the monomer) and that of the Si-CH_3 rocking mode (this absorbance occurs at 835 cm^{-1} in the monomer; see section 3.1.1.[IV]) suggests that although desilylation had taken place, 3-substitution is still inherent in the polymer. This substitution could most likely occur from the coupling of thiophene units to this position.

Intense bands at 788 and 730 cm^{-1}, indicative of poly 2,5- and 2,4- thienylenes respectively[159,160] (figure 6.10), and the overall similarity of the spectra with that of doped polythiophene, would strongly suggest that the polymer [30] is mainly composed of randomly-linked (α-α' and α-β') thienylene units.

---

*Details of the methodology are contained in the experimental section (chapter 8).

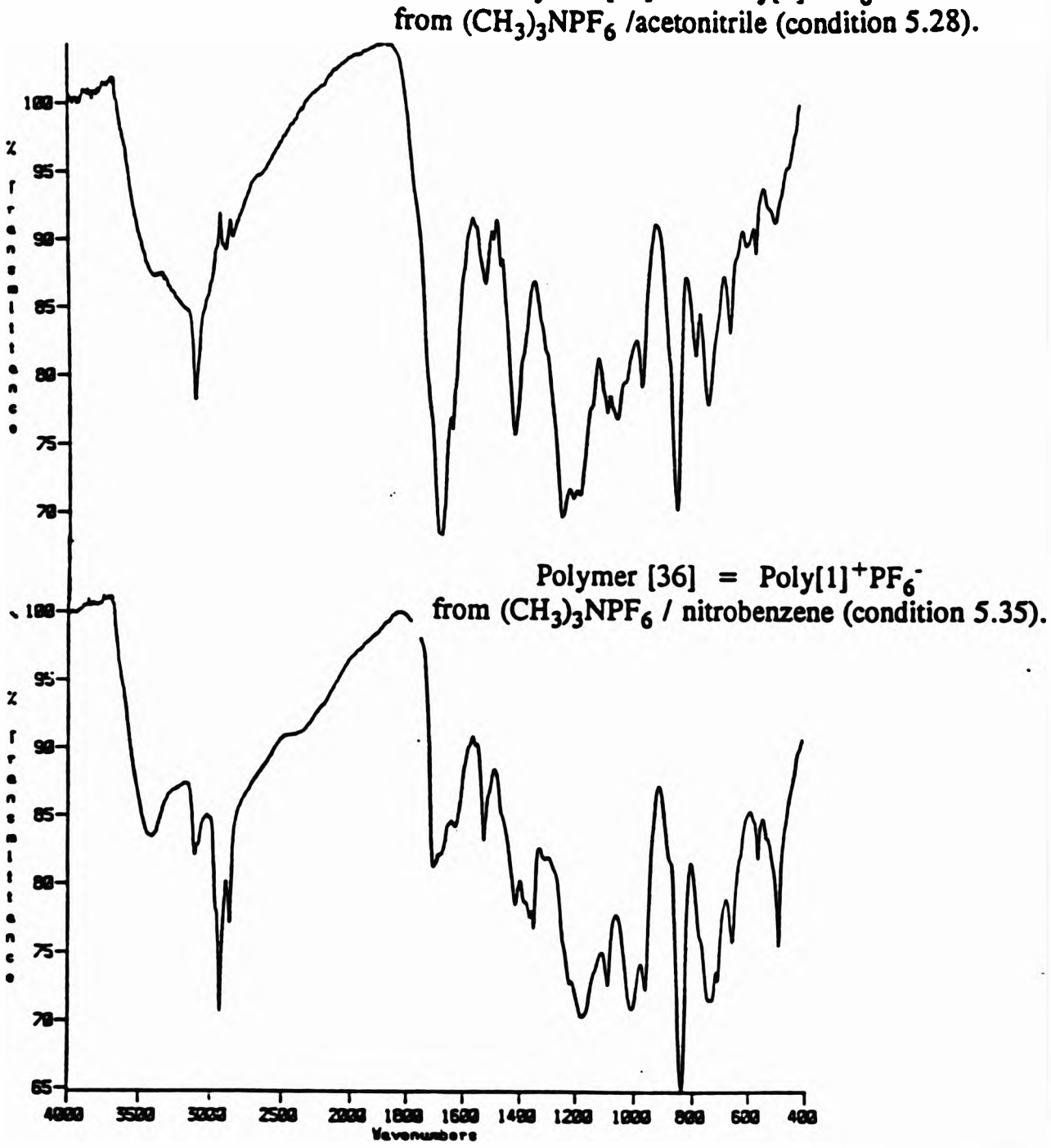

Figure 6.7
FTIR spectra of polymeric materials (a), [34] and (b), [36]; derived from the electropolymerisation of compound [1] in acetonitrile (condition 5.28) and nitrobenzene (condition 5.35) respectively

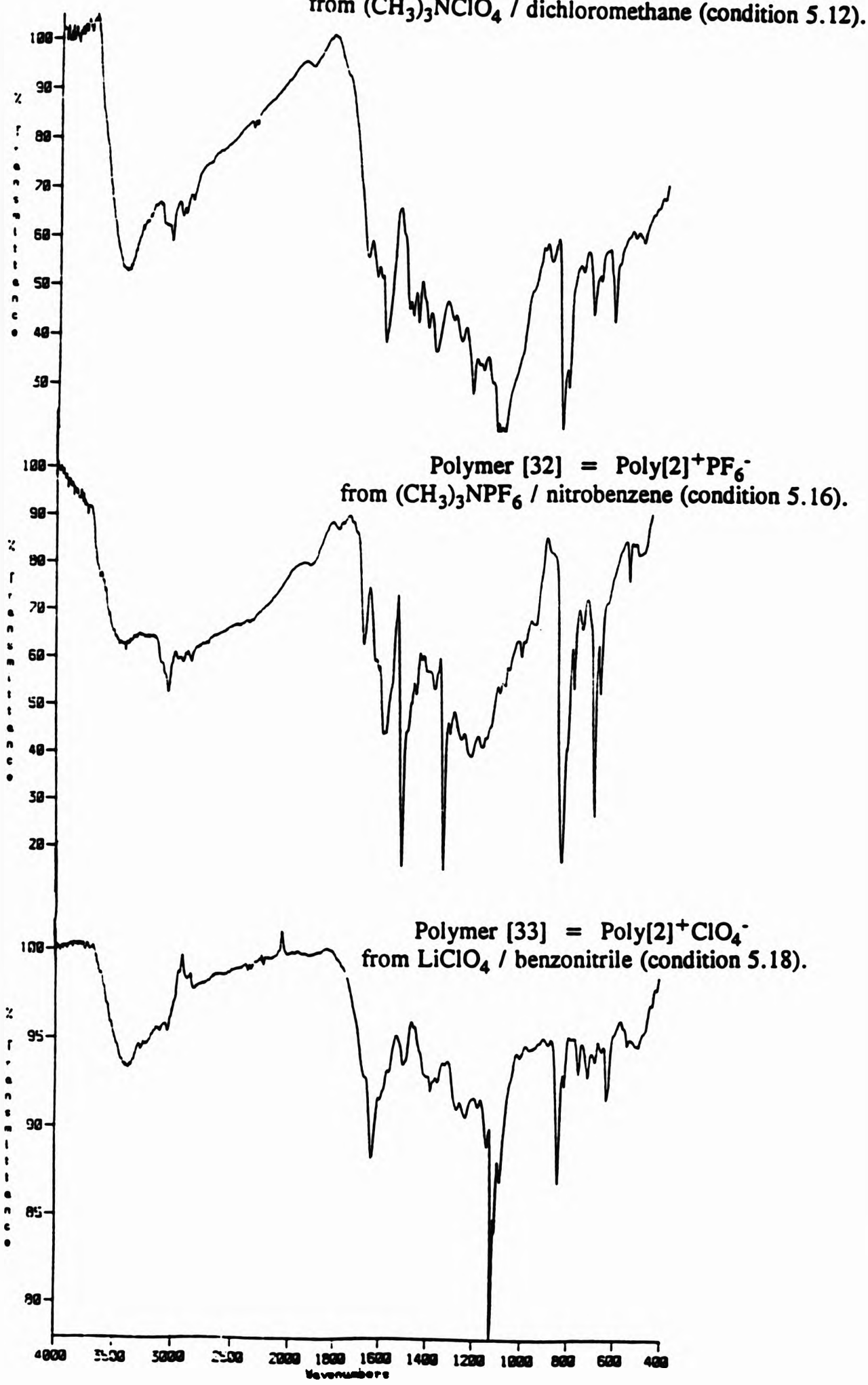

Figure 6.8
FTIR spectra of polymeric materials (a), [31]; (b), [32]; and (c), [33]; derived from the electropolymerisation of [2] in dichloromethane (condition 5.12), nitrobenzene (condition 5.16) and benzonitrile (condition 5.18) respectively

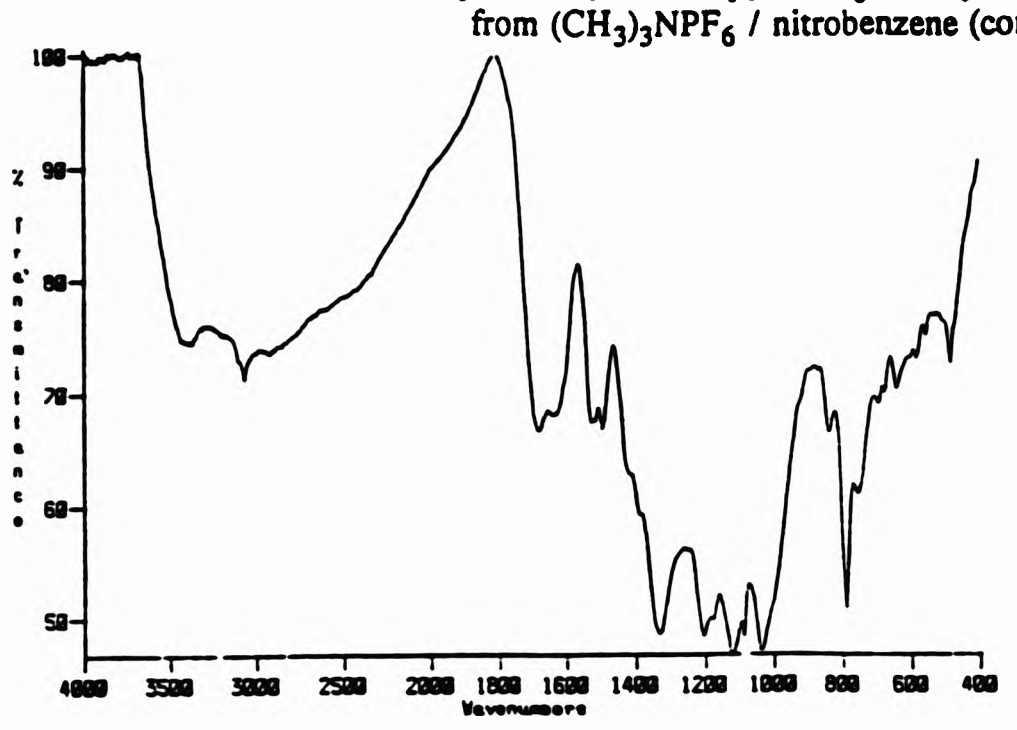

Figure 6.9
The FTIR spectrum of the polymeric material [30], derived from the electropolymerisation of compound [9] in nitrobenzene (condition 5.6)

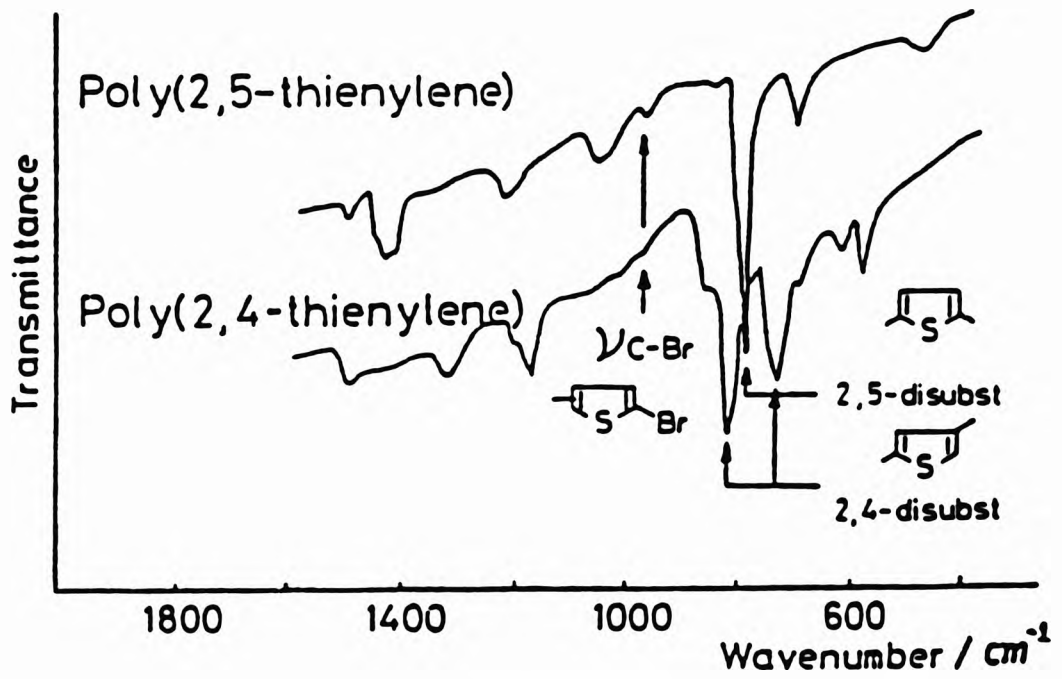

Figure 6.10
The FTIR spectra of chemically synthesised poly(2,4-) & (2.5-) thienylenes

6.2.2 The impact of doping on the IR spectra

In agreement with studies of the IR spectra of oxidised polythiophene and fused thiophene-ring-based polymers,[161] an increase in the dopant ion concentration led to an increase in the intensity of absorptions in the high energy region (4000 - 1900 cm^{-1}) of the spectra of all the polymers studied. This increase in intensity corresponds to an increase in the quasi-metallic behaviour of these polymers, instigated by the presence of anion-induced free-carriers (*i.e* polarons and bipolarons).

There was also an enhancement of all bands in the 1636 - 1000 cm^{-1} region ascribable to absorbances involving ring and skeletal (C=C) vibrations, and probably resultant of the coupling of these vibrations with those of the free-carriers.[162] An increase in the PF_6^- content of Poly[1] led to the observation of intense bands at 1411, 1345, 1240, and 1004 cm^{-1} (figure 6.7). Increases in the ClO_4^- content of Poly[2] resulted in the amplified bands at 1596, 1585, 1458, 1416, and 1315 cm^{-1} (figure 6.8), whilst the oxidative electropolymerisation of [9] also led to the enhanced absorbances at 1523, 1491 1410, 1330 and 1034 cm^{-1}.

6.2.3 Dopant-specific absorptions

Rather than base the configuration of polymer:anion associations on "purely statistical" results obtained from the elemental analysis of an oxidised polymer, an elucidation of the coordination pattern between polymers and their respective dopant anions could be established from the identification of the intrinsic symmetry of the anion in the polymeric ensemble; as it is well established that changes in the symmetry of any anion are reflected in the number(s) and intensity(ies) of its fundamental IR-active vibrations. Documented modes of perchlorate bonding[163] would appear to indicate that the bands observed in all the perchlorate-doped polymers at 1190, 1120, 623, and 635 cm^{-1} arise from a splitting of the ν_3 and ν_4 observable for the prechlorate anion. This splitting is due to a change in the mode of perchlorate bonding; a lowering of symmetry from that of an ionic-Td perchlorate (which is the symmetry of the perchlorate ion in the supporting electrolyte), to a bridging (C_{2v}) perchlorate (which is the symmetry of the perchlorate ion in the polymer:anion ensemble, and is due to a fixation of the ion in the polymer lattice). These two bonding modes are illustrated in figure 6.11. Although not previously reported, a band at 705 cm^{-1} seems characteristic of the PF_6 anion.

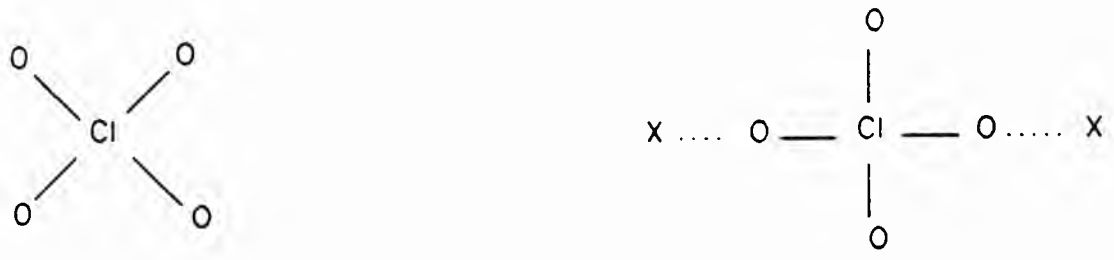

ionic-Td bridging-C_{2v}

Figure 6.11
The ionic and bridging modes of perchlorate bonding.

6.2.4 The exsistence of a C=O function?

Most polymers generated from the oxidation of thiophene and its derivatives exibit a characteristic band at 1675 cm^{-1}. In most cases this absorption has been overlooked,[164,165,166] or speculatively attributed to a vibration involving a carbonyl (C=O) function which has presumably been incorporated into the polythiophene backbone due to the presence atmospheric oxygen and/or water in the electrolytic medium,[21,167] during the oxidative coupling process.

Since appended TGA/DTG results (Chapter 6.3) show no loss of carbon monoxide, and solid-state ^{13}C-NMR data (Chapter 6.4) fail to support the existence of a C=O function, this assignment seems unlikely. This band is therefore tentatively assigned to a doping-activated vibration of the extensively conjugated C=C skeleton of the charged polymers, or more specifically, as a result of strong electrostatic interractions between the positively-charged conjugated ethylenic skeleton, and the fluorine (from PF_6^-) or oxygen (from ClO_4^-) fractions of the dopant anion. Whilst the latter could give rise to absorptions at wavenumbers comparable to that of a ketonic function, the C=C streching frequency of halogenated alkenes[168] is known to range anywhere from 1645 to 1798 cm^{-1}. Also, some disubstituted alkenes[169] are known to absorb at, or near 1670 cm^{-1}.

6.3 THERMOGRAVIMETRIC ANALYSIS (TGA), COUPLED WITH DERIVATIVE THERMOGRAVIMETRIC (DTG) STUDIES[170,*]

6.3.1 The thermal stability of Poly[(2´,5´-thiophenediyl)-1-(1˜-pyrenyl)-2-(3´-thienyl)ethene]$^{+}$ PF_6^{-}, [32]

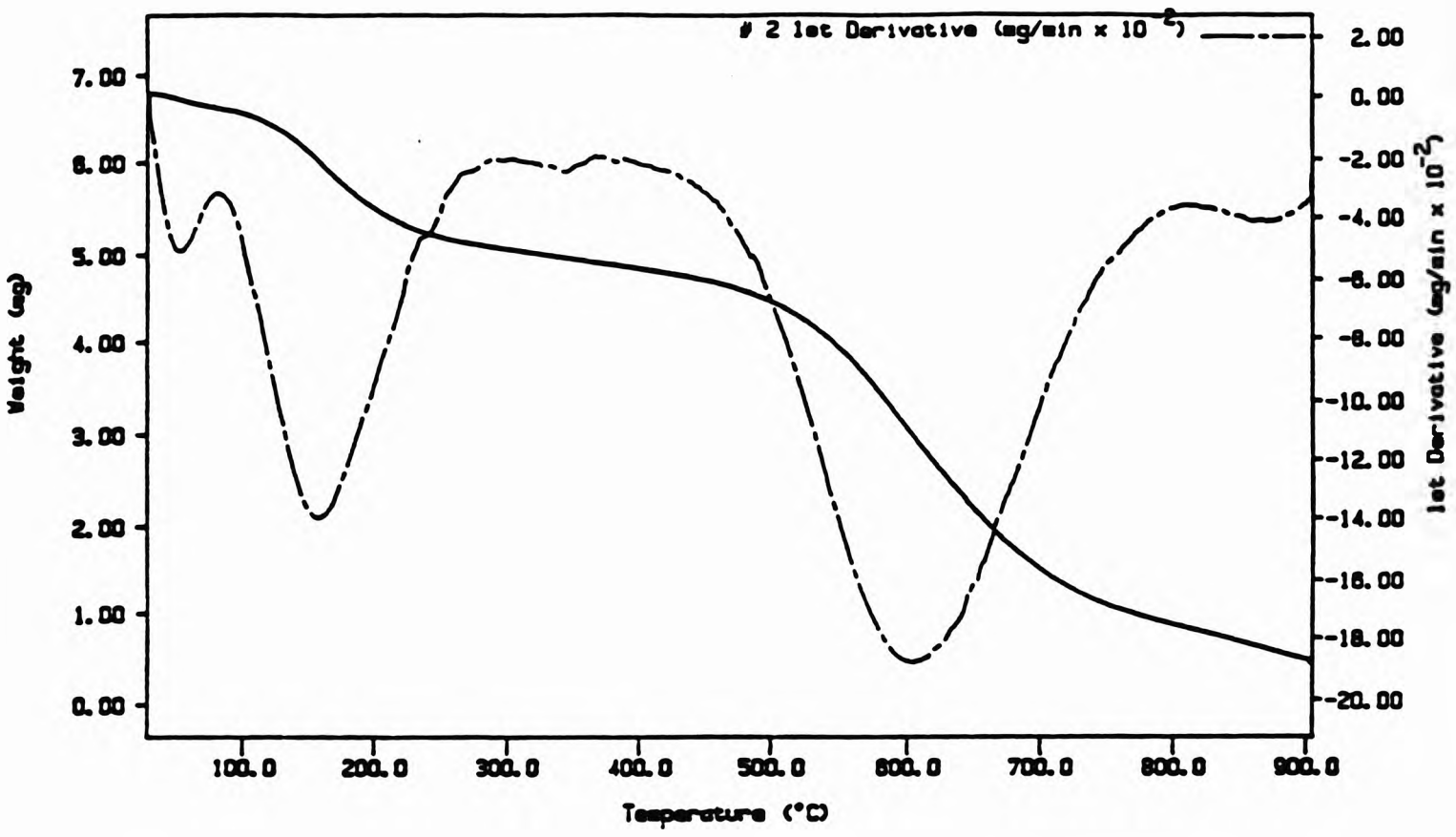

Figure 6.12
(--------) The thermogravimetric profile of the Poly[2]$^{+}PF_6^{-}$ polymer [32] (derived from compound [2]), in nitrogen and within the temperature regions of 30 - 900°C . The rate of temperature increase was 10°C min^{-1}.
(--- - ---) The curve of the first derivative (mg/min x 10^{-2}).

The profile due to the thermal degradation of [32] is depicted in figure 6.12. The first degradation process [A], with a DTG maxima at 56°C, resulted in the 3% weight loss of the polymer mass. This loss is undoubtedly due to the evaporation of the residual acetone used to wash the polymer after its removal from the electrolytic solution, as this temperature corresponds to the boiling point of acetone. The evaporation of residual solvent was followed by a degradation process [B] which was optimum at approximately 165°C. The sharp single DTG maximum observed for this process, coupled with the subsequent relative stability of the profile within the region 250 - 460°C (before the degradation process which involves the pyrolysis of the polymer backbone itself),

*Details of the methodology are contained in the experimental section (chapter 8).

suggests that this degradation is a consequence of expulsion of the dopant ion in a single step, and without any major remodification of the engendered neutral polymer*. The degradation of this resultant dedoped polymer was maximum at 605°C, and a residual mass fraction of 7.36% was obtained after the fixed end-of-test temperature of 900°C.

*Since the temperature-of-commencement of this dopant-exclusion process (90°C) could be regarded as the temperature limit of the thermal stability of [32] in an inert atmosphere, it could be expected that the decomposition of this material upon air storage would occur at a lower temperature and would at least include the process(es) resulting in a one-step loss of dopant.

6.3.2 The thermal stability of [Poly-(2´,5´-thiophenediyl)-1,2-bis(3´-thienyl)ethene]$^{+}$ PF_6^{-}, [36]

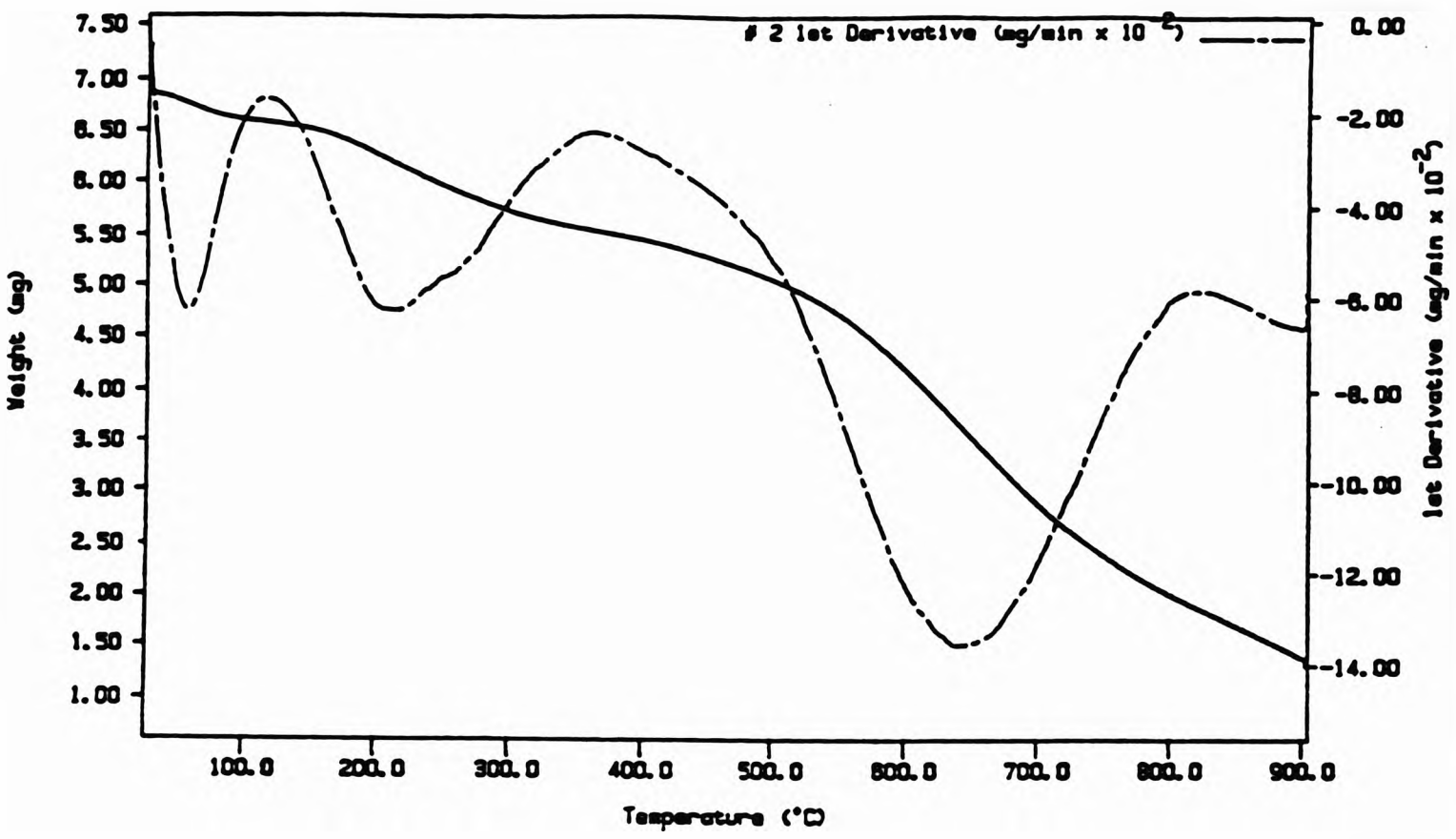

Figure 6.13
(--------) The thermogravimetric profile of the Poly[1]$^{+}PF_6^{-}$ polymer [36] (derived from compound [1]), in nitrogen and within the temperature regions of 30 - 900°C . The rate of temperature increase was 10°C min^{-1}.
(--- - ---) The curve of the first derivative (mg/min x 10^{-2}).

The TGA/DTG curves of [36] shows a biphasic decomposition pattern similar to that observed for decomposition of [32]. The evaporation of residual acetone led to a 3.65% loss of polymer weight (figure 6.13 [A]), whilst the 15.75% mass loss at 208°C is attributed to degradation processes leading to the loss of electric conductivity as a result of thermal dedoping (figure 6.13 [B]). However, the superior thermal stability of this polymer, in comparison with that of [32] is evident in:

i. The higher temperature needed for the optimisation of the dedoping process (208°C in contrast to 165°C). This may be due to a higher degree of planarity of the polymer backbone which correspondingly ensures a better fitting of the anion within the polymer matrix and leads to a superiorly ordered polymer:anion ensemble.

ii. The higher temperature needed to effect the degradation of the dedoped polymer backbone (640°C in contrast to 605°C).

iii. The rate of polymer degradation was also 27.80% slower than that of [32]. The lower rate of degradation, probably due to better inter-chain contacts, resulted in an increased amount of remnant material at the end-of-test temperature of 900°C (20%).

6.3.3 The thermal stability of the PF_6-doped polymer [30], derived from the electropolymerisation of 3-(trimethylsilyl)thiophene, [9]

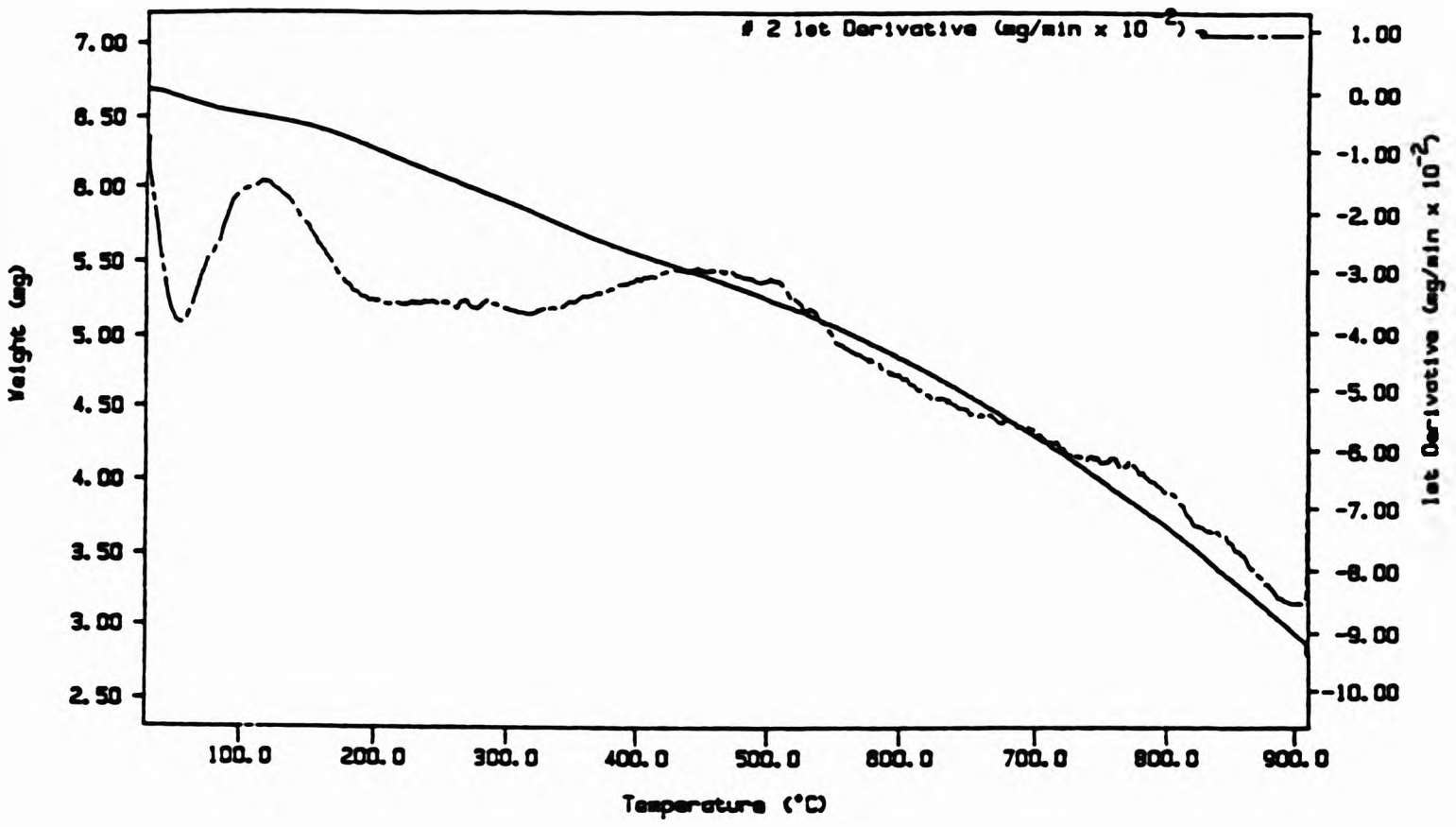

Figure 6.14
(--------) The thermogravimetric profile of the PF_6 doped polymer [30] (derived from compound [9]), in nitrogen and within the temperature regions of 30 - 900°C . The rate of temperature increase was 10°C min^{-1}.
(--- - ---) The curve of the first derivative, (mg/min x 10^{-2}).

After the evaporation of residual acetone which resulted in a 2.65% loss of polymer mass (figure 6.14 [A]), the thermal degradation profile of [30] showed a gradual weight loss resulting from a two-stage deterioration of the polymer (figure 6.14 [B] & [C]). The initial stage occurred between 130 - 500°C and resulted in a 18.70% loss. The DTG profile (in contrast to those for the simple dedoping processes observed in [32] & [36] in their first decomposition stage) is reminiscent of those attributed to coupled reactions. This leads to the assumption that the thermal disruption of the electrically neutral dopant-polymer charge-transfer ensemble, leads to complex structural reorganisation(s) within the polymer matrix. These reorganisation(s) could arise from one or all of the following thermal processes:

i. The reaction between an oxidised portion of the polymer backbone and a neutral, neighbouring polymer chain.

ii. Cross-linking of the monomeric units upon loss of the thermolabile trimethylsilane pendant group.

iii. Reaction of the polymer with the thermally-labile PF_6 anion *via* processes which includes the fluorination of the polymer upon the breakage of the very weak P-F bonds that constitute the dopant anion.

Between 500 & 900°C (stage C) the rate of pyrolysis increases due to the inclusion of processes involving the breakdown of the polymer-chain itself. This leads to the degradation of twice as much material (35.2%) as in the first stage, but the slow rate of degradation still results in a very high residual mass fraction of 43.4% after the fixed end-of-test temperature of 900°C.

6.4 SOLID-STATE ^{13}C-CPMAS NMR SPECTRUM ANALYSIS*

6.4.1 Analysis of the ^{13}C (CPMAS) NMR spectrum of [Poly-(2´,5´-thiophenediyl)-1,2-bis(3´-thienyl)ethene]$^{+}$ PF_6^{-}, [36]

The ^{13}C-NMR spectra of compound [1], and that of its oxidised polymer [36], are shown in figures 6.15 and 6.16 respectively. As a consequence of the decrease in electron density about the oxidised polymer, a slight downfield shift of resonances accorded the polymer in contrast to that of the monomer was expected. Whilst the monomer gave rise a well-resolved spectrum (figure 6.15), that of the polymer contained only one broad signal; centred at 125.59 ppm and with a half-height width of 17 ppm (figure 6.16). Although unresolved, the position of this signal however suggests that the monomeric units are wholly (and intactly) incorporated into the polymeric ensemble.

*Details of the methodology are contained in the experimental section (chapter 8).

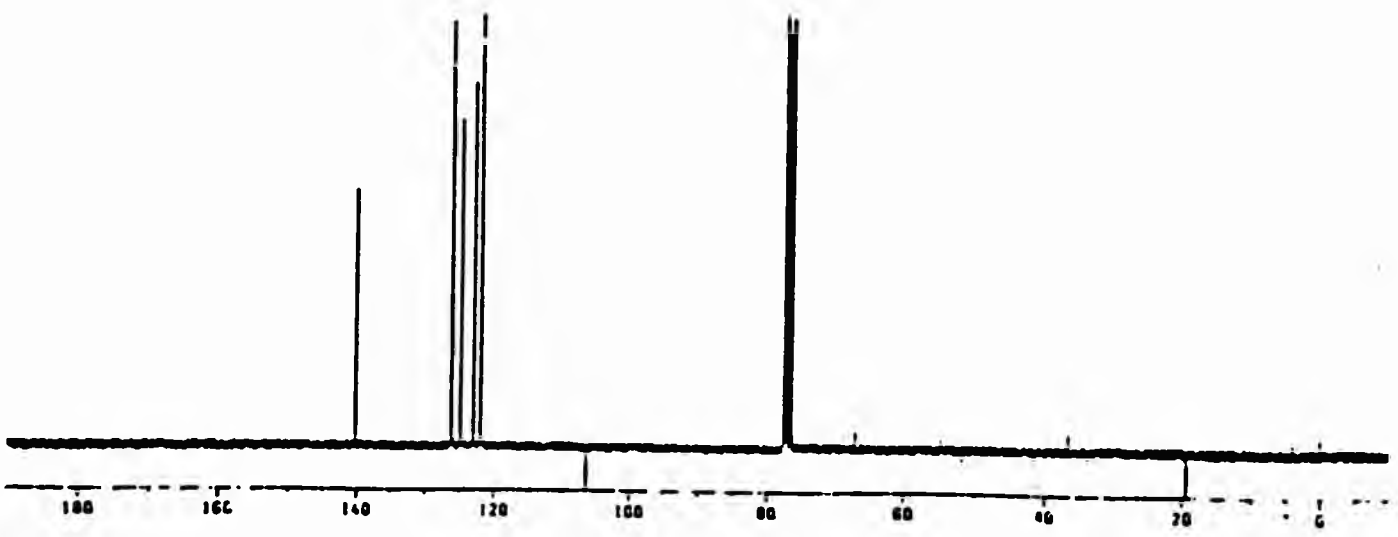

Figure 6.15
The ^{13}C-NMR spectrum of 1,2-bis(3´-thienyl)ethene obtained in $CDCl_3$
(δ) 140.06, C_3; 126.14, C_4; 124.78, C_5; 122.93, C_6; 121.89, C_2.

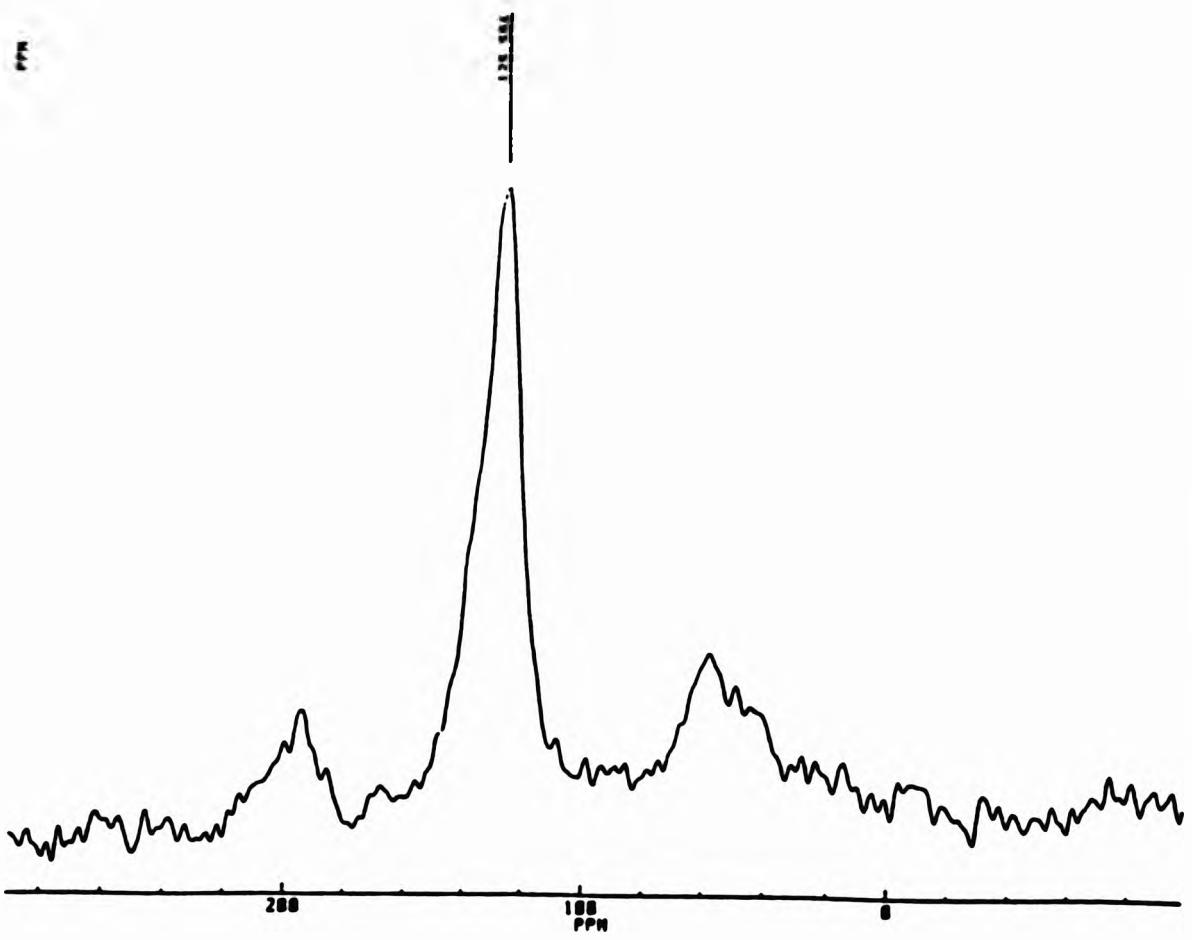

Figure 6.16
The ^{13}C(CPMAS)-NMR spectrum of [Poly-(2´,5´-thiophenediyl)-1,2-bis(3´-thienyl)ethene]$^+$ PF_6^-, [36].

6.4.2 Analysis of the ^{13}C (CPMAS) NMR spectrum of the PF_6-doped polymer [30] derived from the electropolymerisation of 3-(trimethylsilyl)thiophene [9]

Figure 6.17 depicts the ^{13}C spectrum of 3-(trimethylsilyl)thiophene, [9]. In comparison, the spectrum of the PF_6-doped polymer [30], derived from its electropolymerisation as described in condition 5.6, illustrates the presence of five overlapping signals between 120 - 145 ppm (half-height width: 19 ppm). This indicates the presence of five chemically-distinct carbon environments on the polymer framework (figure 6.18). Although unresolved, some of these overlapped signals are at frequencies similar to those present in the spectra of doped poly-2,5-thienylene (figure 6.18: inset). There was also a complete absence of the high-frequency resonances so characteristic of the methyl-carbons of the pendant trimethylsilyl group, and which is observed with high intensity in the spectrum of the monomer at -0.577 ppm.

With these observations, it could be tentatively concluded that the implementation of condition 5.6 (chapter 5) does not result in the expected formation of a Poly[(2´,5´-thiophenediyl)-3´-(trimethylsilyl)thiophene]$^+$ PF_6^- ensemble, but in the formation of a PF_6-doped polymer predominantly made up of thiophene units which are randomly linked by α-α´ and α-β´ bonds, and thus by 2,5- 2,4- and 3,5- couplings.

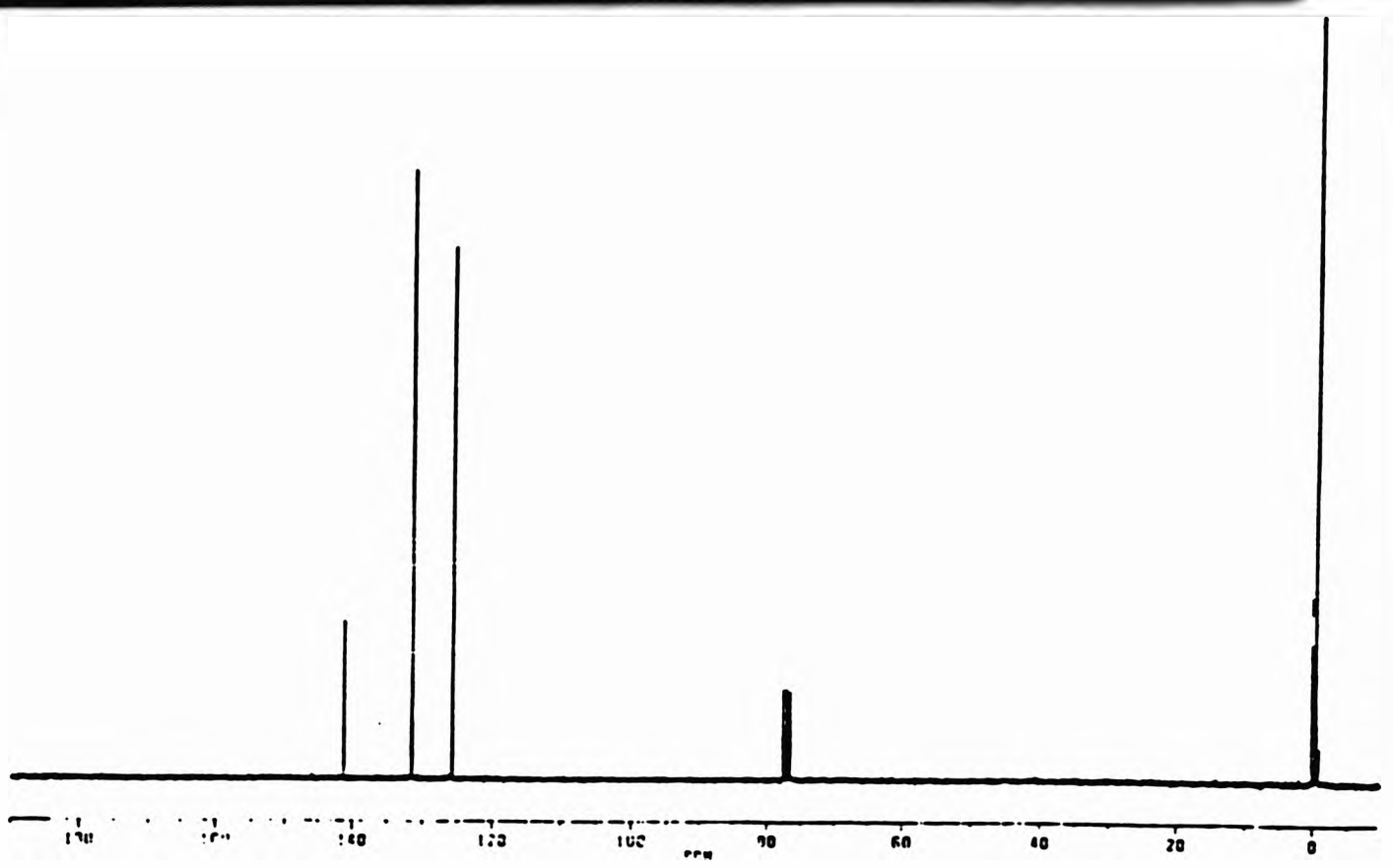

Figure 6.17
The ^{13}C-NMR spectrum of 3-(trimethylsilyl)thiophene obtained in $CDCl_3$ (δ) 141.08, C_3; 131.32, C_2 & C_4; 125.56, C_5; -0.58, -CH_3

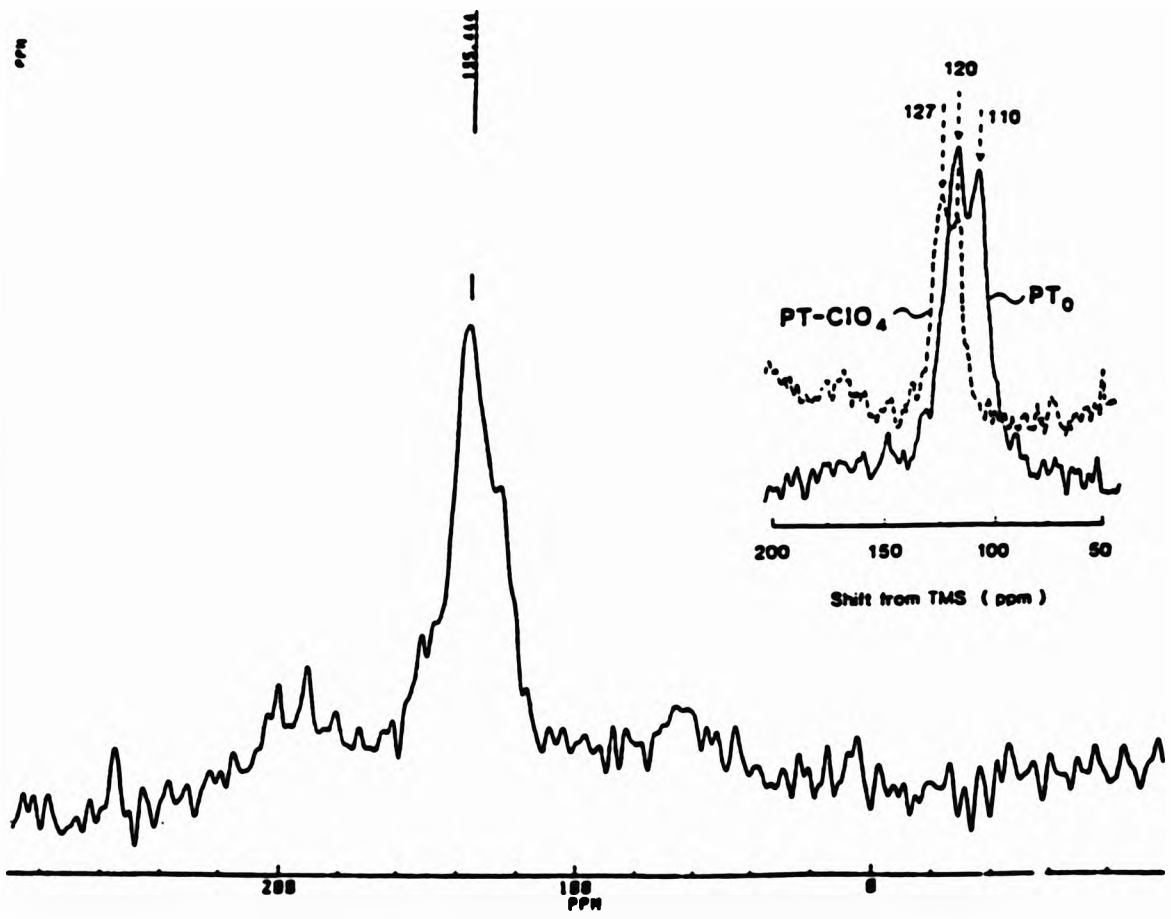

Figure 6.18
The ^{13}C (CPMAS)-NMR spectrum of the PF_6-doped polymer [30] derived from the electropolymerisation of 3-(trimethylsilyl)thiophene [9]. Inset: the strikingly-similar ^{13}C-NMR spectra of ClO_4^- doped poly 2,5-thienylene (broken line) and undoped poly-2,5-thienylene (solid line).[171] The doped poly 2,5-thienylene shows two broad absorption bands at 120 and 127 ppm with a half-height width of 14 ppm

CHAPTER 7

CONCLUSION

7.1 INTRODUCTION

Attempts to produce p-doped, conducting polymers from thiophenes functionalised with a range of active substituents have led to the fabrication of polymeric materials from three of the starting monomers, *viz*; compounds [1], [2] and [9]. Although a low level of doping was achieved in each case, the polymers produced were all semi-conducting and exhibited differences in conductivity values, surface microstructure, thermal stability and material flexibility. The experimental conditions leading to the syntheses of these polymers also reveals a dependency of electropolymerisation process on such variables as the nature of solvent and electrolyte used, the concentration of monomer, and the ratio of monomer to supporting-electrolyte. Similar behaviour has been proposed for polythiophene.[74]

This chapter seeks to:

- describe the experimental variables which require to be controlled and the means by which this could be achieved,
- establish criteria which might optimise the polymerisation process for a given monomer,
- propose avenues which might increase the propensity of the monomers which did not polymerise to do so,
- identify other research interests which might complement this field of study.

7.2 GENERAL DISCUSSION

7.2.1 Factors Affecting Polymer Generation & Yield

The need for a meaningful and comparable set of results necessitated the imposition of a generalised set of conditions on the cyclic voltammetric studies and during constant potential electrolysis. In agreement with published data,[172] films prepared in acetonitrile, the most widely used solvent in electrochemical studies, adhered so firmly to the electrode that they could only be detached with the aid of scraping. With the use of acetonitrile, the anodic oxidation of compound [9] did not result in the localisation of polymeric material on the electrode surface, but in the formation of coloured and oxidised oligomers in the electrolytic solution. Additionally, the material yields obtained from the polymerisation of compounds [1] and [2] were less than 30%. These disappointing results are likely to be due to the generation of soluble reaction products from competing reaction pathways which have stoichiometries different from that relating to the polymerisation process. These reactions, leading to the formation of unwanted products, have constituted a source of mechanistic ambiguity which could not be investigated due to the lack of time. Radical cationic species are highly reactive and susceptible to scavenging-electrophilic and indiscriminate reactions[173] with either acetonitrile or the small amount of water ubiquitously present in it.

With the use of nitrobenzene as solvent, the CV's of all applicable compounds showed an improved stability of the engendered cationic species. Consequently, the electropolymerisation of [9] in nitrobenzene, with conditions analogous to that used in acetonitrile, led to the production of a conducting and free-standing, p-doped polymer [30]. Improved yields of polymeric material were also obtained from the oxidation of [1] and [2]. Generally, and in contrast to acetonitrile, anodic electropolymerisation in nitrobenzene led to the production of free-standing films which harnessed superior yields, improved adhesion properties and consistent reproducibility. The solvent dependency of the polymerisation process thus suggests that the radical cations exhibit a lower reactivity towards nitrobenzene than acetonitrile. These disparate reactivities might be indicative of disparate geometries. Suitable conditions for the adhesion of aromatic nuclei (considered as slightly basic on a metallic surface) are fulfilled in acidic media.[174] It is therefore plausible for the search of conditions leading to the effective polymerisation of those monomers which did not polymerise in this instance, to diverge from the use of acetonitrile as solvent, and find a renaissance in the use of solvents such

as dichloromethane, nitromethane and nitrobenzene.

7.2.2 The Use of Mass-Spectroscopy in Predicting the Propensity of a Monomer to Polymerise.

The multidisciplinary nature of this field of study demands that the organic chemist synthesises a target monomer that is thereafter sent to the electrochemist for studies of its suitability as a p-doped conducting polymer; a procedure that generally works on a "hit or miss" basis. This is because, although it is possible to synthesise monomeric compounds to fit the theoretical requirements of conducting polymers, there is at present, no way to accurately predict the sort of physicochemical properties the engendered polymer would exhibit. However, it should be possible for the organic chemist to use the fragmentation patterns obtained from electron-impact (EI) mass-spectroscopy, to elucidate or forecast the behaviour of aromatic compounds upon electrochemical oxidation, and thus, have a basic idea of the propensity of an aromatic compound to polymerise.

The radical cation formed from either the oxidation of a compound at a suitable potential, or due to EI ionisation, arise from electron loss from the region of lowest ionisation potential or the region of highest electron density. EI mass spectroscopy gives an indication of where the positive charge is localised on the radical cation and which primary process(es) of chemical transformation accompany the formation of the radical cation (i.e., how stable the radical cation is). The capacity of a compound to couple and subsequently aromatise is reflected in the ease with which its radical cation loses a proton, or any other susceptible functionality. This ease can also be identified by EI mass spectroscopy. A study of the spectra of all the compounds prepared showed that all those monomers with intense and successive $[M^+ - 1]$ and $[M^+ - 2]$ peaks underwent oxidative coupling. The quasi-reversibility displayed by the ferrocenyl analogues [4] - [6] during CV studies, indicative of the stability of their generated cations, was also manifest in their mass-spectra; where the respective parent ions of [4] - [6] represented the base peak in all cases. Although with a knowledge of electrochemistry it was easy to relate the primary oxidation process of these compounds to the formation of a stable ferrocenium ion, in the analysis of the EI mass spectroscopy profiles, charge localisation on the iron component was supported by the domination of fragmentation processes by cleavages attributed to the ferrocene moiety.

From the fragmentation patterns of compounds [1], [2], [4] and [3] (chapter 3.2) it is

also possible to predict the secondary reactions or chemical transformations that might occur upon the formation of a radical cation and which ensues low yields of polymeric material. These include oxidative cyclisation to yield stable entities such as [23a], [23b], [23d] and the *m/z* 185 radical cation respectively.

7.2.3 The Fluorescence Efficiency of Compound [32]

Conducting polymers containing fluorescent chromophores have potential revolutionary and wide-ranging device applications. Unfortunately, solid-state fluorescence studies* revealed a low fluorescence efficiency for the poly[2]$^{+}$ PF_6^{-} material, [32]. Although this low fluorescence efficiency could arise from dopant-induced fluorescence quenching, it could also be due to an inability of the pendant pyrene moiety to adopt the conformation that gives rise to its characteristic emission. Even though it is spectroscopically difficult to identify the geometric distortions of polymer chains, this inability of the pyrene moiety to adopt the conformation that leads to fluorescence could be a consequence of steric bulk or, more likely, fixation of the moiety by electrochemical coupling via its 3-, 6-, and 8- positions.[175,176] Coupling of the pyrene moiety in this fashion is expected to result in non-planar conformations and a diminished conductivity; as non-planar conformations leads to the prevalence of poor interchain contacts (see chapter 6.1), which in turn, reduces the probability of charge-carrier hopping.[177]

Taking these factors into consideration, the substitution of the pyrene moiety with long-chained, aliphatic electron donating or withdrawing substituents at its 3-, 6-, and 8-positions is recommended. It is hoped that this would help to suppress the participation of these electron-dense sites in the coupling process and concomitantly generate fluorescent and solution processible conducting polymers.

---

*Solid-state fluorescence studies were conducted at the School of Chemistry, Queen's University of Belfast, Northern Ireland.

7.2.4 The Electropolymerisation of 3-(trimethylsilyl)thiophene [9]

Since the electropolymerisation of [9] resulted in the formation of a polymer that had not retained the trimethylsilyl moiety, it is evident that the mechanism of polymerisation of this monomer involves the contribution of a chemical process which culminates in its desilylation.

The susceptibility of any given compound towards electrophilic substitution is a valid index in determining its' overall reaction sites, and thus, any possible polymer linkage sites.[178] The C-Si bond, which is weaker than the C-H bond,[179] cleaves readily in aromatic-electrophilic reactions, and while the 3-position of thiophene is generally reactive only under forcing conditions, it is still 115 times more prone to protodesilylation than phenyltrimethylsilane.[180] Also the demetalation of group-IV entities upon attempted electropolymerisation has been reported.[181] It is yet undetermined whether the desilylation of [9] occurs as a spontaneous consequence of the formation of the radical cation, or due to protodesilylation of the unoxidised monomeric species in an electrolytic medium which progressively increases in acidity as the time span of the polymerisation process increases. What was evident from the electropolymerisation of [9] in nitrobenzene however, was the production of an electroactive material [30], that harnessed properties which make it one of the most flexible and compressible electroactive polymers derived from a functionalised thiophene to date*.

It is strongly suspected that, whatever the mechanism, the thiophene radical generated by the cleavage of the trimethylsilyl group is likely to result in an increase in the number of coupling routes (and coupling sites), and therefore in indiscriminate β - β' and α --β' couplings. This, in conjunction with competitive α - α' couplings, leads to an increase in the mean conjugation length of the polymer and the generation of a fibrillar morphology upon which microcrystallites are formed as the polymer increases in thickness. The ease of desilylation could therefore lead to the attribution of site activation, to the process of replacing hydrogen with a trimethylsilyl group. Unfortunately however, these scavenging α - β' couplings also lead to structural disorder which is suspected to drastically affect the conductivity values that could otherwise be achieved.

---

* Lately, the polymer has shown promise as an active element in gas sensing, and further studies on this aspect are in progress.

In the study of the polymeric material [30], SEM and EPMA findings have illustrated the importance of the under-utilised technique of microstructure analysis in the elucidation of the physicochemical properties of conducting polymers. Microstructural analysis led to the identification of anisotropic morphologies to the disparate conductivities of the two sides of the polymer, and provided tentative proof of desilylation in the material.

7.2.5 The Oxidation of the Ferrocene-Substituted Thiophenes; compounds [4] - [6]

The propensity for [4] - [6] to exist as stable iron-centred cations and dications respectively results in difficulty in effecting their polymerisation through the α - α' coupling of their respective thiophene components. Efforts to derive polymers from [4] and [5] should be concentrated on co-polymerisation in solvents other than acetonitrile and with monomers which oxidatively electropolymerise at between +0.8 V and +1.3-V (e.g., N-methylpyrrole [+1.12 V] & indole [+1.26 V]). Attempts could also be made to "activate" the 2,5-positions of the thiophene moiety with the insertion of labile and activating functionalities such as the trimethylsilyl group. Polymerisation attempts, using a platinum working-electrode that has been surface modified with a thin film of poly[9], could also be undertaken on these compounds and each of the other synthesised monomers. The crystal structure of [4] has recently been determined by X-ray crystallography,[182] and detailed studies of the electrochemical behaviour of both [4] and [5] are currently in progress.

7.2.6 Factors Affecting Polymer Quality

EPMA and TGA studies have shown the density of monomeric packing and the polymer stability (respectively) to be in the increasing order poly[2] < poly[1] < poly[9]. The same trend was also observed for polymer flexibility and alas, conductivity. The one-step thermal de-doping of the PF_6-oxidised polymers [32] and [36] (derived from poly[2] and poly[1] respectively) as observed in chapter 6.3, is suspected to ensue from a low binding energy between the dopant and the polymeric chains. This is due to steric limitations in the respective polymer:anion ensembles.

In addition to playing a role in the quality of polymers generated, steric limitations may also totally hinder the formation and coupling of any of the radical cations produced during the process of anodic oxidation. The ineffectiveness of the p-toluenesulphonate

anion in supporting polymerisation (chapter 5) could be as a result of these limitations (self- and monomer- imposed), kinetic limitations, or difficulty in the formation of an electrically neutral polymer:anion ensemble.

From the overall results obtained, two generalised assumptions could be made:

- The ability of an anion to coordinate effectively is regulated by the competition it receives from the solvent system used, the bases present, inherent steric restrictions and activation energy limitations as the electrically-neutral ensemble seeks a minimum free energy.

- Polymer quality (arising from flexibility, thermal stability, density of monomeric packing), and inherent conductivity are regulated by the formation of a electrically-neutral polymer/dopant complex which neither exhibits high polymer strain nor contain a large volume fraction of voids of molecular dimensions.

In an effort to suppress the steric effects imposed by the bulkiness of active substituents and thus electropolymerise monomers which incorporate moieties with potential research and device applications, factors which enforce and enhance the polymerisation process, including the neatness of chain-packing should be explored. These should encompass the use of low temperatures as an aid to the stabilisation of generated radical cations and thus instigate an increased effectiveness in the polymerisation process (this could involve experimentation with sulphur dioxide as solvent), the suspension of molecular sieve in the electrolytic solution so as to achieve and maintain "super-dry" conditions (or as recently suggested, the use of an excess of P_2O_5[183] or superactive alumina[184]), and the utilisation of repeating trimer or tetramer-equivalents of the desired monomeric unit with the hope that these oligomers would polymerise at a lower oxidation potential than their corresponding monomers.

7.3 COMPLEMENTARY AREAS OF RESEARCH

Although the main reason for the development of the novel compounds has been for the study of their spectroscopic and electrochemical properties; including the physicochemical properties of their p-doped polymeric ensembles, it is hoped that a there is a more versatile approach towards their possible end uses, and that a wider range of applications could ensue. The following avenues illustrate areas in which the monomers, polymers and the techniques used could be ideally developed into complementary areas of research.

7.3.1 Non-Linear Optics (NLO)[185,186]

The field of NLO has emerged as a new frontier of science and technology which has captured the imagination of scientists and engineers worldwide. Applications of devices based on non-linear optical materials have been identified in the fields of instrumentation, optical communications, sensing, and signal processing. Whilst the absolute material requirements for the optimisation of second and third order non-linearities are presently ill-defined, the presence of a highly extendable and polarisable system of π-electrons appears to be important.

Since polymers derived from the electropolymerisation of thiophene exhibit a propensity for head-to-tail coupling (resulting from S-*cis* coupling) and electrochemical fabrication seems an alternative to the Langmuir-Blodgett (LB) technique normally employed for the fabrication of well-ordered thin films,[187] the phenomenon of non-linear optical activity in optimally (and electrochemically) grown, wafer-thin polymers should be explored.

7.3.2 Pharmacological Studies

Interest in the development of biologically active derivatives of thiophene has led to a series of comprehensive reviews.[188] The substitution of pharmacologically-active benzene systems with analogous thiophene systems have resulted in a range of disparities in the solubility, bioavailability, and metabolic fate of such isosteres. In some cases these isosteres have resulted in up to a 1,000-fold increase in activity.[189] In view of the above, including the structure/reactivity relationships reported for various thiophene series[190] and the observed nematocidal activity of 1,2-bis(2´-thienyl)ethene,[191] samples of monomers [1], [2], [3], [7] & [8] could be screened for any potential

nematocidal and pesticidal activity.

CHAPTER 8

EXPERIMENTAL

8.1 MEASUREMENT TECHNIQUES

The Fourier-Transform Infra-Red (FTIR) spectra of all the synthesised compounds (Chapter 3.1) and the engendered polymers (Chapter 6.2) were obtained as pressed KBr discs on a Bio-Rad (Digilab Division) FTS-40 FTIR spectrophotometer. Each spectrum was acquired by averaging 64 interferrograms between 400 - 4000 cm^{-1}. The polymers, made by the conditions in Chapter 5, were either peeled or scraped-off the platinum electrode. All recorded frequencies are accurate within ± 4 cm^{-1}.

The Mass Spectra (MS) of compounds [1] to [9] (Chapter 3.2) was recorded on a prototype Kratos Profile GC/MS spectrometer operating at 70 eV. Cyclic Voltammetry (CV) measurements in a two-compartment electrochemical cell arrangement (Chapter 4.4) were made using a PAR 173/276 (EG & G Instruments). The platinum working electrode was cleaned in *Aqua regia*, thoroughly rinsed with distilled water and anodised before each use. Melting points were determined using an Electrothermal-Digital melting point apparatus and are uncorrected. C, H, N microanalyses were performed on a Carlo-Erba Strumentazione Elemental Analyser (Model 1106).

The surface morphology of the oxidised polymers (Chapter 6.1) was investigated by Scanning Electron Microscopy (SEM), and by Energy Dispersive Electron Probe X-ray Microanalysis (EPMA) using a Hitachi S-570 Scanning Electron Microscope attached to a Link Analytical AN10/25-S EDAX system. The energy beam used for both procedures was 20 K eV. A deft manipulation of the parameters of contrast and magnification was required, as the charging of the polymers led to a picture-quality handicap. Thermogravimetric Analysis (TGA) coupled with Derivative Thermogravimetric studies (DTG)[192] (Chapter 6.3) were performed on a Perkin-Elmer 7 Series Analysis System in a nitrogen-purged atmosphere. The solid-state ^{13}C-NMR spectra of the oxidised polymers [36] and [30] (Chapter 6.4) were obtained with a Brüker MSL-500 multinuclear spectrometer using high resolution Solid-State Cross Polarisation and Magic Angle Spinning techniques (CPMAS).[193,194]

The ^{13}C-NMR spectra of their respective monomers [1] and [9] (Chapter 6.4), and the ^{1}H-NMR spectra of all the monomers (Chapter 3.3) were obtained as solutions in deuterated chloroform ($CDCl_3$) with the aid of a Brüker AM-250 spectrometer operating at 62.896 MHz for the carbon nucleus and 250.133 MHz for the proton nucleus. All chemical shifts are given in ppm and are relative to tetramethylsilane (TMS) at 0.00 ppm.

Reagents were used as supplied and solvents were dried by standard procedures.

8.2 SYNTHETIC PROCEDURE

(i) *trans*-1,2-Bis(3´-thienyl)ethene, [1]

The following illustrates the general procedure used for the syntheses of the ethene-substituted thiophenes. 3-(Dimethoxyphosphinylmethyl)thiophene (3.6 g., 1.75 x 10^{-2} moles) and sodium methoxide (1 g., 1.85 x 10^{-2} moles) were combined with dimethylformamide (25 ml.) in a 100 ml. round bottom flask fitted with a condenser, drying tube, and magnetic stirrer. After stirring at room temperature for 30 minutes, a solution of thiophene-3-carboxaldehyde (1.63 g., 1.45 x 10^{-2} moles) in DMF (25 ml) was added and the stirred mixture was heated at 85 °C for 8 hours. Upon cooling the solution was poured onto 200 ml. of crushed ice and slurred for 30 minutes. The white precipitate was filtered at the pump, washed with water and dried. Recrystallisation from ethanol yielded silvery-white plates of [1] (1.81 g., 65% yield based on the aldehyde). M.pt 172 - 173 °C. Analysis found: C, 62.53; H, 4.10%. Calculated for $C_{10}H_8S_2$: C, 62.46; H, 4.19%.

(ii) *trans*-1-(1´-Pyrenyl)-2-(3˜-thienyl)ethene, [2]

In a manner essentially identical to that described for the formation of [1], a solution of 3-(dimethoxyphosphinylmethyl)thiophene (3.6 g., 1.75 x 10^{-2} moles), sodium methoxide (1 g., 1.85 x 10^{-2} moles), and pyrene-1-carboxaldehyde (3.4 g., 1.48 x 10^{-2} moles) in DMF (50 ml.) was heated at 85 °C for 5 hours. The crude yellow powder recovered after work-up was chromatographed on silica (70 - 230 mesh) using a 3:7 mixture of carbon tetrachloride/ dichloromethane. The main yellow band was eluted to give, after evaporation of solvent, bright-yellow crystals of [2] (3.8 g., 83%). M.pt 169.5 - 170.4 °C. Analysis found: C, 85.13; H, 4.48%. Calculated for $C_{22}H_{14}S$: C, 85.14; H, 4.55%.

(iii) *trans*-1-(p-N,N-Dimethylaminophenyl)-2-(3´-thienyl)ethene, [3]

In a manner essentially identical to that described for the formation of [1], a solution of 3-(dimethoxyphosphinylmethyl)thiophene (3.6 g., 1.75 x 10^{-2} moles), sodium methoxide (1 g., 1.85 x 10^{-2} moles), and 4-dimethylaminobenzaldehyde (2.2 g., 1.48 x 10^{-2} moles) in DMF (50 ml.) was heated at 85 °C for 8 hours. The crude chalky-white powder recovered after work-up was chromatographed on silica using a 3:7 mixture of carbon-tetrachloride/dichloromethane. Compound [3] was isolated as a chalky-white powder

(2.71 g., 80% yield). M.pt 179.8 - 181.9 °C. Analysis found: C, 73.26; H, 6.65; N, 6.11%. Calculated for $C_{14}H_{15}NS$: C, 73.33; H, 6.60; N, 6.11%.

(iv) *trans*-1-(Ferrocenyl)-2-(3´-thienyl)ethene, [4]

In a manner essentially identical to that described for the formation of [1], a solution of 3-(dimethoxyphosphinylmethyl)thiophene (2.31 g., 1.12 x 10^{-2} moles), sodium methoxide (0.73 g., 1.35 x 10^{-2} moles), and ferrocene-1-carboxaldehyde (2 g., 9.34 x 10^{-3} moles) in DMF (50 ml.) was heated at 65 °C for 8 h. Ethanolic recrystallisation of the crude material recovered after work-up afforded [4] as orange needles (2.42 g., 88% yield). M.pt 146 - 148 °C. Analysis found: C, 65.38; H, 4.77%. Calculated for $C_{16}H_{14}FeS$: C, 65.30; H, 4.80%.

(v) (*E,E*)-3,4 *Bis*-(2´-ethenylferrocenyl)thiophene, [5]

In a manner essentially identical to that described for the formation of [1], a solution of 3,4-*bis*(dimethoxyphosphinylmethyl)thiophene (2.20 g., 6.68 x 10^{-3} moles), sodium methoxide (0.87 g., 1.61 x 10^{-2} moles), and ferrocene-1-carboxaldehyde (3 g., 1.4 x 10^{-2} moles) in DMF (50 ml.) was heated at 65 °C for 8 hours. The crude precipitate recovered after work-up was purified by column chromatography on silica using dichloromethane as solvent to obtain [5] as deep-red crystals. Yield 2.46 g., (73%). M.pt 172 - 174 °C. Analysis found: C, 66.76; H, 4.77%. Calculated for $C_{28}H_{24}Fe_2S$: C, 66.66; H, 4.80%.

(vi) 1-(Ferrocenyl)-3-(3´-thienyl)prop-2-en-1-one, [6]

A solution of sodium hydroxide (2 g, 0.05 mole) in water (12 ml.) was added to a cooled (10 °C) stirred solution of acetylferrocene (2.5 g, 0.011 moles) and thiophene-3-carboxaldehyde (2.2 g, 0.0196 moles) in ethanol (90 ml.). After the addition was completed, the temperature of the reaction mixture was maintained at 26 °C whilst being stirred for a further 3 h. Upon standing overnight at 0 °C, the resulting purple-red crystals were separated by filtration, washed with ice-cold water until the washings were neutral to litmus, and then with cold aqueous ethanol. Recrystallisation from ethanol afforded purple-red crystals of [6] (2.61 g, 73% based on acetylferrocene). M.pt 159 - 161.5 °C. Analysis found: C, 63.43; H, 4.35%. Calculated for $C_{17}H_{14}FeSO$: C, 63.35; H, 4.38%.

(vii) (*E,E*)-1,5-*Bis*(3´-thienyl)penta-1,4-dien-3-one, [7]

To a stirred solution of sodium hydroxide (1.78 g, 4.45 x 10^{-2} moles) in 50% aqueous ethanol (40 ml.), was added half of a mixture of thiophene-3-carboxaldehyde (2 g, 0.018 moles) and dry acetone (0.52 g., 8.95 x 10^{-3} moles). The temperature was maintained at 28 °C throughout the whole procedure and a flocculent product appeared within 3 minutes. After 15 minutes, the remainder of the mixture was added and stirring was continued for another 40 minutes. The precipitate formed was filtered and washed with three 100 ml portions of ice-cold water. It was then dried to yield [7] as a cream powder (3.7 g., 84% yield). M.pt 134.6 - 138 °C. Analysis found: C, 63.34; H, 4.02%. Calculated for $C_{13}H_{10}S_2O$: C, 63.38; H, 4.09%.

(viii) *all-trans* 1,9-*Bis*(3´-thienyl)nona-1,3,6,8-tetraen-5-one, [8]

A reaction between *trans*-3-(3-thienyl)acrolein (1 g., 7.23 x 10^{-3} moles), acetone (0.12 g., 3.62 x 10^{-3} moles) and a stirred solution of sodium hydroxide (0.72 g., 1.81 x 10^{-2} moles) in ethanol (18 ml., 50% aqueous) in the manner described above for [7], yielded [8] as a bright yellow powder (1.72 g., 80%). M.pt 124 - 127 °C. Analysis found: C, 64.03; H, 4.69%. Calculated for $C_{17}H_{14}S_2O$: C, 68.45; H, 4.73%.

(ix) 3-(Trimethylsilyl)thiophene, [9]

A solution of 3-bromothiophene (10 g. 6.13 x 10^{-2} moles) in diethyl ether (50 ml.) was introduced by syringe into a 2-necked flask containing 29.4 ml. of a precooled (-70 °C) and stirred 2.5 M etheral solution of n-butyllitiium (4.7 g.) at such a rate that the temperature of the reaction mixture did not exceed -70 °C. Prior to use, the flask had been successively flame-dried and air-purged with nitrogen. After 45 minutes, a cold etheral solution of chlorotrimethylsilane (7.33 g., 6.75 x 10^{-2} moles) was slowly added by syringe and the mixture stirred for a further period of 2 hours, after which the cooling bath was removed and the flow of nitrogen stopped. Upon warming to room temperature, the reaction was quenched with water (60 ml.) and stirred for 30 minutes; the ether fraction separated and successively washed with three portions of water. After drying over anhydrous magnesium sulphate, filtration of the drying agent, and removal of solvent, the residue was fractionated to yield [9] as a colourless liquid that slowly decomposed upon prolonged storage at room temperature and on exposure to light. Yield: 5.56 g. (58%); B.pt 168 - 169 °C. MS [156.32] (*m/z*, ion, relative %): 141.00,

$C_4H_3S^{28}Si(CH_3)_2^+$, 100.0; 156.00, $C_4H_3S^{28}Si(CH_3)_3^+$, 38.3; 43.00, $^{28}Si(CH_3)^+$, 16.4; 45.10 CHS^+, 12.8; 83.00, $C_4H_3S^+$, 10.8; 39.05, $C_3H_3^+$, 5.6; 73.05, $^{28}Si(CH_3)_3^+$, 5.2.

(x) 3-(Dimethoxyphosphinylmethyl)thiophene, [10]

A magnetically stirred mixture of 3-(bromomethyl)thiophene (60 g, 3.39×10^{-1} moles) and trimethyl phosphite (42 g, 3.39×10^{-1} moles) was heated at 120 °C in a silicon-oil bath. The distillation of ethylbromide was spontaneous and continued over a period of 30 minutes. After 4 h the mixture was fractionated under reduced pressure to yield the phosphonate as a faint-yellow oil (45.5 g, 65% yield). B.pt 164 - 171 °C (25 mm Hg).

(xi) 3,4-Dimethylthiophene

A solution of 3,4-dibromothiophene (15 g., 6.2×10^{-2} moles) in diethyl ether (80 ml.) was placed in a two-necked round bottomed flask that had previously been flame-dried and flushed with dry nitrogen. The flask was cooled to -70 °C in a cardice/acetone bath and 62.5 ml. of a cooled 2.5 M etheral solution of n-butyllithium (10 g. 1.55×10^{-1} moles) was added under a nitrogen atmosphere at such a rate that the temperature of the reaction mixture did not exceed -50 °C. After 45 minutes, a cold etheral solution of dimethylsulfate (16.4 g., 1.3×10^{-1} moles) was added. The mixture was stirred for 30 minutes after which the cooling bath was removed and the flow of nitrogen stopped. An aqueous solution of sodium hydroxide (6.3 g., 1.58×10^{-1} moles) was added and the mixture stirred for 1 hour. The etheral layer was separated, washed three times with water (50 ml.) and subsequently dried over anhydrous magnesium sulphate. The drying agent was filtered off, solvent evaporated on a rotary evaporator, and the residue fractionally distilled to give the desired compound as an oil; yield: 5.7 g. (82%); B.pt. 142 - 145 °C. Lit. b.pt 144 - 146 °C.[195]

(xii) 3,4-*Bis*(bromomethyl)thiophene

In a 250 ml. round bottom flask fitted with a condenser and calcium chloride drying tube, a mixture of 3.4-dimethylthiophene (5.1 g., 4.55 x 10^{-2} moles) and N-bromosuccinimide (16.2 g., 9.10 x 10^{-2} moles) in carbon tetrachloride (100 ml.) was refluxed over a 200 W tungsten bulb for a period of 3 hours and 20 minutes. After cooling, the suspended succinimide was filtered-off at the pump and the solvent was evaporated under reduced pressure. The crude material was diluted with cold 70% ethanol to precipitate the desired compound (9.83 g.) as a white, lachrymatory powder (80% yield). Analysis found: C, 26.90; H, 2.32%. Calculated for $C_6H_6Br_2S$: C, 26.69; H,2.24; Br, 59.19; S, 11.87%.

(xiii) 3-(Bromomethyl)thiophene

The general method above was followed. Distillation of the yellow crude oil obtained from the reaction between 44 g. 3-methylthiophene (0.45 moles), and 80.1 g. N-bromosuccinimide (0.45 moles) in 150 ml. carbon tetrachloride for a period of 8 h. yielded a faint-yellow lachrymatory oil, 67.7 g (84% based on 3-methylthiophene). B.pt. 78 - 81 °C (2 mm Hg). Analysis found C, 34.10; H, 2.80%. Calculated for C_5H_5BrS: C, 33.92; H, 2.85; Br, 45.13; S, 18.11%. Lit. B.pt 78 - 82°C (2 mm Hg).[196]

(xiv) *trans*-3-(3-Thienyl)acrolein

To an ice-cold, vigorously stirred solution of thiophene-3-carboxaldehyde (2.1 g, 0.0187 mole) and sodium hydroxide (0.5 g, 0.0125 mole) in ethanol (8 ml., 63% aqueous), was added over a period of two hours, 5 ml. of a 40% aqueous solution of acetaldehyde. The mixture was stirred for a further 20 minutes, neutralised with ice-cold 20% acetic acid, and extracted with ether. The ether extract was washed successively with dilute aqueous sodium bicarbonate solution and water, dried with anhydrous magnesium sulphate and evaporated under reduced pressure. The residual light-brown liquid was distilled in vacuo to yield the desired compound as a light-yellow liquid (1.35 g, 52% based on thiophene-3-carboxaldehyde). B.pt 126 - 128 °C (5 mm Hg). Analysis found C, 60.75; H, 4.33%. Calculated for C_7H_6SO: C, 60.84; H, 4.38; O, 11.58; S, 23.20%.

(xv) 3,4-*Bis*(dimethoxyphosphinylmethyl)thiophene

A stirred mixture of 3,4-*bis*(bromomethyl)thiophene (4 g, 1.48 x 10^{-2} moles) and trimethyl phosphite (3.68 g, 2.97 x 10^{-2} moles) was heated at 110 °C in a silicon-oil bath. The immediate evolution of bromomethane lasted for 20 minutes, and stirring was continued for a total period of 3 hours. The ^{1}H-nmr of the viscous deep-yellow oil obtained confirmed the formation of the desired phosphonate.* No further purification was carried out.

(xvi) Ferrocene-1-carboxaldehyde

Ferrocene (11.16 g., 0.06 mole) was added in small portions over a period of 20 minutes to a vigorously stirred solution prepared from 21.6 g. (0.16 mole) of N-methylformanilide and 15.3 g. (0.10 mole) of phosphorous oxychloride. The purple viscous mixture formed was stirred for 90 minutes at room temperature and later at 70 °C for 2 hours under a blanket of nitrogen. The mixture was then cooled to 0 °C, sodium acetate (50 g.) dissolved in water (400 ml.) was added, and the solution stirred overnight. The reaction mixture was then extracted three times with ether (400 ml.) and the combined ether extracts washed successively with 1 M HCl, water, saturated sodium bicarbonate solution and finally saturated sodium chloride. The ether extract was concentrated to a volume of 80 ml. and shaken with a cold solution of sodium bisulphite (40 g.) in water (100 ml.). The yellow bisulphite addition compound was collected, washed respectively with ice-cold saturated sodium bisulphite and ether and was finally dried (yield 16 g.).

200 ml. of 2 N sodium hydroxide was added to the bisulphite addition complex and the liberated aldehyde was extracted into ether (3 x 100 ml.). The combined ether extracts were washed with saturated sodium chloride solution and then dried over anhydrous magnesium sulphate. Evaporation of the solvent under water pressure yielded 10.8 g. of deep-red crystals of the required aldehyde. M.pt 120 - 121 °C. Lit. M.pt 124.5°C.[197]

---

*See the ^{1}H-nmr spectra in appendix section.

CHAPTER 9
REFERENCES

1. Innovation 128, *Technical Trends,* Report on Electromagnetic Shielding.

2. (a) J. Mort and G. Pfister, eds., *Electronic Properties of Polymers,* Wiley (1982), p. 215; (b) R. P. Kusy and D. T. Turner, *J. Appl. Polym. Sci.*, **17**, 1631 (1973); (c) S. K. Bhattacharya, S. Basu, and S. K. De, *J. Appl. Polym. Sci.*, **25**, 111 (1980).

3. *Carbon Black Polymer Composites*, E.K. Sichel, ed., Dekker, New York (1982).

4. S. Maiti, *Jnr. Sci. Ind. Res.*, **48**, 577 (1989).

5. *Conducting Polymers*, R. B. Seymour, ed., Plenum Press, New York (1981), p. 23.

6. (a) H. Naarmann, F. Beck, and E. G. Kastning, *DB Patent 1 178 529*, 11 April 1964/20 May 1965; (b) *DB Patent 1 195 497*, 01 February 1963/24 June 1965; (c) D*B Patent 1 092 137*, 12 March 1964/22 November 1967. BASF AG Ludwigshafen.

7. V. V. Walatka, M. M. Vabes, and J. H. Perlstein, *Phys. Rev. Lett.*, **31**, 1139 (1973).

8. R. L. Greene, G. B. Street, and L. J. Sutter, *Phys. Rev. Lett.*, **34**, 577 (1975).

9. C. K. Chiang, Y. W. Park, A. J. Heeger, H. Shirakawa, E. J. Louis, and A. G. McDiarmid, *Phys. Rev. Lett.*, **39**, 1098 (1977).

10. T. Ito, H. Shirakawa, and S. Ikeda, *J. Polym. Sci., Polym. Chem. Ed.*, **12**, 11 (1974).

11. A. F. Diaz, K. K. Kanazawa, and G. P. Gardini, *J. Chem. Soc., Chem. Commun.*, 635 (1979).

12. (a) A. Angeli, *Gazz. Chim. Ital.*, **46**, 279 (1916); (b) G. P. Gardini, *Adv. Heterocycl. Chem.*, **15**, 67 (1973); (c) P. Kovacic and M. B. Jones, *Chem. Rev.*, **87**, 357 (1987).

13. G. Kossmehl and G. Chatzitheodorou, *Mol. Cryst. Liq. Cryst.*, **83**, 291 (1982).

14. M. A. Druy, R. J. Seymour, and S. K. Tripathy, *ACS. Symp. Ser. 242 (Polymer Electronics)*, 473 (1984).

15. M. Delamar, P. C. Lacaze, J. Y. Doumousseau, and J. E. Dubois, *Electrochim. Acta.*, **27**, 61 (1982).

16. G. Mengoli, and M. M. Musiani, *J. Electrochem. Soc.*, **134**, 6436 (1987).

17. N. Oyama, T. Ohsaka, and T. Shimizu, *Anal. Chem.*, **57**, 1526 (1985).

18. J. F. Ambrose and R. F. Nelson, *J. Electrochemical. Soc.*, **115**, 1159 (1968).

19. J. Bargon, S. Mohamand, and R. J. Waltman, *Mol. Cryst. Liq. Cryst.*, **93**, 279 (1983).

20. J. Bargon, S. Mohamand, and R. J. Waltman, *IBM J. Res. Develop.*, **27**, 330 (1983).

21. G. Tourillon and F. Garnier, *J. Electroanal. Chem.*, **135**, 173 (1982).

22. W. R. Salaneck, D. T. Clark, and E. J. Samuelson, *Science and Applications of Conducting Polymers: Proc. of the 6th Europhysics Industrial Workshop*, Adam Hilger, 1991.

23. (a) G. P. Evans in "*The electrochemistry of Conducting Polymers*", *Adv. Electrochem. Sci. and Eng., Vol. 1*, H. Gerischer and C. W. Tobias, eds., VCH Publishers Inc., New York (1990), pp. 1 - 74; (b) J. Heinz, *Topics in Current Chemistry*, Springer-Verlag, Berlin, **152**, 1 (1990).

24. G. L. Baker, *Electronic and Photonic applications of Polymers*; M. J. Bowden, S. R. Turner, eds., *ACS Advances in Chemistry Series 210*; American Chemical Society, Washington DC (1988), p. 271.

25. A. O. Patil, A. J. Heeger, and F. Wudl, *Chem. Rev.*, **88**, 183 (1988).

26. D. J. Walton, *Materials & Design*, **11** (3), 142 (1990).

27. A more rigorous mathematical approach could be found in: B. Moraghar, *J. Molecular Elect.*, **3**, 183 (1987).

28. H. A. Lorentz, *The Theory of Electrons*. Teubner, Leipzig. 1916.

29. C. Kittel, *Introduction to solid state physics*, 6th edition, Wiley, New York. 1986.

30. R. R. Chance, J. L. Brédas, and R. Silbey, *Phys. Rev.*, **B29**, 4491 (1984).

31. (a) J. L. Brédas, R. R. Chance, R. Silbey, *Mol. Cryst. Liq. Cryst.*, **77**, 319 (1981); (b) *Phys. Rev.*, **B26**, 5843 (1982).

32. J. L. Brédas, J. C. Scott, K. Yakushi, and G. B. Street, *Phys. Rev.*, **B30**, 1023 (1985).

33. J. L. Brédas and G. B. Street, *Acc. Chem. Res.*, **18**, 309 (1985).

34. J. L. Brédas, B. Themans, J. G. Fripiat, J. M. André, and R. R. Chance, *Synth. Met.*, **9**, 265 (1984).

35. S. Kivelson in '*Solitons*, S. E. Trullinger, V. E. Zakharov, and V. L. Pokrovsky, eds., Elsevier, Amsterdam. 301 (1986).

36. W. P. Su, J. R. Schrieffer and A. J. Heeger, *Phys. Rev. Lett.*, **42**, 1698 (1979); *Phys. Rev.*, **B22**, 2209 (1980).

37. S. Kivelson, *Phys. Rev.*, **B25**, 3798 (1982).

38. (a) M. -A. DePaoli, R. J. Waltman, A. F. Diaz, and J. Bargon, *J. Polym. Sci. Polym. Chem. Ed.*, **26**, 1687 (1985); (b) S. F. Lindsey and G. B. Street, *Synth. Met.*, **10**, 67 (1984/'85).

39. H. Naarmann, *Electronic properties of conjugated polymers*, H. Kuzmany, M. Mehring, and S. Roth, eds., *Solid State Sciences*, **76**, 12, Springer-Verlag, Berlin (1987).

40. L. Pietronero, *Syn. Metals*, **8**, 285 (1983).

41. W. A. Little, *Phys. Rev.*, **134A**, 1416 (1964); *Sci. Am.*, **212**, 21 (1965).

42. *Chemical Week*, July 20 1983, p. 38.

43. (a) T. Hanawa, S. Kuwabata, H. Hashimoto, and H. Yoneyama, *Synth. Met.*, **30**, 173 (1989); (b) D. Kim, and H. Reiss, *J. Phys. Chem.*, **89**, 2728 (1985); (c) J. Miasik, A. Hooper, and B. C. Tofield, *J. Chem. Soc. Faraday Trans.*, **182**, 1117 (1986).

44. R. L. Blankespoor, and L. L. Miller, *J. Chem. Soc., Chem. Commun.*, 90 (1985).

45. H. Naarmann, *Synth. Met.*, **17**, 223 (1987).

46. *Japanese Patent Application JP62/249906 A2* assigned to Showa Denko KK (1987);

47. (a) F. R. Fan, B. L. Wheeler, A.J. Bard, and R. N. Noufi, *J. Electrochem., Soc.*, **128**, 2042 (1981); (b) G. Horowitz, and F. Garnier, *J. Electrochem. Soc.*, **132**, 634 (1985).

48. A. R. Kmetz, and F. K. Von Willisen, *Non-Emissive Electrooptic Displays*, Plenum, New York (1976).

49. T. Yamamoto, *Spring Electrochemical Society Meeting Extended Abstracts*, **Vol. 82-1**. Electrochemical Society, 1982. p 987.

50. M. Aizawa, T. Yamada, H. Shinohara, K. Akagi, and H. Shirakawa, *J. Chem. Soc., Chem. Commun.*, 1315 (1986).

51. W. H. Meyer, H. Kiess, B. Binggeli, E. Meier, and G. Harbeke, *Synth. Met.*, **10**, 255 (1983).

52. G. E. Wnek, *Polym. Mater. Sci. Eng.*, **64**, 338 (1991).

53. S. Glenis, G. Horowitz, G. Tourillon, and F. Garnier, *Thin Solid Films*, **111**, 93 (1984).

54. S. L. Meisel, G. C. Johnson, and H. D. Hartough, *J. Am. Chem. Soc.*, **72**, 1910 (1950).

55. (a) A. F. Diaz, *Chem. Scripta*, **17**, 145 (1981); (b) A. F. Diaz, J.I. Crowley, J. Bargon, G.P. Gardini, and J.B. Torrance, *J. Electroanal. Chem.*, **121**, 355 (1981).

56. G. Tourillon, and F. Garnier, *J. Electroanal. Chem.*, **161**, 51 (1984).

57. J. Heinze, J. Mortensen, and K. Hinckleman, *Synth. Met.*, **21**, 209 (1987).

58. J. M. Bureau, M. Gazard, M. Champagne, J. C. Dubois, G. Tourillon, and F. Garnier, *Mol. Cryst. Liq. Cryst.*, **118**, 325 (1985).

59. Y. Yumoto and S. Yoshimura, *Synth. Met.*, **13**, 185 (1986).

60. F. Wudl, M. Kobayashi, A. J. Heeger, *J. Org. Chem.*, **49**, 3382 (1984).

61. For examples involving dithienothiophenes and their benzene analogues see: (a) A. Bolognesi, M. Catellani, S. Destri, R. Zamboni, and C. Taliani, *J. Chem. Soc., Chem. Commun.*, **246** (1988); (b) A. Bolognesi, M. Catellani, S. Destri, R. Zamboni, C. Taliani, W. Porzio, R. Danieli, S. Rossini, and P. Ostoja, *Synth. Met.*, **28**, C521 (1989); (c) T. L. Lambert and J. P. Ferraris, *J. Chem. Soc., Chem. Commun.*, 752 (1991); (e) M. K. Shepherd and P. Kathirgamanathan, *J. Electroanal. Chem.*, **354**, 305 (1993).

62. B. L. Funt, E. M. Peters, and J. D. Van Dyke, *J. Pol. Sci., Part A; Pol. Chem.*, **24**, 1529 (1986).

63. O. Inganas, B. Liedberg, and W. Chag-Ru, *Synth. Met.*, **11**, 239 (1985).

64. M. R. Bryce, A. Chissel, P. Kathirgamanathan, D. Parker, and N. R. M. Smith, *J. Chem. Soc., Chem Commun.*, 466 (1987).

65. A. O. Patil, Y. Ikenaue, N. Basescu, N. Colaneri, J. Chen, F. Wudl, and A. J. Heeger, *Synth. Met.*, **20**, 151 (1987).

66. (a) G. Tourillon, and F. Garnier, *J. Electrochem. Soc.*, **130**, 2043 (1983); (b) G. Tourillon, and F. Garnier, *J. Electroanal. Chem.*, **161**, 407 (1984); (c) K. Kaneto, Y. Kohno, K. Yoshino,and Y. Inuishi, *J. Chem. Soc., Chem. Commun.*, 382 (1983).

67. (a) G. B. Street and T. C. Clarke, *IBM J. Res. Dev.*, **25**, 51 (1981); (b) A. G. MacDiarmid, M. Aldissi, R. B. Kaner, M. Maxfield, and R. J. Mammone, *Extended Abstracts in Spring Electrochemical Society Meeting*, San Fransisco, **Vol. 83-1**, (1983). p. 842; (c) L. W. Shacklette, R. L. Elsenbaumer, and J. M. Sowa, *ibid.*, p. 985.

68. R. J. Watlman and J. Bargon, *Can. J. Chem.*, **64**, 76 (1986).

69. R. J. Waltman, J. Bargon, and A. F. Diaz, *J. Phys. Chem.*, **87**, 1459 (1983); (b) A. F. Diaz, J. I. Castillo, J. A. Logan, and W. -Y. Lee, *J. Electroanal. Chem.*, **129**, 115 (1982).

70. *Proceedings of International Conference on Science and Technology of Synthetic Metals*, Santa Fe, USA, June 1988; *Synth. Met.*, **27 - 29** (1989).

71. R. J. Watlman and J. Bargon, *Tetrahedron*, **40(20)**, 3963 (1984).

72. G. M. Gamaggi, G. Deluca, and A. Tundo, *J. Chem. Soc., Perkin Trans.*, **2**, 1594 (1972).

73. J. Roncalli, M. Lemaire, R. Garreau and F. Garnier, *Synth. Met.*, **18**, 139 (1987).

74. K. Tanaka, T. Schichiri, S. Wang, and T. Yamabe, *Synth. Met.*, **24**, 203 (1988).

75. A. J. Downard and D. Pletcher, *J. Electroanal. Chem.*, **206**, 139 & 147 (1986).

76. (a) T. F. Otero, R. Tejada and A. S. Eloa, *Polymer*, **28**, 651 (1987); (b) T. F. Otero and E. de Larreta-Azelain, *ibid*, **29**, 1522 (1988).

77. A. E. Arbuzov: *J. Russ. Phys. Chem. Soc.*, **38**, 687 (1906).

78. A. Michaelis and R. Kaehoe, *Chem. Ber.*, **31**, 1048 (1898).

79. R. G. Harvey and E. R. DeSombre, *Topics in Phosphorous Chemistry,* **Vol. 1**, M. Grayson and E. J.Griffith, eds., John Wiley & Sons, New York, 1964. pp 57-112.

80. (a) L. Horner, H. Hoffmann, and H. G. Wippel, *Chem. Ber.*, **91**, 61 (1958); (b) L. Horner, H. Hoffmann, H. G. Wippel, and G. Klahre, *Chem. Ber.*, **92**, 2499 (1959).

81. W. S. Wadsworth, Jr. and W. D. Emmons, *J. Am. Chem. Soc.*, **83**, 1733 (1961).

82. L. Horner, W. Klink, and H. Hoffmann, *Chem. Ber.*, **96**, 3133 (1963).

83. (a) A. Maercker, *Org. React.*, **14**, 270 (1965); (b) I. Gosney and A. G. Rowley in *Organophosphorous Reagents in Organic Synthesis*, J. I. G. Cadogan, ed., Academic Press, London, 1979. pp. 17-153; (c) B. E. Maryanoff and A. B. Reitz, *Chem. Rev.*, **89**, 863 (1989).

84. (a) J. Boutagy and R. Thomas, *Chem. Rev.*, **74**, 87 (1974); (b) W. S. Wadsworth Jr., *Org. React.*, **25**, 73 (1977); (c) H. Gross and I. Keitels, *Z. Chem.*, **22**, 117 (1982).

85. M. Schlosser, *Top. Streochem.*, **5**, 1 (1970).

86. R. O. Larsen and G. Aksnes, *Phosphorus Sulphur*, **15**, 219 & 229 (1983).

87. (a) R. A. Cherkasov and N. A. Polezharva, *Russ. Chem. Rev. (Engl. Transl.)* **56**, 163 (1987); (b) J. Emsley and D. Hall, *The Chemistry of Phosphorus;* Wiley, New York, 1976, Chapters 2 & 6; (c) T. Bottin-Strzalko and J. Seyden-Penne, *Bull. Soc. Chim. Fr.*, 161 (1984 [II]).

88. (a) G. Lefébvre, and J. Seydne-Penne, *Chem. Commun.*, 1308 (1970); (b) D. Danion, and R. Carrie, *C. R. Acad. Sci.*, **267**, 735 (1968).

89. H. O. House, *Modern Synthetic Reactions*. 2nd Edition, *The Organic Chemistry Monograph Series*, W.A. Benjamin Inc., London (1972). pp. 707 - 709.

90. H. E. Zimmerman, *Molecular Rearrangements*, **1**, P. deMayo, ed., Wiley Interscience, New York (1963). pp. 345 - 406.

91. D. Y. Curtin, *Rec. Chem. Progr.*, **15**, 111 (1954).

92. S. Gronowitz, *Arkiv f. Kemi.*, **7**, 361 (1954).

93. (a) A. R. Katritzky and P. J. Taylor, *Physical Methods in Heterocyclic Chemistry*, **Vol 4**, A. R. Katritzky, ed., Academic Press, New York (1971). p. 265; (b) L. J. Bellamy, *The Infra-Red Spectra of Complex Molecules*, 2nd Edition, Methuen & Co. Ltd., London (1966); (c) M. St. C. Flett, *Chacteristic Frequencies of Chemical Groups in the Infra-Red*, Elsevier monographs, Elsevier Publishing Company, New-York (1962).

94. *CRC Handbook of Spectroscopy, Vol. 2*, J. W. Robinson, ed., CRC press, Ohio (1974).

95. Coblentz, *Investigations of Infra-Red Spectra, Part 1*, Carnegie Institution, Washington (1905). p. 35 & 98.

96. (a) G. Paliani, A. Poletti, and R. Cataliotti, *Chem. Phys. Letters*, **18**, 525 (1973); (b) E. N. Bolotina and L. M. Suerdlov, *Opt. Spectry.*, **22**, 357 (1967); (c) D. N. Scott, *J. Mol. Specrty.*, **31**, 451 (1969); (d) J. H. S. Green, *Spectrochim. Acta.*, **27A**, 2015 (1971); (e) J. J. Péron, P. Saumagne, and J. M. Lebas, *Spectrochim. Acta.*, **26A**, 1651 (1970); (f) J. C. Evans, *J. Opt. Soc. Am.*, **50**, 1337 (1950); (g) S. Brodersen and T. Johanesen, *J. Molec. Spectry.*, **23**, 293 (1967).

97. M. Rico, J. M. Orza, and J. Morcillo, *Spectrochim. Acta.*, **21**, 689 (1965).

98. B. N. Cyvin and S. J. Cyvin, *Acta. Chem. Scand.*, **23**, 3139 (1969).

99. (a) H. Rosatzin, *Spectrochim. Acta.*, **19**, 1107 (1963); (b) S. Fisichella, G. Scarlata, and M. Torre, *Gazz. Chim. Ital.*, **104**, 1237 (1974).

100. (a) C. G. Cannon and G. B. B. M. Sutherland, *Spectrochim. Acta.*, **4**, 373 (1951); (b) R. T. Conley, *Infrared Spectroscopy*, 2nd edition, Allyn & Bacon, Boston (1972); (c) N. B. Colthrup, L. H. Daly, and S. E. Wilberly, *Introduction to Infrared and Raman spectroscopy*, 2nd edition, Academic Press, New York and London (1975).

101. (a) I. Shimizu, Y. Kamei, T. Tezuka, T. Izumi, and A. Kasahara, *Bull. Chem. Soc. Jpn.*, **56**, 192 (1983); (b) I. Shimizu, H. Umezawa, T. Kanno, T. Izumi, and A. Kasahara, *Bull. Chem. Soc. Jpn.*, **56**, 2023 (1983).

102. P. J. Taylor, *Spectrochim. Acta.*, **26A**, 165 (1970).

103. B. Antoine, J. J. Péron, P. Saumagne, and R. Guilard, *J. Chim. Phys.*, 232 (1970).

104. D. J. Chadwick, J. Chambers, G. D. Meakins, and R. L. Snowden, *J. Chem. Soc., Perkin Trans. II*, 604 (1975).

105. H. Satonaka, *Bull. Chem. Soc. Jpn.*, **56**, 3337 (1983).

106. V. I. Savin, S. A. Flegontov, and Yu. P. Kitaev, *Khim. Geterotsikl. Soedin.*, 1188 (1970).

107. G. Paliani, R. Cataliotti, and M. R. Pelleti, *Spectrochim. Acta., Part A*, **39A**, 1013 (1983).

108. Groenewege, *Spectrochim. Acta.*, **11**, 579 (1958).

109. T. Yamamoto, K. Sanechika, and A. Yamamoto, *Bull. Chem. Soc. Jpn.*, **56**, 1497 (1983).

110. S. Meyerson and E. K. Fields, *Org. Mass Spectrom.*, 2, 241 (1969).

111. C. A. Crowder and D. W. Scott, *J. Molec. Spectroscopy*, **16**, 122 (1965).

112. D. B. Adebimpe and M. K. Shepherd, Unpublished results.

113. (a) R. G. Cooks, *Org. Mass Spectrom.*, **2**, 481 (1969); (b) T. Nishiwaki, *Heterocycles*, **2(4)**, 473 (1974).

114. R. V. Hoffman, G. G. Orphanides, and H. Shechter, *J. Am. Chem. Soc.*, **100**(25), 7926 (1978).

115. (a) H. Wynberg, R. M. Kellog, H. Van Driel, and G. E. Berkins, *J. Am. Chem. Soc.*, **89**, 3501 (1967); (b) H. Wynberg, R. M. Kellog, and H. van Driel, *Organosulphur Chemistry: reviews of current research*, M. J. Janssen, ed., John Wiley & Sons Inc., New York (1967), Chapter 9; (c) M. J. Janssen and F. de Jong, *Z. Chem.*, **10**, 216 (1970); (d) R. M. Kellog, M. Groen, and H. Wynberg, *J. Org. Chem.*, **32**, 3093 (1967); (d) R. M. Kellog, J. K. Dik, H. van Driel and H. Wynberg, *J. Org. Chem.*, 2737 (1970).

116. G. M. Badger, J. H. Bowie, J. A. Elix, G. E. Lewis, and U. P. Singh, *Aust. J. Chem.*, **20**, 2669 (1967).

117. R. M. Dawson and R. Gillis, *Aust. J. Chem.*, **25**, 1221 (1972); (b) S. Meyerson and E. K. Fields, *Org. Mass Spectrom.*, **1**, 263 (1968).

118. (a) Q. N. Porter, *Aust. J. Chem.*, **20**, 103 (1967); (b) R. G. Cooks, I. Howe, S. W. Tam, and D. H. Williams, *J. Am. Chem. Soc.*, **90**, 4064 (1968).

119. For the complete assignment of shifts and coupling constants of the A_2B_2 spectra of thiophene see: R. A. Hoffman and S. Gronowitz, *Arkiv. Kemi.*, **15**, 45 (1959).

120. For the spectra of a variety of thiophene derivatives see:
(a) R. J. Abraham and H. J. Bernstein, *Can. J. Chem.*, **37**, 2095 (1959); (b) D. H. Grant, R. C. Hirst, and H. S. Gutowsky, *J. Chem. Phys.*, **38**, 470 (1963); *Chem. Abstr.*, **61**, 14032b (1964); (c) S. Gronowitz and B. Gestblom, *Arkiv. Kemi.*, **18**, 513 (1962); (d) K. Takahasi, Y. Matsuki, Y. Miyake, and G. Hazato, *Bull. Chem. Soc. Jpn.*, **84**, 1599 (1961); (e) A. D. Cohen and K. A. Mclauchlan, *Discuss. Faraday Soc.*, 132, (1962); (f) S. Gronowitz and L. Karlsson, *Acta Chem. Scand.*, **17**, 2120 (1963); (g) H. Hirohashi, S. Inaba, and H. Yamamoto, *Bull. Chem. Soc. Jpn.*, **49**, 1395 (1976); (h) M. K. Mahanti, *Indian J. Chem., Sect. B*, **15B**, 168 (1977); (i) V. Galasso, *Chem. Phys. Letts.*, **21**, 54 (1973); (j) B. Östman, *Acta Chem. Scand.*, **21**, 1257 (1967); (k) S. Gronowitz, I. Johnson, and A. -B. Hörnfeldt, *Chemica Scripta*, **7**, 211 (1975); (l) R. Radeglia, H. Hartmann, and S. Scheithauer, *Z. Naturforsch*, **B24**, 286 (1969); (m) F. Fringuelli, S. Gronowitz, A. -B. Hörnfeldt, I. Johnson, and A. Taticchi, *Acta Chem. Scand.*, **B28**, 175 (1974).

121. S. Gronowitz, *Advances in Heterocyclic Chemistry*, **1**, 9 (1963).

122. R. M. Silverstein, G. Clayton Bassler, and T. C. Morrill, *Spectroscopic Identification of Organic Compounds*, 4th edition, John Wiley & Sons, New York (1981), p. 235.

123. (a) R. A. Hoffman and S. Gronowitz, *Arkiv. Chemi.*, **16**, 515 (1960); (b) G. Gestblom, S. Gronowitz, R. A. Hoffman, B. Mathiasson, and S. Rodmar, *Arkiv. Kemi.*, **23**, 483 (1965).

124. S. Gronowitz and R. A. Hoffman, *Acta Chem. Scand.*, **13**, 1687 (1959).

125. (a) P. L. Corio and I. Weinberg, *J. Chem. Phys.*, **31**, 569 (1959); (b) S. Gronowitz and R. A. Hoffman, *Arkiv. Kemi.*, **15**, 499 (1960).

126. M. Faraday, *Ann. Phys. Chem. [2]*, 33, 438 (1834).

127. (a) E. Laviron in A. J. Bard's *Electroanalytical Chemistry*, Vol 12, Marcel Dekker, New York (1982). p. 53. (b) P. J. Pearce and A. J. Bard, *J. Electroanal. Chem.*, **114**, 89 (1980); (c) F. C. Anson, J. M. Savéant, and K. Shigehara, *J. Phys. Chem.*, **87**, 241 (1983); (d) E. Laviron, *J. Electroanal. Chem.*, **112**, 1 (1980).

128. D. H. Evans, K. M. O'Connel, R. A. Peterson, and M. J. Kelly, *J. Chem. Educ.*, 60(4), 290 (1983).

129. J. G. Dick and S. Nadler, *Metrohm Monographs; "Electrode Reaction Kinetics Determined by Cyclic Sweep Triangular Wave Voltammetry"* Metrohm Ltd., Switzerland (1993).

130. H. H. Willard, L. L. Merritt, and J. A. Dean, *Instrumental Methods of Analysis*, Van Nostrand-Reinhold. New York (1965). p.531.

131. H. Schafer, *Angew. Chem. Intl. Ed. Engl.*, 20, 911 (1981); (b) N. L. Weinberg, *J. Chem. Educ.*, **49**, 120 (1972); (c) H. Lund, *Organic*

Electrochemistry, M. M. Baizer and H. Lund, eds., 2nd Edition, Dekker, New York (1983), Chapter 5.

132. C. K. Mann, *Electroanal. Chem.*, 3, 57 (1969).

133. K. J. Vetter, *Electrochemische Kinetik*, Springer, Berlin (1961).

134. R. S. Nicholson, *Anal. Chem.*, 37, 1351 (1965).

135. R. S. Nicholson and I. Shain, *Anal. Chem.*, 36, 706 (1964); *Anal. Chem.*, 37, 190 (1965).

136. R. S. Nicholson and I. Shain, *Anal. Chem.*, 36, 722 (1964).

137. J. A. Page and G. Wilkinson, *J. Am. Chem. Soc.*, 74, 6149 (1952).

138. (a) R. E. Dessey, and L. A. Bares, *Acc. Chem. Res.*, 5, 415 (1972); (b) M. M. Bazier, Ed., *Organic Electrochemistry*, Dekker, New York (1973); (c) S. P. Gubin, *Pure Appl. Chem.*, 23, 463 (1970).

139. J. Heinze, *Angew. Chem. Intl. Ed. Eng.*, 23(11), 836 (1984).

140. G. M. Brown, T. J. Meyer, D. O. Cowan, C. LeVanda, F. Kaufman, P. V. Roling, and M. D. Rausch, *Inorg. Chem.*, 14, 506 (1975).

141. W. H. Morrison Jr. and D. N. Hendrickson, *J. Chem. Phys.*, 59, 380 (1973).

142. C. LeVanda, K. Bechgaard, D. O. Cowan, and M. D. Rausch, *J. Am. Chem. Soc.*, 99, 2964 (1977).

143. J. A. Kramer and D. N. Hendrickson, *Inorg. Chem.*, 19, 3330 (1980).

144. M. J. Powers and T. J. Meyer, *J. Am. Chem. Soc.*, 100, 4394 (1978).

145. (a) G. Tourillion, *Handbook of Conducting Polymers, Vol 1*, A. T. Skotheim, ed., Marcel Dekker, New York (1986), p. 293; (b) E. W. Tsai, S. Bassak, J. P. Ruiz, J. R. Reynolds, and K.Rajeshwar, *J. Electrochem. Sci.*, 136, 3683 (1989).

146. D. T. Sawyer and J. L. Roberts Jnr., *Experimental Electrochemistry for Chemists*, Wiley, New York (1974).

147. P. T. Kissinger and W. R. Hienemann, eds., *Laboratory Techniques in Electroanalytical Chemistry*, Dekker, New York (1984).

148. M. Fleischman and D. Fletcher, *Tett. Lett.*, 6255 (1968).

149. (a) M. Sato, S. Tanaka, and K. Kaeriyama, *J. Chem. Soc., Chem. Commun.*, 713 (1985); (b) M. Sato, S. Tanaka, K. Kaeriyama, and F. Tomonaga, *Polymer*, 28, 1071 (1987).

150. These electrodes were made by Keith Goodchild of Exeter University.

151. K. Yoshida, T. Saeki and T. Fueno, *J. Org. Chem.*, 24, 3673 (1971).

152. M. Nemec, M. Janda, and K. Srogl, *Coll. Czech. Chem. Commun.*, 38, 3857 (1973).

153. M. K. Shepherd, Unpublished Results.

154. (a) L. F. Warren, J. A. Walker, D. P. Andersen, and C. G. Rhodes, *J. Electrochem. Soc.*, 136, 2286 (1989); (b) J. D. Nisson, and O. Inganās, *Synth. Met.*, 31, 359 (1989).

155. M. R. Bryce, A. D. Chissel, N. R. M. Smith, D. Parker and P. Kathirgamanathan, *Synth. Met.*, 26, 153 (1988).

156. F. J. Pern and A. J. Frank, *J. Electrochem. Soc.*, 137(9), 2769 (1970).

157. R. J. Waltmann and A. F. Diaz, *J. Electrochem. Soc.*, 132(3), 631 (1985).

158. Y. Furukawa, Y. Imai, and M. Tasumi, *Synth. Met.*, 32(2), 253 (1989).

159. C. J. Pouchert, *The Aldrich Library of Infrared Spectra*, Aldrich, Milwaukee (1975).

160. M. Akimoto, Y. Fukuyama, H. Takouchi, I. Harada, Y. Soma, and M. Soma, *Synth. Met.*, 15, 353 (1986).

161. C. Taliani, R. Danieli, R. Zamboni, P. Ostoja, and W. Porzio, *Synth. Met.*, 18, 177 (1987).

162. J. F. Rabolt, T. C. Clark, and G. B. Street, *J. Chem. Phys.*, 71, 4614 (1979).

163. (a). B. J. Hathaway and A. E. Underhill, *J. Chem. Soc.*, 3091 (1961). (b). S. F. Pavkovic and D. W. Meek, *Inorg. Chem.*, 4, 1091 (1965).

164. M. B. Inuoe, E. F. Velazquez, and M. Inuoe, *Synth. Met.*, 24, 223 (1988).

165. S. Kuwabata, S. Ito, and H. Yoneyama, *J. Electrochem. Soc.*, 135(7), 1691 (1988).

166. O. Inganās, B. Liedberg, and W. Chang-Ru, *Synth. Met.*, 11, 239 (1985).

167. H. Neugebauer, A. Neckel, and N. Brinda-Konopik in H. Kuzmany et al (eds.), *Electronic Properties of Polymers and Related Compounds*, Springer, Berlin-Heidelberg-New York, (1985), p. 227.

168. L. J. Bellamy, *The Infra-Red Spectra of Complex Molecules*, 1st. edition, Methuen & Co. Ltd., London (1954), p. 37.

169. See reference 122, p. 108.

170. *Thermal Analysis*, 3rd edition, *Vol. 19 of Chemical Analysis: A Series of Monographs on Analytical Chemistry and its applications*. P. J. Elving and J. D. Winefordner, eds., John Wiley & Sons, New York (1986).

171. S. Hotta, T. Hosaka, and W. Shimotsuma, *J. Chem. Phys.*, 80(2), 954 (1984).

172. S. Hotta, T. Hosaka, and W. Shinotsuma, *Synth. Met.*, 6, 69 (1983).

173. One of such reactions is anodic hydroxylation. For a discussion of this process see: V. D. Parker, *J. Electroanal. Chem.*, 21, App. 1 (1969).

174. F. M. Fowkes, *Physicochemical Aspects of Polymer Surfaces*, Vol. 2, K. L. Mittal, ed., Plenum Press, New York (1983), p. 583.

175. (a) A. Camerman and J. Trotter, *Acta Crystallogr.*, 18, 636 (1965); (b) J. T. Cooper and W. F. Forbes, *Can. J. Chem.*, **46**, 1158 (1968); (c) J. Cooper, *Can. J. Chem.*, **48**, 1996 (1970).

176. J. A. Pople and D. L. Beveridge, *Approximate molecular orbital theory*, McGraw Hill, New York (1970).

177. M. Leclerc and R. E. Prud'homme, *Macromolecules*, 20, 2153 (1987).

178. A. F. Diaz, J. Bargon, and R. J. Waltman, *Proceedings of the Symposium on Membranes and Ionic and Electronic Conducting Polymers*, 83, 332 (1982).

179. D. Häbich and F. Effenberger, *Synthesis*, 841 (1979).

180. F. B. Deans and C. Eaborn, *J.*, 2299 (1959).

181. (a) M. Lemaire, W. Büchner, R. Garreau, H. A. Hoa, A. Guy, and J. Roncali, *J. Electroanal. Chem.*, 281, 293 (1990); (b) S. K. Ritter and R. E. Noftle, *Chem. Mater.*, **4**, 872 (1992).

182. L. Dowd, *Final Year Project*, School of Applied Chemistry, University of North London (1993).

183. S. Aeiyach, J. E. Dubois, and P. C. Lacaze, *J. Chem. Soc., Chem. Commun.*, 1668 (1986).

184. O. Hammerich and V. D. Parker, *Electrochim. Acta*, 18, 5 (1973).

185. *Organic Materials for Non-linear Optics*, R. A. Hann and D. Bloor, eds., Royal Society of Chemistry, London (1989).

186. For a comprehensive treatise on this subject see: *Nonlinear Optical Properties of Organic Molecules and Crystals*, Volumes 1 and 2, D. S. Chemla and J. Zyss, eds., Orlando: Academic (1987).

187. For a review on this technique see: G. G. Roberts, *Contemp. Phys.*, 2, 109 (1984).

188. Excellent reviews include: (a) J. B. Press, in *Chemistry of Heterocyclic Compounds*, Vol. 44, *Thiophene and Its Derivatives: Part 1*, S. Gronowitz,

ed., Wiley, New York (1985), pp. 353-456; (b) J. B. Press, *ibid*, Part 4, (1991), pp. 398-478; (c) R. Pech and R. Böhm, *Pharmazie*, 39, 4 (1984).

189. T. M. Bargar, R. J. Broersma, L. C. Creemer, J. R. McCarthy, J. M. Hornsperger, M. G. Palfreyman, J. Wagner, and M. J. Jung, *J. Med. Chem.*, 29, 315 (1986).

190. G. Drehsen and J. Engel, *Sulphur Repts.*, 3, 171 (1983).

191. W. Drenth, and M. J. Handele, *Recl. Trav. Chim. Pays-Bas*, 91(5), 688 (1972).

192. L. Erdey, F. Paulik, and J. Paulik, *Nature*, 174, 885 (1954).

193. J. R. Lyerla in *Contemporary Topics in Polymer Science*, Volume 3, M. Shan, ed., Plenum, New York (1979), pp. 143-213.

194. J. Shaefer and E. O. Stejskal in *Topics in Carbon-13 NMR Spectroscopy*, Volume 3, G.C.Levy, ed., Wiley Interscience. New York (1979).

195. H. Nishimura and J. Mizutani, *J. Org. Chem.*, 40, 1574 (1975).

196. E. Campaigne and B. F. Tullar, *Organic Syntheses Coll. Vol. IV*, p 921.

197. P. J. Graham, R. V. Lindsey, G. W. Parshall, M. L. Peterson and G. M. Whitmann, *J. Am. Chem. Soc.*, **79**, 3416 (1957).

APPENDICES

APPENDIX I

The ^{1}H-nmr spectrum of
3,4-*Bis*(dimethoxyphosphinylmethyl)thiophene

APPENDIX II

Papers and Publications

The following section details published material deemed relevant to the thesis.

PUBLISHED PAPERS NOT FILMED FOR COPYRIGHT REASONS

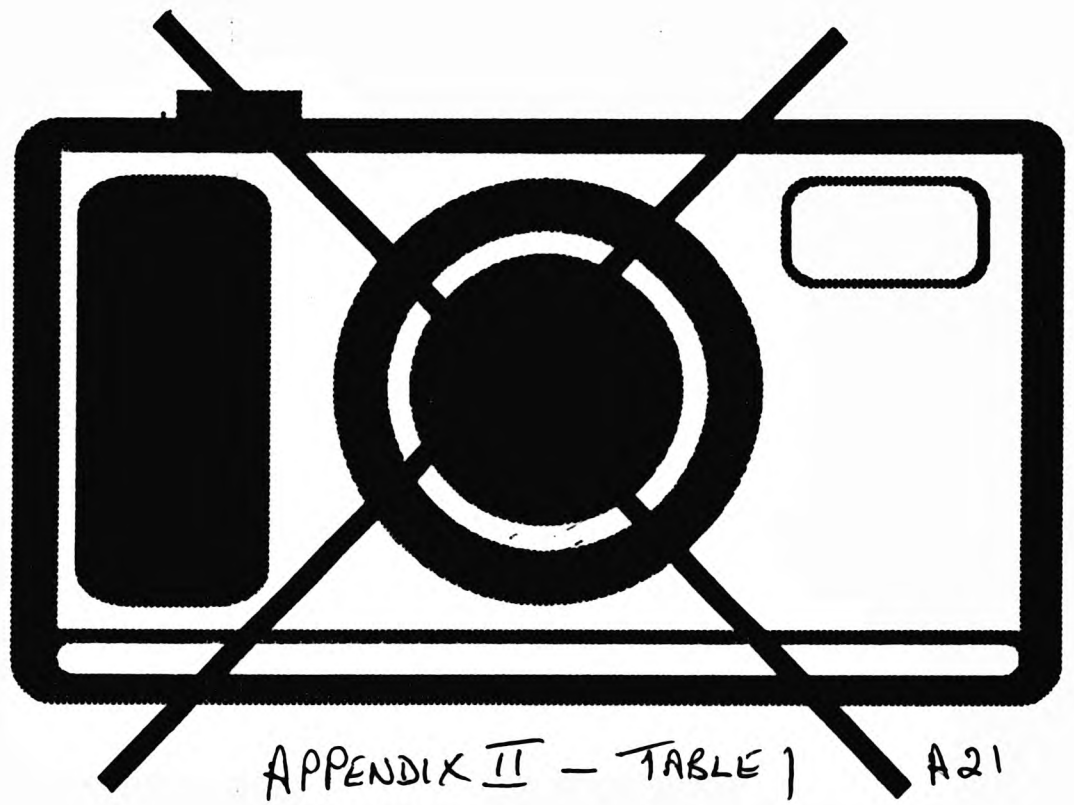

APPENDIX II – TABLE 1 A21

Table 1

Electropolymerisation of Poly(pyrrole)-hexafluorophosphate in Acetonitrile

Pyrrole: 2mM; tetrabutylammonium hexafluorophosphate = 10mM.
Electrode: Tin oxide coated glass.

No	Temp/°C	Potential /V vs SCE	Conductivity /S cm^{-1}	Comments
1.	20°C	-0.5 - 1.5 potentiodynamic	too thin to measure	granular deposits (4-40 μm) see Figure 1A
2.	20°C	1.10	too thin to measure	granular deposits with large valleys (20-30 μm) see Figure 1B
3.	20°C	1.20	7.8 ± 0.5	granular deposits with mountains see Figure 1C
4.	20°C	1.30	4.5 ± 0.5	granular deposits with large mountains (60-80 μm) see Figure 1D
5.	10°C	1.20	55.0±1.0	small globular mountains (10μm) with secondary growth see Figure 2B
6.	0°C	1.20	86.0±4.0	small globular mountains with secondary growth more densely packed than 5; see Figure 2C

Table 2

Electropolymerisation of Poly(pyrrole) trifluoromethansulphonate on Tin Oxide Electrode In Acetonitride

No	Temp/°C	Potential /V vs SCE	Conductivity /S cm^{-1}	Comments
1.	20°C	-0.5 - 1.5	too thin to measure	long nodules see Figure 3A
2.	20°C	1.20	27.5 ± 2.5	small nodular growth (10μm long) see Figure 3B
3.	20°C	1.30	too thin to measure	ill-defined crystallites on amorphous globular deposits see Figure 3C
4.	20°C	1.40	too thin to measure	well defined crystals (1-2μm) on amorphous globular deposits (Figure 3D)

Table 3

Influence of Anion On the Conductivity of Poly(pyrrole)*

No	Temp/°C	Anion	Conductivity /S cm^{-1}	Comments
1.	20°C	Trifluoro -methane sulphonate	27.5 ± 2.5	globular deposits (2 - 20 μm) see Figure 5A
2.	20°C	p-toluene sulphonate	30.0 ± 5.0	fine particulate deposit (~0.1μm) on amorphous deposit compact structure see Figure 5B
3.	20°C	perchlorate	6.0 ± 1.0	compact amorphous structure particulate deposit (#0.1 μm) see Figure 5C

* Monomer = 2mM, Anion = 10mM

Solvent = acetonitrile, Electrode = SnO_2.

Potential = 1.2V vs SCE.

Table 4

Electropolymerisation of Co-poly(3-methylthiophen-pyrrole) Perchlorate on Tin Oxide Electrode in Acetonitrile[a]

No	Temp/°C	Potential /V vs SCE	Conductivity /S cm^{-1}	Comments
1.	20°C	1.15	9.0 ± 1.0	granular deposits (0.1 - 1 μm) see Figure 6A
2.	20°C	1.25	6.0 ± 1.0	globular structure (10μm) with secondary spherical growth (2-3 μm) see Figure 6B
3.	20°C	1.35	8.0 ± 1.0	globular structure with secondary growth see Figure 6C

Table 5

Electropolymerisation of Co-poly(3-methylthiophen-pyrrole) Trifluoromethanesulphonate on SnO_2 Electrode in Acetonitrile at 20°C (a)

No	Potential/ V vs SCE	Conductivity /S cm^{-1}	Comments
1.	1.10	too thin to measure	Fibrous network (see Figure 7A)
2.	1.20	too thin to measure	much more dense fibrous network (see Figure 7B)
3.	1.30	2.0 ± 1.0	(see Figure 7C) three dimensional globular network
4.	1.65	2.0 ± 1.0	-

a: pyrrole 2mM; 3-methylthiophen 10mM, tetrabutyammoniumtrifluoromethanesulphonate 10mM.

Table 6

Electropolymerisation of Co-poly(3-methylthiophen-pyrrole) hexfluorophosphate at 0°C on a SnO_2 Electrode

No	Potential /V vs SCE	Conductivity /S cm^{-1}	Comments
1.	1.10	too thin to measure	globular structure with fibrous secondary growth (see Figure 8A)
2.	1.20	29.0 ± 1.0	fibrous structure on a globular matrix see Figure 8B
3.	1.30	17.0 ± 1.0	globular deposit (see Figure 8C)

Table 7

Electropolymerisation of Poly(pyrrole) under Galvanostatic Conditions

No	Current Density MA cm^{-2}	Anion	Conductivity /S cm^{-1}	Comments
1.	1.50	p-toluene sulphonate	30.0 ± 5.0	flaky structure
2.	1.00	as above	17.5 ± 2.5	50 - 350 µm, irregular platelets see Figure 12A
3.	1.00	laurylsulphate	100.0 ± 8.0	10 - 80 µm, irregular plates see Figure 12B

Table 8

CYCLIC VOLTAMMMETRY DATA

	Epa/V	Epc/V	$\frac{(Epa + Epc)/V}{2}$	Epa - Epc
Pyr/ClO_4^-	0.675	+0.050	0.363	0.625
Pyr/PF_6^-	0.590	-0.145	0.223	0.735
Pyr/ $CF3SO_3^-$	0.625	-0.285	0.170	0.910

WORKING ELECTRODE: TIN OXIDE COATED GLASS

All potentials in volts vs SCE

Table 9

Electropolymerisation of Dimethylisothianaphthene hexafluorophosphate At a Platinum Electrode in Acetonitrile

No	Potential/V vs Ag/AgCl	Conductivity /S cm^{-1}	Comments
1.	1.10	(0.50 ± 0.10)	0.1 - 2μm size granules (see Figure 1(A)
2.	1.30	(5.0 ± 2.0)	0.1 - 4μm size granules and flakes (see Figure 1(B)
3.	1.50	(80.0 ± 4.0)	0.1 - 2μm granules and 2-4μm long tubes (see Figure 1(C)

POLY(PYRROLE)HEXAFLUOROPHOSPHATE:
DEPENDENCE OF MICROSTRUCTURE ON APPLIED POTENTIAL.

A 0.5 - 1.5V.

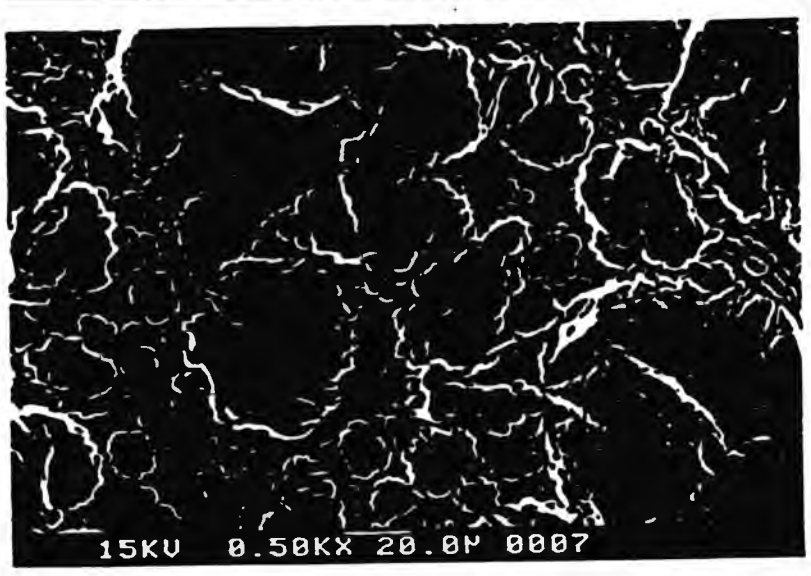

B 1.1V.

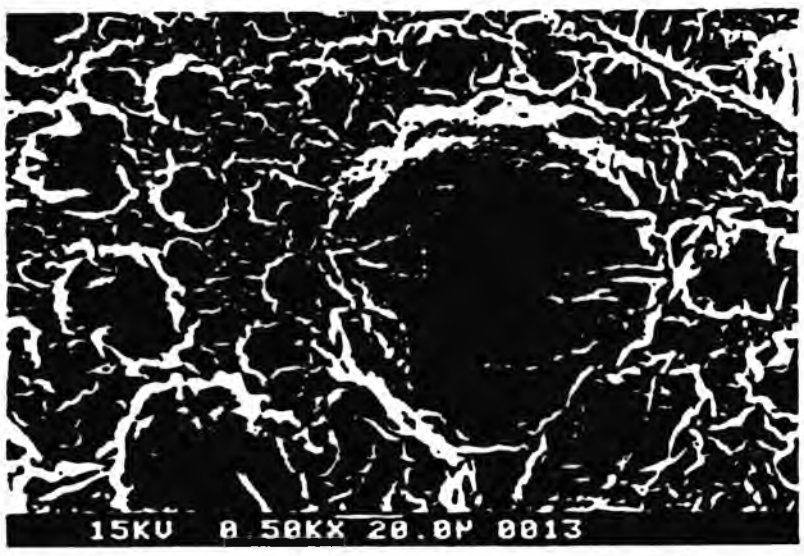

C 1.2V.

D 1.3V.

CONDITIONS EMPLOYED: PYRROLE:2mM: $Bu_4N^+PF_6^-$:10mM: ELECTRODE:SnO_2
TEMP.:20°C: SOLVENT:CH_3CN

FIGURE 1.

POLY(PYRROLE)HEXAFLUOROPHOSPHATE:
DEPENDENCE OF MICROSTRUCTURE ON TEMPERATURE OF GROWTH.

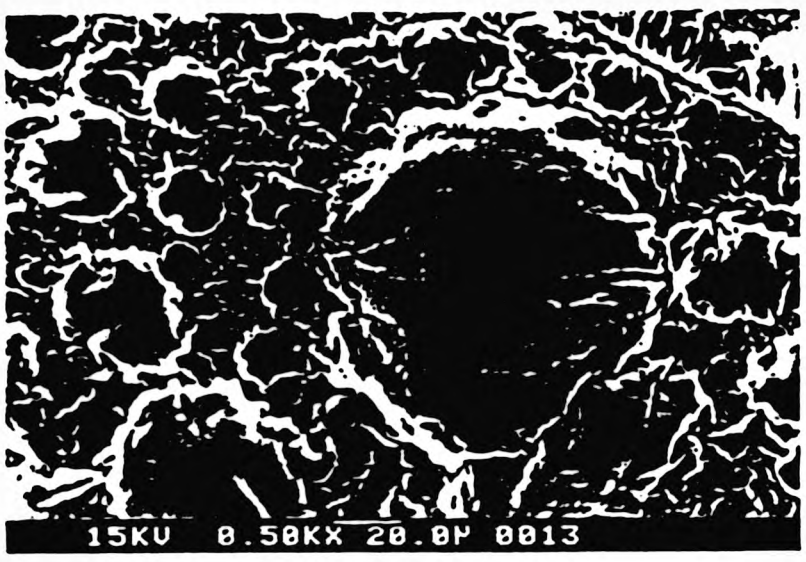

A 1.2V 20°C $7\ Scm^{-1}$

B 1.2V 10°C $55\ Scm^{-1}$

C 1.2V 0°C $83\ Scm^{-1}$

FIGURE 2. CONDITIONS EMPLOYED: PYRROLE: 2mM; $Bu_4N^+PF_6^-$: 10mM; ELECTRODE: SnO_2 SOLVENT: CH_3CN;

POLY(PYRROLE)TRIFLUOROMETHANE SULPHONATE:
DEPENDENCE OF MICROSTRUCTURE ON APPLIED POTENTIAL.

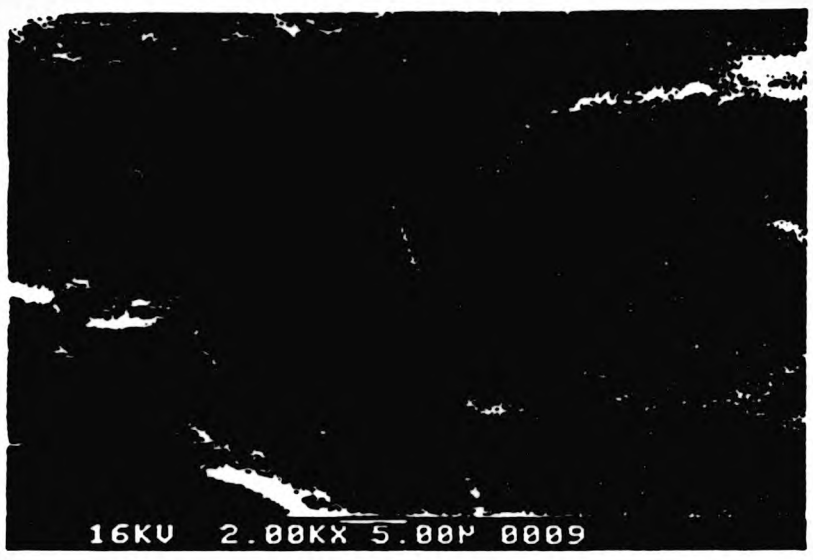

A -0.5 - 1.5V.

B 1.2V.

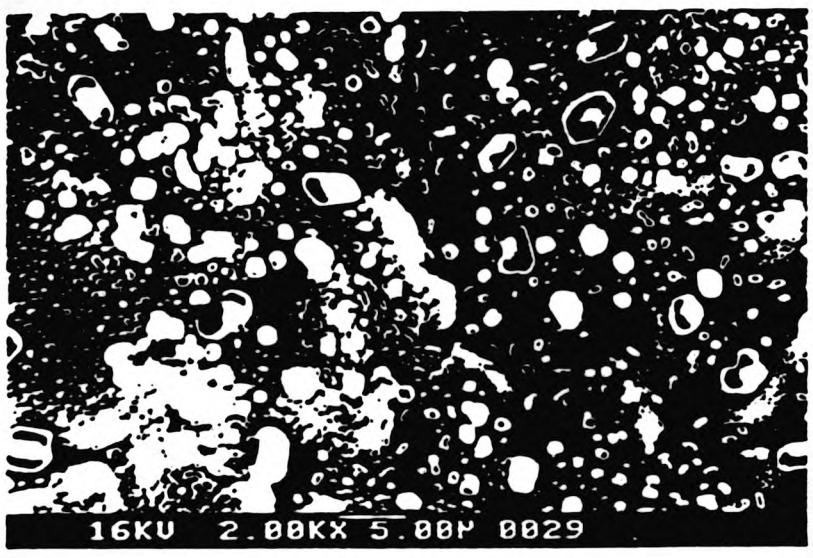

C 1.3V.

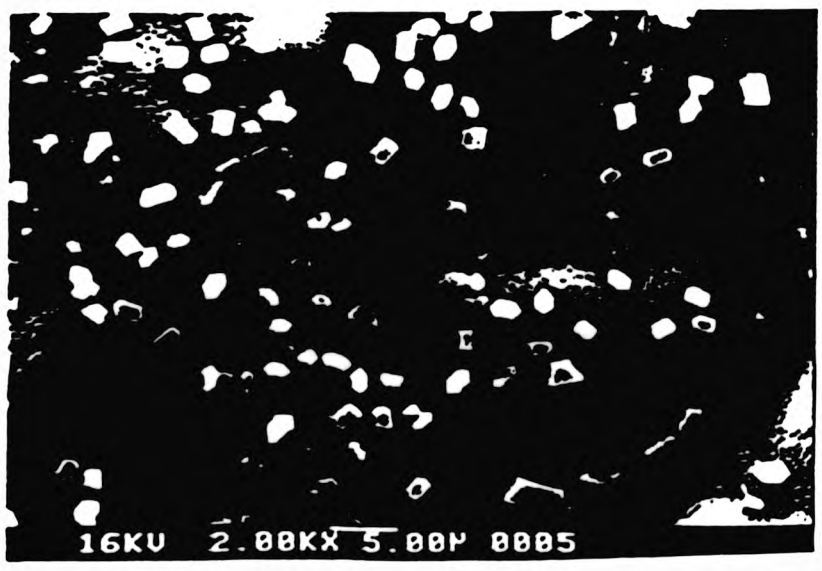

D 1.4V

FIGURE 3. CONDITIONS EMPLOYED: PYRROLE:2mM: $TFMS^-$:10mM: ELECTRODE:SnO_2 TEMP.:20°C: SOLVENT:CH_3CN.

POLY(PYRROLE)HEXAFLUOROPHOSPHATE:
DEPENDENCE OF MICROSTRUCTURE ON SOLVENTS.

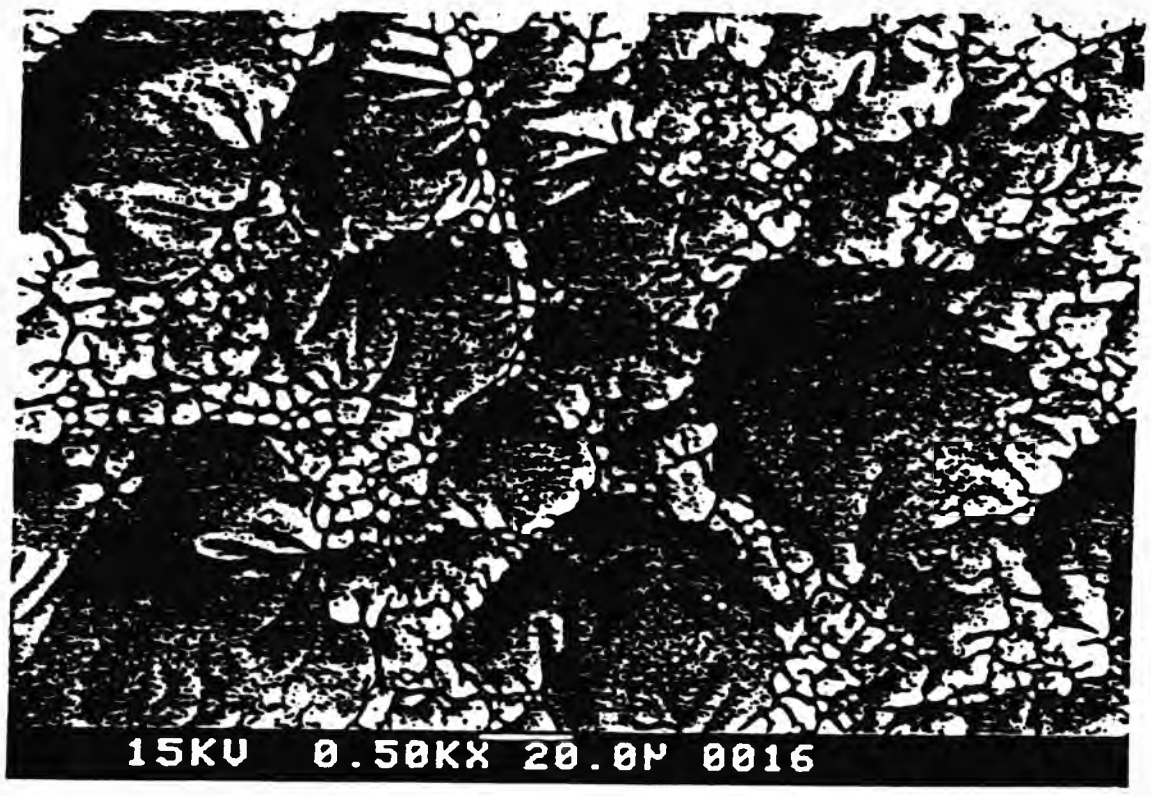

A

1.3V
PYRROLE: 2mM
PF_6^-: 10mM
SOLVENT: CH_3CN
TEMP.: 20 C

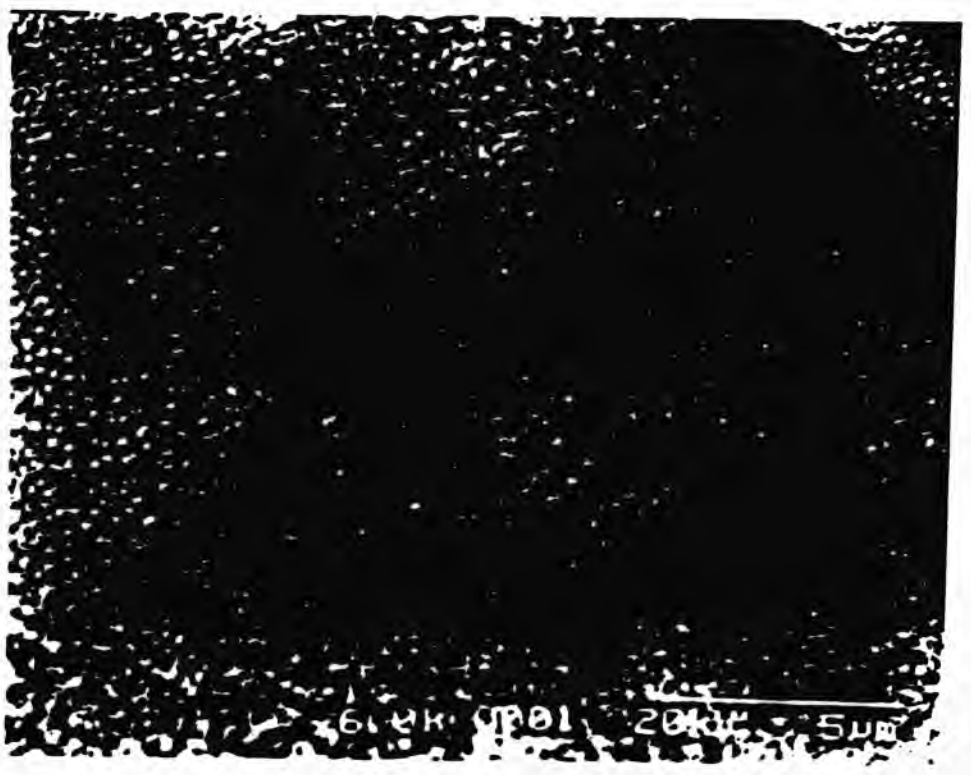

B

1.3V
PYRROLE: 2mM
PF_6^-: 10mM
SOLVENT: $C_6H_5NO_2$
TEMP.: 20 C

FIGURE 4.

POLY(PYRROLE)HEXAFLUOROPHOSPHATE:
DEPENDENCE OF MICROSTRUCTURE ON THE NATURE OF ANIONS.

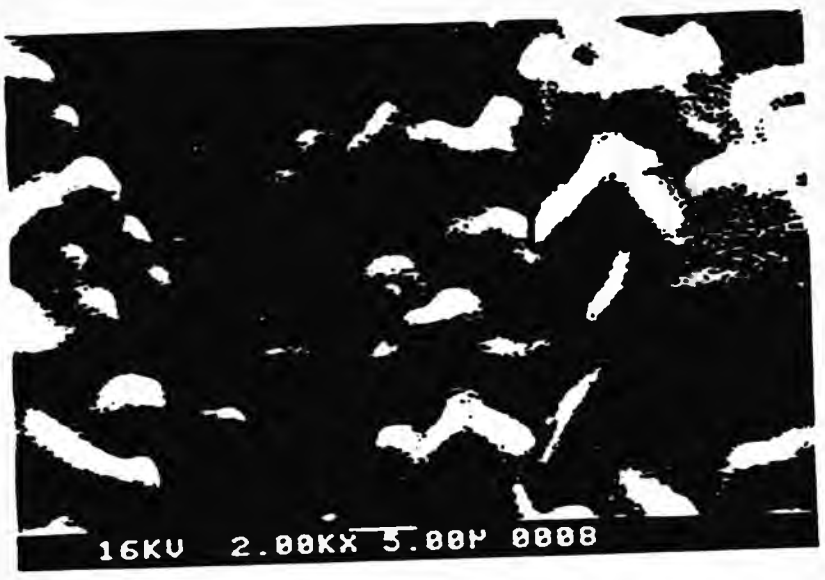

A $CF_3SO_3^-$
27.5 + 2.5 Scm^{-1}

B PTS^-
30.0 + 5.0 Scm^{-1}

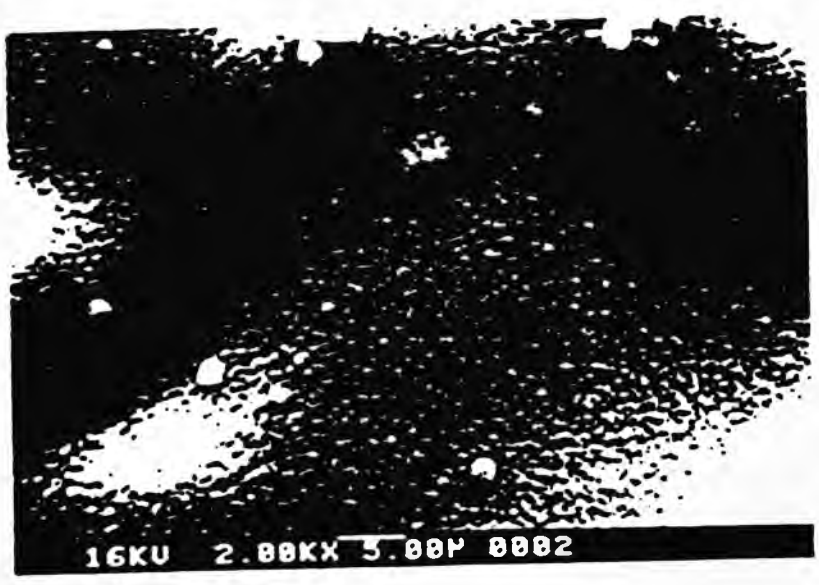

C ClO_4^-
6.0 + 1.0 Scm^{-1}

FIGURE 5. CONDITIONS EMPLOYED: PYRROLE: 2mM; ANION: 10mM; ELECTRODE: SnO_2
TEMP.: 20°C; SOLVENT: CH_3CN; V= 1.2V Vs SCE

CO-POLY(3-METHYLTHIOPHENE/PYRROLE)PERCHLORATE:
DEPENDENCE OF MICROSTRUCTURE ON APPLIED POTENTIAL.

A

1.15V
9 Scm^{-1}

B

1.25V
6 Scm^{-1}

C

1.35V
8 Scm^{-1}

FIGURE 6. POTENTIAL EMPLOYED: PYRROLE:2mM; $Bu_4N^+ClO_4^-$:10mM; ELECTRODE:SnO_2
TEMP.:20°C; SOLVENT:CH_3CN; 3-MT:2mM.

CO-POLY(3-METHYLTHIOPHENE/PYRROLE:TRIFLUOROMETHANE SULPHON.
DEPENDENCE OF MICROSTRUCTURE ON APPLIED POTENTIAL.

7A

(1.1V)

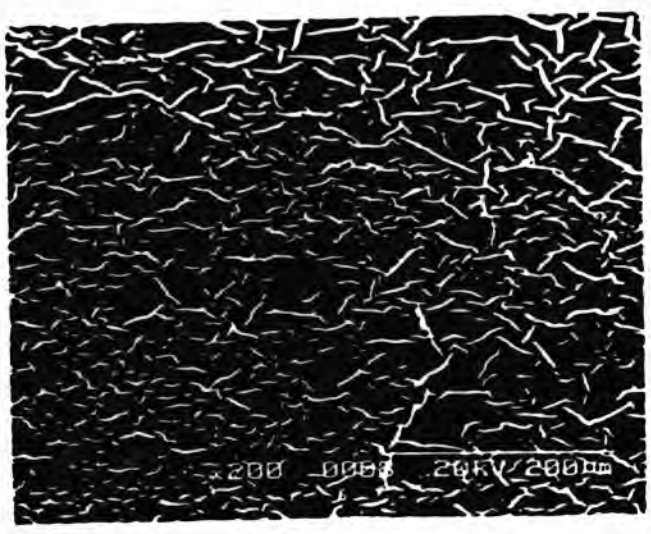

7B

(1.2V)

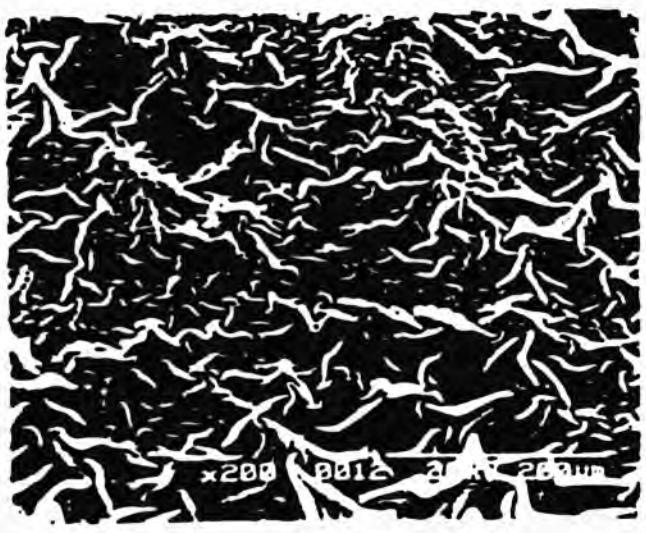

7C

(1.3V)

FIGURE 7. [illegible] EMPLOYED: PYRROLE:2mM; [illegible]; TMT:5mM;
TEMP.:20°C; SOLVENT: [illegible]-MET[illegible]M.

CO-POLY(3-METHYLTHIOPHENE/PYRROLE)HEXAFLUOROPHOSPHATE: DEPENDENCE OF MICROSTRUCTURE ON APPLIED POTENTIAL.

A

1.1V Vs SCE

B

1.2V Vs SCE

29 Scm^{-1}

C

1.3V Vs SCE

17 Scm^{-1}

FIGURE 8. CONDITIONS EMPLOYED: PYRROLE: 2mM; $Bu_4N^+PF_6^-$: 10mM; ELECTRODE: SnO_2 TEMP.: 0^oC; SOLVENT: CH_3CN; 3-MT: 10mM.

Influence of Anions on the Cyclic Voltammetric Behaviour Of Poly(pyrrole) Growth.

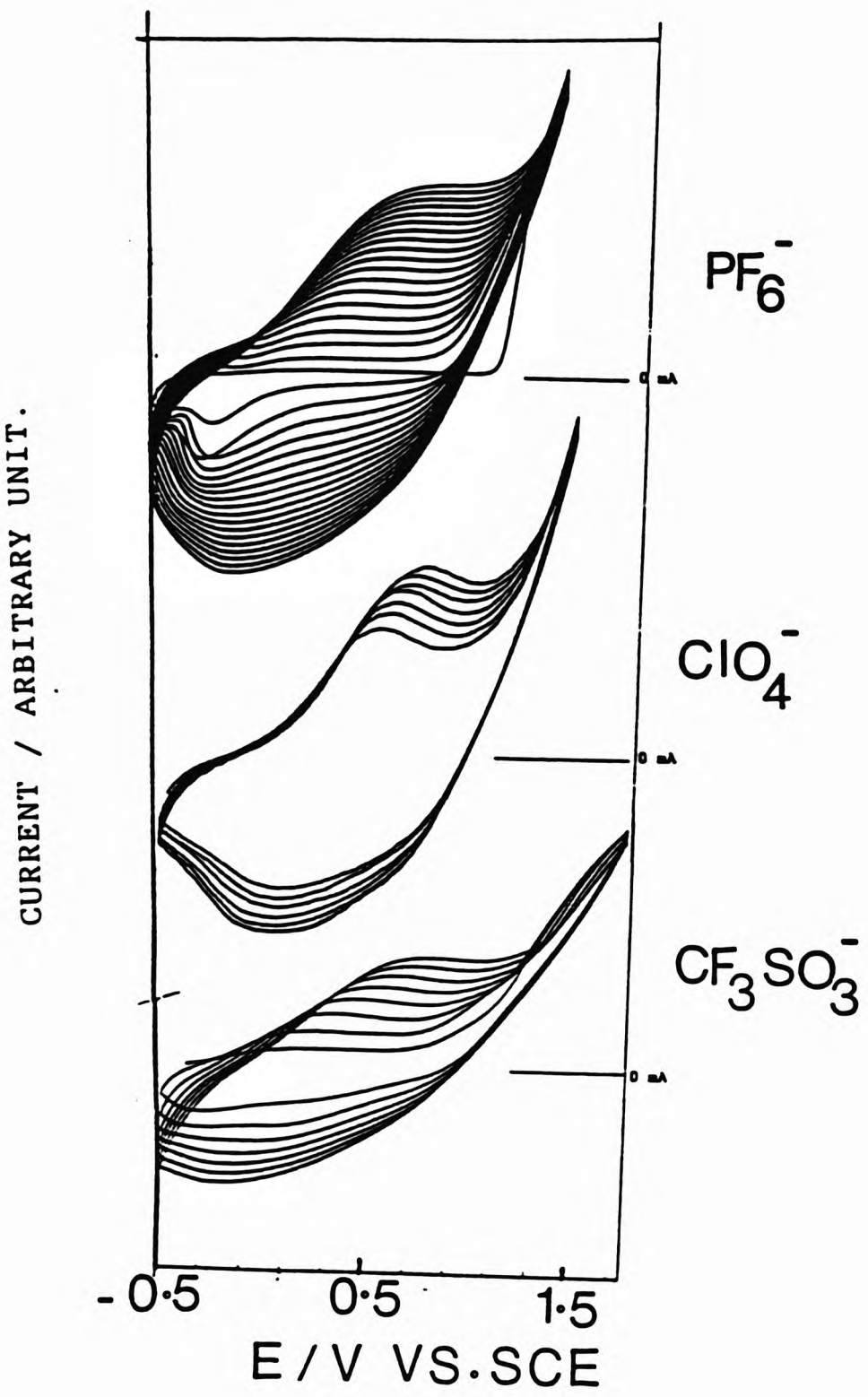

Conditions: Pyrrole : 2 mM.,Anion : 10 mM. ,

Electrode: Tin Oxide , Scan rate : 25 mV / s.

FIGURE 9.

INFLUENCE OF PYRROLE ON THE ELECTROPOLYMERISATION CHARACTERISTICS OF 3-METHYLTHIOPHEN.

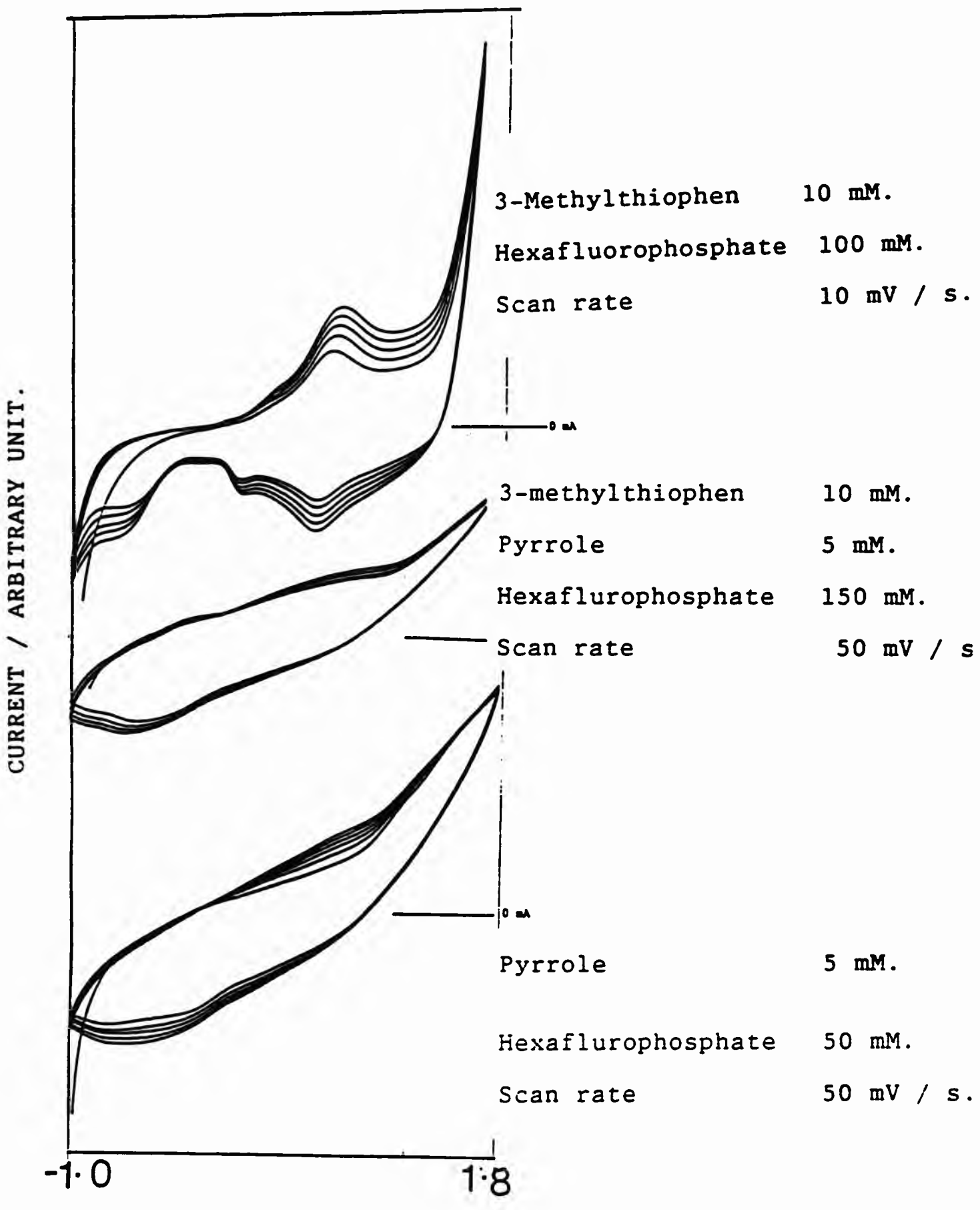

FIGURE 10.

Solvent in all cases : nitrobenzene.

POLY(DIMETHYLISOTHIONAPTHTHENE)HEXAFLUOROPHOSPHATE:
DEPENDENCE OF MICROSTRUCTURE ON APPLIED POTENTIAL.

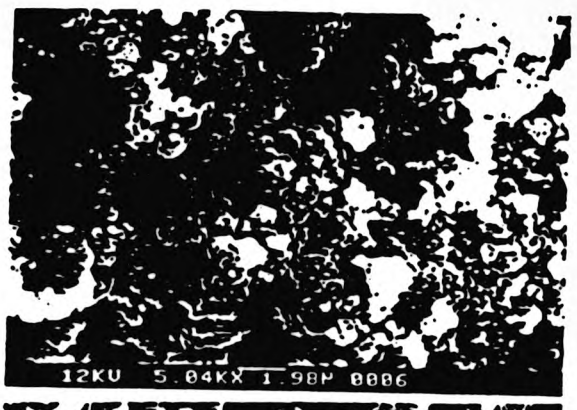

A

1.1V

5×10^{-1} Scm^{-1}

B

1.3V

5 Scm^{-1}

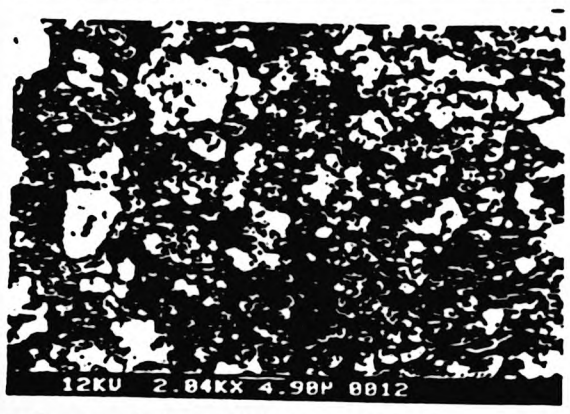

1.5V

80 Scm^{-1}

C

FIGURE 11.

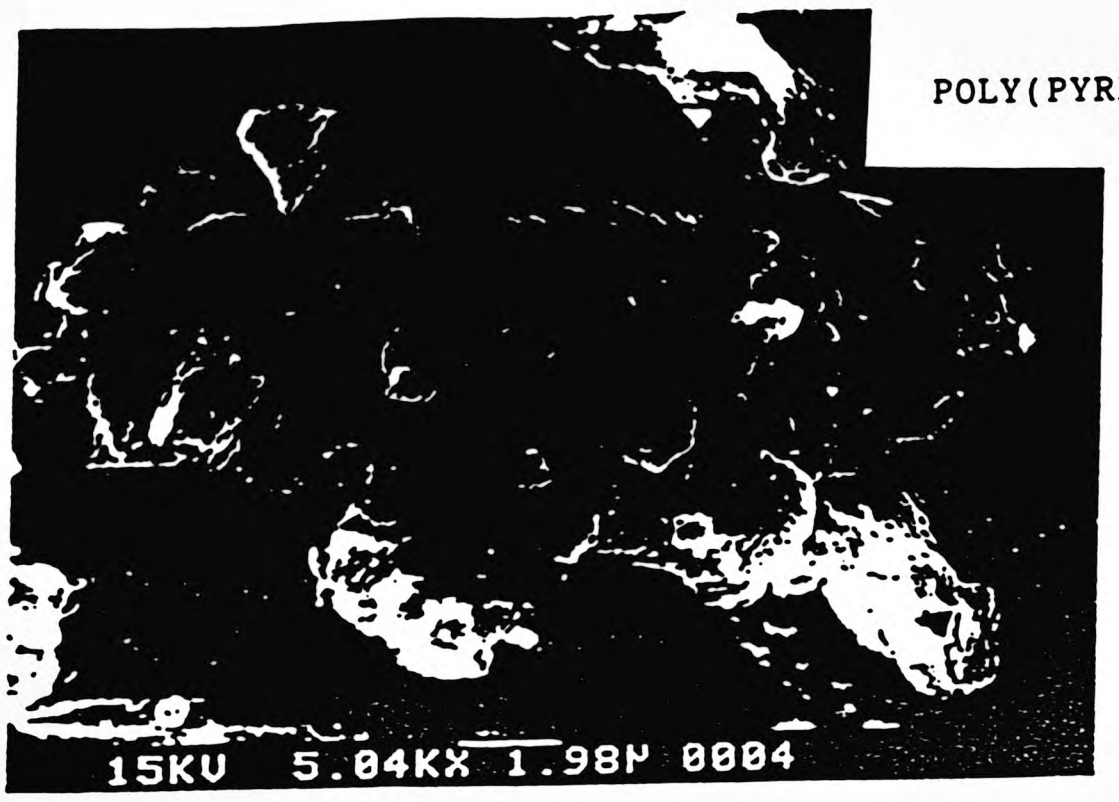

POLY(PYRROLE) p-TOLUENESULPHONATE

A

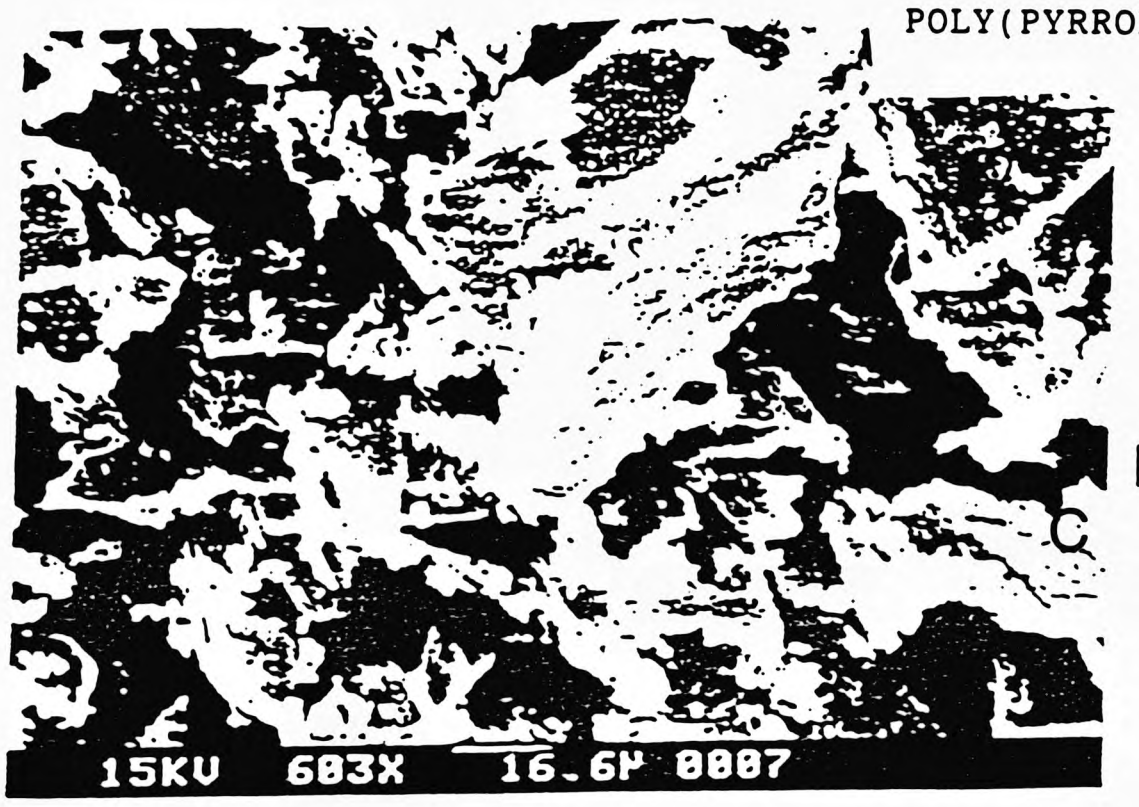

POLY(PYRROLE) LAURYLSULPHONATE

B

C

FIGURE 12.

ERRATA

The following represents mistakes made in the thesis:

page v, line : "dispropotionation" should read "disproportionation"

page 10, line 2: "proccessible" should read "processible"

page 17, line 3: "supression" should read "suppression"

page 22, paragraph 2, line 10: "phosphorous" should read "phosphorus"

page 23, bottom line: "Wiitg" should read "Wittig"

page 39, paragraph 2, line 1: "fragementation" should read "fragmentation"

page 41, paragraph 2, line 1: "fragementation" should read "fragmentation"

page 49, line 6: "transforamations" should read "transformations"

page 51, paragraph 2, line 6: "capaticance" should read "capacitance"

page 51, paragraph 2, line 7: "faradic" should read "faradaic"

page 54, paragraph 1, line 7: "atall" should read "at all"

page 54, paragraph 2, line 3: "investigtation" should read "investigation"

page 56, paragraph 2, line 3: "equilibrum" should read "equilibrium"

page 56, paragraph 2, line 4: "boundry" and "pricipally" should read "boundary" and "principally"

page 57, line 3: "transter" should read "transfer"

page 60, paragraph 1, line 3: "proflies" should read "profiles"

page 90, line 1: "Bromosuccinimide" should read "bromosuccinimide"

page 92, line 8: "$(CH_3)_3NPF_6$" should read "$(CH_3)_4NPF_6$"

page 97, paragraph 1, line 1: "moities" should read "moieties"

page 106, line 2: "polymeriation" should read "polymerisation"

page 121, paragraph 2, line 5: "interractions" should read "interactions"

page 144, paragraph 1, line 5: "slurred" should read "slurrried"

page 146, paragraph 3, line 3: "butyllitiium" should read "butyllithium"

DX

184648